IDENTIFYING GRADINGS AND BINDER COMBINATIONS FOR IMPROVING THE GREY WATER RESISTANCE OF ASPHALT

by
Christiaan Ludolph Marais Nel

Thesis presented in fulfilment of the requirements for the degree of Master of Engineering in the Faculty of Engineering at Stellenbosch University

Supervisor: Prof. Kim Jonathan Jenkins

March 2017

DECLARATION

By submitting this thesis electronically, I declare that the entirety of the work contained therein is my own, original work, that I am the sole author thereof (save to the extent explicitly otherwise stated), that reproduction and publication thereof by Stellenbosch University will not infringe any third party rights and that I have not previously in its entirety or in part submitted it for obtaining any qualification.

Full Names and Surname: Christiaan Ludolph Marais Nel

Date: March 2017

ABSTRACT

Premature failure of asphalt surfacing was observed on roads in areas within and surrounding informal settlements in Cape Town. It was concluded that the main source of failure was as a result of grey water spillage onto these road surfaces. Mew Way, located in the Khayelitsha area on the Cape Flats, required treatment and surfacing at least every 5 years to address grey water related problems. This has prompted the City of Cape Town and SABITA to initiate the Grey Water Resistant Asphalt Study to investigate the influence of grey water on the performance of asphalt.

As part of the Grey Water Resistant Asphalt Study, extensive laboratory experiments and testing were required to investigate the grey water resistance of asphalt. The University of Stellenbosch was approached by the Grey Water Research Group under the leadership of Mr A. Greyling, Technical Director at BVi Consulting Engineers (Pty) Ltd, to develop a research methodology for this unique study. This research methodology was executed at the University of Stellenbosch where all results and conclusions related to this study were reported.

The Researcher, after initiating an extensive literature study and identifying factors for improving the grey water resistance of asphalt, developed primary and secondary research methodologies. The objective of the primary research methodology was to identify gradings and binder combinations to improve the grey water resistance of asphalt. This research methodology consisted of two phases.

Phase 1 included moisture inducing simulating tests (MIST) for moisture conditioning purposes and indirect tensile strength (ITS) tests. Tensile strength ratio (TSR) results of binder combinations that were tested during Phase 1, indicated that the retained strength of asphalt mixtures after grey water MIST was significantly lower when compared to clean water MIST conditioning. Results also indicated that a medium graded asphalt mixture achieved greater strength after grey water MIST conditioning when compared to fine graded asphalt mixtures. The binder additive EVA contributed significantly to achieving greater asphalt mixture strength after grey water MIST conditioning.

Phase 2 consisted of laboratory scale model mobile load simulating (MMLS) and ITS testing of asphalt briquettes subjected to trafficking under dry (no water) and wet (grey water) conditions. Results from Phase 1 assisted with setting up asphalt gradations and binder combinations for testing during Phase 2 of the primary research methodology.

TSR results from Phase 2 did not show significant variations between the performance of medium and fine graded asphalt mixtures after being subjected to wet (grey water) MMLS3 trafficking. However,

permanent deformation results indicated that medium graded asphalt mixtures with EVA and SBS modified binders produced significantly lower deformations when compared to virgin binder (50/70 penetration grade) combinations after being subjected to wet MMLS3 trafficking. A binder additive, ZycoTherm®, in combination with an EVA modified binder and Sasobit did not only assist in reducing the permanent deformation, but also significantly increased the strength of the asphalt. ITS, permanent deformation, texture and material loss results of Phase 2 were combined to establish a rating criteria for determining suitable grey water resistant asphalt mixtures for high and low volume roads. Medium graded asphalt mixtures may provide a suitable grey water resistant asphalt mixture for high volume roads, whereas fine graded asphalt mixtures may provide a suitable solution for low volume roads. Based on the results of the rating criteria, the following asphalt mixtures showed significant resistance to grey water:

- EVA + 1%Sasobit® + Extra Lime (COLTO Medium Continuous Graded)
- EVA + Extra Lime (COLTO Medium Continuous Graded)
- EVA + 1%Sasobit® (COLTO Fine Continuous Graded)
- EVA + 1%Sasobit® + 0.1%ZycoTherm® (COLTO Fine Continuous Graded)

After completing laboratory scale MMLS trafficking during Phase 2 of the primary research methodology, trafficked asphalt briquettes were subjected to ITS testing. Each asphalt briquette had a diameter of 150 mm, and during the preparation of test specimens for laboratory scale MMLS trafficking, two opposite segments with parallel chords and each having a 19 mm mid-ordinate, had to be machined-off from each briquette with a dual saw. This was done to fit nine asphalt briquettes in a test bed specifically designed for executing the laboratory scale MMLS trafficking procedure. This led to the setup of a secondary research methodology for investigating the influence of these removed segments on the indirect tensile strength of the shaped asphalt briquettes. This investigation was accomplished through linear-elastic finite element modelling.

Results of the secondary research methodology indicated that a decrease of up to 8% in the maximum tensile strength can be expected at the centre of a shaped asphalt briquette (with removed segments as described above) when compared to an unshaped asphalt briquette. Results also indicate that no significant changes occurred in compressive stresses due to the shaping of briquettes.

This study provides insight on the development of grey water susceptible asphalt mixtures, which serves as a starting point for ensuring that durability and user specifications for roads exposed to grey water are met.

OPSOMMING

Die storting van gryswater oor die asfaltlaag van interne paaie binne en aangrensend tot informele nedersettings in Kaapstad, was geïdentifiseer as sleutelprobleem tot versnelde faling van die padstruktuur. Mew-weg, 'n pad aan die buitewyke van Khayelitsha op die Kaapse Vlakte, is een van hierdie paaie waar gryswater-verwante probleme tot behandeling en herbedekking ten minste elke 5 jaar gelei het. Die Stad Kaapstad en SABITA het saamgespan om die Gryswater Weerstandige Asfalt Studie te loods om invloed van gryswater op die gedrag van asfalt te ondersoek.

Deel van die Gryswater Weerstandige Asfalt Studie behels die uitvoer van toepaslike en uitgebreide laboratorium eksperimente rondom die gryswater-weerstandigheid van asfalt. Die Universiteit van Stellenbosch was genader deur die Gryswater Navorsings-groep, onderleiding van Mnr A. Greyling van BVi Raadgewende Ingenieurs (Edms) Bpk, om 'n navorsingsmetodiek vir hierdie unieke studie saam te stel. Hierdie navorsingsmetodiek was ook by die Universiteit van Stellenbosch uitgevoer van waar die verwante resultate en gevolgtrekkings van die studie geraportteer was.

Die Navorser het 'n primêre en sekondêre navorsingsmetodiek vir hierdie studie saamgestel wat deur 'n uitgebreide literatuurstudie voorafgegaan is. Vanuit hierdie literatuurstudie was sleutelfaktore om gryswater-weerstandigheid van asfalt te verbeter, geïdentifiseer. Die primêre-navorsingsmetodiek het die identifisering van graderings- en bindstofkombinasies om die gryswater weerstandigheid van asfalt te verbeter, behels. Die primêre navorsingsmetodiek het uit twee fases bestaan.

Fase 1 het uit voginduserende-simulasietoetse (E: MIST) asook indirekte-treksterktetoetse (ITS) bestaan. Treksterkte-verhoudings van hierdie fase het aangedui dat gryswater 'n beduidende invloed op die sterkte van asfalt in vergelyking met skoon water het. Resultate van Fase 1 het ook aangetoon dat medium-gegradeerde asfalt 'n verbeterde sterkte teenoor fyn-gegradeerde asfalt na gryswater kondisionering behaal. Die EVA-bindstofbymiddel het ook tot 'n beduidend beter mengselsterkte na gryswater kondisionering gelei.

Fase 2 het uit laboratoriumtoetse met 'n model mobiele lassimileerder (MMLS) bestaan, asook ITS-toetse op asfaltbrikette wat aan droë (geen water) en nat (gryswater) verkeerstoestande onderhewig was. Resultate vanuit Fase 1 het bygedra tot die keuse van asfaltgraderings- en bindstof-kombinasies wat tydens Fase 2 van die primêre navorsingsmetodiek getoets was.

Treksterkte-verhoudings van Fase 2 het nie enige beduidende verskille tussen die medium- en fyn-gegradeerde asfaltmengsels na gryswater kondisionering getoon nie. Permanente vervormingsresultate

het wel aangetoon dat medium-gegradeerde asfalt mengsels met EVA en SBS gemodifiseerde bindstowwe tot laer vervorming gelei het in vergelyking met skoon bindstof kombinasies na gryswater MMLS3 verkeers-kondisionering. 'n Bindstof bymiddel, genaamd ZycoTherm®, in kombinasie met EVA gemodifiseerde bindstof en Sasobit®, het nie net permanente vervorming verlaag nie, maar ook tot verbeterde asfalt-sterkte gelei. Die resultate van Fase 2 se ITS, permanente vervorming, tekstuur en materiaalverlies was saamgevoeg om beoordelingskriteria saam te stel. Die doel van die kriteria was om 'n geskikte gryswater-weerstandige asfaltmengsel vir hoë en lae verkeervolumes te identifiseer. Medium-gegradeerde asfaltmengsels kan as 'n geskikte oplossing dien om 'n gryswater-weerstandige asfaltmengsel vir hoë verkeervolumes te produseer. Fyngegradeerde asfaltmengels kan as 'n geskikte oplossing vir lae verkeervolumes dien. Gebaseer op die resultate van die beoordelingskriteria, het die volgende asfaltmengsels beduidende weerstand teen gryswater getoon:

- EVA + 1%Sasobit® + Extra Lime (COLTO Medium Deurlopende Gradering)
- EVA + Extra Lime (COLTO Medium Deurlopende Gradering)
- EVA + 1%Sasobit® (COLTO Fyn Deurlopende Gradering)
- EVA + 1%Sasobit® + 0.1%ZycoTherm® (COLTO Fyn Deurlopende Gradering)

Na voltooiing van die laboratoriumskaalse MMLS-toetse tydens Fase 2 van die primêre navorsings-metodiek, was 150 mm diameter asfaltbrikette wat aan verkeer onderhewig was, gebruik vir die uitvoer van ITS-toetse. Die voorbereiding van die asfaltbriket-monsters vir MMLS-toetse het behels die masjinering daarvan deur twee segmente met parallelle koorde en 19 mm mid-ordinate van elk af te saag. Hierdie vereiste het dit moontlik gemaak om nege asfaltbrikette op die toetsbed te installer wat spesifiek vir hierdie doel ontwerp is. Dit het gelei tot die samestelling van 'n sekondêre navorsingsmetodiek om die invloed van die gemasjineerde asfaltbrikette op die maksimum treksterkte resultaat na 'n ITS-toets te ondersoek. Die ondersoek was deur middel van lineêr-elastiese eindige-elementmodelle tot stand gebring.

Resultate van die sekondêre-navorsingsmetodiek het aangedui dat 'n verskil van 8% in die maksimum trekstrekte-resultaat in die middel van gemasjineerde en ongemasjineerde asfaltbrikette verwag kan word. Resultate het ook getoon dat die drukspannings in die briket nie beïnvloed was deur masjinering soos hierbo aangedui nie.

Insig tot die ontwikkeling van gryswater-weerstandige asfalt word in hierdie verslag aangebied.

ACKNOWLEDGMENTS

I would like to acknowledge the following persons and companies:

- University of Stellenbosch: My promoter, Prof Kim Jenkins, and Mrs Chantal Rudman for affording me the opportunity to develop my interest and knowledge in the field of pavement engineering. Without their guidance and support, this study would not have been completed successfully.
- BVi Consulting Engineers (PTY) Ltd: Messrs André Greyling and Nicolaas van Aardt for their assistance and arrangements with study materials. In addition, their practical knowledge in the field of asphalt technology proved vital in setting up the experimental procedures for this thesis.
- University of Stellenbosch laboratory manager, technicians and staff: Messrs Riaan Briedenhann, Gavin Williams, Collin Isaac and Eric Nojewu for their assistance during the execution of laboratory experiments.
- Colas (Cape Town): Mr Morné Labuschagne for preparing modified binders used during this study.
- Much Asphalt: For supplying aggregate, bitumen and filler materials.
- My family for providing support and assistance in the completion of my post-graduate studies.

TABLE OF CONTENTS

LIST OF FIGURES

LIST OF TABLES

LIST OF ABBREVIATIONS

AASHTO	– American Association of State Highway and Transport Officials
ACV	– Aggregate Crushing Value
ASTM	– American Society for Testing and Materials
CCC	– City of Cape Town fine grade asphalt mixture
COLTO	– Committee of Land Transport Officials
DHU	– Dry Heating Unit
EVA	– Ethylene Vinyl Acetate
FACT	– Fines Aggregate Crushing Test
HMA	– Hot Mix Asphalt
ITS	– Indirect Tensile Strength
ITT	– Indirect Tensile Test
LTM	– Laser Texture Meter
MIST	– Moisture Inducing Simulating Test
MMLS	– Model Mobile Load Simulator
MTS	– Material Testing System
PG	– Performance Grade
PSV	– Polished Stone Value
SABITA	– Southern Africa Bitumen Association
SANS (SABS)	– South African National Standards (South African Bureau of Standards)
SAPEM	– South African Pavement Engineering Manual
SBR	– Styrene-Butadiene-Rubber
SBS	– Styrene-Butadiene-Styrene
TRH	– Technical Recommendations for Highways
TSR	– Tensile Strength Ratio
VFB	– Voids Filled with Binder
VIM	– Voids in Mix
VMA	– Voids in the Mineral Aggregate
WHU	– Water Heating Unit

CHAPTER 1 – INTRODUCTION

1.1 BACKGROUND

Premature failure of asphalt surfacing was observed on roads in areas within and surrounding informal settlements in Cape Town. It was concluded that the main source of failure was as a result of grey water spillage onto these road surfaces. Mew Way, located in the Khayelitsha area on the Cape Flats, required treatment and surfacing at least every 5 years to address grey water related problems. This has prompted the City of Cape Town and SABITA to initiate the Grey Water Resistant Asphalt Study to investigate the influence of grey water on the performance of asphalt.

In developing areas in Cape Town, conventional binder combinations and asphalt mixtures proved inadequate to resists the effect of surfactants present in grey water in combination with traffic. A visual inspection of Mew Way indicated that severe damage to asphalt surfacing occurred in areas of standpipes and local businesses such as car washes. In these areas loss of the bitumen-aggregate mastic between larger aggregate particles, scour, potholes and crocodile cracking were observed (Greyling, 2015).

Based on this scenario, improving the grey water resistance will require improving asphalt properties through unconventional binder and aggregate grading combinations.

1.2 OBJECTIVES OF RESEARCH

Primary and secondary objectives were established for this study. The primary objective of this study was to identify gradings and binder combinations for improving the grey water resistance of asphalt. Accomplishing the primary objective required completing various sub-objectives:

i) Understanding compositions, properties as well as mechanisms of moisture failure in asphalt surfacing.

> This objective was accomplished by compiling an extensive literature study. Knowledge on these topics assisted with the selection of appropriate aggregate and modified binders for addressing premature failure of asphalt surfacing exposed to grey water.

ii) Setting up of an extensive experimental research methodology to identify variables that influence the grey water susceptibility of various asphalt mixture compositions.

This objective was achieved through accelerated pavement testing of asphalt under different levels of grey water exposure. The identification of the variables that influence grey water susceptibility of asphalt mixtures was accomplished through MIST conditioning, MMLS3 trafficking and ITS tests. MIST conditioning consists of submerging asphalt briquettes in a triaxial cell with grey water and subjecting it to repeated pressure pulses of 150 kPa for a duration of 6 hours to simulate traffic loads. ITS tests are performed to measure the damage caused by grey water conditioning. MMLS3 trafficking consists of subjecting asphalt mixtures to dry and wet conditions during trafficking on a laboratory scale.

iii) Executing the Experimental Research Methodology and processing of data obtained to conclude the finding of this study.

This objective was accomplished by determining whether grey water had an influence on the performance of asphalt mixtures. In addition, four asphalt mixtures with the most effective grey water resistance were selected based on laboratory results. Two of these mixtures were selected for developing suitable solutions for surfacing of high volume roads, whereas the remaining two were selected as suitable surfacing solutions for low volume roads.

A secondary objective was established to investigate the influence of the geometry of a 150 mm diameter asphalt briquette on the result of an ITS test through finite element analysis. Laboratory scale MMLS testing using the test bed procedure, two opposite segments with parallel chords and each having a 19 mm mid-ordinate, had to be removed from each briquette by the saw method. This was done to fit nine asphalt briquettes in a test bed specifically designed for executing the laboratory scale MMLS trafficking procedure. This led to the setup of a secondary research methodology for investigating the influence of these removed segments on the indirect tensile strength of the machined asphalt briquettes. This investigation was accomplished through linear-elastic finite element modelling. A secondary research methodology, known as the finite element analysis research methodology, were established to complete this objective.

1.3 LIMITATIONS OF STUDY

This study was limited to sand skeleton asphalt mixtures as prepared by Much Asphalt. Virgin and modified binders for this study were selected based on local supply and for improving adhesive properties of asphalt mixtures.

A grey water concentrate was mixed during execution of the laboratory research methodology. The concentrate consisted of 0.5% Sunlight® dishwashing liquid and 0.5% OMO® laundry detergent per 100 litres clean water. MIST conditioning was done at 60°C, whereas MMLS tests were completed at 40°C and 100 000 MMLS3 load cycles. All indirect tensile strength (ITS) tests were completed at a temperature of 25°C and a loading rate of 50.8 mm/min.

1.4 LAYOUT OF THESIS

The layout of this thesis is presented in Table 1.1.

Table 1. 1 - Layout of the thesis.

Chapter	Description
1	Brief background, objectives of research and study limitations.
2	A literature review is focussing on key areas related to this study.
3	Experimental research methodology consisting of MIST conditioning, ITS testing and laboratory scale MMLS testing.
4	Finite Element Analysis Research Methodology inclusive of model set-up.
5	Results obtained from of the Laboratory Research Methodology.
6	Results obtained from the Finite Element Research Methodology.
7	Conclusions and Recommendations.

CHAPTER 2 – LITERATURE REVIEW

2.1 INTRODUCTION

This literature review discusses aspects relevant to the research topic and gives a brief overview of the application of hot-mix-asphalt (HMA) in South Africa, as well as the purpose of asphalt surfacing and failure mechanisms related to asphalt pavements. In addition, the following concepts related to asphalt mixtures are covered: moisture susceptibility, cohesion and adhesion theories, disbonding mechanisms related to moisture damage, factors influencing the bitumen-aggregate bond, the composition of grey water, the effects of chemicals on the moisture susceptibility, test methods for evaluating moisture susceptibility and the MMLS3 accelerated pavement tester. A conclusion is formulated to establish factors to be considered for improving an asphalt mixture's grey water resistance and to assist with the development of a research methodology.

2.2 BRIEF OVERVIEW OF ASPHALT SURFACING IN SOUTH AFRICA

In South Africa, 80% of the roads are surfaced with seals, leaving a small percentage of roads surfaced with either asphalt or concrete (SAPEM Chapter 2, 2014). This distribution of surfacing layer types is influenced by various factors such as traffic loads, as well as the nature of materials used for constructing South African roads.

Asphalt surfacing in South Africa is predominately found in areas subjected to heavy traffic loads where surfacing seals are not sufficient. The thin layer design of asphalt surfacing is something unique to South Africa. Minimum layer thicknesses range from 20 mm for ultra-thin asphalt surfacing, 40 mm for conventional asphalt surfacing and 80 mm for asphalt bases.

The design of asphalt surfacing in South Africa is contained in the *Interim Guidelines for the Design of Hot-Mix Asphalt in South Africa (2001)* and *Technical Recommendations for Highways 8 (TRH8)* (1987). Although these manuals are available for use, SABITA compiled a new Hot-Mix Asphalt (HMA) design manual. SABITA Manual 35/TRH 8 (2016) was published in February 2016 for the design and use of asphalt in road pavements. These manuals establish methods for designing ultra-thin surfacing, conventional surfacing and asphalt bases. The South African design manuals include traffic considerations, selection of asphalt components, asphalt volumetric design and methods to evaluate rutting and fatigue performance to produce sufficient asphalt mixes.

2.3 ASPHALT SURFACING PURPOSE

The purpose of asphalt surfacing can be of a structural or functional nature. In South Africa, asphalt surfacing serves a structural purpose when constructed in layer thicknesses of 30 mm and greater. Also referred to as structural asphalt layers, these layer contributes to the structural integrity of the pavement structure as well as providing skid resistance against environmental elements. Structural asphalt layers are constructed with low permeability to protect the substratum for moisture ingress.

In South Africa, asphalt surfacing serves a functional purpose when constructed in layer thicknesses of 30 mm and less. Referred to as functional asphalt layers, these layers do not have a significant contribution to the structural integrity of the pavement structure. Functional asphalt layers conform to a specific functional criteria such as providing skid resistance, surface drainage and noise reduction. These layers also protect the substratum from water ingress as well as providing sufficient riding quality. HMA is designed according to specification and to meet certain engineering properties. The primary engineering properties for HMA are illustrated in Figure 2.1 (SAPEM Chapter 9, 2014).

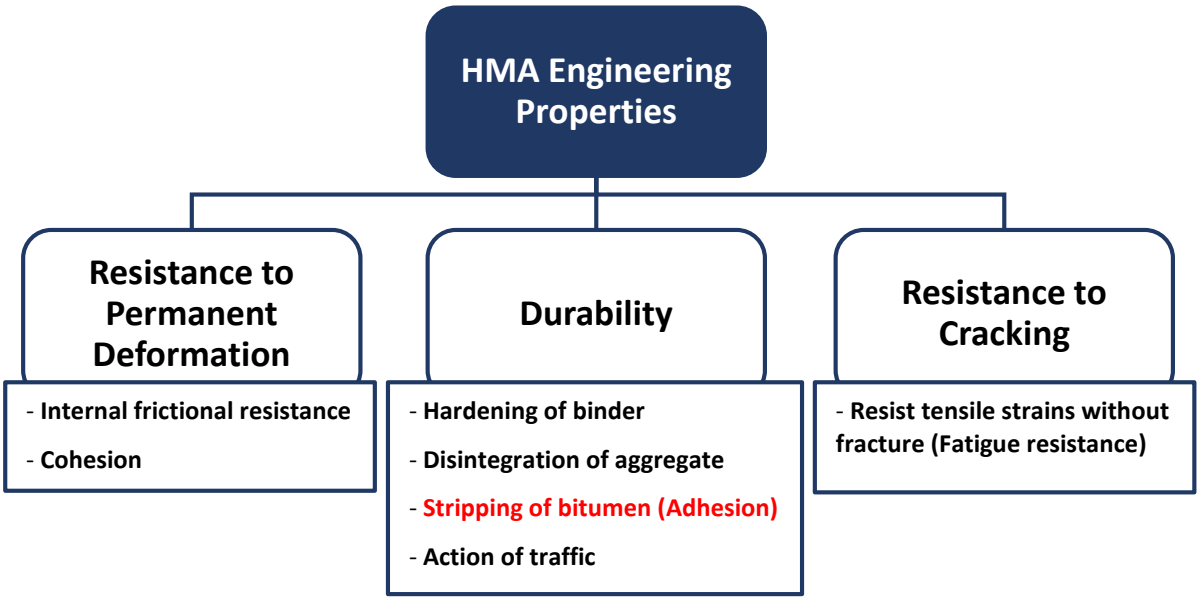

Figure 2. 1 - Hot-Mix-Asphalt Engineering properties (SAPEM Chapter 9, 2014).

In addition to the primary engineering properties, other properties such as flexibility, skid resistance, permeability, stiffness and workability are also important to consider during the design of HMA. In the sections that follow important aspects of asphalt surfacing is discussed to establish an understanding of the material's performance and how engineering properties are incorporated to produce sufficient asphalt mix designs.

2.4 ASPHALT FAILURE MECHANISMS

The predominant failure mechanisms of asphalt surfacing are permanent deformation and fatigue. The *Technical Methods for Highways 9* (TMH 9) manual provide guidelines for visually assessing the performance of flexible pavements in South Africa. From the TMH 9 it is concluded that various other distresses can be connected to the ability of the asphalt mix to resist permanent deformation and fatigue. Poor asphalt mix design can lead to distresses such as cracking, potholing, rutting, pumping and bleeding to occur.

In addition to permanent deformation and fatigue, moisture susceptibility of asphalt mixes is also considered important. Ingress of water through micro cracks in the bitumen mastic has been found to significantly increase the rate at which permanent deformation and fatigue of the asphalt surfacing occur (Little & Jones IV, 2003). Brief discussions on permanent deformation, fatigue and moisture susceptibility of asphalt mixes are presented in the sections that follow.

2.4.1 PERMANENT DEFORMATION

Permanent deformation occurs in the wheel path on asphalt surfacing due to shear deformation caused by repetitive traffic loading. The distress permanent deformation is also referred to as 'rutting'. The shape of the deformation is a good indicator of where the problem is located in the pavement structure. A wide and even deformed shape indicates that the problem is usually located within the lower pavement layers, whereas a narrow and sharp deformed shape indicates that the problem is most likely located within the upper pavement structure. The latter case is usually the result of a poor asphalt mix design (TRH 9, 1992). Figure 2.2 illustrates a severe condition of permanent deformation.

Figure 2. 2 - Severe condition of permanent deformation (TMH 9, 1992).

Asphalt's ability to resist permanent deformation is dependent on environmental and mixture aspects. Environmental aspects include temperature, traffic loading rate and the stress state associated with a particular loading and pavement situation (shear stress and bulk stress). Mix aspects include the viscosity

of the bitumen mastic, packing characteristics of the mix, volumetric aspects and aggregate characteristics (Taute, et al., 2001).

Due to the composition of asphalt, its material behaviour is regarded visco-elastic. Figure 2.3 illustrates the relationship between viscous and elastic material behaviour. The complex shear modulus (G*) is used to quantify the resistance of the binder to deformation when repeated shear loads are applied. The complex shear modulus is determined from dividing the maximum shear stress by the maximum shear strain as represented by the length of the vector shown in Figure 2.3. In addition, a shear angle (δ) is determined to quantify the relationship between the recoverable and non-recoverable deformation as indicated in Figure 2.3 (Douries, 2004). This means that at low temperatures and high loading frequencies, greater elastic (recoverable) behaviour is expected due to the nature of the bitumen and asphalt mixture (Figure 2.3 scenario 1). At high temperatures and long loadings times, the viscous (non-recoverable) component of the bitumen and asphalt mix is dominant (Figure 2.3 scenario 2).

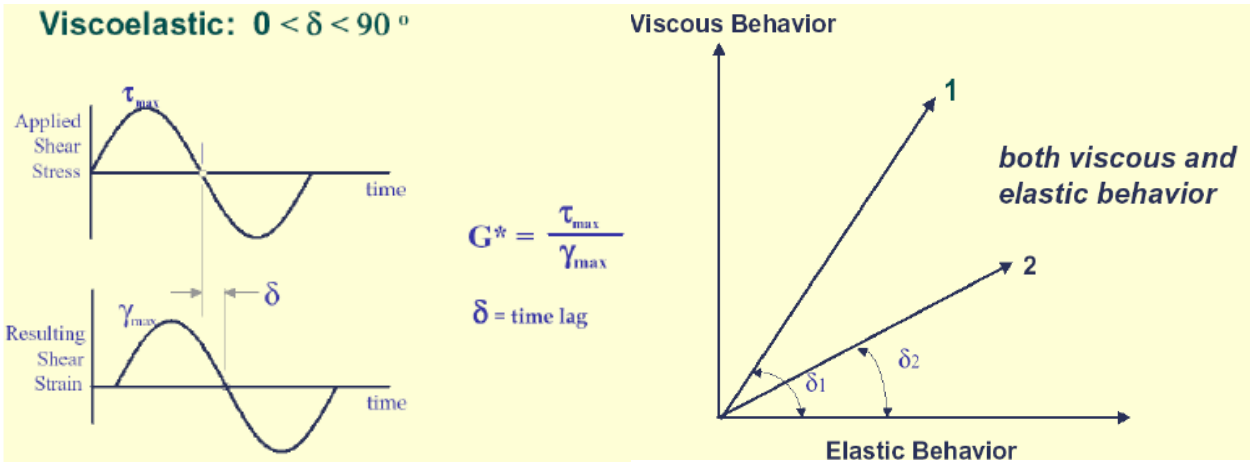

Figure 2. 3 - Viscous and elastic material behaviour of the binder (Douries, 2004).

The cohesion and internal angle of friction of an asphalt mixture is dependent on the nature and content of the binder, aggregate properties and temperature. These material parameters determine the shear resistance of a mixture. As the temperature of the mixture increases above the softening point of the bitumen, the material behaviour becomes dominated by the viscous component of the binder. At these temperatures the bitumen is less viscous and the cohesion of the mixture is reduced. Therefore, binders with a low softening point exposed to high temperatures and long loading times have less cohesion, meaning it is less resistant to shear compared to binders with higher softening points. As the binder content increases, the excess binder or free binder increases and pushes the aggregate particles apart to enhance fluidity and to reduce shear resistance (Anderson, 1987). An optimum binder content is therefore

determined for asphalt mixtures to establish a suitable relationship between the required performance parameters. Aggregate properties such as the angularity also influences the shear resistance of asphalt. The aggregate interlocking of an asphalt mixture increases with an increase in the angularity of the aggregate (De Sombre, et al., 1998). Testing for permanent deformation should be done at high temperatures as the shear strength of an asphalt mix is dependent thereon (Douries, 2004). Improving asphalt's ability to resist permanent deformation requires investigating the internal frictional resistance, as well as the cohesion of the asphalt mixture.

Wheel tracking tests have been found to produce the strongest correlation between rutting in the field and laboratory testing. However, these tests require large asphalt slabs to be compacted before testing, making it expensive to perform. In South Africa wheel tracking test devices include the Model Mobile Load Simulator (MMLS) and Transporttek Wheel Tracking Device (Taute, et al., 2001).

2.4.2 FATIGUE

Failure of an asphalt layer due to repetitive traffic loading is known as fatigue failure. An asphalt layer acts as a flexible beam when subjected to traffic loads. Repetitive traffic loading causes accumulated strain to develop at the bottom of the asphalt layer. Once the accumulated strain is beyond what the asphalt can sustain, cracks will start to form. These cracks usually form in the wheel path at the bottom of the asphalt layer and can migrate from hair line cracks to macroscopic cracks if left unattended. In most cases, macroscopic cracking causes complete loss in the structural integrity of the asphalt layer. Fatigue failure is usually identified by the formation of 'crocodile' cracking-pattern on the asphalt surface (Soenen, 2015). Figure 2.4 illustrates a severe condition of 'crocodile' cracking.

Testing asphalt's resistance to fatigue requires an understanding of the asphalt properties, pavement structure and environment it is subjected to. It has been suggested that fatigue evaluation may easily become oversimplified as it incorporates a significant amount of factors. The Indirect Tensile Strength (ITS) test is an inexpensive method to evaluate relative fatigue performance of asphalt subjected to low traffic volumes. In the

Figure 2. 4 - Cracking of the asphalt due to fatigue (TMH 9, 1992).

case of heavy trafficked roads, the four-point beam test is suggested (Taute, et al., 2001).

The presence of water has shown to significantly influence the rate of crack formation caused by fatigue. Water penetrates through the cracks causing a significant loss of adhesion. Therefore. investigating the moisture susceptibility of asphalt mixes is considered important.

2.4.3 MOISTURE SUSCEPTIBILITY

The moisture susceptibility of asphalt surfacing determines its ability to resist stripping of bitumen from the aggregate surface. Stripping of bitumen is the result of disbonding mechanisms such as detachment, displacement, hydraulic scour and pore pressures. These disbonding mechanisms occur in the presence of moisture ingress, where moisture physically separates the bitumen film from the aggregate surface. As expected, traffic loading has shown to increase the rate of stripping due to stresses induced.

Improving the moisture susceptibility of asphalt requires investigating adhesion properties. The adhesion of asphalt is primarily determined by factors such as the aggregate and bitumen properties. In addition, investigating the volumetric properties may also provide improvements as it is connected to the permeability of asphalt. Evaluating the moisture susceptibility of asphalt mixes has become standard protocol as various types of tests have been developed to measure the stripping of bitumen.

The durability of asphalt is the engineering property influenced by stripping of bitumen (see Figure 2.1). Understanding disbonding mechanisms and composition of HMA shall provide solutions for improving asphalt's resistance against grey water.

2.5 COHESION AND ADHESION

Improving the moisture susceptibility of asphalt requires investigating the cohesive and adhesive properties of an asphalt mixture. Damage in an asphalt mixture can occur either by the fracturing of the bitumen mastic (cohesive failure) or fracturing of the bitumen-aggregate bond (adhesive failure) (Little & Jones IV, 2003). Defining these concepts are required to understand the disbonding mechanism associated with moisture susceptibility of asphalt.

2.5.1 COHESION

Cohesion is a term used to describe the strength of a material when unconfined. Coulomb developed an equation incorporating the cohesion to determine the shear strength of materials. This relationship between the shear strength and cohesion of a material is represented by Equation 2.1

$$\tau = c + \sigma tan\phi \qquad \textit{Equation 2.1}$$

where τ = *shear strength*

c = *cohesion*

σ = *confining pressure*

ϕ = *angle of internal friction*

De Sombre et al (1998) states that asphalt mixtures exhibit cohesive behaviour somewhere between a cohesive and non-cohesive soil. During compaction aggregates in the asphalt mixture are distorted and reorientation occurs much like a cohesive material. The cohesiveness of an asphalt mixture decreases with an increase in binder content. During compaction, friction between the aggregates also provide resistance to the reorientation of the particles, therefore exhibiting cohesive behaviour similar to a non-cohesive soil. This behaviour supports acceptability of using Coulomb's equation for determining the shear stress of an asphalt mixture. In asphalt pavement layers, traffic-induced stresses are transferred to underlying layers through a combination of inter-particle contact and resistance to flow of the binder. Therefore, the asphalt mixture is required to resist high shear stresses due to traffic loading. Shear resistance is dependent on the aggregate structure and cohesion of the binder.

The bitumen mastic is responsible for providing cohesion within an asphalt mixture and is greatly dependent on the rheology of the bitumen. Terrel and Al-Swailmi (1994) stated the presence of water saturates the bitumen mastic causing swelling of the voids in the asphalt mixture. This weakens the bitumen mastic resulting in loss of cohesion. The addition of filler materials such as lime and cement have shown to improve the cohesion of an asphalt mixture and thus the shear resistance. This was investigated by Kim et al. (2002) who concluded that the dispersion of filler material greatly influences the bitumen mastic's resistance to microcracking. Hydrated lime has shown to improve the bitumen-aggregate adhesion through its interaction between the carboxylic acids in the bitumen (Plancher, et al., 1977). This interaction is discussed in further detail in *Section 2.7.3.3.*

The cohesion of an asphalt mix is also dependent on the temperature at compaction. An indirect relationship between cohesion and temperature of an asphalt mix exists. Increasing the temperature will decrease the cohesion of the mix and vice versa (De Sombre, et al., 1998).

Cohesion not only has an influence on bitumen mastic properties but also has a significant influence on other properties such as the stiffness of an asphalt mixture. Research done by Schmidt and Graf (1972) investigated the effect of water saturation on the stiffness of asphalt mixtures. They concluded that asphalt can lose up to 50 percent of its stiffness when saturated with water. However, they also established that loss in stiffness can be regained upon drying. Cheng et al. (2002) discussed that the saturation and the rate of moisture damage in asphalt mixtures is related to the diffusion of water into the asphalt mastic and the migration of water through the bitumen-aggregate interface. He further stated that asphalt mixtures with the ability to hold large quantities of water, accumulate moisture damage at a faster rate. It is also apparent that the extent of saturation is related to the permeability of the asphalt.

2.5.2 ADHESION

Adhesion of an asphalt mix is determined by the bitumen-aggregate bond. Terrel and Shute (1989) identified four theories to describe the adhesion between the bitumen and aggregate in an asphalt mix. These theories include chemical reaction, surface energy, molecular orientation and mechanical adhesion. Terrel and Shute (1989) stated that adhesion of an asphalt mixture may be the result of more than one theory combined. Therefore, no single theory is available to describe the adhesion of an asphalt mixture. They further stated that these adhesion theories may be affected by factors such as:

- Aggregate and bitumen surface tension
- Aggregate and bitumen chemical composition
- Bitumen viscosity
- Aggregate porosity, cleanliness, moisture content and temperature (During mixing)

From these factors, it is clear that the aggregate and bitumen properties significantly influence the adhesion of an asphalt mix.

2.5.2.1 Chemical reaction (Adhesion Theory 1)

The chemical reaction theory states that water-soluble compounds form between the acidic and basic components of the bitumen to form a strong adhesive bond. Therefore, a chemical reaction is established through attraction of surface charges and is also governed by the pH-level. Aggregates consist of both acidic and basic components. However, the silica content of an aggregate determines whether it is primarily acidic or basic. The acidity of an aggregate increase with an increase in the silica content. Rice (1958) suggested that the selection of aggregates and bitumen should be based on improving the chemical reaction between the bitumen and aggregates. In the presence of moisture acidic aggregates have shown greater loss of adhesion when compared to basic aggregates. This is due to their surface charge in the

presence of water. However, the adhesion between the acidic aggregates and bitumen can be improved upon with amines. Amines are further discussed in *Section 2.7.2.3*.

Robertson (2000) investigated the types of chemical reactions that occur between bitumen and aggregates due to the polar nature of these materials. He explains that basic nitrogen molecules from the bitumen react tenaciously with the aggregate surface to form adhesive bonds. He continued by explaining that carboxylic acids in the bitumen are quite polar and tend to be attracted to the aggregate surface. However, this attraction vanishes in the presence of water and is dependent on the type of acid. This is also substantiated by Plancher et al (1977), where they explained that monovalent cation salts (sodium and potassium) present in the carboxylic acids of bitumen are considered to be surfactants, therefore acting as soap causing disbonding especially during traffic loading.

Robertson (2000) established that divalent charge salts of acids, such as calcium from hydrated lime, have shown to significantly improve the bitumen-aggregate bond strength against the action of water. Research done by Williams et al. (1998) at the Western Research Institute indicated that aged asphalt mixtures are more susceptible to moisture damage compared to unaged asphalt mixtures. Ageing of the bitumen through oxidation causes a strong acidic material to appear, causing loss of adhesion. However, this is not the case for all asphalt mixtures. Robertson (2000) indicated that a detergent may form if bitumen acids are converted to sodium salts (which is the case for some aggregates). Whereas calcium salt compounds from detergents are less moisture sensitive, they can also deactivated with the addition of lime filler.

2.5.2.2 Surface energy and Molecular orientation (Adhesion Theory 2 and 3)

The relative wettability of aggregate surfaces, either by bitumen or water, is used to formulate the surface energy adhesion theory. The low viscosity and low surface tension of water make it a better wetting agent compared to bitumen (Little & Jones IV, 2003). The surface energy theory can be used to calculate the cohesive strength of the bitumen mastic as well as determining the adhesive bond energy between the bitumen and aggregate. Cheng et al. (2002) provided a method for measuring the surface energy of bitumen using the Wilhelmy plate method. He also provided a method for measuring the surface energy of aggregates using the universal sorption device (USD). Cheng et al. (2002) further explained how to relate these measurements to the fracturing of the bitumen mastic (cohesion) and fracturing of the bitumen-aggregate bond (adhesion). However, this method requires detail discussion and will not be presented in this literature study.

The molecular orientation theory works together with the surface energy theory to form a synergistic process, as both these theories are involved with the structuring of bitumen molecules at the bitumen-aggregates interface (Kiggundu & Roberts, 1988). The molecular orientation theory assumes the adhesion between bitumen and aggregate is established by a reduction in surface energy due to the aggregate surface absorbing the bitumen.

2.5.2.3 Mechanical adhesion (Adhesion Theory 4)

The mechanical adhesion theory includes adhesion formed by the aggregate's properties. These properties include the surface texture, absorption, surface coating, physical particle size and surface area (Terrel & Al-Swailmi, 1994). This theory involves selecting aggregates with large surface areas and rough texture to produce a strong mechanical interlocking bond that improves the moisture susceptibility of an asphalt mixture (Little & Jones IV, 2003). *Section 2.7.1* of this Literature Review elaborates on the significance of aggregate properties on the moisture susceptibility of asphalt mixtures.

2.6 DISBONDING MECHANISMS

Loss of durability and strength of asphalt mixtures due to the ingress of water is referred to as moisture damage. As already established, moisture damage can either cause failure of the bitumen-aggregate bond or failure of the bitumen mastic. In the latter case, moisture penetrates the bitumen mastic and weakens it. Once moisture has penetrated, traffic loadings may significantly increase the rate of damage making the asphalt mix more susceptible to moisture (Little & Jones IV, 2003).

Failure of an asphalt mixture due to moisture damage may be cohesive or adhesive. It has been established that failure related to the bitumen mastic is cohesive, whereas failure related to the bitumen-aggregate bond is adhesive. In the latter case, stripping of the bitumen from the aggregate surface is the result of adhesive failure. Five primary disbonding mechanisms have been established to explain the methods associated with moisture damage. The layout of disbonding mechanisms is illustrated in Figure 2.5. Moisture damage is usually the result of combined disbonding mechanisms.

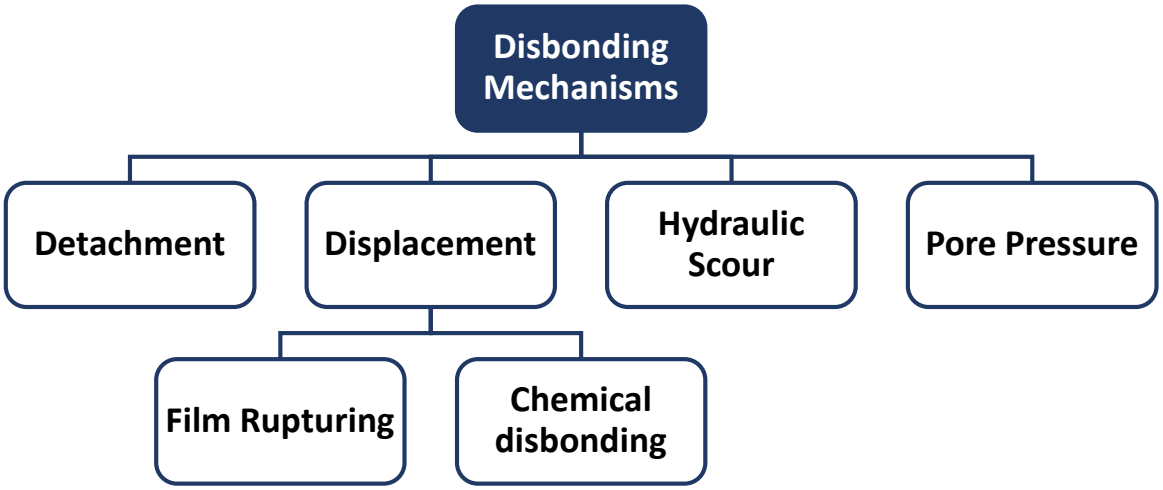

Figure 2. 5 - Disbonding mechanisms related to moisture damage.

2.6.1 DETACHMENT

Majidzadeh and Brovold (1968) described detachment as the separation of the bitumen film from the aggregate surface due to a thin film of water being present between the bitumen-aggregate interface without a clear break in the bitumen film. Detachment in this context is substantiated by the surface energy adhesive theory. As established, the surface energy adhesive theory relates the adhesive bond strength between the bitumen and aggregate to the ability of the bitumen to wet the aggregate's surface. Wettability of aggregates is, therefore, dependent on the surface energy as Majidzadeh and Brovold (1968) stated that increased wettability of aggregates decreases the surface energy. However, water has a significantly greater wetting ability as it satisfies the surface energy demands of the aggregate better than bitumen.

Majidzadeh and Brovold (1996) described a three-phase interface system consisting of aggregate, bitumen and water to explain the surface energy adhesion theory in terms of thermodynamics. They explained that water reduces the surface energy of the aggregate more than bitumen, therefore it produces a much more thermodynamically stable condition. This concept was validated by surface energy measurements done at the Texas A&M University, where it was concluded that energy is released at the bitumen-aggregate interface when the asphalt mixture is subjected to water. This means that the aggregate surface strongly prefers water over bitumen to produce a thermodynamically stable condition. Table 2.1 summarises surface energy of adhesion results for four asphalt mixtures using the method established by Cheng et al. (2002).

Table 2. 1 - The Surface energy of adhesion results from measurements done at Texas A&M University (Little & Jones IV, 2003).

Asphalt Mixtures	Surface Energy of Adhesion (Dry) (J/m^2)	Surface Energy of Adhesion (Wet) (J/m^2)
AAD + Texas Limestone	0.141	-0.067
AAM + Texas Limestone	0.205	-0.031
AAD + Georgia Granite	0.150	-0.048
AAM + Georgia Granite	0.199	-0.030

Columns two and three from Table 2.1 summarise the surface energy of adhesion results for four asphalt mixtures under dry and wet conditions. Notice the significant decrease in surface energy due to the presence of water. The more negative the surface energy in the presence of water, the greater the chance is of detachment of bitumen to occurring (Little & Jones IV, 2003).

The Road Research Laboratory (United Kingdom) suggested in 1962 that bitumen has a relatively low polarity causing weak dispersion forces to form the bond between bitumen and aggregates. Dispersion forces occur due to the intermolecular attraction between molecules. However, water molecules have a high polarity that can disrupt the bitumen-aggregate interface by replacing the bitumen. This theory was established by Cheng et al. (2002) and was the reason for developing a method to measure surface energies and calculating the adhesive bond strengths of asphalt mixtures. Figure 2.6 illustrates that low polarity is exhibited by the bitumen compared to the polarity of water as suggested by the Road Research Laboratory.

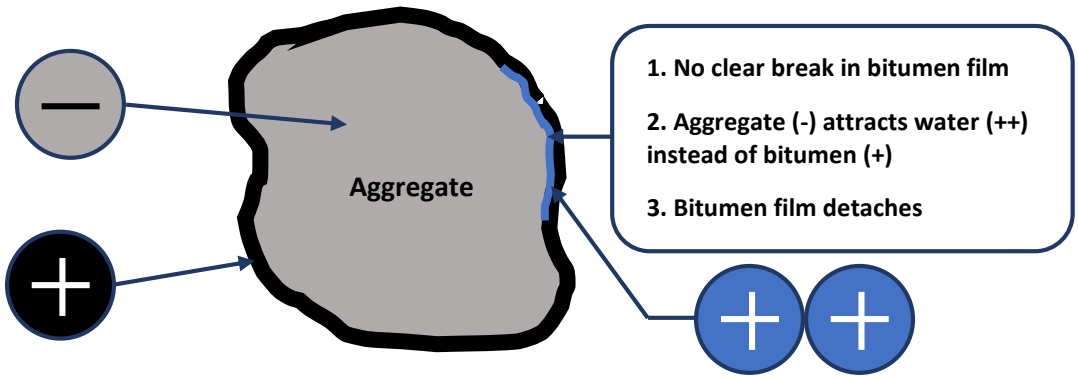

Figure 2. 6 - Illustration of detachment theory as suggested by the Road Research Laboratory.

In *The Shell Bitumen Handbook*, Read and Whiteoak (2003) stated that although the bitumen film fully encapsulates the aggregate, it is easy to peel off when detachment occurs. The detachment process is irreversible and traffic loading accelerates this process due to continuous tension and compression cycles

in the surface voids. Read and Whiteoak (2003) further explained that: "*Suspended dust and silt in the water can act as an abrasive and can accelerate detachment.*"

2.6.2 DISPLACEMENT

Displacement is the result of either a disruption in the bitumen film due to inadequate coating of the aggregate surface with bitumen, or a break in the bitumen film at sharp edges of the aggregate (Tarrer & Wagh, 1991). Moisture penetrates these disruptions or breaks and displaces the bitumen from the aggregate surface.

The displacement theory is also explained according to thermodynamic equilibrium as established for the detachment theory by Majidzadeh and Brovold (1996). Surface energy calculations have shown that the presence of water causes bitumen to retract from the aggregate surface as water produces a more stable thermodynamic condition. Figure 2.7 illustrates the change in the thermodynamic condition of an asphalt mixture in the presence of moisture. Point A represents the thermodynamic condition of the bitumen-aggregate bond in absence of moisture. Once water is added to an asphalt mix the thermodynamic condition slowly shifts to Point B as the displacement of the bitumen film occurs. The difference in Point A and B represents the retraction of the bitumen film.

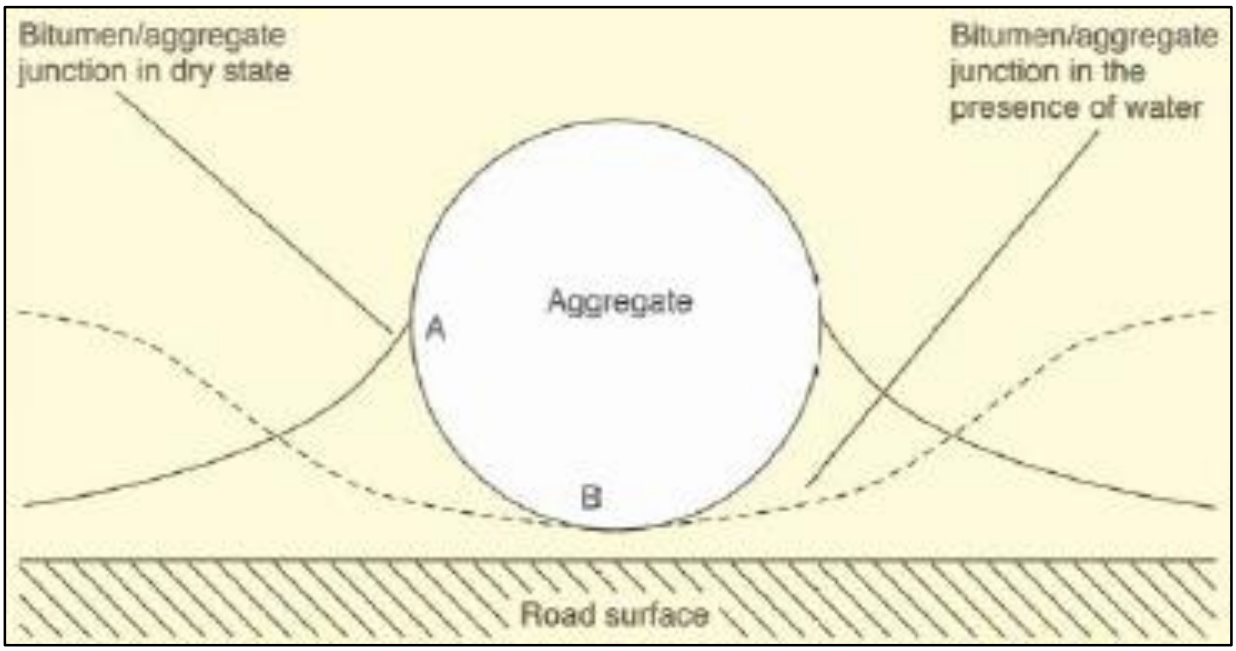

Figure 2. 7 - Retraction of bitumen due to the presence of water to form a thermodynamic stable condition (Read & Whiteoak, 2003).

As established before, the Wilhelmy plate method is used to determine the surface energy of bitumen. The new interface between the bitumen and aggregate at Point B has a new contact angle that needs to

be determined by this method in order to calculate the change in surface energy. The new contact angle is dependent on the bitumen type and its viscosity.

Displacement of the bitumen film may also occur due to changes in the pH-level of water on the aggregate's surface that ingresses through points of disruption or breakage. This phenomenon is known as chemical disbonding. Changes in the pH-level of water cause a build-up of negative polarity on the opposing bitumen and aggregate surfaces. In order to achieve equilibrium, more water is attracted to the aggregate's surface causing displacement of the bitumen there from (Little & Jones IV, 2003). Hughes et al. (1960) and Scott (1978) substantiated this theory by reporting that significant adhesion losses between the bitumen and aggregate occur when the pH of a water solution is increased from 7.0 to 9.0. Kiggundu and Roberts (1988) investigated the pH sensitivity at the bitumen-aggregate interface and concluded that stabilisation of the pH level at this interface increased the bond strength and decreased stripping. Little and Jones (2003) established that the dislodging of amines from the surface of acidic aggregates will not occur at pH-levels between 9 and 10. Although hydrated lime may be used to control the pH-level, a pH-level below 4 dissolves hydrate lime and causes dislodging of amines from the aggregate's surface (Little & Jones IV, 2003).

Displacement of the bitumen film may also occur due to rupturing thereof. Rupturing usually occurs at sharp edges of the aggregate creating a point for moisture to ingresses that displace the bitumen film. Rupturing of the bitumen film may also be caused by the combined action of traffic and environmental effects such as weathering of the asphalt mixture. Once rupturing occurs, the rate of displacement is dependent on the following factors (Greyling, et al., 2015 (1)):

- Bitumen rheology such as the viscosity
- Nature of aggregate surface
- Bitumen film thickness
- Presence of filler material and binder modifying agents

2.6.3 HYDRAULIC SCOUR

Hydraulic scour causes stripping of a saturated pavement surface due to the action of the vehicle tyres. The action of the tyres forces the water on the asphalt surface to be sucked underneath the tyre and pushed into the asphalt layer. Osmosis is a term used to describe the process where solvent fluid molecules pass or diffuse through a semi-permeable membrane from a low to a high solute concentration. Hydraulic scour is related to repetitive osmosis and pullback of water in the aggregate pores. Salt or salt

solutions present in the aggregate pores produce an osmotic pressure gradient which forces the moisture through the bitumen film. The osmotic pressure gradient created by the action of tyres causes water to be sucked through the bitumen film (Fromm, 1974). Figure 2.8 illustrates the process of hydraulic scour.

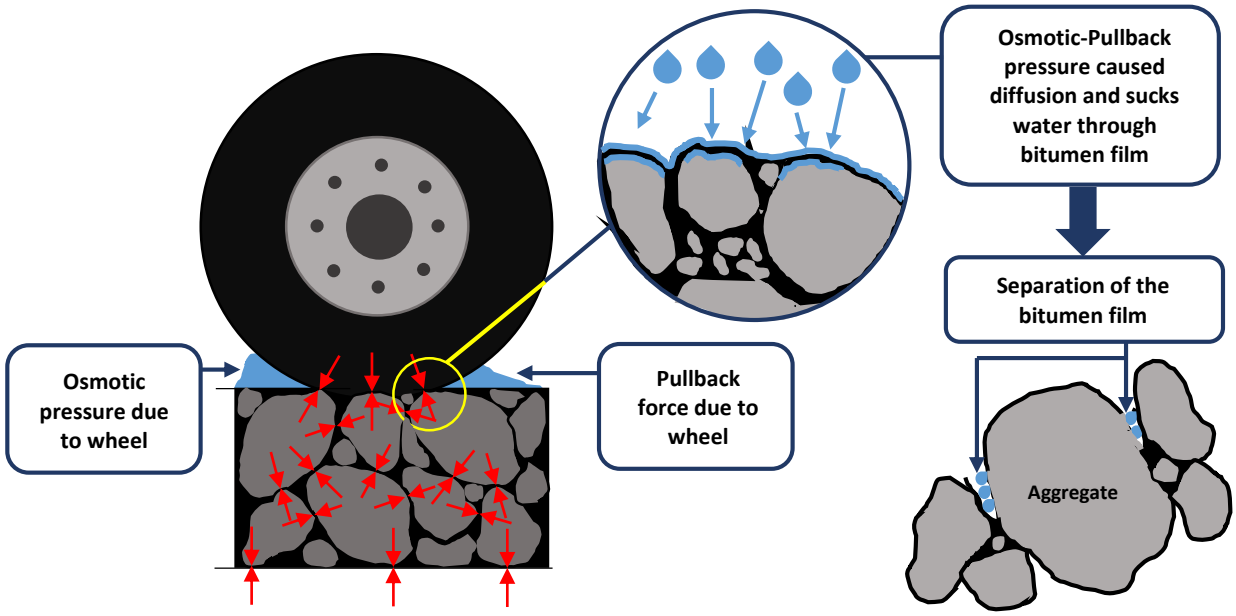

Figure 2. 8 - Diffusion of water through bitumen film due to osmosis.

Cheng et al. (2002) investigated the diffusion of water vapour through bitumen and concluded that the bitumen film is permeable. This substantiated the theory that water can penetrate the bitumen film based on an osmotic process. They further concluded that the bitumen mastic of an asphalt mixture can store considerable amounts of water. The presence of salts on the aggregate's surface and permeability of the bitumen film makes hydraulic scour a plausible disbonding mechanism (Little & Jones IV, 2003).

2.6.4 PORE PRESSURE

Pore pressure damage occurs when water entrapped in the air voids of an asphalt mix is stressed. Pore pressures cumulatively build-up in the asphalt layer due to repetitive traffic loading. Pore pressure build-up damages the bitumen film on the aggregates surface causing the growth of micro-cracks in the bitumen mastic. These cracks provide additional channels for moisture to ingresses, further leading to moisture damage. Figure 2.9 illustrates the distribution traffic induced stresses throughout the asphalt layer. Once the bitumen-aggregate bond is disrupted the water forces separation that causes cracks to form.

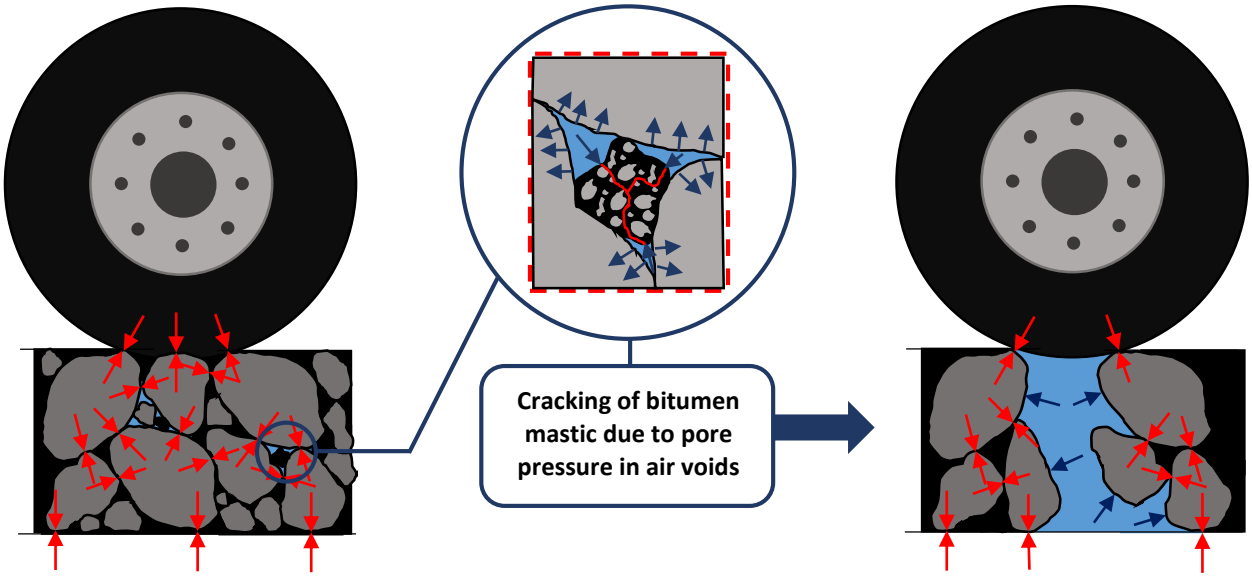

Figure 2. 9 - Distribution of stresses through pavement surface and water induced stresses due to pore pressure.

Pore pressure damage is considered to be important when designing for moisture susceptibility of an asphalt mixture. Cracks formed by pore pressure damage may result in water penetrating the substratum causing erosion as in the case of a granular base layer. The asphalt layer's resistance to permanent deformation and fatigue may be significantly influenced.

Pessimum air void range is a concept described by Terrel and Al-Swailmi (1994). This entails an air void content specification, usually between 8% and 10%, within which most asphalt mixes are compacted too. Terrel and Al-Swailmi (1994) suggested that an air void content within this specification may cause air voids to become saturated with water. Moisture can enter this non-interconnected voids with no escape, thus creating an ideal environment for pore pressure build-up that causes moisture damage. An air void content of 10% or greater results in air voids becoming interconnected, thus providing channels for moisture to flow out under a stress gradient created by traffic loading. An air void content of at least 4 % or lower creates a relatively impermeable asphalt mixture with no interconnected air voids.

2.7 FACTORS INFLUENCING THE BITUMEN-AGGREGATE BOND

Read and Whiteoak (2003) established factors influencing the bitumen-aggregate bond. These factors are divided into four categories, namely: aggregate properties, bitumen properties, mixing properties and external factors. Each category consists of a number of factors influencing the bitumen-aggregate bond. Read and Whiteoak (2003) states 80% of these factors can be controlled during asphalt production and construction. These factors are illustrated in Figure 2.10.

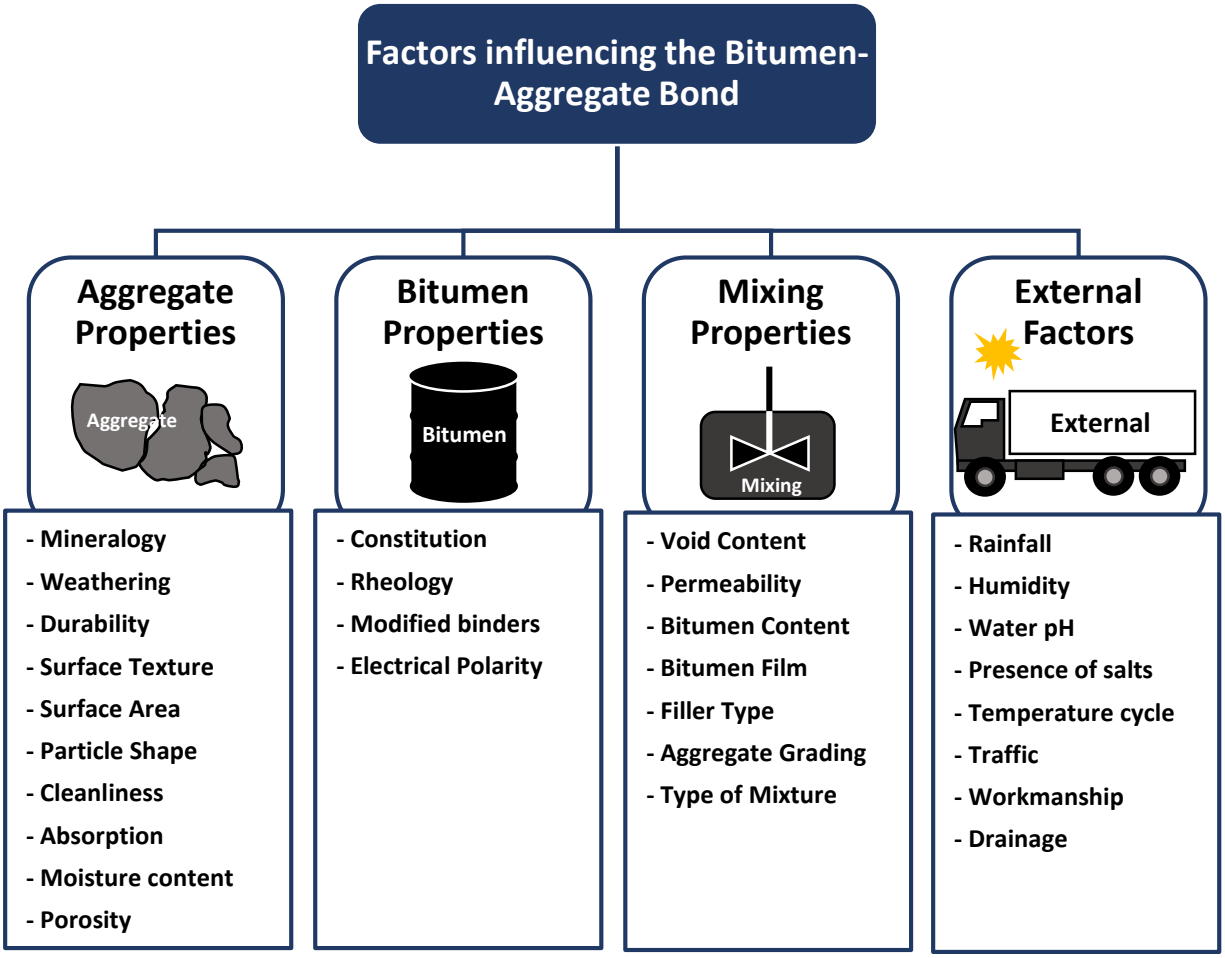

Figure 2. 10 - Factors influencing the bitumen aggregate bond as adapted from Read and Whiteoak (2003).

2.7.1 AGGREGATE PROPERTIES

Aggregate properties have a significant influence on the bitumen-aggregate bond. The moisture susceptibility of asphalt is therefore influenced by these properties. Additional information on aggregates and it availability in South Africa is given in *Appendix A Section A.3*. The following aggregate properties should be considered when selecting the appropriated aggregate for asphalt:

2.7.1.1 Aggregate Mineralogy

Most aggregates are considered to be hydrophilic or oleophobic, meaning that they attract water or repel oil. This property is determined by the mineralogy of the aggregate. Aggregates consisting of a high silicon oxide content, also known as siliceous aggregates, prove to be more difficult to coat with bitumen as the majority of adhesive failures have been associated with these aggregate types. Siliceous aggregates include granites, rhyolites, quartzite and cherts. Read and Whiteoak (2003) suggested the use of basic rocks, such as limestone and basalt, as they improve the moisture susceptibility of asphalt due to good resistance to stripping.

Mineralogy determines the surface charge (also known as surface energy) of aggregates. Should this surface charge be unbalanced, aggregates will attract liquids with an opposite charge to form a neutral state. In the case of bitumen and water, the aggregate will attract the liquid that best satisfies the surface charges. Stripping of the bitumen occurs when water is attracted instead of bitumen (Read & Whiteoak, 2003). Residual moisture on the aggregate surface should be removed before mixing asphalt.

2.7.1.2 Hardness and Toughness (Weathering)

Aggregates need to be hard and tough to withstand abrasive wear during crushing, screening, asphalt mixing, construction and traffic loads. This property of aggregates influences the HMA resistance to permanent deformation as well as providing low-speed skid-resistance due to its micro-texture. Three tests are required to evaluate the hard and toughness of aggregates: Fines Aggregate Crushing Test (FACT), Aggregate Crushing Value (ACV) and Los Angeles Abrasion Test. The South African design specification suggests a minimum FACT value of 160 kN and a maximum ACV value of 25% for HMA base and surfacing. No specification is set for the Los Angeles Abrasion test, but a value of 10% for this test indicates a very hard aggregate, whereas a value of 60% indicates a very soft aggregate (Taute, et al., 2001).

2.7.1.3 Durability and Soundness

An aggregate's ability to resist breakdown and disintegration due to environmental elements is determined by its durability and soundness. Environmental elements such as wetting and drying, as well as freeze and thaw cycles, degrade aggregates over time. It has been suggested that durability of aggregates is determined by both its physical and chemical properties. The soundness of aggregates is tested by performing the sulphate soundness test. The South African specification accepts a sulphate soundness test value of 12% to 20%. No standard test are available to evaluate the durability of aggregates, but it has been suggested that the ethylene glycol soundness test is performed. During this

test, the ethylene glycol breaks down the aggregate by reacting with deleterious clay minerals causing swelling within the aggregate.

2.7.1.4 Surface Texture, Particle Shape and Surface Area

Aggregate texture and shape have significant effects on the workability and stability of HMA. Rough textured aggregate provides good resistance to permanent deformation as it increases the stability of HMA. Rough textured aggregates are, therefore, especially important for heavy traffic roads. Smooth textured aggregates are considered acceptable for roads with low traffic volumes. Workability of asphalt during mixing increases with a reduction in aggregate texture. Coating of smooth textured aggregates with bitumen are much easier, but the bond between the bitumen and aggregate has been proven not being as strong and durable as for rough textured aggregates (Taute, et al., 2001).

When investigating the moisture susceptibility of HMA, it has been suggested that rough textured aggregates should be used for improved adhesion due to mechanical interlocking (Greyling, et al., 2015 (1)). However, Maupin (1982) suggested that rough texture affects the aggregates ability to be properly coated with bitumen, therefore stripping is more severe. The surface area of the aggregate increases as the surface roughness increases. Maupin (1982) further stated that pre-coating of aggregates may prevent this problem.

The angularity of aggregates improves the stability of HMA. This is especially important for roads with heavy traffic volumes. In most cases the angularity of the aggregate is greatly dependent on the crushing process (Taute, et al., 2001). Flat and elongated aggregate shapes should be avoided as slip planes are created and aggregate interlocking reduced (WesTrack Forensic Team, 2001).

Test methods in use to evaluate the aggregate texture and shape includes: Flakiness Index Test, Particle Index Test, Polished Stone Value (PSV) and Fractured Faces Test.

2.7.1.5 Cleanliness (Presence of dust)

The absence of deleterious and foreign materials in aggregate fractions are referred to as cleanliness. Deleterious and foreign materials include: clay on the aggregate surface, shale, vegetation and dust from crushing (Taute, et al., 2001). Aggregates with high amounts of surface dust increase the surface area to be coated with bitumen. This decreases the wetting potential of larger aggregate fractions causing poor bitumen-aggregate bonds to form (Greyling, et al., 2015 (1)). Castan (1968) stated that dust on the surface of the aggregates promotes stripping as it prevents sufficient bonding to form between the bitumen and

aggregate. Castan (1968) explained that small channels form between the bitumen coated dust and aggregate surface thus providing a pathway for water to penetrate.

2.7.1.6 Porosity and Absorption

Porosity describes the void spaces located in aggregates that can be filled with a liquid. The porosity is calculated as a fraction by dividing the volume of voids by the total volume of the aggregate. Absorption describes the filling of the porous voids on the aggregate's surface with bitumen. Increased porosity of aggregates will increase the absorption of bitumen on the aggregate's surface, thus improving the bond strength between the bitumen and aggregates.

The influence of porosity of aggregates on the absorption of bitumen was investigated by Jeon and Curtis (1990). They explained that the surface of porous aggregates may cause separation of the high and low molecular weight fractions of the bitumen. Curtis et al. (1989) stated that during absorption bitumen on the aggregate's surface becomes hard and brittle, thus leading to the formation of a weak boundary layer susceptible to moisture damage.

2.7.1.7 Variability in source

Variability in aggregate quality is expected from quarries due to the geology of the quarried materials as well as the crushing and screening processes. When narrow aggregate gradation envelopes are required, the costs of production may increase as additional processing are required (Taute, et al., 2001).

2.7.2 BITUMEN PROPERTIES

2.7.2.1 Constituent of bitumen

Bitumen is a chemical mixture consisting of hydrocarbon molecules and small amounts of functional groups comprising of nitrogen, sulphur, oxygen and some metals molecules. Bitumen is a by-product from the crude oil distilling process. The proportions of these hydrocarbon molecules and functional groups within the bitumen are determined by the crude oil source, of which the latter is variable and contributing to bitumen complexity. However, bitumen can be separated into two broader groups called asphaltenes and maltenes. The maltenes group is further subdivided into resins, aromatics and saturates (Greyling, 2012). The breakdown of bitumen is illustrated in Figure 2.11.

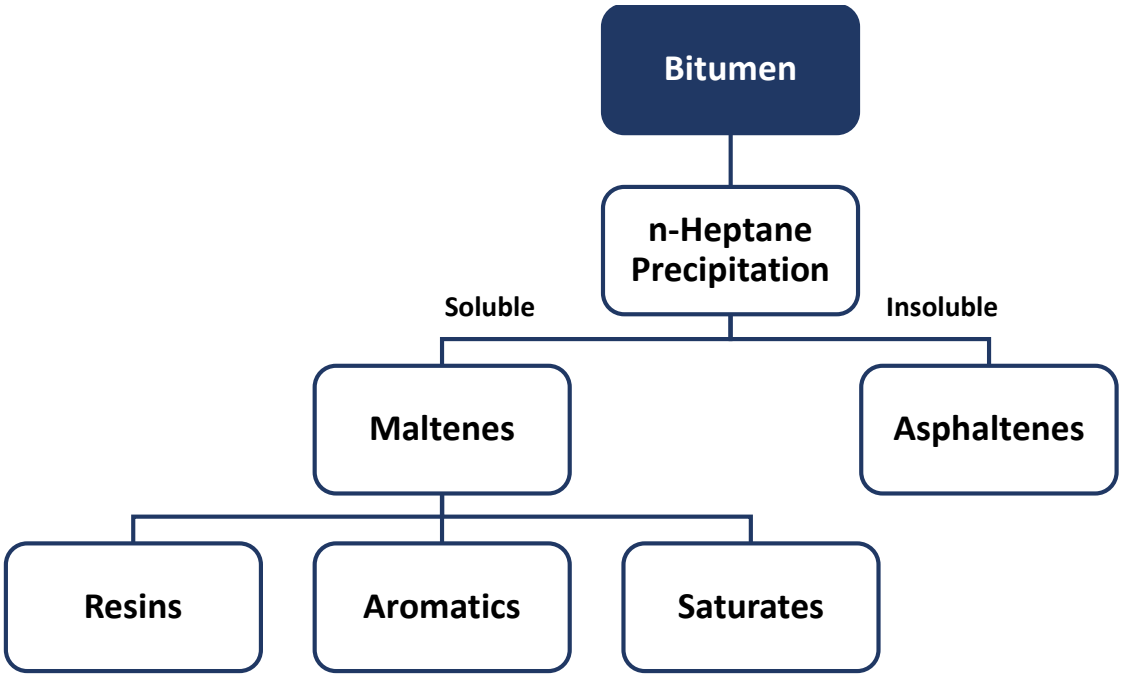

Figure 2. 11 - Bitumen composition based on broader groups (Read & Whiteoak, 2003).

The *Shell Bitumen Handbook* (Read & Whiteoak, 2003) provides a detailed description of these broader groups. Therefore, only a brief description of each broader group is presented:

- **Asphaltenes** – Asphaltenes are the insoluble precipitate of n-heptane and consist of black and brown amorphous carbon and hydrogen solids. In addition, this broader group also consists of nitrogen, sulphur and oxygen. It constitutes 5% to 25% of the bitumen and is considered highly polar. Asphaltenes determine the hardness as well as the viscosity of bitumen.
- **Resins (Maltenes)** – Resins are part of the maltenes broader group originating from the soluble n-heptane precipitate. Consisting of oxygen, carbon and hydrogen, this broader group is dark brown in colour and have a strong polarity which makes it strongly adhesive.
- **Aromatics (Maltenes)** – Aromatics are viscous liquids dark brown in colour and consist of non-polar carbon chains. It constitutes 40% to 60% of bitumen.
- **Saturates (Maltenes)** – Saturates are viscous oils, white in colour and constitute 5% to 20% of bitumen. Saturates are also non-polar. It consists of aliphatic hydrocarbons with alkyl-naphthenes saturates to form straight and branch chains.

2.7.2.2 Rheology of bitumen

Rheology involves studying the deformation behaviour as well as the flow of materials. Bitumen is regarded as a visco-elastic material, therefore its behaviour is influenced by temperature and loading

time. When subjected to long loading times or high temperature, bitumen exhibits viscous behaviour resulting in permanent deformation. During short loading times or low temperatures, bitumen exhibits elastic behaviour resulting in recoverable deformation (Asphalt Academy-TG1, 2007).

The constituents of bitumen determine its rheology as shown by systematic blending of the broader groups separated from the bitumen. Read and Whiteoak (2003) explained that by holding the asphaltenes constant, the following effects are expected on the bitumen rheology:

- **Increasing Aromatics** - Increasing the aromatics content while keeping the content of saturates and resins constant has shown little effect on the rheology of bitumen.
- **Increasing Saturates –** Increasing the saturates content while keeping the aromatics and resins content constant have shown to soften the bitumen.
- **Increasing Resins –** Increasing the resins content while keeping the aromatics and saturates content constant has shown to increase the viscosity and reducing the shear susceptibility and penetration index of the bitumen.

Rheology of bitumens is usually tested by performing penetration, softening point and viscosity tests at various temperatures. These tests are important to conduct in order to determine required mixing and compaction temperature and viscosity. Greyling et al. (2015) suggested the following rheological properties have shown to increase bitumen adhesion and cohesion against chemical attack:

- Bitumen with low viscosities ranging from 200-500 mPa.s at asphalt mixing temperatures ranging from 150-180^{o}C. The low viscosity promotes coating of the aggregate resulting in a thicker bitumen film thickness.
- Bitumen exhibiting high viscosity at service temperatures ranging from 0 to 60^{o}C has shown to improve adhesion and cohesion. At these temperatures, the increased viscosity promotes the asphalt mix stiffness due to elastic material behaviour.

The three important stages of bitumen's life as a binder include: coating of the aggregate, compaction of the asphalt mixture and the service performance of the compacted asphalt layer. The performance of bitumen at these stages is viscosity or stiffness-related. One of the most important performance relationships for bitumen is that of viscosity change with a change in temperature as illustrated in Figure 2.12 (Hunter, 1994).

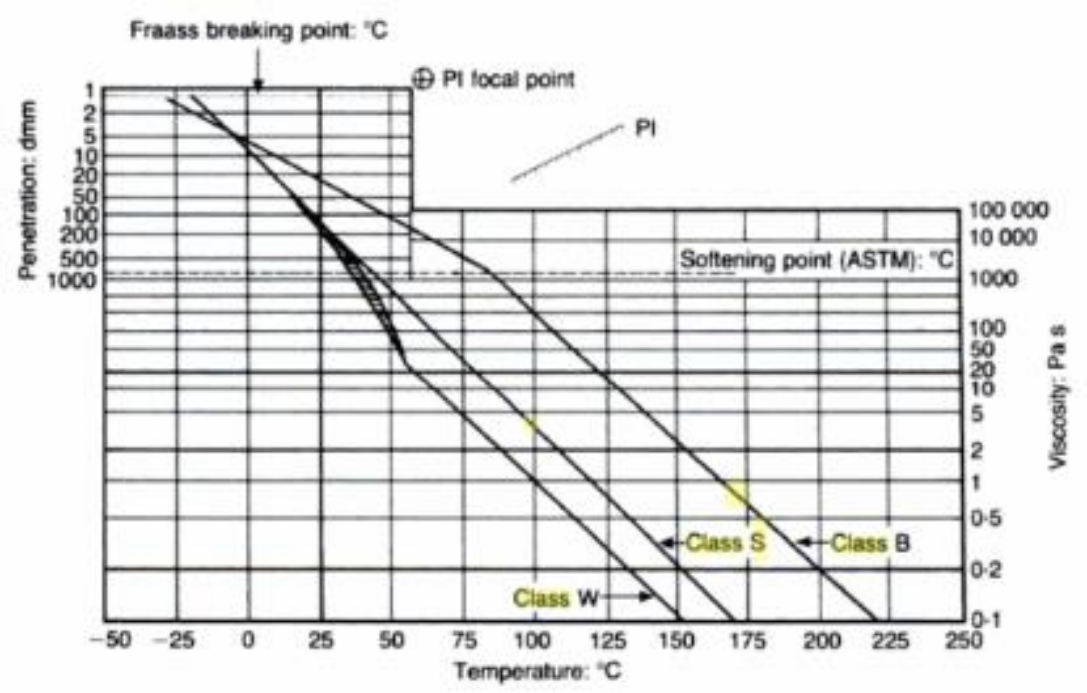

Figure 2. 12 - Heukenlom bitumen test data sheet (Hunter, 1994).

Figure 2.12 also illustrates the three bitumen classification classes (Hunter, 1994):

- **Class S** is used for road construction purposes (also known as a straight line). Their test data can be presented by a linear line on the Heukenlom bitumen test data sheet as illustrated in Figure 2.12. These bitumens are produced under vacuum without modifying its chemical structure. Class S bitumen is the basis for producing penetration grade bitumen.
- **Class W** consist of bitumens classified with a relatively high wax content. Due to the wax content, these bitumens will exhibit less viscous material behaviour during in-service temperatures compared to a Class S bitumen.
- **Class B** bitumen, also known as blown bitumen, are air-rectified during production. Due to air-rectification, these bitumens have an oxidized chemical structure. Class B bitumen require significantly higher temperatures to ensure workability when compared to Class S bitumens. It is not considered suitable for road construction.

Rheological properties of the bitumen to prevent chemical attack, are seldom achieved with Class S bitumen as they their deviate from the ideal viscosities and adhesion capabilities as suggested by Greyling et al. (2015). However, this can be overcome through bitumen modification of penetration grade bitumen, which is predominately done in the road construction industry in South Africa. Determining the optimum mixing and compaction temperatures at viscosities of 170 and 280 Pa.s are not applicable to modified

binders. Unrealistically high temperatures are obtained at these viscosities, which are related to a phenomenon known as shear thinning that is experienced with these type of binders. Shear thinning relates to a reduction in the viscosity of a liquid as the shear rate increases (Hunter, et al., 2015). Modified bitumen does not display Newtonian behaviour above its softening point, therefore, using the Brookfield viscosity test at one shear rate may not be appropriate (Asphalt Academy-TG1, 2007).

2.7.2.3 Modified binders

Present day factors such as increased traffic volumes, increased truck loads and increased tyre pressures have a significant influence on the performance of HMA pavements. Due to the strain these factors place on HMA performance, premature failure is the result in most cases. Engineers are therefore required to investigate and improve the engineering properties of HMA. Unmodified binders have in most cases been found to be insufficient to satisfy the following HMA performance requirements (Hunter & et al., 2000):

- Sufficient flexibility to prevent fatigue cracking caused by traffic-induced stresses
- Sufficient adhesive bond between the bitumen and aggregate
- Sufficient in-service temperature performance range
- Sufficient cohesion developed in the bitumen mastic

Modifiers are used to improve the engineering properties of bitumen as well as the performance of pavement materials such as hot-mix asphalt, surface seals and bitumen stabilised materials (BSMs). In South Africa the *Asphalt Academy Technical Guidelines 1: The use of Modified Bituminous Binders in Road Construction (2007)* provide assistance with the modification of bitumen for road construction purposes. Modified binders provide benefits compared to conventional bitumen, but are not solutions to all situations. The following benefits are associated with modified bitumen (Asphalt Academy-TG1, 2007):

- Improved consistency
- Reduced temperature susceptibility
- Improved stiffness and cohesion
- Improved flexibility, resilience and toughness
- Improved binder aggregate adhesion
- Improved resistance to in-service ageing

Although various types of binder modifiers are available, this research focusses on elastomer modifiers, plastomer modifiers and anti-stripping agents as modifier groups. The modifier group depends on the type of modifier used in the modification process and Figure 2.13 presents these classification groups as well as the type of modifiers associated with each group.

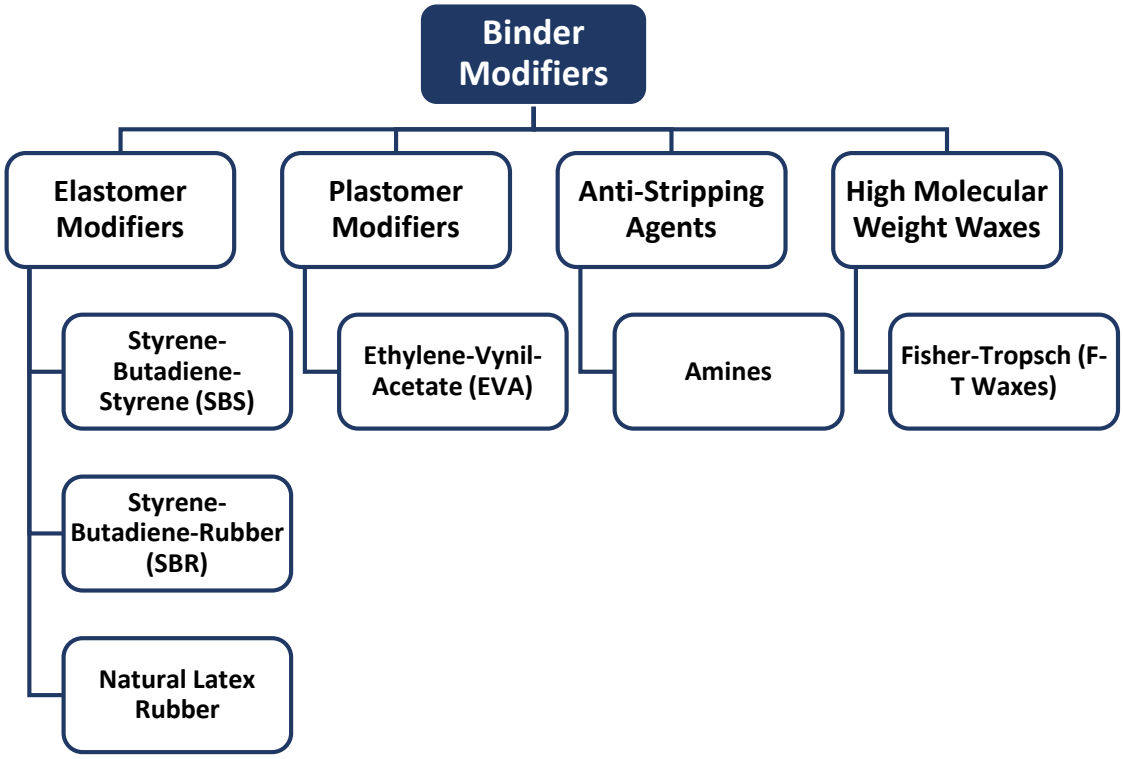

Figure 2. 13 - Binder modifiers type and classification groups.

Elastomer modifiers

Elastomer modifiers promote the elastic behaviour of bitumen. The bitumen properties have been found to improve significantly with modification with elastomeric modifiers (Hunter & et al., 2000). The most common types of elastomer modifiers used in South Africa are Styrene-Butadiene-Styrene (SBS), Styrene-Butadiene-Rubber (SBR) and natural rubber latex.

SBS modifier is absorbed by the maltenes broad group in the bitumen and improves the elastic recovery of the bitumen. The concentration of SBS influences the properties of the modified bitumen. At concentrations ranging from 3% to 4% only fragmented molecular networks are formed. However, at concentrations ranging from 4% to 6%, the softening point of the bitumen is significantly increased as continuous molecular networks are formed. The molecular network improves the elasticity of the bitumen, therefore improving the asphalt mixture's resistance to permanent deformation. At low

temperatures, SBS modified binders exhibit improved flexibility and resistance to cracking compared to conventional binders (Asphalt Academy-TG1, 2007). Additional information on SBS modified binders is given in *Appendix A Section A.2.3.1*.

SBR modifier can be used for modifying hot and emulsions. However, SBR modifier is predominantly used in emulsions where it improves adhesive properties, elasticity and flexibility. SBR modifier used in hot bituminous binders reduces its resistance to permanent deformation, fatigue and cracking and is therefore not recommended for improving the moisture susceptibility of HMA (Asphalt Academy-TG1, 2007).

Natural rubber latex increases the elasticity of bitumen. It is predominantly used for modification of cold bituminous binders as it is extremely sensitive to temperature. However, natural rubber latex modified binders have been used for producing porous asphalt wearing courses. This modification improved the durability of the asphalt mixture. Additional effects of this modification include increased viscosity and bitumen film thickness as well as a reduction in binder drainage (Douries, 2004).

Plastomer modifiers

Thermoplastic polymers, also known as plastomers, have a similar although less dramatic temperature susceptibility to bitumen. They exhibit low viscous behaviour at high temperatures and high viscous behaviour at low temperatures. Modifications of bitumen using plastomers tend to have a greater influence on the penetration of bitumen than the softening point. As the concentration of a plastomer modifier in the bitumen increases, the softening point of the bitumen will be increased, however, this is only true until a maximum softening point is reached. No increase in the softening point with an increase in polymer concentration occurs beyond the maximum softening point (Douries, 2004).

King et al (1992) states asphalt pavement failures related to the binder may include poor resistance to permanent deformation as the binder exhibits low stiffness at high temperatures, poor resistance to cracking due to brittle behaviour of the binder at low temperatures, disbonding of bitumen from the aggregate surface due to moisture, bitumen oxidation and traffic loading.

The most common used plastomer modifiers in South Africa is EVA. EVA improves the stiffness of HMA, therefore it improves the asphalt mixture's resistance to permanent deformation. In addition to improving the stiffness of HMA, EVA also improves the workability of an asphalt mixture at low temperatures (Hunter & et al., 2000). It has been found that plastomer modified binders are more tough and rigid compared to

elastomer modified binders (Douries, 2004). Additional information on EVA modified binders is given in *Appendix A Section A.2.3.3*.

Anti-stripping agents

Amine, such as polyamine, is used as an anti-stripping agent which increases Hot-Mix Asphalt's moisture susceptibility. Amines are mixed with the bitumen and are capable of chemically modifying the tension between the bitumen and aggregate surfaces. Amines consist of a hydrocarbon chain that interacts with the bitumen. In the presence of water, the amine is ionized to form an amine ion ($R\text{-}NH_3$) that is positively charged. Fatty amines react with the aggregate surface while its hydrocarbon chain is fixed to the bitumen. In case of hydrophobic or acidic aggregates, these hydrocarbon chains improve the adhesion with the hydrophobic bitumen surface by acting as a bridge between the two components of asphalt (Porubszky, et al., 1969).

An anti-stripping-agent known as ZycoTherm® has shown to improve the moisture susceptibility of an asphalt mixture. This anti-stripping agent improves the moisture susceptibility of an asphalt mixture by producing a strong chemical bond between the bitumen and aggregate surfaces which reduces stripping of the bitumen. It has been found that ZycoTherm® improves the wetting ability of binders which results in complete coating of fines in a short period of time. It has also been found that better mechanical interlocking is achieved in asphalt mixtures with ZycoTherm® anti-stripping agent (Zydex Industries, 2015(2)).

A boil test was performed on asphalt mixtures with Zycotherm® anti-stripping agent to determine stripping of the bitumen when subjected to grey water. The asphalt mixtures tested were a control mixture, a mixture with 1% ZycoTherm anti-stripping agent and a mixture with SBS and 1% ZycoTherm® anti-stripping agent. The grey water solution consisted of a 4% salt content and a 1% washing detergent content. During the boil test, complete disintegration of the control sample occurred after 3 hours. Meanwhile, the asphalt mixtures with ZycoTherm® anti-stripping agent showed no signs of stripping. After 6 hours of testing the asphalt mixture with SBS and 1% ZycoTherm® anti-stripping agent showed a bitumen coating retention of 85 percent (Zydex Industries, 2015(1)).

Anti-stripping agents are produced to improve an asphalt mixture's resistance to stripping of the bitumen and may provide an effective solution to improve the asphalt mixture's resistance against grey water.

High Molecular Weight Waxes

The use of waxes is not generally considered by practitioners. However, there is a difference in the waxes derived from crude oil and the high molecular weight waxes which are derived from the Fischer-Tropsch (F-T) process and used for bitumen modification (Asphalt Academy-TG1, 2007).

F-T waxes consist of long carbon alkane chains and originate from the coal gasification process. Chain lengths for F-T waxes vary from 40 to 100 carbon atoms as opposed to the crude oil waxes which vary from 20 to 40 carbon atoms. The purpose of F-T waxes modifications is to reduce the viscosity of the modified binder during mixing and compaction temperatures without having a negative effect on the characteristics of the bitumen at low temperatures. F-T wax modified bitumen has shown good adhesive properties and stiffness at high operating temperatures. At low operating temperatures the resistance to cracking is also satisfied (Asphalt Academy-TG1, 2007).

Sasobit® is a wax based additive developed by Sasol and is used to modify bitumen by increasing its workability. An increase in workability is the result of a decrease in viscosity which improves the level of compaction of an asphalt mixture (Prowell & Hurley, 2005). Improving the level of compaction will improve the volumetric properties of an asphalt mixture and make it more susceptible to moisture. Additional information on F-T wax modified binders is given in *Appendix A Section A.2.3.2*.

2.7.2.4 Electrical Polarity

The electrical polarity of bitumen is determined by asphaltenes and resins broader groups. Both these constituents are highly polar and responsible for adhesive bonding with the aggregate. It has been established that the polarity of water is greater than that of bitumen and that aggregates will attract the liquid satisfying their surface polarity the best (Read & Whiteoak, 2003).

2.7.3 MIXING PROPERTIES

2.7.3.1 Volumetric properties

The volumetric properties of an asphalt mixture are dependent on aggregate grading as well as the compactibility of the mixture. The volumetric properties determine the permeability of the asphalt mixture and the moisture susceptibility thereof is controlled by these properties. Figure 2.14 illustrates the interaction between the air voids, bitumen and aggregates of an asphalt mixture.

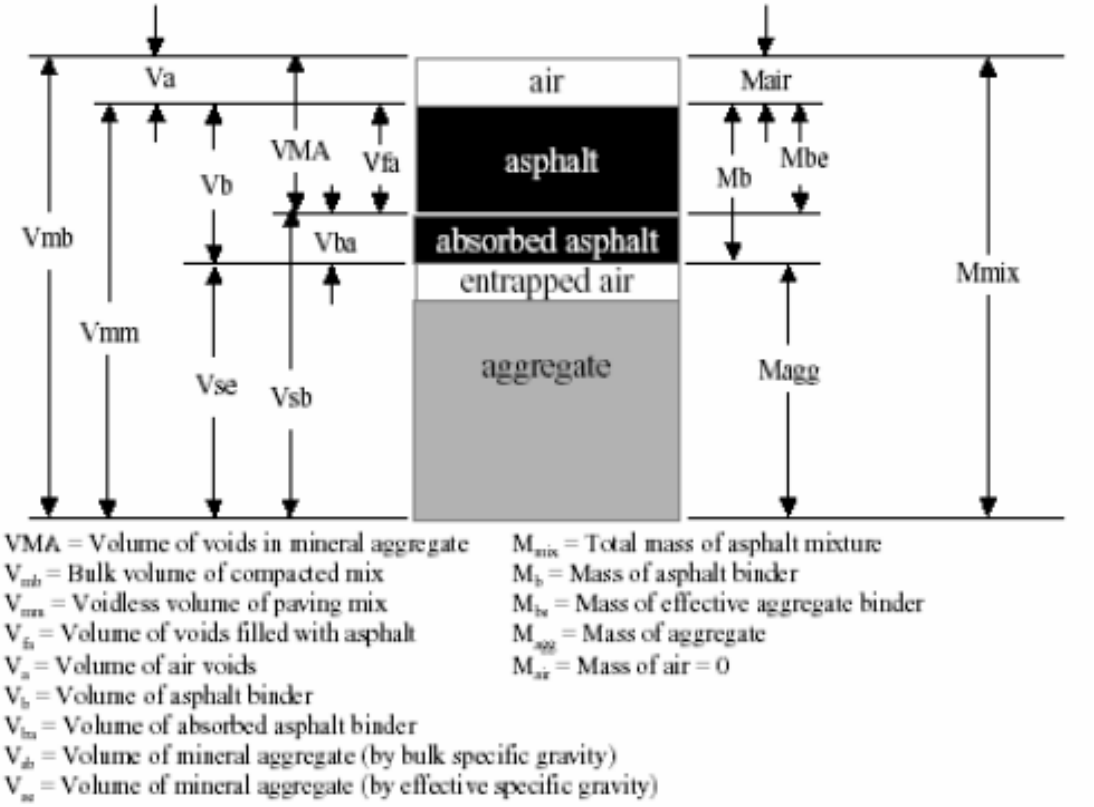

Figure 2. 14 - Volumetric components of an asphalt mixture (Hunner & Brown,

The required volumetric properties in an asphalt mixture include the voids in the mix (VIM), voids in the mineral aggregate (VMA) and voids filled with binder (VFB) (Roberts, et al., 1991). These properties are defined as follows (Douries, 2004):

- **Voids in the Mix (VIM)** – The VIM measures the total volume of air pockets located between the coated aggregate particles of a compacted asphalt mixture and is expressed as a percentage of the total volume of the compacted asphalt mixture.
- **Voids in the Mineral Aggregate (VMA)** – The VMA measures the volume intergranular void spaces between the aggregate particles of an asphalt mixture. The percentage VMA is calculated from the sum of the volumes of air voids and binder not absorbed by aggregates, divided by the total volume of the compacted asphalt mixture.
- **Voids Filled with Binder (VFB)** – The VFB is calculated as the percentage VMA volume that is filled with binder, divided by the total volume VMA of the compacted asphalt mixture.

The VIM is directly related to the VMA while indirectly related to the VFB. Decreasing the VIM of an asphalt mixture will also decrease the VMA, but the VFB of the mixture will increase. As established the moisture susceptibility is determined by the volumetric properties of an asphalt mixture. Decreasing the air void content decreases the permeability of an asphalt mixture. The air void content can be decreased by either increasing the bitumen content or increasing the extent to which the mixture is compacted. However, the extent of compaction is dependent on the aggregate grading of the asphalt mixture (Douries, 2004).

2.7.3.2 Bitumen Content and Film Thickness

Increasing the binder content of an asphalt mixture will improve its moisture susceptibility. As the moisture susceptibility is dependent on air void content and permeability, increasing the binder content will decrease both of these properties. The bitumen film thickness will also increase with an increase in binder content, therefore improving the asphalt mixture's resistance against disbonding mechanisms (Read & Whiteoak, 2003).

Furthermore, by increasing the binder content too much may have a significant influence the volumetric properties of an asphalt mixture. For example, from Figure 2.14 it is clear that an increase in the binder content will lead to a decrease in the VMA of an asphalt mixture. However, the VMA will only decrease up to a certain point as the binder content of the asphalt mixture is increased. Once the VMA reaches its minimum, the VIM will start to fill with binder. Should the VIM become overfilled with binder, the aggregates will be forced apart during compaction. This is due to the binder acting as a lubricant, therefore reducing the contact pressure points between the aggregates. The shear resistance of such a mixture will be very poor as the bitumen carries the traffic load and not the aggregate skeleton. Large permanent shear strains will develop in such an asphalt mixture causing permanent deformation and bleeding (Douries, 2004).

An asphalt mixture is usually constructed with the VFB ranging from 50% to 70%. However, under traffic, the asphalt mixture densifies over time leading to an increase in the VFB of the mixture. Once the VFB reaches 80% to 85%, permanent deformation will occur as the asphalt mixture becomes unstable (Douries, 2004). As the binder content of an asphalt mixture increase, so will the VFB. This will produce an asphalt mixture susceptible to permanent deformation at an early stage of its service life. Selecting the appropriate binder content to improve the moisture susceptibility of an asphalt mixture should, therefore, involve satisfying the volumetric specifications of the mixture.

2.7.3.3 Filler Material Type

Material passing through the 0.075 mm-sieve is regarded as filler material. Filler material stiffens the bitumen mastic and therefore increases the stability of the mix. The addition of fillers in asphalt mixes also influence volumetric properties as they act as void-filling materials. In the correct amounts, filler materials improve the tensile strength and toughness of an asphalt mixture by providing shear resistance which is especially relevant to sand-skeleton asphalt mixtures.

Filler materials are classified as active or inert. Active fillers include hydrated lime and Portland cement. Inert fillers include baghouse fines, limestone dust and fly ash. Additional information on filler materials is given in *Appendix A Section A.3.3*. Hydrated lime has shown to improve the adhesion of asphalt mixes and is added in quantities ranging from 1% to 3% of an asphalt mixture. The reaction of hydrated lime in asphalt mixes was investigated by Plancher et al. (1977) and Petersen et al. (1987) where the following were concluded:

- **Asphalt mixes without hydrated lime** – Silicon hydroxide (SiOH) compounds on the aggregate's surface reacts with carboxylic acid ($COOH^-$) to form hydrogen bonds and adhesion between the bitumen and aggregate. In the presence of water, these hydrogen bonds dissociate and react with the water (H_20) to form new hydrogen bonds. The hydrogen bond between carboxylic acid ($COOH^-$) and water (H_20) is therefore preferred over the one formed by the carboxylic acid ($COOH^-$) and silicon hydroxides (SiOH). Detachment of the bitumen film is the result of this reaction (Plancher, et al., 1977).
- **Addition of hydrated lime** – The addition of hydrated lime leads to partial dissociation of the $Ca(OH)_2$ molecules resulting in calcium ions (Ca^{2+}) to react with the carboxylic acids ($COOH^-$) of bitumen. Petersen et al. (1987) further explain that this reaction creates insoluble calcium organic salts to form. Petersen et al. (1987) also stated that the remaining silicon hydroxides (SiOH) react with the nitrogen (N) components of the bitumen to form strong adhesive bonds.

The viscosity of the bitumen mastic is influenced by too much filler material which results in poor compaction of the asphalt layer. A filler-binder ratio has been developed to assist in selecting the appropriate filler content. Sabita Manual 35/TRH8 (2016) suggested a binder-filler ratio of not more than 1.5 for thin asphalt layers and not more than 1.6 for thick asphalt bases.

2.7.3.4 Type of Mixture and Aggregate Grading

The HMA mixture type is dependent on performance requirements. The aggregate packing characteristics of HMA mixture influence these performance requirements and therefore determine the HMA mixture type. The types of HMA mixtures are classified into two categories according to mix gradations (Sabita Manual 35/TRH8, 2016):

- **Sand-Skeleton Mixes** – In sand-skeleton asphalt mixtures the traffic loads are mainly transferred to the finer aggregate fractions, with the coarser aggregate fractions providing bulk to the mixture. No contact exists between the coarser aggregate fractions of a sand-skeleton asphalt mixture as it is enclosed by the finer aggregate fractions that provide the stability of the mixture. Sand-skeleton mixes are dense and are used for low to high traffic volume roads. Types of sand-skeleton asphalt mixtures are medium/fine continuous graded asphalt, semi-gap graded asphalt and gap-graded asphalt.
- **Stone-Skeleton Mixes** – In stone-skeleton mixes the traffic loads are mainly transferred to a matrix of coarser aggregate fractions with the finer aggregate fractions filling the spaces in-between. Selecting the correct grading is important to ensure that contact between the coarser aggregate fractions exists from which the stability of the mixture is derived. This type of asphalt mixture is predominately used for high traffic volume situations as it provides good resistance to permanent deformation, skid resistance and noise reduction.

The volumetric properties of HMA are determined by the aggregate gradation selected for the asphalt mixture. The VMA and VIM are greatly influenced by small changes in the aggregate characteristics (Douries, 2004). Factors such as density and aggregate surface are related to aggregate gradation and have a significant influence on the VMA as stated by Chadbourn et al. (2000).

Nijboer developed the 0.45 power grading chart in 1943 when he investigated the densities of gravel and crushed aggregates. The 0.45 power grading chart plots the log passing percentage versus the log particle size and consists of a straight line, known as the maximum density line, through the origin at an angle of 45 degrees (Douries, 2004). Chadbourn et al. (2000) explained that by moving the aggregate gradation away from the maximum density line, the VMA of an asphalt mixture increase for fine and coarse gradations. Figure 2.15 illustrates the 0.45 gradation chart developed by Nijboer.

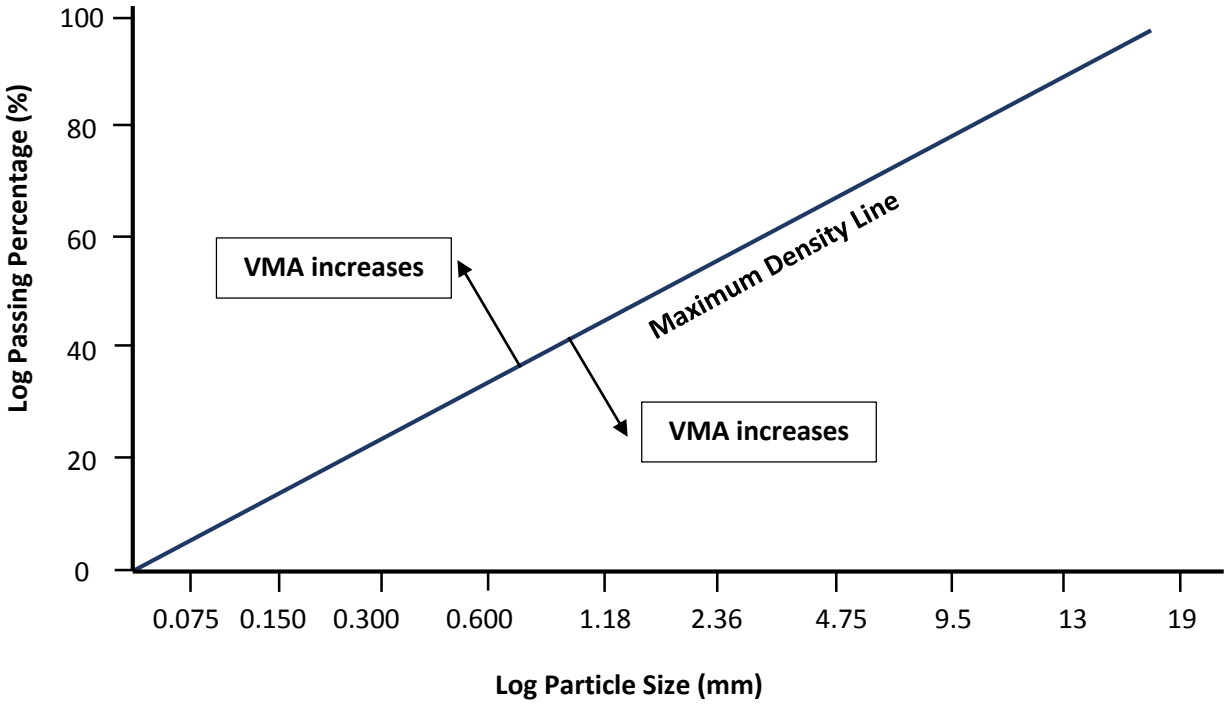

Figure 2. 15 - Nijboer's 0.45 power grading chart adapted by Douries (2004).

From the 0.45 power grading chart, Nijboer derived the 0.45 grading exponent at which the maximum packing density of aggregates is achieved. This means that the VMA and the VIM of an asphalt mixture will be at its lowest for a gradation exponent of 0.45 (Douries, 2004).

An asphalt mixture with low VMA and VIM will produce a mixture with low permeability, therefore the moisture susceptibility of such a mixture will be significant. However, asphalt mixtures with low VMA and VIM have the potential for developing permanent deformation and bleeding. A balance should, therefore, be established between the binder and volumetric properties of an asphalt mixture to prevent poor performance and durability (Douries, 2004). From this section, it is clear that the asphalt mixture type as well as the aggregate grading have a significant influence on the moisture susceptibility of the mixture and should therefore be considered carefully.

2.7.4 EXTERNAL FACTORS

2.7.4.1 Rainfall and Humidity

Asphalt pavements in areas with high rainfall and water tables experience greater amounts of moisture damage and stripping of the bitumen. In the United States of America (USA) significant amounts of

moisture related problems occur in the eastern and south-eastern part of the Texas State. These problems are related to the high rainfall and high water tables found in these parts of the state (Ruth, 1984). Taute et al. (2001) stated that rainfall may significantly influence aggregate, filler and bitumen selections required for the design of high moisture susceptible asphalt mixtures.

Humidity influences the rate at which water evaporates from the asphalt surface. Asphalt pavements in areas of high humidity tend to have longer contact time between water and the asphalt, making these pavements more susceptible to moisture (Greyling, et al., 2015 (1)).

2.7.4.2 Water pH and Presence of Salts

It has been established that the pH-level of water may have a significant effect on the stripping resistance of an asphalt mixture. Chemical disbonding is the result of changes in the pH-level of water. Stabilisation of the pH-level at the bitumen-aggregate interface is required to prevent chemical disbonding from occurring (Kiggundu & Roberts, 1988).

The presence of salts in an asphalt mixture is determined by the mineralogy of the aggregate. These salts in the presence of moisture may form a solution in the aggregate pores which produces an osmotic pressure gradient. Pressure forces moisture through the bitumen film which leads to separation of the bitumen film from the aggregate surface (Fromm, 1974).

2.7.4.3 Temperature Cycles

Freeze-thaw is a concept related to sudden changes in the temperature of the environment. Although not so significant in South Africa, countries with very low temperatures, especially during winter months, are susceptible to freeze-thaw cycles in asphalt pavements. As asphalt pavements age, small cracks will eventually develop in the asphalt layer. Without proper maintenance, water ingresses through these cracks and freezes during very low environmental temperatures. The frozen water expands and widens these cracks to cause significant moisture damage. As these cracks widen, more water can ingresses which leads to premature failure of the asphalt layer.

Ageing of HMA pavements is mostly related to hardening of the bitumen due to high temperatures and the presence of air during storage (Jenkins & Twagira, 2008). Further ageing takes place over the service life of the asphalt pavement due to environmental factors. At low temperatures bitumen is especially susceptible to ageing (Taute, et al., 2001).

2.7.4.4 Traffic

Walubita (2000) established that a reduction in stiffness, cracking, stripping and fatigue loss may be expected when an asphalt surface is subjected to trafficking under wet conditions. He explained that the fatigue life is significantly reduced for asphalt materials susceptible to moisture under wet trafficking and light axle loads with high tyre pressures of 690 kPa.

Little and Jones IV (2003) stated that the mechanical action of traffic during wet conditions may cause sodium carboxylates in the bitumen to act as a surfactant, due to a reduction of the bitumen's surface tension. This causes the bitumen to be 'washed' away from the aggregate surface.

2.7.4.5 Workmanship

Poor joint construction and compaction of an asphalt mixture have significant influences on the permeability of the mixture. The degree of compaction determines whether the air voids in the asphalt mixture are interconnected or not. Santucci et al. (1985) explained that a high air void content causes poor strength retaining and rapid hardening of the asphalt mixture. Therefore the stripping resistance of the mixture is significantly influenced. A concept known as the 'pessimum' air void range (8% to 10% air voids) was established by Terrel and Al-Swailmi (1994) this is a specification used to determine whether the air voids in an asphalt mixture is interconnected or not. The objective should, therefore, be to avoid the 'pessimum' air void range by ensuring quality workmanship during compaction.

2.7.4.6 Drainage

Case studies done by Kandhal et al. (1989) established that stripping of the bitumen from the aggregate surface does not occur as a general phenomenon on the of asphalt pavement's surface. They concluded that stripping of the bitumen occurs at localised locations where the asphalt surface is over saturated due to inadequate drainage. At these locations pore pressures build-up in the saturated air voids of the asphalt layer due to the action of the traffic. Pore pressures build-up cause expansion of the air voids resulting in the formation of cracks. Temperature increases also increase the pressure in the saturated air voids which may lead to moisture damage.

2.8 COMPOSITION OF GREY WATER

Wastewater produced by households can be categorised as grey or black water. In terms of science, the dictionary defines black water as: *"wastewater containing bodily or other biological wastes, as from toilets, dish washers or kitchen drains"* (Dictionary.com, 2015). Grey water in terms of science is defined

according to the dictionary as: *"wastewater from baths, bathroom sinks, and washing machines that do not contain body or food wastes"* (Dictionary.com, 2015).

Various factors influence grey water characteristics of such as water supply quality and household activities. Ingredients present in the grey water will depend on the lifestyle and use of chemical products by households and will, therefore, vary from sources (Eriksson, et al., 2002).

Peterson (2013) conducted research titled: "*Investigating the effects of Grey Water on various bitumen asphalt grades*" for his B.Tech thesis. A door to door survey was carried out in Khayelitsha, an area with informal settlement in Cape Town, where it was determined that OMO® washing powder and Sunlight® dishwashing liquid is the most common detergents used by residents. This survey provided him with insight on the major ingredients of grey water effluent in the Municipal region of the City of Cape Town. Petersen's conclusion is further substantiated by water quality tests conducted at retention ponds in the same area by the City of Cape Town's Department of Water and Sanitation, which showed high phosphor and ammonia levels. These compounds are typically found in washing powders and dishwashing soaps (Greyling, et al., 2015 (1)).

Detergents such as OMO® washing powder and Sunlight dishwashing liquid consist of anionic surfactants. These type of detergents are excellent cleaning products as that ionise when in contact with water. Surfactants serve several purposes such as (American Cleaning Institute, 2016):

- Wetting agent
- Emulsifying agent
- Foaming agent
- Dispersant

Surfactants are used to decrease the surface tension between liquids and between a solid and liquid, therefore acting as a wetting agent. Surfactants emulsify oily contents and keep them in a dispersed form to prevent settlement. Typical surfactants found in washing powder and dishwashing liquid are listed in Tables 2.2 and 2.3.

Table 2. 2 - Surfactants present in washing powder (Unilever, 2015)

Washing Powder Ingredients	
Ingredient	**Function**
C 12-15 Pareth-7	Surfactant
Stearic Acid	Surfactant
Sodium Dodecyl-benzene-sulfonate	Surfactant

Table 2. 3 - Surfactants present in Sunlight dishwashing liquid (Diversey, 2011).

Sunlight® liquid Ingredients		
Ingredient	**Weight %**	**Function**
Di-ethanolamine	0.1 - 1.5%	-
Magnesium Oxide	1 - 5%	-
Ethyl Alcohol	1 - 5%	-
Dodecylbenzene Sulfonic Acid	20 - 30%	Surfactant
Sodium Laurel Ether Sulphate	10 - 20%	Surfactant

2.9 PREVIOUS RESEARCH ON GREY WATER RESISTANT ASPHALT

As indicated, Petersen (2013) has done research on the effect of grey water on various asphalt gradations. In this section, conclusions from Petersen's research are discussed according to the static and dynamic disbonding mechanisms as established in this Literature Review. In addition, findings of research done on the grey water resistance of asphalt at the University of Stellenbosch, are presented.

2.9.1 STATIC DISBONDING MECHANISMS

Static disbonding mechanisms include detachment and displacement. Displacement consists of chemical disbonding and bitumen film rupturing. These disbonding mechanisms are classified as static as only the presence of clean water is required for these mechanisms to initiate (Greyling, et al., 2015 (1)). From research done by Petersen (2013), it can be determined that the presence of surfactants in grey water accelerates these disbonding mechanisms.

Petersen (2013) concluded from his research that water with a high surfactant content will lead to premature failure of an asphalt mixture due to a loss of adhesion being caused by the presence of the surfactants. His research methodology included preparation of asphalt briquettes for six asphalt mixture combinations. These briquettes were submerged into distilled water for testing as the control samples.

In addition, he prepared four separate water solutions with a surfactant content of 1 percent. Petersen identified the following surfactants that are used in OMO® washing powder and Sunlight® liquid to prepare these water solutions (Petersen, 2013):

- Dodecylbenzene sulfonic Acid
- Sodium Lauryl Ether Sulphate
- Nonylphenol ethoxylate
- Trisodium phosphate

Similar to the control samples, Pietersen (2013) prepared asphalt briquettes that were submerged in each of the four surfactant water solutions. The water solutions were preheated to 60°C before the asphalt briquettes were submerged.

Petersen (2013) conducted a series of tests on the asphalt briquettes after 30 minutes, 24 hours and 7 days of submergence. He concluded that all the asphalt briquettes submerged in the surfactant water solutions completely disintegrated after 3 to 4 days. After seven days these samples were impossible to recover for further testing. From these results, it are clear that a high concentration of surfactants in a water solution affects the rate at which asphalt mixtures lose their cohesive and adhesive properties (Petersen, 2013).

Petersen (2013) had confirmation from Mr Kobus Louw from COLAS in Cape Town that all base binders used for his research were pre-tested to determine whether the bitumen is resistant to the surfactants he used for the water solutions. The tests showed that the surfactants have little effect on the bitumen. It is therefore concluded that grey water has a significant effect on the bond between the bitumen and aggregate.

Morgan and Mulder (1995) stated that bitumen generally has good resistance against most chemicals. In the *Shell Industrial Bitumen Handbook,* Morgan and Mulder (1995) published a list of chemicals where bitumen's resistance against these chemicals is evaluated. Trisodium phosphate, sulphated detergents and stearic acid, which are typical surfactants to be found in grey water, were amongst the chemicals on this list. Figure 2.16 illustrates bitumen's resistance against these chemicals.

From Figure 2.16 follows that stearic acid is the only chemical capable of having a significant effect on bitumen, but only in its pure form. However, in grey water stearic acid is present in low concentrations, therefore it can be concluded that it will have little effect on the bitumen of an asphalt mixture.

From the research Petersen (2013) conducted, as well as information provided by Read and Whiteoak (2003), it can be concluded that grey water will have little effect on the individual material constitutes of an asphalt mixture. However, surfactants in grey water accelerate disbonding mechanisms, which cause an asphalt mixture to lose its adhesive and cohesive properties.

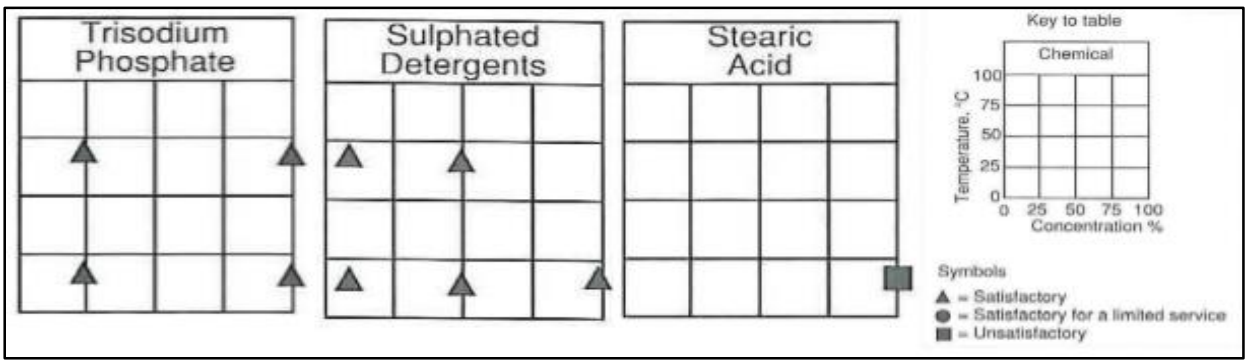

Figure 2. 16 - Bitumen's resistance against chemicals (Morgan & Mulder, 1995).

2.9.2 DYNAMIC DISBONDING MECHANISMS

Dynamic disbonding mechanisms include hydraulic scour and pore pressure. These disbonding mechanisms are classified as dynamic as the presence of water and traffic loading are required for these mechanisms to initiate. The rate of deterioration caused by these dynamic disbonding mechanisms increase with an increase in the traffic loading, temperature and chemical concentration (Greyling, et al., 2015 (1)).

The effect of dynamic disbonding mechanisms was not directly proven by Petersen (2013) during his research. However, he performed Marvel permeability tests on the asphalt briquettes before and after they were completely submerged in clean and surfactant water during a static-immersion test. Permeability measurements before submergence were 10 seconds and greater for all asphalt briquettes. After the asphalt briquettes were submerged for 24 hours, all asphalt briquettes showed permeability measurements of less than 1 second. Permeability measurements of the asphalt briquettes submerged in clean water were also among these results.

From these results, it can be concluded that the air voids in the asphalt mixtures may become interconnected once it is submerged in clean and surfactant water. These voids are filled with water which promotes the occurrence of disbonding mechanisms (Greyling, et al., 2015 (1)). The effect of traffic may influence the rate of moisture damage caused by disbonding mechanisms. This is due to a ‘wash’-action that may be produced by traffic-induced stresses. This ‘wash’-action may, therefore, accelerate the stripping of bitumen from the aggregate surface.

2.9.3 RESEARCH DONE AT THE UNIVERSITY OF STELLENBOSCH

Briedenhann and Jenkins (2015), as well as Greyling et al. (2015(2)), researched the grey water resistance of asphalt at the University of Stellenbosch. Their research indicated that significant damage was done to asphalt mixtures subjected to clean water conditioning. However, based on ITS results, the presence of surfactants in grey water accelerates this damage by reducing the strength of the asphalt mixture (Greyling, et al., 2015 (2)). Figure 2.17 illustrates the reduction in strength of asphalt mixtures over time after conditioning with moisture inducing simulating test (MIST), using clean and grey water at various temperatures.

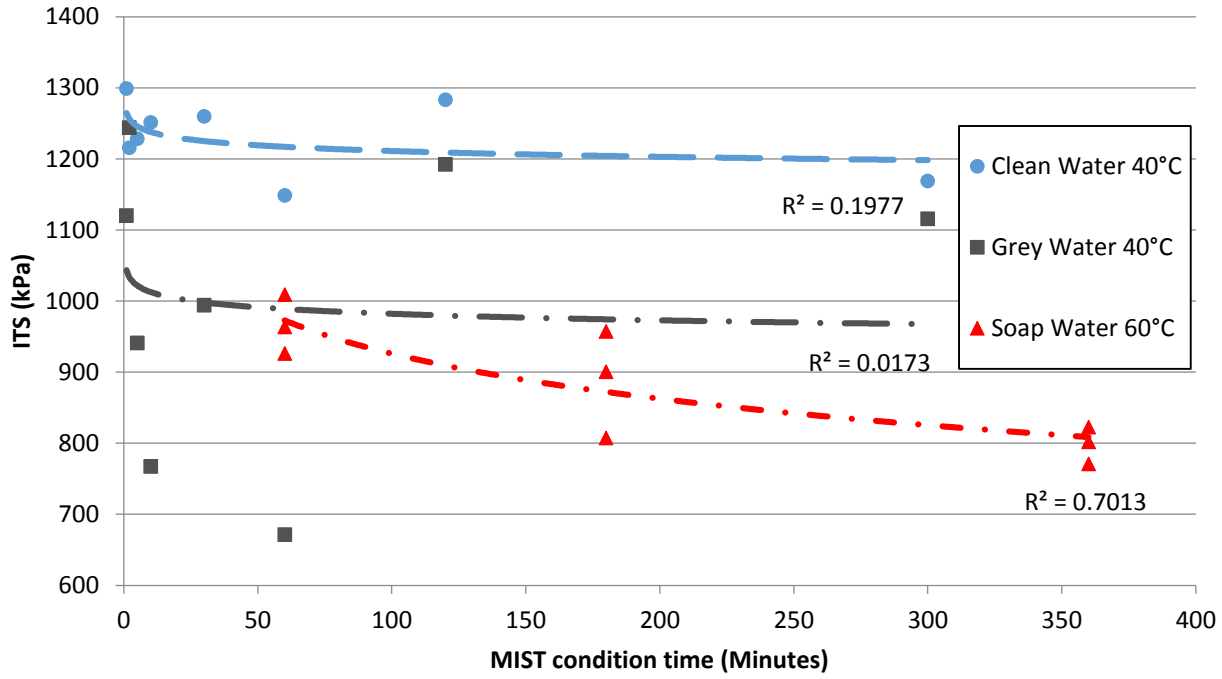

Figure 2. 17 - Reduction in asphalt mixture strength as a result of grey water (Briedenhann & Jenkins, 2015).

It is apparent that the ITS results versus MIST conditioning time for clean and grey water conditioning at 40°C did not show a significant trend due to a determination coefficient of less than 0.7. However, conditioning at this temperature with clean water did not show significant variation in the ITS results for short and long periods of conditioning. Conditioning at 40°C with grey water did show large variation in the ITS result for short and long periods of conditioning compared to clean water. Increasing the conditioning temperature to 60°C showed accelerated moisture damage as the conditioning time increased.

The effect of grey water conditioning was also tested for the composition, binder additives and compaction of various asphalt mixtures during this research.

Greyling et al (2015(2)) established that the gradation of an asphalt mixture influences its resistance to grey water conditioning. Due to a reduction in the void content of a semi-gap graded asphalt mixture, greater resistance to grey water conditioning was achieved by this gradation. However, limitations related to the rut resistance of a semi-gap graded mixture need to be considered in order to develop a suitable grey water resistance asphalt mixture. Greyling et al (2015(2)) further established that the use of a continuous grade asphalt mixture with a suitable modified binder may provide an effective asphalt solution to address rut and grey water related problems.

In terms of binder additives, Greyling et al (2015(2)) found that modified binders significantly improved the grey water resistance of asphalt. It was established that modified binders, made up from a combination of anti-stripping and polymer additives, provided better solutions to the grey water resistance of asphalt compared to using these additives individually. This is illustrated in Figure 2.18. It should be noted that ITS result presented in Figure 2.18 are less than the COLTO specification of 800 kPa. However, COLTO specification is set for ITS testing at 25^{o}C, whereas results in Figure 2.18 were obtained after ITS testing at 40^{o}C.

Greyling et al. (2015(2)) also found that the lime content should be limited to two percent to prevent embrittlement of the asphalt mixture. From this research, it was also concluded that a modified EVA plastomer binder, in combination with two percent lime, proved to be the most effective solution to improve the grey water resistance of asphalt.

Greyling et al. (2015(2)) also found that compaction affects the grey water resistance of the asphalt mixture. Semi-gap graded mixtures tend to compact better compared to continuous grade mixtures, as the former relates to a lower void content and resultant improvement in resistance to grey water conditioning. Increasing the compaction effort indicated an improved grey water resistance as the voids content of the mixtures are reduced with an increase in compaction effort.

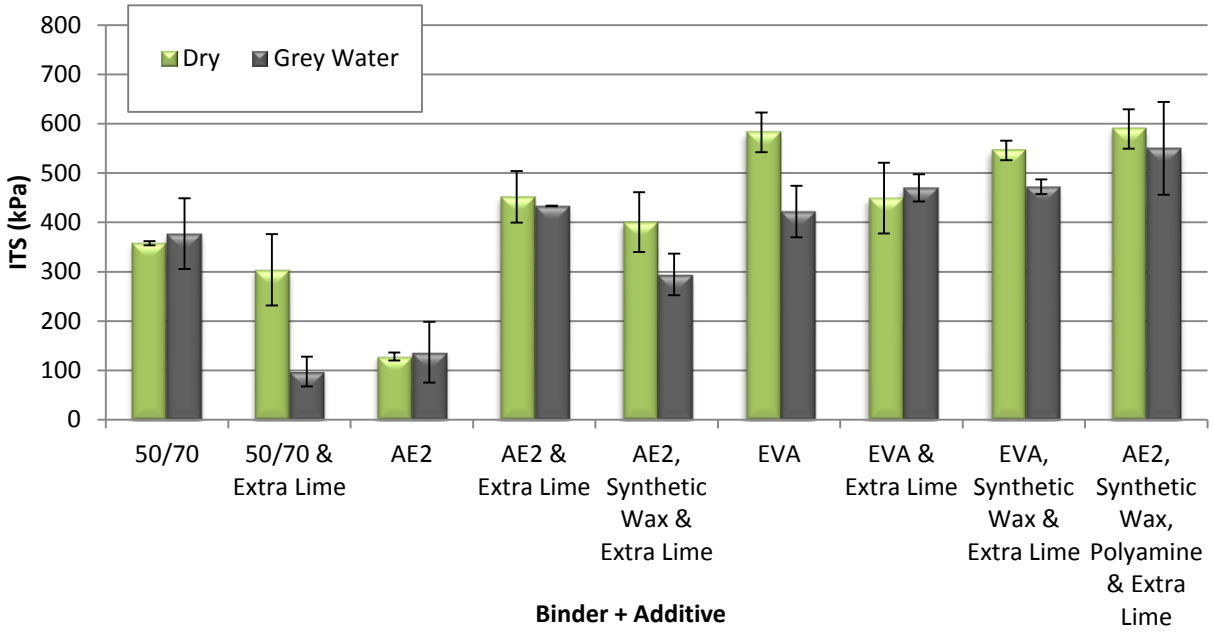

Figure 2. 18 - ITS results of continuous grade asphalt mixtures compacted to N_{max}, using gyratory compactor (Briedenhann & Jenkins, 2015).

The strength of the asphalt mixtures subjected to no water, clean water and grey water conditioning were compared with the void content by Briedenhann and Jenkins (2015). They found that no water conditioning did not produce any significant changes in the strength of asphalt with an increase in the void content of the mixture. However, a decrease in the mixture strength with an increase in the void content was observed after grey water conditioning. This is illustrated in Figure 2.19.

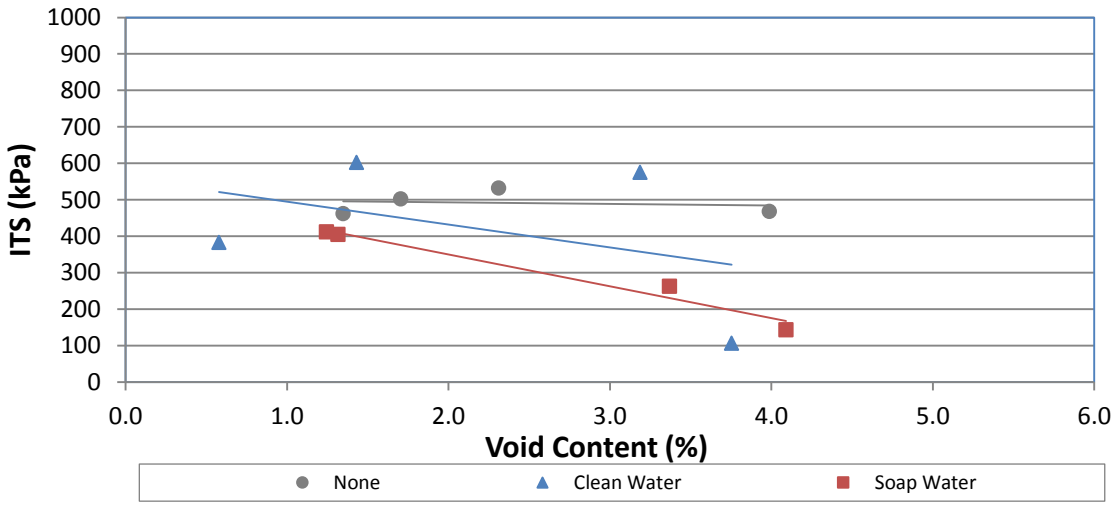

Figure 2. 19 - Asphalt mixture strength versus void content (Briedenhann & Jenkins, 2015).

Laboratory test results were confirmed with an Analysis of Variance (ANOVA) that was completed by Briedenhann and Jenkins (2015) on the gradation, binder additives and compaction of asphalt mixtures subjected to grey water conditioning. The results of this analysis are presented in Table 2.4.

Table 2. 4 - Results of ANOVA analysis (Briedenhann & Jenkins, 2015).

Key area of interest	Grading	Additives	Compaction
Populations to compare	Continuously graded mix	9 different combinations of additives	N_{Design}
	Semi-gap graded mix		N_{Max}
Distinguishable probability (p-value)	95%	99%	68%

From Table 2.4 follows that a 95 percent probability exists that a distinctive result related to the grey water resistance of asphalt mixtures with different gradations will be achieved. The ANOVA analysis further indicated that a significant unique result related to the grey water resistance of asphalt mixtures with different binder additive combinations will also be achieved. ANOVA results also indicted that there is a 68 percent probability that a unique result related to the grey water resistance of asphalt will be produced by increasing the compaction effort (Briedenhann & Jenkins, 2015).

Research done at the University of Stellenbosch provides vital information on the composition, modified binders and compaction of asphalt mixtures. This research information serves as the basis for setting up the research methodology of this study.

2.10 TESTING THE MOISTURE SUSCEPTIBILITY OF ASPHALT MIXTURES

Various types of tests have been developed to evaluate the moisture susceptibility of asphalt mixtures. These tests were developed to evaluate the moisture susceptibility of asphalt in its loose or compacted form. However, for the purpose of this research report, the focus is only placed on tests performed on compacted asphalt mixes. Moisture susceptibility tests on compacted asphalt mixtures are performed using laboratory prepared samples, field cores or slabs. The advantage of these tests is that the effect of mixture properties, mechanical properties, traffic loading and pore pressures can be accounted for. These tests require longer testing times, the correct laboratory equipment and more laborious test procedures (Solaimanian, et al., 2003).

2.10.1 IMMERSION-COMPRESSION TEST AND MARSHALL IMMERSION TEST

The immersion-compression test was one of the first tests to evaluate the moisture susceptibility of compacted asphalt mixtures. The full test procedure is explained by Goode (1959) in ASTM Special Technical Publication 252. However, as a brief description of the test procedure is presented (Solaimanian, et al., 2003).

The immersion-compression test includes compaction of two groups of asphalt briquettes. The first group is conditioned for four days in a bath of water with a temperature of 50°C. An alternative method to condition the asphalt samples is to submerge it in a bath of water for 24 hours at 60°C. The second group receives no conditioning as its represents the control samples. After conditioning the compressive strength of the control and the conditioned asphalt samples are tested. The compressive strength tests are performed at a temperature of 25°C and a deformation rate of 5.08 mm/min for a sample height of 100 millimetres. A compressive strength ratio is determined by dividing the average compressive strength of the conditioned asphalt samples by the average compressive strength of the control asphalt samples. The compressive strength ratio is then used to measure the moisture susceptibility of the asphalt mixture. A compressive strength ratio of at least 70 percent is required for the asphalt mixture to pass the moisture susceptibility test (Solaimanian, et al., 2003).

The Marshall immersion test is similar to the immersion-compression test. However, instead of using a compressive strength ratio, a Marshall stability ratio is determined and used to measure the moisture susceptibility of the asphalt mixture (Solaimanian, et al., 2003).

2.10.2 MOISTURE VAPOUR SUSCEPTIBILITY

The California Department of Transport (2000) developed the moisture vapour susceptibility test. During this test, two asphalt briquettes are compacted using the Gyratory compactor. Figure 2.22 illustrates the complete sample setup for the moisture vapour susceptibility test.

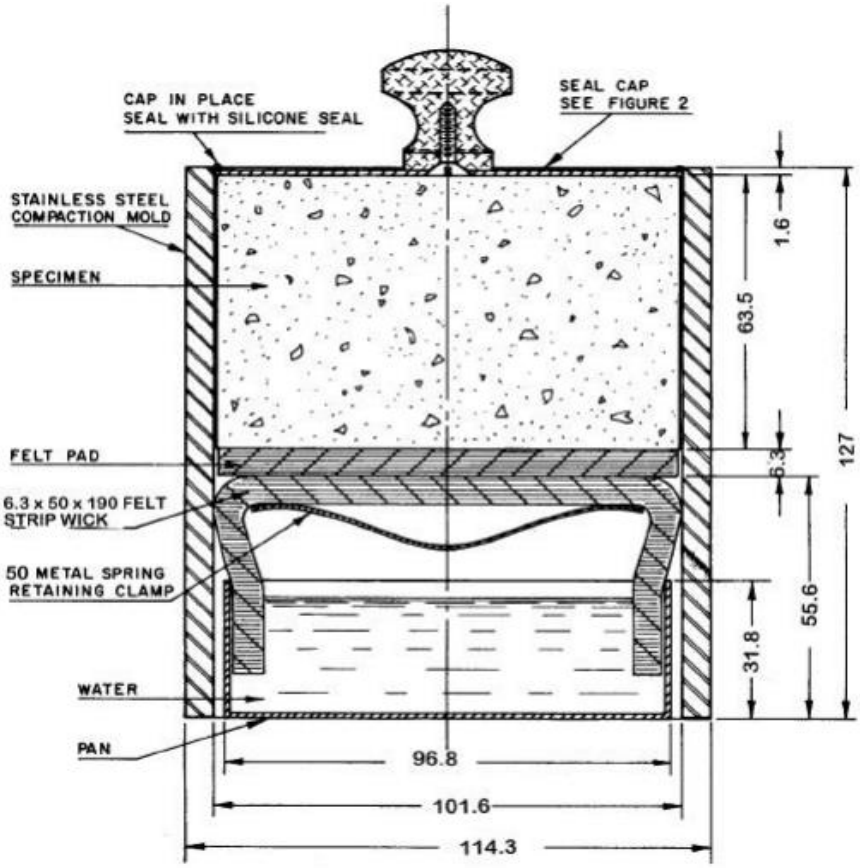

Figure 2. 20 - Asphalt sample setup for moisture vapour susceptibility test (California Department of Transport, 2000).

Figure 2.20 shows that a stainless steel compaction mould is prepared for each sample by placing a pan of water at the bottom of the mould. On top of the pan of water, a pre-soaked felt strip wick is installed and secured by a metal spring clamp. A circular pre-soaked felt pad is installed on top of the felt strip wick. The compacted surface of the asphalt specimen is covered with an aluminium seal cap and placed in the stainless steel mould. Silicon sealant is used to seal the edges around the aluminium seal cap to prevent moisture vapour from escaping (California Department of Transport, 2000).

The complete test assembly is then placed in an oven set to a temperature of 60^{o}C for 75 hours. After 75 hours the samples are removed from the oven and tested using the Hveem stabilometer. The Hveem stabilometer is used to determine the stability of an asphalt mixture and is a test apparatus developed for the Hveem mixture design method. For the moisture susceptibility criterion of the asphalt mixture to be satisfied, the average Hveem stabilometer value for the wet asphalt samples should be less than the dry asphalt samples tested for the same asphalt mixture design (California Department of Transport, 2000).

2.10.3 ORIGINAL LOTTMAN INDIRECT TENSION TEST

Lottman (1978) developed the original Lottman indirect tension test at the University of Idaho. Two groups of asphalt briquettes are prepared for this test. The first group of asphalt briquettes receives conditioning while the second group represents the control briquettes. Each briquette is 100 millimetre in diameter and about 60 millimetres thick (Solaimanian, et al., 2003).

The first group of asphalt briquettes is conditioned by vacuum saturation for 30 minutes at a pressure of 3.4 kPa. Thereafter this group is left at atmospheric pressure for 30 minutes, where after thermal conditioning is simulated by freezing and thawing conditions. Thermal conditioning involves the freezing of briquettes at -18 ^{o}C for 15 hours, followed by heating at 60^{o}C for 24 hours in a water bath. An alternative method of thermal conditioning is to alternate the temperature cycles for 4 hours at -18^{o}C and then followed by 4 hours at 50^{o}C. The total thermal cycle for this method is completed in 8 hours for a total of 18 cycles (Solaimanian, et al., 2003).

After conditioning the indirect tensile strength as well as the tensile resilient modulus of the conditioned and control groups are determined. Figure 2.21 illustrates the indirect tensile strength test of an asphalt briquette. Two loading rates are specified for the Lottman indirect tension test. The first loading rate is at 1.65 mm/min at a test temperature of 13^{o}C, whereas the second loading rate is specified at 3.8 mm/min at a test temperature of 23^{o}C. A tensile strength ratio (TSR) is determined from dividing of the average indirect tensile strength of the conditioned asphalt briquettes by the average indirect tensile strength of the control asphalt briquettes. The TSR is used to determine the moisture susceptibility of the asphalt mixture (Solaimanian, et al., 2003).

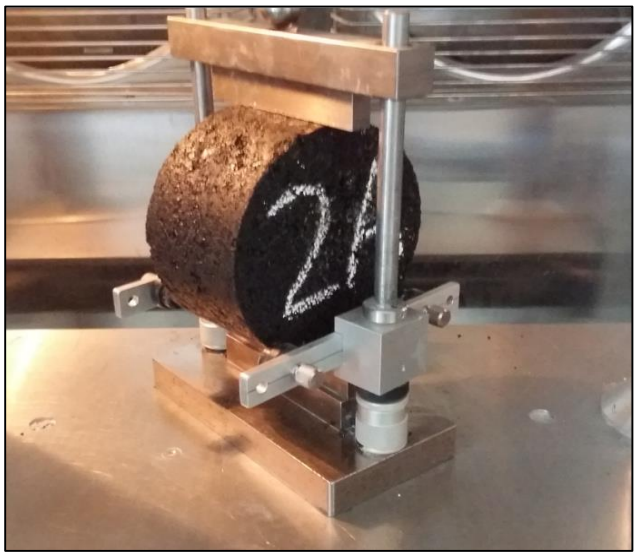

Figure 2. 21 - Indirect tensile strength testing.

2.10.4 MODIFIED LOTTMAN INDIRECT TENSION TEST

The modified Lottman indirect tension test is also known as AASHTO Standard Method of Test T283. This is the most common method used to evaluate the moisture susceptibility of hot-mix asphalt mixtures. Although the original Lottman tension test forms the basis of this test procedure, a few modifications

were made to the method used for conditioning of asphalt briquettes as well as the method used for indirect tensile strength testing (Solaimanian, et al., 2003).

The vacuum saturation conditioning was modified to continue until 70 to 80 percent of the saturation level is achieved, instead of the 30 minute time requirement set for the original Lottman method. The temperature and loading rate used to perform the indirect tensile strength test were also modified. The modified Lottman indirect tension test specified a loading rate of 50.8 mm/min at a test temperature of 25°C. With this new specification, the indirect tensile strength tests are performed using the Marshall stability tester. This is convenient as most laboratories have a Marshall stability tester available (Solaimanian, et al., 2003).

The modified Lottman indirect tension test includes curing of the loose asphalt mixture at 60°C for 16 hours, followed by additional 2 hours at 135°C. Enough asphalt is mixed to produce six briquettes. The void content of the asphalt briquettes is tested after compaction for a required 6.5% to 7.5%. The six asphalt briquettes are separated into two group of three. The first group will represent the control briquettes and the second group is conditioned (Solaimanian, et al., 2003).

The conditioning procedure consists of vacuum saturating the asphalt briquettes to a saturation level of 50% to 80%. Once the correct saturation level is achieved, thermal conditioning is applied to the asphalt briquettes. Thermal conditioning includes keeping the briquettes in a freezer at a temperature of -18°C for 16 hours. Thereafter the briquettes are placed in a water bath at 60°C for 24 hours. The asphalt briquettes are considered conditioned after this process (Solaimanian, et al., 2003).

After conditioning, all asphalt briquettes prepared for indirect tensile strength testing. The briquettes are placed in an oven to ensure a constant temperature is achieved prior testing. The indirect tensile strength for the control and conditioned asphalt briquettes are determined from which a tensile strength ratio (TSR) is calculated. A TSR of 80% is required to ensure the moisture susceptibility of an asphalt mixture is acceptable (Solaimanian, et al., 2003).

The modified Lottman indirect tension test has major shortcomings as its ability to predict the moisture susceptibility of asphalt mixtures accurately is doubtful (Solaimanian & Kennedy, 2000). However, the modified Lottman indirect tension test was adopted by the Superpave mix design system as a standard test for determining the moisture susceptibility of asphalt mixtures. Epps et al. (2000) investigated the modified Lottman test to improve the test method for the Superpave mix design system. The investigation evaluated the effect of different types of compaction, diameter of asphalt briquettes, thermal

conditioning methods and the levels of saturation. Epps et al (2000) concluded the following from his investigation:

- 100 mm diameter Superpave and Hveem prepared control specimens showed greater strength compared to the 150 mm diameter Superpave prepared control specimens.
- 100 mm diameter Marshall prepared control specimens showed similar strength as 150 mm diameter Superpave prepared control specimens.
- The strength of 100 mm diameter Superpave prepared control specimens was the same as for 100 mm diameter Hveem prepared control specimens.
- The strength of control specimens increases with the ageing of a loose mix.
- The tensile strength of specimens subjected to freeze-thaw cycles was the same as for specimens subjected to no freeze-thaw cycles.
- The TSR of 150 mm diameter Superpave prepared specimens was greater than the TSR of 100 mm diameter Superpave and Hveem prepared specimens.
- The TSR of 150 mm Superpave prepared specimens was the same as the TSR of 100 mm Marshall prepared specimens.

Several research projects have been launched to investigate the shortcomings of the modified Lottman indirect tension test. However, only suggestions have been made to improve the shortcomings of this test procedure which is still empirical and provides mixed results in terms of the moisture susceptibility of asphalt mixtures (Solaimanian, et al., 2003).

2.11 ACCELERATED PAVEMENT TESTING – MMLS3

2.11.1 BACKGROUND OF MMLS3

The concept of the Mobile Load Simulator (MLS) was initiated in 1988 by the Texas Highway Department. The Texas Highway Department launched a project to investigate the development of a full-scale accelerated pavement testing system. However, at the time only two types of accelerated pavement testing systems existed. The South Africans developed the Heavy Vehicle Simulator (HVS) in the 1960's whereas the Australians and United States used the Accelerated Loading Facility (ALF) to investigate the performance of bituminous road pavements under accelerated trafficking. Both these accelerated trafficking systems consisted of a single double bogie configured truck wheel to produce traffic stresses on the pavement surface (Kemp, 2006).

Professor Fred Hugo, who was the team leader of the Texas Highway Department project, developed a unique closed loop accelerated trafficking system in the late 1980's. The MLS system was developed to test the rutting performance of asphalt mixes on a laboratory scale at the Institute for Transport Technology at the University of Stellenbosch (Hugo & Steyn, 2015). His team proposed and built a 1 to 10 scale model of the MLS by implementing this closed loop concept. Development of a full-scale MLS version was approved by the Texas Steering Committee in 1990 after the presentation of the 1 to 10 scale model MLS developed by Hugo's team. The first full-scale MLS was known as the Texas Mobile Load Simulator (TxMLS) (Kemp, 2006).

After the scale model MLS was developed, it was decided to develop a MLS system for laboratory operations. This was done by upgrading the original scale model MLS which was demonstrated at the University of Stellenbosch. This MLS system was known as the MMLS1. The first laboratory scale model MLS was eventually sold to the University of Texas and was used for the development of the full-scale TxMLS system. Meanwhile, a second laboratory scale model MLS system was developed and used for research purposes at the University of Stellenbosch (Kemp, 2006).

However, the 1 to 10 scale modelling of pavement structures seemed challenging and lead to the development of a more feasible MLS system for laboratory purposes. The MMLS3 was developed as a solution to the scale modelling of pavement structures. Completed in 1997, the MMLS3 was a third scale model mobile load simulator. It consisted of four bogies fitted with a single third scale tyre. The third scale tyre represents a third of a single truck wheel that forms part of a dual wheel configuration (Kemp, 2006). The MMLS3 schematics is illustrated in Figure 2.22.

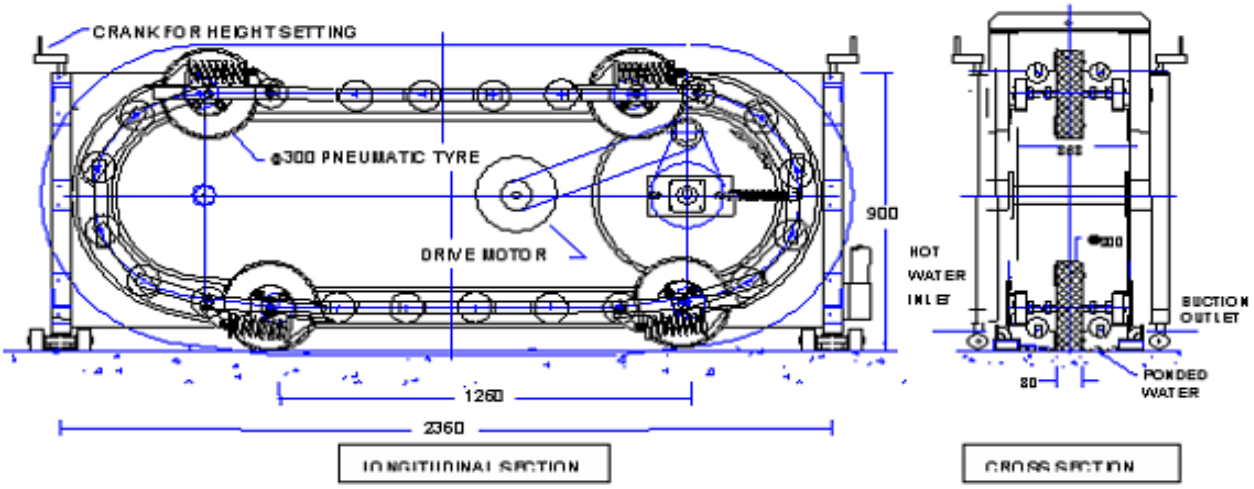

Figure 2. 22 - Schematics of third-scale Model Mobile Load Simulator (MMLS3) (Abrahams, 2015).

The advantages of the MMLS3 are its high speed of trafficking, the load moves in one direction only and in a short time period many load repetitions are possible. In addition to these advantages, the MMLS3 can be used for field and laboratory testing as well as testing in wet or dry conditions (Douries, 2004).

The first MMLS3 system was sold to the United States after completion in 1997, followed by systems sold to universities in Europe and the United States (Kemp, 2006). A total of twenty-four MMLS3 systems are to be found globally at present. SANS 3001-PD1 2015 is being compiled to incorporate the MMLS3 system as a SANS certified test to evaluate the performance of asphalt pavements (Hugo & Steyn, 2015).

2.11.2 MML3 TEST METHODS

The Draft Protocol Guideline 1 (DGP1) was released in 2008 and describes a *Method for evaluation of permanent deformation and susceptibility to moisture damage of bituminous road paving mixtures using the Model Mobile Load Simulator (MMLS)*. This guideline provided an international standard test protocol for evaluating the rutting and moisture susceptibility of asphalt pavements, especially under controlled environmental conditions.

The MMLS3 is a third-scale heavy vehicle simulator (HVS) used for evaluating the performance of bituminous bases and surfacing under accelerated trafficking. It consists of four single wheels, each 300 mm in diameter, and is capable of producing 7200 real loads per hour. The recommended testing tyre pressure is 700 kPa, but it can be increased up to 850 kPa depending on the test requirements. A wheel load of 1.9 kN to 2.7 kN can be set which also depends on the test requirements (Douries, 2004). Three test types have been developed using the MMLS3 and are presented in DGP1. The first test type is used for laboratory purposes and consists of performing third-scale mobile model load simulating tests on nine compacted asphalt briquettes or field cores installed in a test bed. Asphalt briquettes, 150 mm in diameter and 30 mm to 90 mm in thickness, are prepared and compacted using the gyratory compactor. The briquettes are each machined by sawing-off two parallel segments of which the long chords are 112 mm apart. The

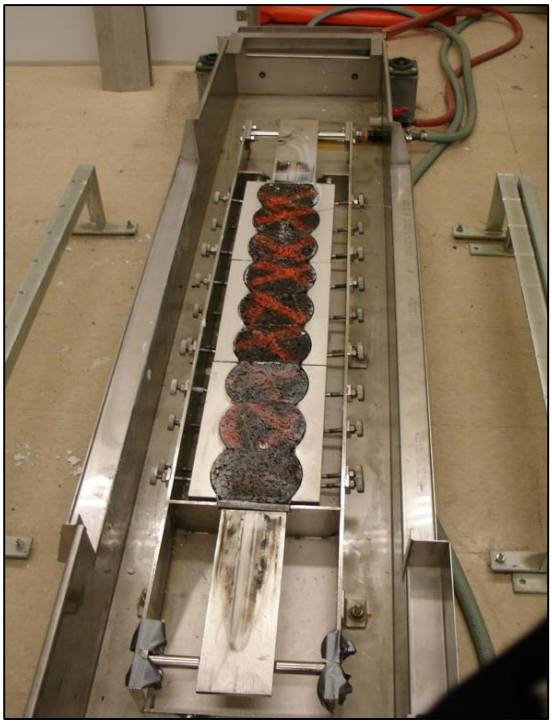

Figure 2. 23 - Asphalt briquettes installed in test bed (Hugo & Steyn, 2015).

asphalt briquettes are installed next to each other with the parallel chords perpendicular to the direction of trafficking. Screws and clamps are used to keep the briquettes in place during the test. Trafficking is applied to the asphalt briquettes while the test temperature is constantly monitored. The trafficking is stopped at predetermined intervals to measure the cross-sectional profile of each asphalt briquette (Draft Protocol Guideline, 2008). Multiple environmental conditions can be produced using the dry heating and water heating units which are part of the MMLS3 system. Figure 2.23 illustrates laboratory testing of asphalt briquettes using the test bed and MMLS3 system.

Figure 2. 24 - Vibratory roller for compacting asphalt slabs (Hugo & Steyn, 2015).

The second test type is also used for laboratory purposes by performing third-scale mobile model load simulating tests on asphalt slabs. The slabs are compacted using a vibratory roller specifically designed for compacting laboratory scale asphalt slabs. Once these slabs are compacted the initial cross-sectional profiles are measured. Trafficking is also applied and stopped at predetermined intervals to measure the cross-sectional profiles. Similar to the test bed, multiple environmental conditions are simulated using the dry heating and water heating units. Figure 2.24 illustrates the vibratory roller for compacting asphalt slabs as well as an environmental chamber used for simulated environmental conditions.

Figure 2. 25 - Field testing using MMLS3 system (Hugo & Steyn, 2015).

The third test type is performed in the field. The MMLS3 system is setup on an existing pavement structure to determine the remaining service life and failure mechanisms as well as the prediction of the future performance of structure under investigation. The field test is developed to produce multiple environmental conditions such as wet conditions by constructing an artificial dam to flood the pavement surface with water. Field testing eliminates the various variables that are difficult to simulate in controlled testing environments. These variables include temperature fluctuations

and parameters related to wet trafficking of the asphalt surface. Field testing using the MMLS3 system is illustrated in Figure 2.25.

2.11.3 PREVIOUS RESEARCH ON MOISTURE SUSCEPTIBILITY USING MLS SYSTEM

Hugo and Steyn (2015) explained that field testing done in Texas have shown physical evidence of stripping of a high modulus asphalt surface after 1.45 million MMLS3 load cycles under wet conditions. This was confirmed after a 62% reduction in the asphalt stiffness was noticed. Dry trafficking tests were also conducted on the same asphalt surface on which a 1.8 ± 0.2 mm rut depth was observed after 1.0 million MMLS3 load cycles. It was observed that the stiffness of the high modulus asphalt surface subjected to dry trafficking tests also increased by 25%. This provides evidence of the effects moisture has on the performance of asphalt mixtures (Hugo, et al., 1999).

Increased distress was noticed during trafficking under wet conditions using the MMLS3 on a selected section of the NCAT test track. Cores were extracted from the trafficked asphalt surface and were found to be completely fractured due to the effect of trafficking in conjunction with wet conditions (Hugo, et al., 2004). MMLS3 tests conducted in Switzerland also showed evidence of variability in the effect moisture has on the performance of asphalt mixtures under wet trafficking and lateral wandering. A total of 48 cores from different asphalt pavements across Switzerland were extracted after wet trafficking. Improved performance was observed from some of the cores extracted this provided evidence that trafficking tests under wet conditions may reduce the risk associated with unexpected distresses (Raab, et al., 2005).

Walubita (2000), by performing accelerated pavement tests using the MMLS3, investigated the performance of various asphalt mixtures on US highway 281 in Texas. Accelerated pavement tests were conducted under wet conditions on sections consisting of four different asphalt mixtures. Wet trafficking was done at 45^{o}C with a 1 mm thick film of hot water on the surface of the test sections. After trafficking the moisture susceptibility of the asphalt mixtures were determined through TSR. Semi-Circular-Bending tests (SCB) were performed on asphalt cores extracted from the test sections. The TSR showed significant moisture damage to some asphalt sections whilst the field testing results for the same asphalt section showed otherwise. These observations lead to additional findings related to the moisture susceptibility of asphalt materials and standard test procedures.

The tests conducted on US highway 281 in Texas, provided important findings related to moisture damage caused by wet trafficking of asphalt pavements. During these tests, it was found that AASTHO T283 specification will not always ensure that asphalt mixtures are resistant to moisture damage and stripping

of the bitumen. It was further concluded that a TSR-value less than 80 percent will not always result in stripping of the bitumen or damage to the asphalt surface caused by water (Walubita, et al., 2002).

Findings from research done using the MMLS3 showed that accelerated pavement tests can provide important information related to the performance of asphalt pavements, especially on the moisture susceptibility of asphalt mixtures. It is clear that moisture significantly reduces the performance of an asphalt pavement under trafficking. MMLS3 testing may therefore also provide important information for improving the grey water resistance of asphalt mixtures.

2.12 SUMMARY - IMPROVING THE GREY WATER RESISTANCE OF HMA

This section concludes the Literature Review by presenting a summary of factors to consider for improving the grey water resistance of an asphalt mixture. Four primary factors were identified to have a significant influence on moisture susceptibility and are presented in Figure 2.26. This also serves as a point of reference for establishing a research methodology to investigate grey water resistance.

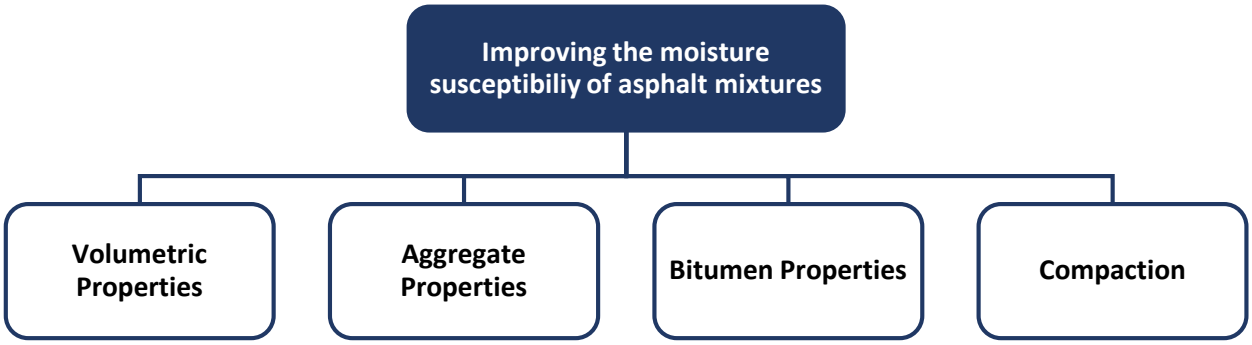

Figure 2. 26 – Primary factors identified to have an influence on the moisture susceptibility of asphalt mixtures.

The primary factors identified were used for developing Table 2.5, which represents performance variables and considerations for improving the moisture susceptibility and grey water resistance of asphalt mixtures.

Considerations shown in Table 2.5 as well as findings by Greyling et al. (2015) and Briedenhann & Jenkins (2015) on composition, binder additives and compaction of asphalt guided the extensive research methodology developed for this thesis report. This research methodology will differ from previous research by including MIST conditioning, ITS testing and laboratory scale model mobile load simulating (MMLS) tests on more asphalt gradations and binder additive combinations.

Table 2. 5 - Factors to consider for improving the moisture susceptibility and grey water resistance of an asphalt mixture.

Primary Factors	Performance Variable	Considerations	Improve adhesive properties
Volumetric Properties	VIM	The VIM of the asphalt mixture should be low but greater that 2% after construction.	-
	VMA	Binder content should be selected to ensure VMA conforms to the specification.	-
	VFB	A VFB of 50% to 70% is required after compaction.	-
	Aggregate grading	Sand-Skeleton aggregate grading is required.	-
	Permeability	Permeability related to VIM. Decreasing VIM decreases permeability.	
Aggregate properties	Surface texture and shape	Aggregates should be rough textured and angular in shape.	☺
	Hardness and Toughness	Hard and tough aggregates should be used.	-
	Durability and Soundness	Durable aggregates should be used that do not wear easily.	-
	Surface area	Greater surface area creates stronger bitumen-aggregate bonds. Surface area increases as the aggregate roughness increases.	☺
	Cleanliness	Clean aggregates improve the adhesion properties of the asphalt mixture.	☺
	Porosity and Absorption	Increased porosity increases the absorption of bitumen and creates strong bitumen-aggregate bonds.	☺
	Hydrated Lime filler	Hydrate filler improves the adhesive properties and regulates pH-levels. Content should range from 1% to 2%.	☺
Bitumen properties	Viscosity	Low viscosity at high temperatures provides a better coating of aggregate.	☺
	Penetration	Determined from SANS. The lower the penetration the harder the bitumen.	-
	Temperature susceptibility	Susceptible to high in-service temperatures.	☺
	Modified binders	Reduces viscosity at high temperatures resulting in better coating of aggregates. Increased flexibility of bitumen and elasticity improves resistance to cracking.	☺
Compaction	Density	Increased level of compaction increases the density of the asphalt mixture.	-
	VIM	Increased level of compaction decreases VIM.	-
	Permeability	Increased level of compaction decreases permeability.	-

CHAPTER 3 – EXPERIMENTAL RESEARCH METHODOLOGY (PRIMARY)

Improving the asphalt mixtures' resistance to grey water is investigated in this study. This led to the development of a primary research methodology (known as the experimental research methodology) as shown in Figure 3.1.

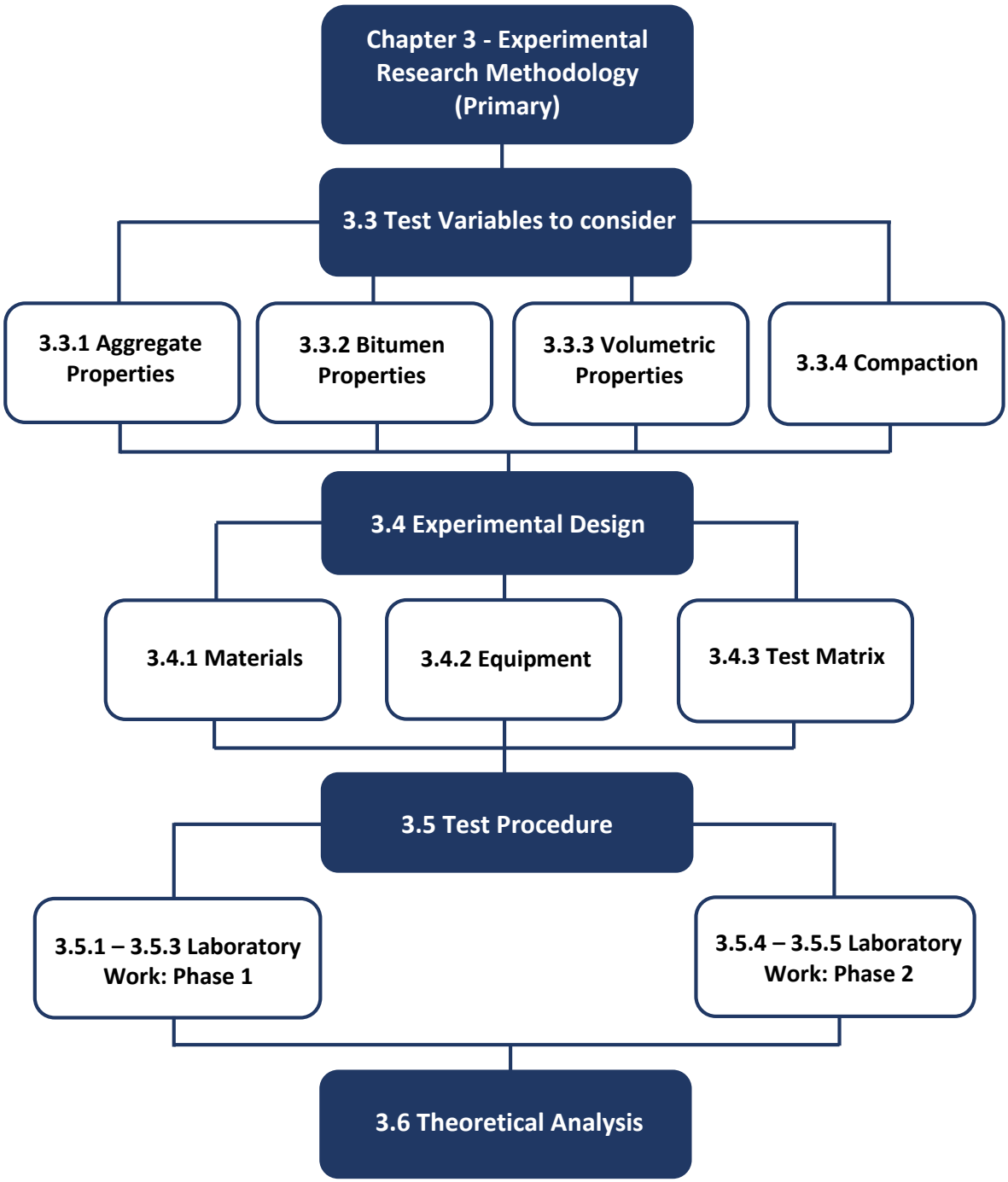

Figure 3. 1 - Outline of the research methodology

3.1 INTRODUCTION

In the Literature Review, factors were established for consideration when the moisture susceptibility of asphalt mixtures are investigated. Previous research provided insight on methods used by researchers to improve the moisture susceptibility of asphalt mixtures. However, Petersen (2013) investigated the effect of grey water on the performance of asphalt mixtures and concluded that the presence of surfactants in grey water significantly increases the rate of moisture damage.

In this Chapter, a research methodology is developed to investigate the moisture susceptibility of asphalt mixtures subjected to grey water. The research focuses on applying methods learned in the Literature Review and South African asphalt design practice for developing improved resistance to surfactants. In this research methodology, a complete breakdown of test variables to consider when investigating the moisture susceptibility of asphalt mixtures, as well as an experimental design and test procedure are presented. Thereafter the theoretical analysis of results procured from test procedures are presented.

3.2 OBJECTIVE

As indicated in *Chapter 1*, the premature failure at some locations along Mew Way located near Khayelitsha (Cape Town) has been observed as a result of grey water spillages on the asphalt surface. The failure is associated with stripping of the bitumen from the aggregate surface causing, in some cases, complete loss of the asphalt mixture's adhesive properties. This led to establishing an objective for developing asphalt mixtures with improved resistance to the chemicals present in grey water.

As failure of an asphalt mixture, subjected to grey water, is related to the moisture susceptibility of the mixture, it is required to investigate the adhesive properties of the mixture as well as the type of materials used to produce the mixture. From the literature review, it was established that factors such as the aggregate properties, bitumen properties, volumetric properties and compaction of an asphalt mixture have a significant influence on the moisture susceptibility of the mixture. The objective is, therefore, to combine these established factors to produce an asphalt mixture with improved moisture susceptibility in order to resist the moisture damage caused by grey water.

3.3 TEST VARIABLES TO CONSIDER

Test variables to consider include the aggregate properties, bitumen properties, volumetric properties and compaction of an asphalt mixture. These variables have a significant influence on the adhesive properties of an asphalt mixture which determines its moisture susceptibility. The test variables are discussed in the sections that follow.

3.3.1 AGGREGATE PROPERTIES

From *Section 2.7.1* of the Literature Review, it was established that aggregate properties such as the aggregate mineralogy, hardness and toughness, durability and soundness, surface texture, particle shape surface area, cleanliness, porosity and absorption influence the adhesive bond between the bitumen and aggregate. Read and Whiteoak (2003) stated that the aggregate has the most dominant influence on the bitumen-aggregate bond due to its properties.

Looking at the mineralogy of aggregates, the objective is to use aggregates with a mineralogy equal to that of basic rocks. Read and Whiteoak (2003) stated that basic rocks, such as limestone and basalt, have shown to improve the moisture susceptibility of asphalt mixtures. In South Africa, the types of aggregate used for asphalt production are dependent on their availability, sources and the location of construction.

Aggregates in asphalt mixtures should be tough and hard to resist the stresses induced by traffic. In addition, it should be durable and sound to resist weathering from environmental and traffic elements. The moisture susceptibility of asphalt mixtures has been shown to improve if aggregates with a rough surface texture, that is with angular shapes and a larger surface area are used in the production of the mixtures. Porosity and absorption are related to the filling of the void spaces located on the aggregate surface with bitumen. Improved porosity and absorption improve the bond strength between the bitumen and aggregate. Therefore, asphalt mixtures produced from aggregates with these properties exhibit improved adhesive properties.

Hornfels aggregate is used in the Western Cape for asphalt production (Sabita Manual 35/TRH8, 2016). Hornfels is a metamorphic rock consisting of shale, limestone, slate, sandstone and diabase. It is a hard and tough rock mined at quarries where its properties are monitored before crushing and screening according to specifications for use in construction. Hornfels aggregate is normally sourced from the nearest quarry that also specializes in asphalt production. Sabita Manual 35/TRH 8 specifies the following specification regarding the properties of aggregates used in asphalt production, as presented in Table 3.1.

Table 3. 1 – Specification for aggregate properties as adapted from Sabita Manual 35/TRH 8 (2016).

Aggregate Property	Test Name	SANS/ASTM Standard	Passing Criteria
Hardness/Toughness	Fines Aggregate Crushing Test: 10% FACT	SANS 3001-AG10	• Asphalt surfacing and base: Minimum 160 kN. • Open-graded surfacing and SMA: 210 kN.
	Aggregate Crushing Value (ACV)	SANS 3001-AG10	• Fine graded: minimum 25% (Fine). • Coarse graded: minimum 21%.
Soundness	Magnesium Sulphate Soundness	SANS 5839 SANS 3001-AG12	• 12% to 20% is normally acceptable. • Some specification requires ≤ 12% loss after 5 cycles.
Durability	Methylene Blue Adsorption Indicator	SANS 6243	• High-quality filler: Maximum value 5. • More than 5: Additional testing needed.
Particle Shape and Texture	Flakiness Index	SANS 3001-AG4	• 20 mm and 14 mm aggregate: Maximum 25. • 10 mm and 7.1 mm aggregate: maximum 30.
	Polished Stone Value (PSV)	SANS 3001-AG11	• Minimum 50.
	Fractured Faces	SANS 3001-AG4	• Fine graded: At least 50% of all particles should have three fractured faces. • Coarse graded and SMA: At least 95% of the plus 5 mm fractions should have one fractured face.
Water Absorption	Coarse Aggregate (> 5 mm)	SANS 3001-AG20	• Maximum 1% by mass.
	Fine Aggregate (< 5 mm)	SANS 3001-AG21	• Maximum 1.5% by mass.
Cleanliness	Sand Equivalency Test	SANS 3001-AG5	• Minimum 50 total fines fraction.
	Clay Lumps and Friable Particles	ASTM C142-97	• Maximum 1%.

Filler material is considered part of the aggregate component of an asphalt mixture. From *Appendix A* it was established that various types of filler materials are available in South Africa. However, research has shown that hydrate lime should be used in asphalt mixtures susceptible to moisture damage. In *Section 2.7.3.3* it was established that a chemical reaction between the hydrated lime and bitumen constituents occurs to produce a strong adhesive bond, which improves the moisture susceptibility of

asphalt mixtures. Hydrate lime was therefore considered to improve the grey water resistance of an asphalt mixture.

3.3.2 BITUMEN PROPERTIES

In *Section 2.7.2.3* of the Literature Review is was established that bitumen properties such as the rheology and modification of bitumen have an influence on the moisture susceptibility of an asphalt mixture. The engineering properties of asphalt mixtures can be improved by adjusting the rheological properties of the bitumen as they are responsible for the adhesive properties as well as the cohesive properties of the mixture. The rheological properties of bitumen can be modified through the addition of modifiers such as elastomers, plastomers and anti-stripping agents. Modifiers such as SBS, EVA, Sasobit Wax, Amine and ZycoTherm anti-stripping agents are available in South Africa and have been identified to improve the engineering properties of asphalt mixtures.

SBS modified binders improve the elastic recovery of asphalt mixtures. As asphalt surfacing tends to develop cracks overtime, it provides an easy way for grey water to ingress and cause distress. Improving the elastic recovery of an asphalt mixture provides increased resistance to cracking as the material is more flexible (Asphalt Academy-TG1, 2007). Therefore SBS modified binders improve the durability and the moisture susceptibility of an asphalt mixture.

EVA modified binders improve the stiffness of an asphalt mixture by providing improved resistance to permanent deformation. EVA modified binders improve the workability of asphalt mixtures, which may improve the compactibility of the mixture. Improved compaction results in a less permeable asphalt layer, which is less susceptible to moisture. EVA modified binders have been used in asphalt mixtures for areas subjected to fuel spillages (Asphalt Academy-TG1, 2007). These mixtures were very successful against chemical attack. Therefore, EVA modified binders may improve an asphalt mixture's resistance to grey water.

Sasobit® Wax is an F-T wax modifier which improves the workability of asphalt mixtures. In most cases it is used as a compaction agent. Mixes with Sasobit® wax have shown to be less susceptible to moisture especially when used in conjunction with an anti-stripping agent. These mixtures achieve low air void contents, which results in a less permeable asphalt layer (Prowell & Hurley, 2005). Therefore, Sasobit® wax modifier should be considered for improving the grey water resistance of asphalt mixtures.

Amine and ZycoTherm® anti-stripping agents are used to improve the asphalt mixtures resistance to stripping. Anti-stripping agents increase the bitumen-aggregate bond strength through chemical bonding. Boil tests were conducted on asphalt specimens produced with ZycoTherm® and SBS

modified binders. These specimens were conditioned with a grey water solutions consisting of salt and washing detergent. After six hours the ZycoTherm® and SBS modified binder samples retained 85% of their coatings (Zydex Industries, 2015(1)). Anti-stripping agents should be considered to improve the grey-water resistance of asphalt mixtures.

Improving the bitumen properties in conjunction with the aggregate properties may result in strong adhesive bonds to form between the bitumen and aggregate, which may improve the ability of the asphalt to resist moisture damage caused by grey water.

3.3.3 VOLUMETRIC PROPERTIES

The volumetric properties of an asphalt mixture will not improve adhesive properties, but it can be adjusted to produce a less permeable asphalt layer. The volumetric properties of an asphalt mixture are greatly influenced by the aggregate gradation, binder content, the presence of filler material and compaction.

From Sabita Manual 35/TRH 8 (2016) it follows that densely-graded sand skeleton mixtures should be considered to improve the moisture susceptibility of asphalt mixtures. Sand skeleton mixtures consist of the following types of asphalt gradations: semi-gap graded, gap-graded, medium continuous-graded and fine-continuous graded. Gap-graded asphalt mixtures are seldom used for economical reasons, due to high binder content requirements and difficulty with manufacturing as a result of material sources. However, continuously graded asphalt mixtures are frequently used (SAPEM Chapter 4, 2014).

Section 2.7.3.2 it was established that by increasing the binder content of an asphalt mixture, the bitumen film thickness will also increase. Therefore, increasing the binder content may improves the moisture susceptibility of asphalt mixtures. However, the binder content may only be increased up to a certain point until the volumetric properties of the asphalt mixture are negatively affected.

As established in *Appendix A,* the filler material serves the purpose of filling the voids in an asphalt mixture. Therefore, depending on the content of filler material used in asphalt mixtures, the permeability is reduced by reducing the air void content of the mixture. Filler material is used to adjust the volumetric properties of an asphalt mixture. It was established in *Section 2.7.3.3* that hydrated lime improves the moisture susceptibility of asphalt mixtures.

The level of compaction also significantly influences the volumetric properties of an asphalt mixture. The densification of an asphalt mixture during compaction is related to the permeability of the mixture. Compaction is discussed in the section that follows.

3.3.4 COMPACTION

As established before, the level of compaction determines the density of the asphalt, which is related to the permeability of the mixture. The permeability measures the penetration of air and water through the asphalt mixture. A less permeable asphalt mixture exhibits long term durability and protects the underlying pavement layers from water damage (Sabita Manual 35/TRH8, 2016). Permeability is controlled not only by compaction but also by aggregate packing characteristics, binder content and the air void content of an asphalt mixture. Compaction is important to achieve an asphalt mixture with improved resistance against grey water.

3.4 EXPERIMENTAL DESIGN

Considering the test variables to consider for improving the grey water susceptibility of asphalt mixtures, an experimental design was established for this study. The experimental design discusses the materials used, test matrix, test procedure and theoretical analysis of data captured.

3.4.1 MATERIALS

Materials used during this study were procured from Much Asphalt in Eersterivier. Since Malmesbury Hornfels is the preferred aggregate for asphalt surfacing in the Western Cape, it was selected for producing the asphalt mixtures identified for this study. Binders used for this study consisted of a combination of penetration grade bitumen and modified binders. These binders were procured from Much Asphalt and Colas (Epping Industria). The modified binders consisted of a combination of anti-stripping adhesive improvers and rutting resistance modifiers commonly used in HMA in South Africa. However, ZycoTherm® was the exception as this modifier was selected to evaluate its general performance in HMA and its capability to resist the effect of grey water. The binders used for this study were as follow:

- 50/70 Penetration Grade
- 50/70 + 1% Sasobit®
- 50/70 + 0.1%ZycoTherm®
- 50/70 + 0.07%ZycoTherm®
- SBS Modified Binder
- SBS + 1%Sasobit® Modified Binder
- SBS + Polyamine + 1% Sasobit®
- SBS + 1%Sasobit® +0.1%ZycoTherm®
- EVA Modified Binder
- EVA + 1%Sasobit® Modified Binder

- EVA+ 1%Sasobit® + 0.1%ZycoTherm®

Tests were conducted on five different asphalt mixture gradations. These gradations were: COLTO medium continuous grade, COTLO fine continuous graded, semi-gap graded, City of Cape Town fine graded (CCC) and a fine gradation mixture prepared by Much Asphalt (Much fine graded). The semi-gap and City of Cape Town fine (CCC) graded asphalt mixtures consisted of natural sand fractions in its gradation. Macassar sand was used for these asphalt mixtures. Lime active filler was used for the COLTO medium continuous and COLTO fine continuous graded asphalt mixtures to improve the adhesive properties thereof. The lime content used was 1% of the aggregate mass, whereas, in the case of extra lime requirements, a lime content of 2% was used for asphalt mixtures.

Additional information related to aggregate, binders and additives is presented in *Appendix A*.

3.4.2 EQUIPMENT

A fair amount of equipment was used during the execution of this experimental research methodology. Equipment used were:

- Gyratory compactor
- Moisture inducing simulating test (MIST) device
- Material Testing System (MTS) for ITS testing
- Mobile Model Load Simulator 3 (MMLS3)
- Laboratory scale MLS test bed setup and dual blade saw
- Water Heating Unit (WHU) and Dry Heating Unit (DHU)
- Laser Profilometer

Full details on equipment are discussed in *Appendix B*, except for the laser profilometer as important background on this equipment is required for this Chapter. Calibration of equipment such as the MIST device and MMLS3 will be discussed in this Chapter in detail.

3.4.2.1 Laser Profilometer

Part of the MLS-system is a laser profilometer, illustrated in Figure 3.2, for scanning the surface area of laboratory produced asphalt briquettes and slabs after MMLS3 trafficking. When laboratory trafficking is done using the MLS-test bed setup, the laser profilometer is used to scan the surface area of all nine asphalt briquettes after predetermined MMLS3 load cycle intervals. Prior to initial trafficking, reference scans of the asphalt briquettes surface are taken. Thereafter, scans are taken at the following load cycle intervals: 2500, 5000, 10 000, 20 000, 50 000 and 100 000. Once the surface area of the all nine asphalt briquettes are scanned at these predetermined load cycles, three-dimensional models of the asphalt surface are produced in Microsoft Excel. An example of a three-

dimensional model is illustrated in Figure 3.2. These models are used to determine the effect trafficking under wet or dry conditions has on the performance of an asphalt mixture.

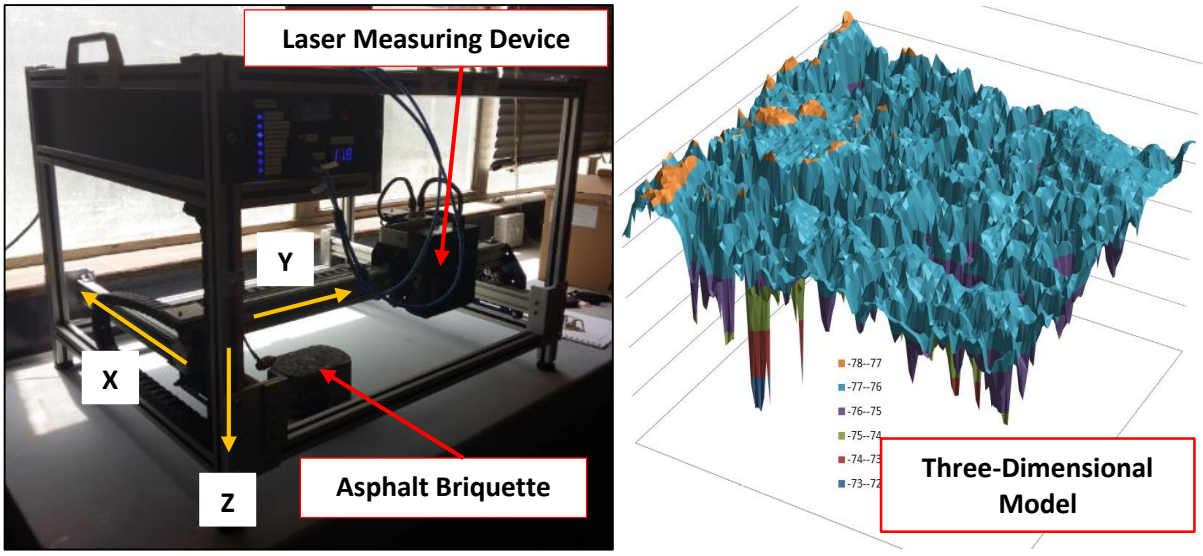

Figure 3. 2 – Laser Profilometer and Three-dimensional model of asphalt briquette surface.

As indicated before, the laser profilometer produces a three-dimensional model that establishes a co-ordinate system having an x-, y-, and z-axes. The z-axis is established in the vertical direction, from the laser measuring device to the surface of the asphalt specimen (see Figure 3.2). The maximum scan size in the x and y-direction is 489 mm and 444 mm respectively, however, the size of the area to scan is set by a specified size and number of incremental steps. The laser measuring device of the profilometer takes cross-sectional readings of the asphalt briquette's surface while it moves in the y-direction for a specified number of incremental steps. A specified number of incremental steps can also be set in the x-direction, which allows the laser measuring device to move in the x-direction while taking cross-sectional readings in the y-direction. A three-dimensional model is a combination of elevation readings in the z-direction and y-directional cross-sectional readings for a number of incremental steps in the x-direction. The minimum size of the incremental steps in both x- and y-direction is 0.25 mm. These small incremental steps provide the ability to investigate the permanent deformation and texture of the asphalt surface during trafficking under dry and wet conditions.

3.4.3 TEST MATRIX

As indicated before, five different asphalt gradations were tested during this study. A test matrix was setup to establish the binder combinations and the test types to be performed on asphalt specimens. The experimental research methodology was divided into two phases. The first phase consisted of tests, perform as part of an initial investigation, to determine the effect grey water has on the performance of asphalt mixtures, whereas the second phase consisted of MMLS3 trafficking.

3.4.3.1 Phase 1 – Initial Investigation

The test matrix for Phase 1 of the experimental research methodology is illustrated in Figures 3.3 and 3.4. Figure 3.3 illustrates seven binder combinations identified to produce COLTO medium continuous graded asphalt. A total of seven 150 mm asphalt briquettes per binder combination were prepared, where one sample was used to perform a maximum theoretical density test. Three briquettes received no water conditioning and three briquettes were subjected to grey water conditioning at 60°C using the MIST device. After conditioning these asphalt briquettes were subjected to indirect tensile strength (ITS) tests. Figure 3.4 illustrates the binder combinations identified to produce COLTO fine continuous graded, CCC fine graded, semi-gap graded and Much fine graded asphalt mixtures. Similar conditioning and tests were completed on these asphalt mixtures as for the COLTO medium continuous graded asphalt mixtures.

3.4.3.2 Phase 2 – Accelerated Pavement Trafficking

The test matrix for Phase 2 of the experimental research methodology is illustrated in Figures 3.5 and 3.6. During this phase, MMLS3 trafficking tests were performed under dry (no water) and wet (grey water) conditions. Figure 3.5 illustrates the binder combinations identified to produce COLTO medium continuous graded asphalt. Figure 3.6 illustrates the binder combinations identified to produce COLTO fine continuous graded, CCC fine graded and Much fine graded asphalt. A total of six asphalt briquettes were prepared per binder combination of which three briquettes were subjected dry MMLS3 trafficking and three subjected to wet MMLS3 trafficking. Each briquette received 100 000 MMLS3 load cycles at a temperature of 40°C.

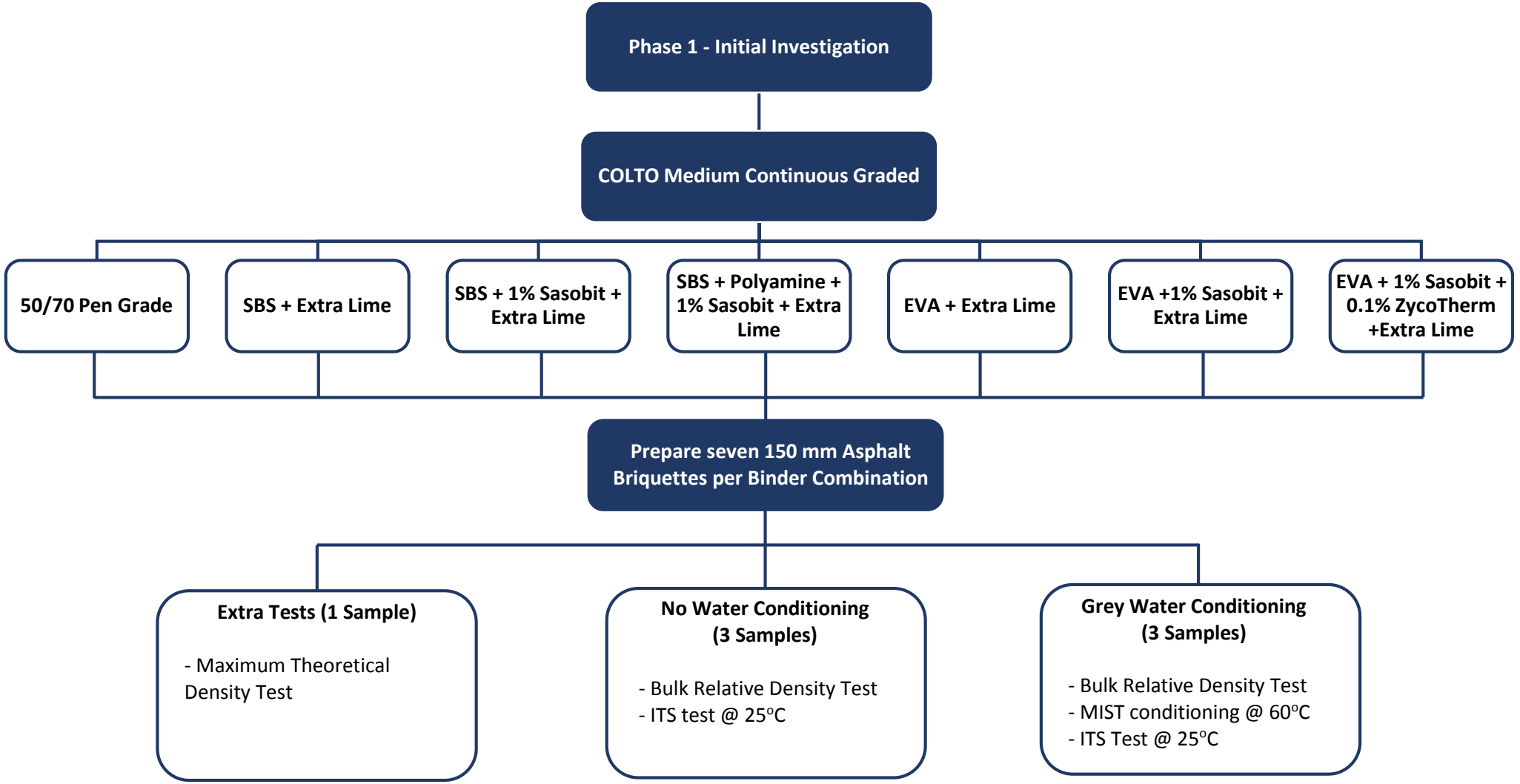

Figure 3. 3 - Phase 1: COLTO medium continuous graded asphalt test matrix.

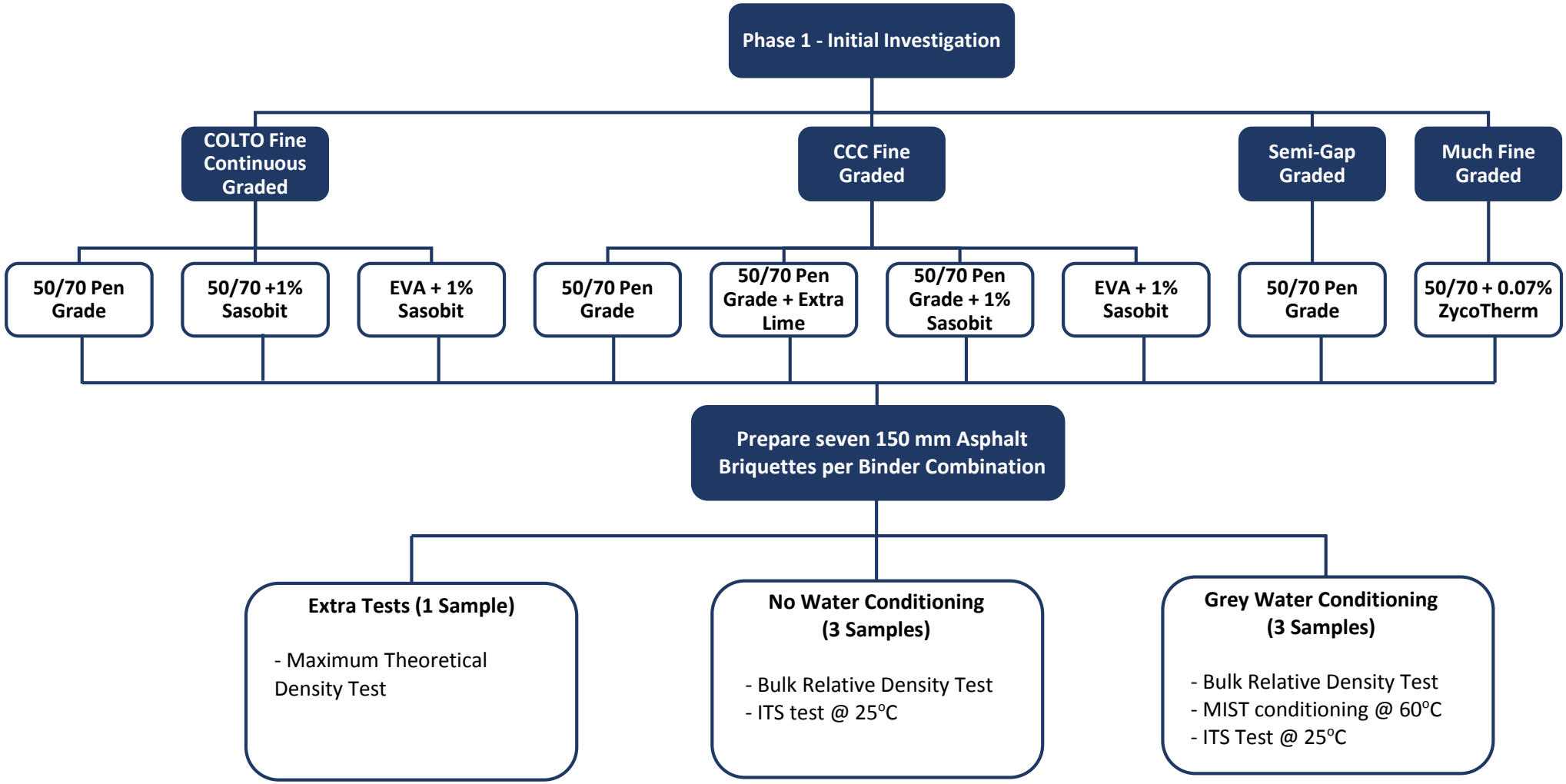

Figure 3. 4 – Phase 1: COLTO fine continuous graded, CCC fine graded, Semi-gap graded and Much Fine graded test matrix.

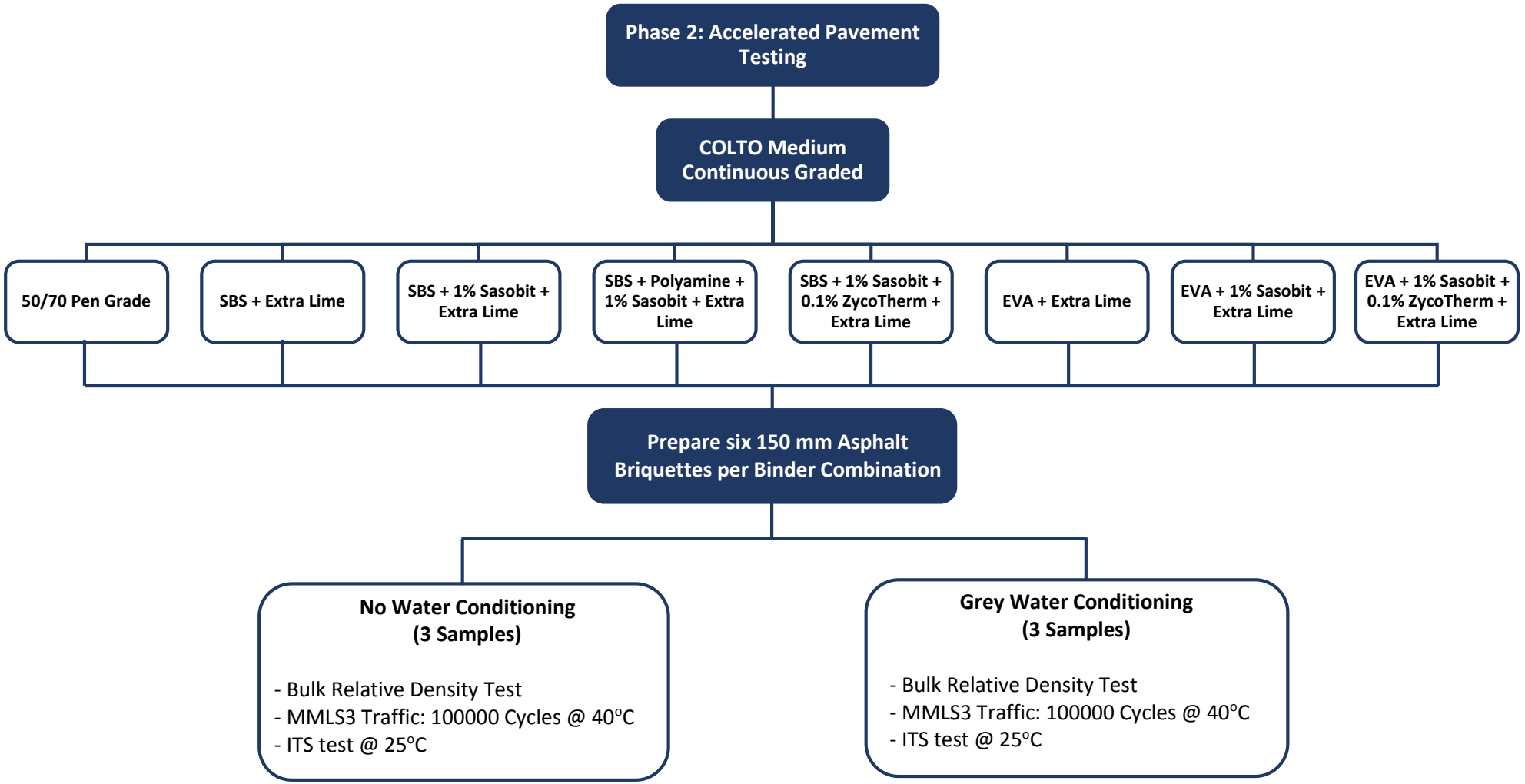

Figure 3. 5 – Phase 2: COLTO continuous graded asphalt test matrix.

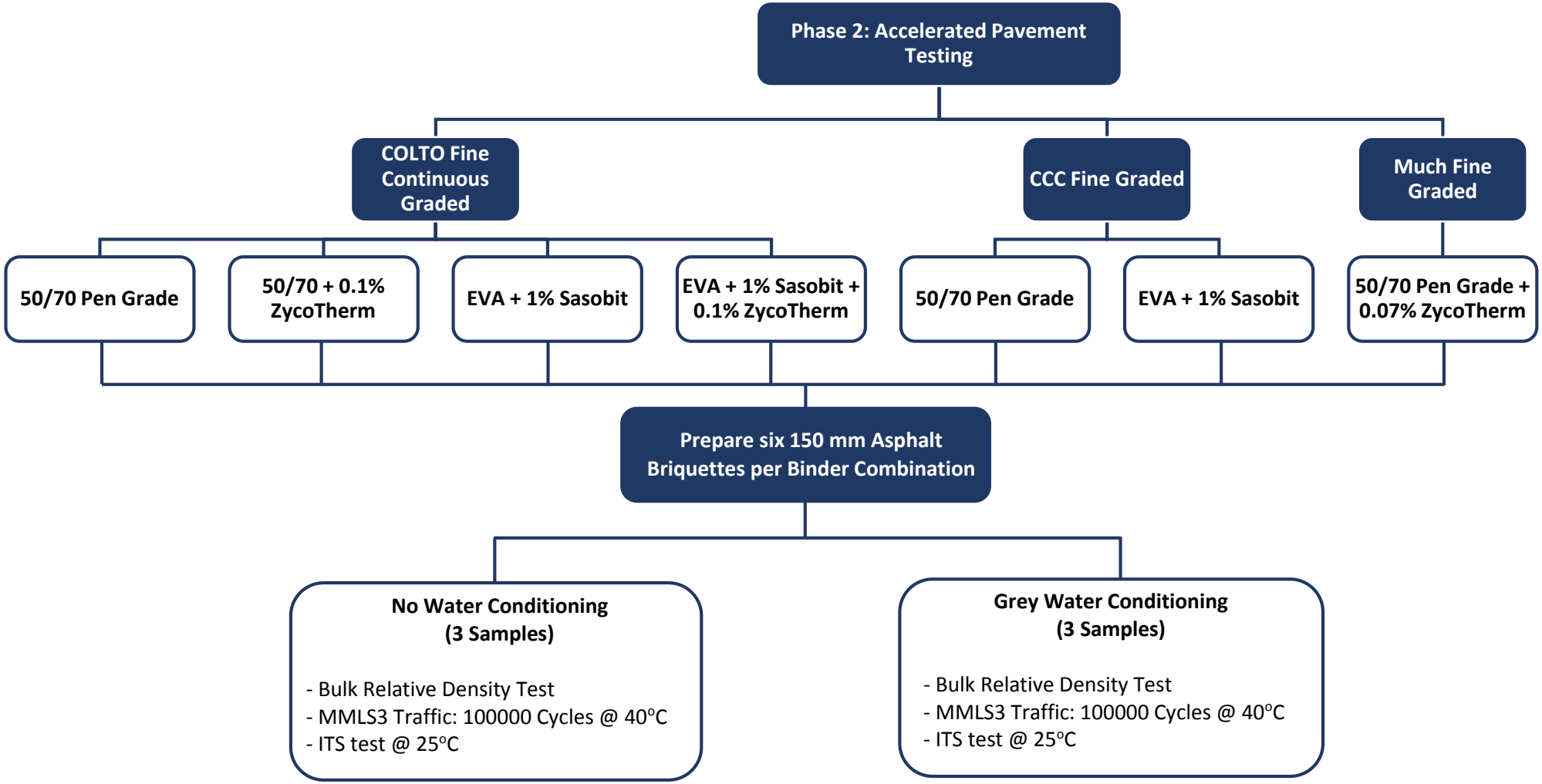

Figure 3. 6 – Phase 2: COLTO fine continuous graded, CCC fine graded and Much fine graded asphalt test matrix.

3.5 TEST PROCEDURE

The layout test procedure for the experimental research methodology is illustrated in Figure 3.7.

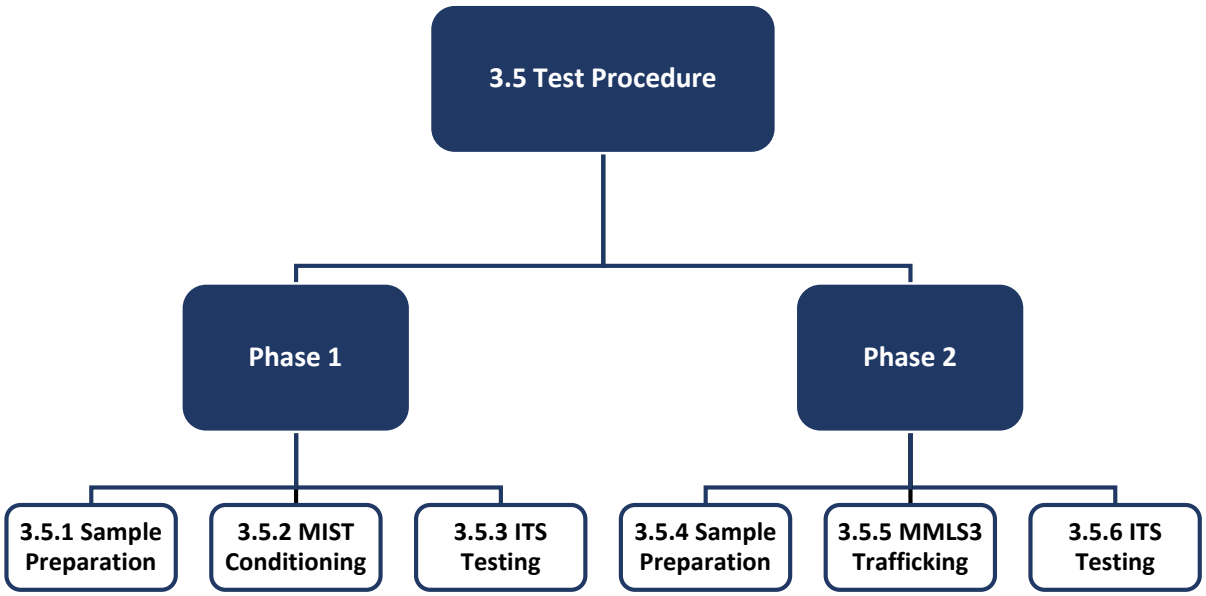

Figure 3. 7 - Layout of test procedure for this research.

3.5.1 PHASE 1: SAMPLE PREPARATION

3.5.1.1 Sample Information Sheet

An asphalt sample information sheet was compiled and completed for each asphalt briquette prepared during phase 1 of this study. This sheet contains quality control procedures and all information related to sample composition, sample preparation, MIST conditioning and ITS results. An example of the sample information sheet is shown in *Appendix D*.

3.5.1.2 Material Requirements

As indicated before, samples prepared for Phase 1 of this experimental research methodology consisted of 150 mm diameter asphalt briquettes with a height of 80 mm. Sample preparation started with the sieving of Malmesbury Hornfels and Macassar sand into material fraction sizes. The following SANS 3001 approved sieve sizes were used for sieving the Malmesbury Hornfels: 20 mm, 14 mm, 10 mm, 7.1 mm, 5 mm, 2 mm, 1 mm, 0.6 mm, 0.3 mm, 0.15 mm and 0.075 mm. Sieve sizes used for sieving the Macassar sand were: 5 mm, 2 mm, 1 mm, 0.6 mm, 0.3 mm, 0.15 mm and 0.075 mm. Thereafter, the sieved materials were combined according to a specific gradation. The five different asphalt gradations for this study were compiled by Much Asphalt according to COLTO specification. The gradation of these five asphalt mixtures

is presented in Table 3.2. Refer also to *Appendix E* for information sheets on asphalt gradations used for this study.

Table 3. 2 - Gradation of asphalt mixtures prepared for the Grey Water Resistant Asphalt Study.

Sieve Size (mm)	Percentage Passing (%)						
	COLTO Medium Continuous Graded	COLTO Fine Continuous Graded	CCC Fine Graded		Semi-Gap graded		Much Asphalt Fine Graded
	H (100%)	H (100%)	H (90%)	S (10%)	H (65%)	S (35%)	H
19	100	-	100	-	100	-	-
14	99	-	98	-	98	-	-
10	87	100	86	-	83	-	100
7.1	73	98	72	-	68	-	98
5	65	85	65	-	55	100	84
2	44	56	46	-	31.2	16.8	55
1	28	37	28.8	3.2	28.6	15.4	39
0.600	18	25	22.5	2.5	22.7	12.3	30
0.300	12	17	15.3	1.7	14.3	7.7	20
0.150	9	11	8.1	0.9	5.2	2.8	10
0.075	7.4	9.1	5.5	0.6	3.2	1.8	6.1

Note: H – Malmesbury Hornfels; S – Macassar Sand

Using the volumetric properties of each mixture design as presented in Appendix D, it was possible to determine the total amount of Malmesbury Hornfels and Macassar sand required per material fraction. Initially, a binder content of 5.5% was used for all asphalt mixtures as presented in Table 3.3, which is suggested by the *Interim Guidelines for the Design of Hot-Mix Asphalt in South Africa (2001).* However, for the COLTO fine continuous graded asphalt mixtures, it was necessary to increase the binder content to 6.0% as volumetric requirements were not achieved with a 5.5% binder content of. The aggregate requirements to produce a single asphalt briquette for each mixture design were determined and are presented in Table 3.3.

Table 3. 3 - Determining mass aggregate required for sample preparation per asphalt mixture.

Requirements	CM @ 5.5% binder content	CF @ 6.0% binder content	CCC @ 5.5% binder content	SG @ 5.5% binder content	MF @ 5.5% binder content
Max. Theoretical Relative Density (kg/m^3)	2 500	2 494	2 498	2 486	2 502
Voids in Mixture (%)	4.6	5.6	2.9	5.3	-
Sample Diameter (m)	0.15	0.15	0.15	0.15	0.15
Sample Height (m)	0.075	0.075	0.075	0.075	0.100
Sample Volume (m^3)	0.0013	0.0013	0.0013	0.0013	
Aggregate Mass (g)	**3161**	**3120**	**3215**	**3120**	-
Lime Content (%)	1	1	-	-	-

Notes: CM – COLTO Medium Graded; CF – COLTO Fine Graded; CCC – City of Cape Town Fine Graded; SG- Semi-Gap Graded; MF- Much Asphalt Fine Graded.

The required aggregate mass as shown in Table 3.3 consists of the Malmesbury Hornfels, or as in some cases, a combination of Malmesbury Hornfels and Macassar sand (See Table 5.4). Aggregate and lime active filler requirements, as presented in the test matrix, were weighed and sealed using plastic bags. Information related to the dry material constituents were captured on the sample information sheet for each prepared sample as mentioned in *Section 3.5.1.1*.

3.5.1.3 Asphalt Mixing

Four of the five asphalt gradations were used to prepare asphalt briquettes at the University of Stellenbosch. These gradations were: COLTO medium continuous graded, COLTO fine continuous graded, CCC fine graded and semi-gap graded. The fifth asphalt gradation, referred to as the Much fine graded, was prepared by Much Asphalt at their Eersterivier plant.

Mixing of asphalt samples required preheating the aggregate, binders and mixing equipment. The aggregate was heated to a temperature of 180°C to ensure that good coating of the aggregate surface with bitumen was achieved. Majority binders were preheated to a temperature of 160°C prior mixing. However, binders consisting of SBS modifier were preheated to a temperature of 170°C as the viscosity of these binders was not suitable for mixing at 160°C.

The mixing procedure started with weighing the preheated aggregate to determine the mass binder to be added. The adding of mass binder was determined from Equation 3.1.

$$BM = AM \times \frac{BC}{(100-BC)} \qquad \textit{Equation 3.1}$$

where:

$BM = Binder\ Mass\ (g)$

$AM = Aggregate\ Mass\ (g)$

$BC = Binder\ Content\ (\%)$

Asphalt samples were mixed individually and not prepared in bulk mixes. The aggregate and binder were hand mixed on a hot-plate using a preheated bowl and spade. The asphalt was mixed until complete coating of the aggregate surface with binder was achieved. Figure 3.8 illustrates the mixing procedure.

Figure 3. 8 - Asphalt mixing procedure.

During mixing, the temperature of the asphalt mixture was constantly measured using a calibrated thermometer. The temperature was recorded on the sample information sheet. After mixing, asphalt samples were placed in an oven set to a temperature of 160°C to ensure that the correct compaction temperature was achieved.

A total of seven asphalt samples were mixed per binder combination as presented in the test matrix (Figures 3.3. and 3.4). Six samples were compacted, while the seventh uncompacted sample was used for conducting maximum theoretical relative density tests on the asphalt mixture.

3.5.1.4 Compaction

Prior to compaction, a 150 mm diameter gyratory compactor mould was preheated to a temperature of 160°C. Compaction temperatures for the four asphalt gradations prepared at the University of Stellenbosch ranged from 138°C to 140°C.

The gyratory compactor was prepared and set to compact asphalt samples to a design number (N_{Design}) of 100 gyrations. The vertical compaction pressure was set to 600 kPa, whereas the compaction angle was set to 1.25 degrees. The gyratory compactor computers required the maximum theoretical relative density in order to determine the change in sample density and height per gyration during compaction. See *Appendix B* for full details on the gyratory compactor.

Once the gyratory compactor's input parameters were set, the asphalt sample was removed from the oven and placed in the gyratory compactor mould. The asphalt's sample mass was determined and entered into the gyratory compactor's computer. The temperature of the asphalt sample and gyratory compactor mould was measured using a calibrated thermometer and recorded on the sample information sheet. It was aimed to achieve an asphalt sample and gyratory compactor mould temperature of 160°C

prior compaction, as the temperature usually drops during compaction to the required temperature range of 138°C to 140°C. After compaction, the asphalt sample was extracted from the mould and left to cool down. Figure 3.9 illustrates the compaction procedure.

Figure 3. 9 - Compaction of asphalt briquettes.

3.5.1.5 Determining Voids in Mixture

The maximum theoretical relative density (Rice Density) and bulk relative density (BRD) were required to establish the void content (VIM) of the prepared asphalt briquettes. The maximum theoretical relative density was determined from an uncompacted asphalt sample per binder combination in accordance with SANS 3001-AS11. BRD's were completed for six compacted asphalt briquettes per binder combination, according to SANS 3001-AS10. Table 3.4 summarizes the volumetric properties determined for each prepared asphalt briquette.

Table 3. 4 - Volumetric properties applicable to research.

Symbol or Calculation	Description	Test method
MVD	Max theoretical relative density (kg/m³)	SANS 3001-AS11
BD_{Mix}	Bulk relative density (kg/m³)	SANS 3001-AS10
$\boldsymbol{VIM} = \frac{(MVD - BD_{Mix})}{MVD} \times 100$	Voids in the Mix (%)	-

The maximum theoretical density and the average bulk relative density results per binder combination for Phase 1 of this study are presented in Table 3.5. The average VIM per asphalt mixture design was calculated and is also presented in Table 3.5.

Table 3. 5 - Asphalt mixture's volumetric properties (Phase 1).

Gradation Type	Binder Type	Maximum Theoretical Relative Density (kg/m³)	Bulk Relative Density (kg/m³)	Voids in the Mix (%)
COLTO Medium	50/70 Penetration Grade Bitumen	2 486	2 358	5.2
COLTO Medium	SBS + Extra Lime	2 479	2 369	4.4
COLTO Medium	SBS + 1%Sasobit+Extra Lime	2 492	2 368	5.0
COLTO Medium	SBS + Polyamine + 1%Sasobit + Extra Lime	2 475	2 367	4.4
COLTO Medium	EVA +Extra Lime	2 487	2 376	4.5
COLTO Medium	EVA +1%Sasobit+Extra Lime	2 479	2 373	4.3
COLTO Medium	EVA + 1%Sasobit + 0.1%ZycoTherm + Extra Lime	2 475	2 379	3.9
COLTO Fine	50/70 Penetration Grade Bitumen	2 422	2 297	5.2
COLTO Fine	50/70 + 1%Sasobit	2 484	2 346	5.6
COLTO Fine	EVA + 1%Sasobit	2 461	2 329	5.4
CCC Fine	50/70 Penetration Grade Bitumen	2 468	2 334	5.4
CCC Fine	50/70 + Extra Lime	2 478	2 337	5.7
CCC Fine	50/70 + 1%Sasobit	2 484	2 346	5.6
CCC Fine	EVA + 1%Sasobit	2 470	2 339	5.3
Semi-Gap	50/70 Penetration Grade Bitumen	2 483	2 342	5.7
Much Fine	50/70 + 0.07%ZycoTherm	2 502	2 345	6.3

3.5.2 PHASE 1: MIST CONDITIONING

Three asphalt briquettes per binder combination were subjected to MIST conditioning during Phase 1 of this study. Refer to *Appendix B* for details on the MIST device used for conditioning purposes. Previous research on the effects of grey water on asphalt, completed by Petersen (2013), used a grey water concentration of 1% of volume of water for conditioning purposes (E.g. 200 gram of surfactant per 20 litre of water). This concentration was considered extremely high and did not simulate a realistic concentration of grey water that is typically spilled onto the road surface. Therefore, the grey water concentration produced during this study consisted of 1% surfactants per 100 litre of clean water. In addition, a survey completed by Petersen (2013) on a section of Lansdowne Road in Khayelitsha indicated that detergents such as OMO laundry detergent and Sunlight dishwashing liquid are predominately used by household. Therefore, MIST conditioning was done at a temperature of 60°C with a grey water concentration of 1% surfactants (0.5% OMO® laundry detergent and 0.5% Sunlight® dishwashing liquid) per mass of clean water. The MIST device has a capacity to condition three 80 mm asphalt briquettes simultaneously. However, trail conditioning tests indicated erosion of the third asphalt briquette which was in direct contact with the water pulse. As a consequence, the number of asphalt briquettes to condition simultaneously in the MIST device was reduced to two. A steel plate was also placed on top of the second asphalt briquette in the triaxle cell to prevent erosion of the briquette surface.

With the temperature and grey water concentration set, asphalt briquettes were placed in the triaxial cell and sealed to prevent pressure loss during testing. The MIST device was switched on and time was given for the triaxle cell to fill with grey water. Once the asphalt briquettes were submerged in the triaxial cell, the pressure of the pulse was set to 150 kPa by adjusting a pressure regulator. MIST conditioning was done for a duration of 6 hours and 2 minutes as suggested by Jenkins and Twagira (2009).

Complete failure of semi-gap and Much fine graded asphalt briquettes was observed before completion of grey water MIST conditioning. Figure 3.10 illustrates the failed asphalt briquettes.

It was possible to complete MIST conditioning of one Much fine graded asphalt briquette for ITS testing. However, the semi-gap graded mixture was unsuccessful in withstanding grey water MIST conditioning. It was therefore decided to remove this asphalt mixture for further testing in Phase 2 experimental research methodology.

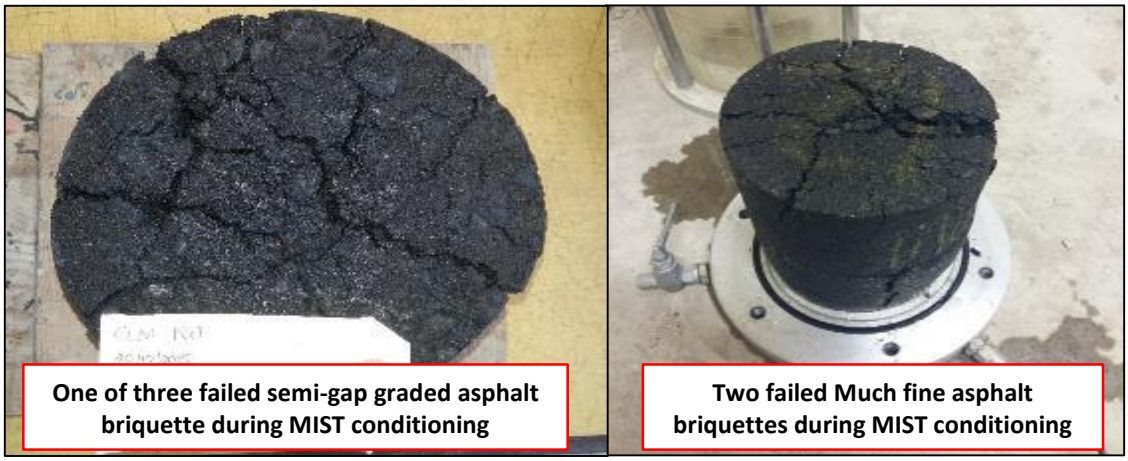

Figure 3. 10 - Failed semi-gap and Much fine graded asphalt briquettes during MIST conditioning.

It was suspected that failure of the semi-gap graded asphalt mixture was related to the high sand content present in this asphalt mixture. The semi-gap graded asphalt mixture required a Macassar sand content of 35%, which is unusually high. COLTO specification sets a maximum sand content limit of 15% for semi-gap grade asphalt mixtures. The angularity of the Macassar sand may also be related to the premature failures.

Clean water MIST conditioning and ITS tests were also done on some binder combinations as spot checks to compare with grey water conditioned ITS results. Although not part of the test matrix, clean water MIST conditioning was done on the following gradations and binder combinations:

- 50/70 Penetration Grade (COLTO medium continuous graded)

- SBS + 1% Sasobit + Extra Lime (COLTO medium continuous graded)
- EVA + 1% Sasobit + Extra Lime (COLTO medium continuous graded)
- EVA + 1% Sasobit (COLTO fine continuous graded)
- EVA + 1% Sasobit (CCC fine graded)

Clean water MIST conditioning indicated whether the grey water has a significant influence on the asphalt's performance. Three asphalt briquettes per binder combination were prepared and subjected to clean water conditioning.

3.5.3 PHASE 1: INDIRECT TENSILE STRENGTH TESTING

ITS tests indicated the effect of grey water conditioning on the performance of asphalt mixtures. These tests were conducted as 25°C at a loading rate of 50.8 mm/min. Refer to *Appendix B* for full details on the MTS device. A test temperature of 25°C was selected as more elastic than viscous material behaviour was required during testing. A summary of average ITS results per binder combination, subjected to no water and grey water conditioning, is presented in Table 3.6.

Table 3. 6 - ITS results for phase 1 of Grey Water study.

Gradation Type	Binder Type	ITS_{NC} (kPa)	ITS_{GW} (kPa)	TSR (%)
COLTO Medium	50/70 Penetration Grade Bitumen	752	490	65
COLTO Medium	SBS + Extra Lime	820	598	73
COLTO Medium	SBS + 1%Sasobit+Extra Lime	850	644	72
COLTO Medium	SBS + Polyamine + 1%Sasobit + Extra Lime	683	628	92
COLTO Medium	EVA +Extra Lime	766	683	72
COLTO Medium	EVA +1%Sasobit+Extra Lime	754	724	96
COLTO Medium	EVA + 1%Sasobit + 0.1%ZycoTherm + Extra Lime	931	942	101
COLTO Fine	50/70 Penetration Grade Bitumen	855	130	15
COLTO Fine	50/70 + 1%Sasobit	750	403	54
COLTO Fine	EVA + 1%Sasobit	793	468	59
CCC Fine	50/70 Penetration Grade Bitumen	992	172	17
CCC Fine	50/70 + Extra Lime	992	438	44
CCC Fine	50/70 + 1%Sasobit	866	271	31
CCC Fine	EVA + 1%Sasobit	1023	179	17
Semi-Gap	50/70 Penetration Grade Bitumen	875	DNF	-
Much Fine	50/70 + 0.07%ZycoTherm	934	561	60

Notes: NC - No-Conditioning; GW - Grey Water Conditioning; DNF - Did Not Finish

From Table 3.6 the tensile strength ratios (TSR) were calculated, which represents the retained strength after grey water conditioning. A ratio of less than 100 percent indicates that the asphalt strength reduced as a result of grey water conditioning. A ratio greater than 100 percent indicates that the asphalt strength was increased as a result of grey water conditioning. ITS result for Phase 1 is discussed in detail in Chapter 5.

3.5.4 PHASE 2: SAMPLE PREPARATION

From the ITS results of Phase 1 of the experimental research methodology, a new test matrix (Figures 3.5 and 3.6) was established to evaluate the grey water resistance and permanent deformation of asphalt mixtures through MMLS3 under dry (no water) and wet (grey water) trafficking conditions. The test matrix for Phase 2 consisted of selected binder combinations from Phase 2 and additional binder combinations. A total of six compacted asphalt briquettes per binder combination were prepared, with three briquettes subjected to dry (no-water) MMLS3 trafficking and three briquettes subjected to wet (grey water) MMLS3 trafficking.

Sample preparation for Phase 2 of the experimental research methodology was approached in a similar as was discussed in *Section 3.5.1*. A sample information sheet was also completed for each asphalt briquette prepared for this phase.

Maximum theoretical relative density tests and BRD's for additional binder combinations were completed to determine the voids in the mixture (VIM). Table 3.7 summarizes the average VIM per binder combination for Phase 2.

Table 3. 7 - Asphalt mixture's volumetric properties (Phase 2).

Gradation Type	Binder Type	Maximum Theoretical Relative Density (kg/m^3)	Bulk Relative Density (kg/m^3)	Voids in the Mix (%)
COLTO Medium	50/70 Penetration Grade Bitumen	2 486	2 362	5.0
COLTO Medium	SBS + Extra Lime	2 479	2 378	4.1
COLTO Medium	SBS + 1%Sasobit+Extra Lime	2 495	2 383	4.5
COLTO Medium	SBS + Polyamine + 1%Sasobit + Extra Lime	2 489	2 366	4.9
COLTO Medium	SBS + 1%Sasobit + 0.1%ZycoTherm + Extra Lime	2 495	2 390	3.9
COLTO Medium	EVA + Extra Lime	2 487	2 381	3.6
COLTO Medium	EVA + 1%Sasobit + Extra Lime	2 470	2 380	3.9
COLTO Medium	EVA + 1%Sasobit + 0.1%ZycoTherm + Extra Lime	2 475	2 374	4.8
COLTO Fine	50/70 Penetration Grade Bitumen	2 422	2 294	5.3
COLTO Fine	50/70 + 0.1%ZycoTherm	2 475	2 351	3.4
COLTO Fine	EVA + 1%Sasobit	2 486	2 357	4.5
COLTO Fine	EVA + 1%Sasobit + 0.1%ZycoTherm	2 433	2 349	5.1
CCC Fine	50/70 Penetration Grade Bitumen	2 467	2 338	5.3
CCC Fine	EVA + 1%Sasobit	2 486	2 351	4.8
Much Fine	50/70 + 0.07%ZycoTherm	2 502	2 345	6.3

After mixing, compaction and determining the volumetric properties two parallel segments were machined-off from the circular asphalt briquettes using a dual blade saw. Full details on the dual blade saw are shown in *Appendix B*. These segments enables one to fit nine asphalt briquettes next to each

other in a test bed designed for laboratory scale MMLS3 trafficking. Refer to *Appendix B* for full details on the test bed.

3.5.5 PHASE 2: MMLS3 (APT)

3.5.5.1 MMLS3: Test Parameters

The MMLS3 Operator's Manual (2012) assisted in preparing the MMLS3 trafficking tests. The MMLS3 is a third scale accelerated pavement trafficking device which scales down a standard 80 kN axle to perform trafficking tests on a laboratory scale. The MMLS3 uses full-scale tyre pressures. However, as a result of a scaled down contact pressure area, the transferred load is reduced by 9 times that of a single tyre of a double bogie configuration of an E80 axle. Before testing, it was required to calibrate the MMLS3.

The calibration process first required the inflation of the four tyres on the MMLS3 to a pressure of 700 kPa (SANS 3001-PD1, 2016). Each of the four wheels of the MMLS3 is connected to a bogie system. The bogie system on the MMLS3 consists of a spring mechanism and a set of rubber stoppers which are adjusted to set the correct load transfer to the pavement surface. A calibration unit supplied with the MMLS3 system was used to set the correct load transfer. The calibration unit presses down on the wheel of the MMLS3 until the set of rubber stoppers moves 10 mm away from the bogie frame. A load is transferred to the wheel which the calibration unit measures and displays. Should the load be less than desired, the spring mechanism should be tightened by turning it clockwise. If the measured load is greater than the desired load, the spring mechanism should be turned counter clockwise in order to loosen it. The desired load for MMLS3 testing was 2.2 kN as suggested for gyratory compacted asphalt specimens with a thickness greater than 75 mm (SANS 3001-PD1, 2016). The calibration process needed to be completed for each of the four wheels on the MMLS3 prior testing. Figure 3.11 illustrates the calibration unit.

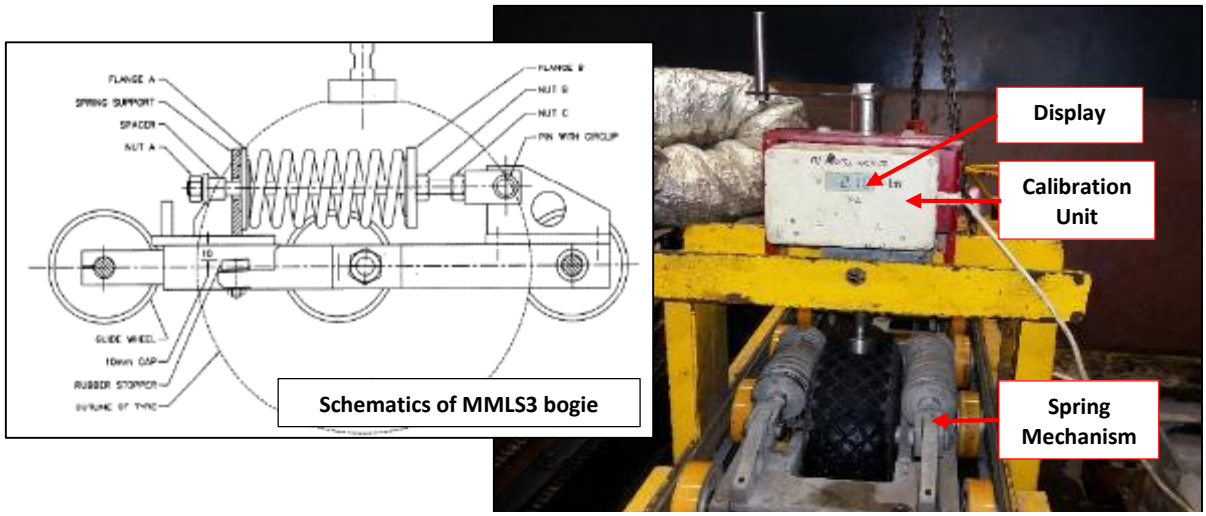

Figure 3. 11 - MMLS3 calibration unit and spring mechanism.

A trafficking speed of 7200 loads repetitions per hour, as suggested by the SANS 3001-PD1 for free flow highway traffic, was selected. MMLS3 trafficking was done at a temperature of 40°C under both dry (no water) and wet (grey water) conditions for a total of 100 000 load repetitions. This temperature deviates from the 60°C as suggested by SANS 3001-PD1. However, permanent deformation was not identified as the primary failure mechanism for Mew Way. Instead stripping of the binder due to grey water conditioning was identified as the primary failure mechanism. A greater indication of the stripping of the binder was given, by lowering the trafficking temperature to 40°C, as this temperature was below the terminal rutting zone of 50°C to 60°C. However, permanent deformation was still evaluated at this temperature.

3.5.5.2 MMLS3: Dry Testing Condition

Under dry conditions, the MMLS3 trafficking was completed without the presence of water. Dry MMLS3 trafficking required a dry heating unit (DHU) to be installed in order to heat the surface of the asphalt briquettes. Refer to *Appendix B* for details of the DHU. SANS 3001-PD1 in conjunction with the MMLS3 Supplementary Items Manual (2011) were used as guidelines to complete the dry MMLS3 trafficking.

The test procedure that was followed for dry MMLS3 trafficking is illustrated in Figure 3.12. The numbered steps below discuss the procedures followed as illustrated in Figure 3.12.

1. Nine prepared asphalt briquettes were installed in a test bed and clamped together to prevent movement during trafficking (see *Appendix B* for details of the test bed). The asphalt briquettes were assigned a location number in the test bed as indicated. SANS 3001-PD1 suggests that nine asphalt briquettes of the same binder combination should be prepared and installed in the test bed. However, it was decided to test three binder combinations in a single MMLS3 test by preparing only three asphalt briquettes per binder combination. This is illustrated in Figure 3.12. The MMLS3 was calibrated as discussed in *Section 3.5.5.1.*

2. The MML3 was placed on the test bed and levelled with its four adjustable legs. The legs were adjusted until the rubber stoppers on each bogie moved 10 mm away from the bogie frame to ensure that the calibrated wheel load (see *Section 3.5.5.1* and *Appendix A*) was exerted on the asphalt briquettes. An initial 100 cycles were completed to ensure that the briquettes were embedded in the test bed.

3. The MMLS3 was removed from the test bed and initial laser profilometer readings were completed (refer to *Section 3.4.2.1* for details of the laser profilometer). The surface of each

asphalt briquette was scanned individually. The laser profilometer was set to measure the elevation (z-coordinates) at 1 mm increments in the y-direction until the total distance measured was equal to 170 mm. Once readings in the y-direction were completed the laser profilometer was set to move in increments of 2 mm in the x-direction where a new line of elevation readings (z-coordinates) in the y-direction were measured. Movement of the laser profilometer in the x-direction was repeated until the total distance measured was equal to 102 mm. This concept is illustrated in Figure 3.12. A reference point was selected for each of the nine asphalt briquettes from where profilometer measurements were started. Correct alignment of the laser profilometer with the reference point was ensured by wooden spacers which were clamped to index bars with markings as indicated in Figure 3.12.

In addition to laser profilometer readings, sand patch tests were performed according to SANS 3001-BT11:2011. Sand patch tests were completed at locations 2, 3, 5, 6, 7 and 8 in the test bed. Due to the small surface area of each asphalt briquette, the standard 50 ml volume glass beats that are suggested to perform this test, could not be used. A constant volume of 3 ml glass beats was therefore selected to perform sand patch tests. The test was executed as specified in the SANS document to determine the texture of the asphalt briquettes' surface.

4. Once the initial profilometer readings were completed, the MMLS3 was placed on the test bed, where it was levelled and the rubber stoppers were checked. An orange canvas was used to cover the MMLS3 during dry trafficking in order to create an environment with a constant temperature. Ventilation pipes and heat transfer boxes, connected to the dry heating unit, were installed on the sides of the test bed to blow heated air on the asphalt briquettes' surface. A thermometer was used to measure the temperature of the asphalt briquettes surface until a temperature of 40^{o}C was achieved. Once the test temperature was reached, the dry heating unit's temperature controller kept the temperature constant at 40^{o}C during testing. MMLS3 testing was stopped after the predetermined number of load cycle intervals was reached, to perform laser profilometer readings and sand patch tests. Table 3.8 summarises the load cycle intervals as suggested by SANS 3001-PD1. The time to complete each load cycle interval is also presented.

Table 3. 8 - Summary of load cycle intervals.

Load Cycle Interval	Time (@ 7200 cycles/hr)	Profilometer Readings	Sand Patch Test
0	0 min	•	•
2 500	21 min	•	
5 000	21 min	•	
10 000	42 min	•	
20 000	1 hr 23 min	•	
50 000	4 hr 10 min	•	•
100 000	6 hr 58 min	•	•

Steps three and four were repeated until a total of 100 000 load cycles were achieved. The MMLS3 had to be calibrated after each load cycle interval before testing could continue.

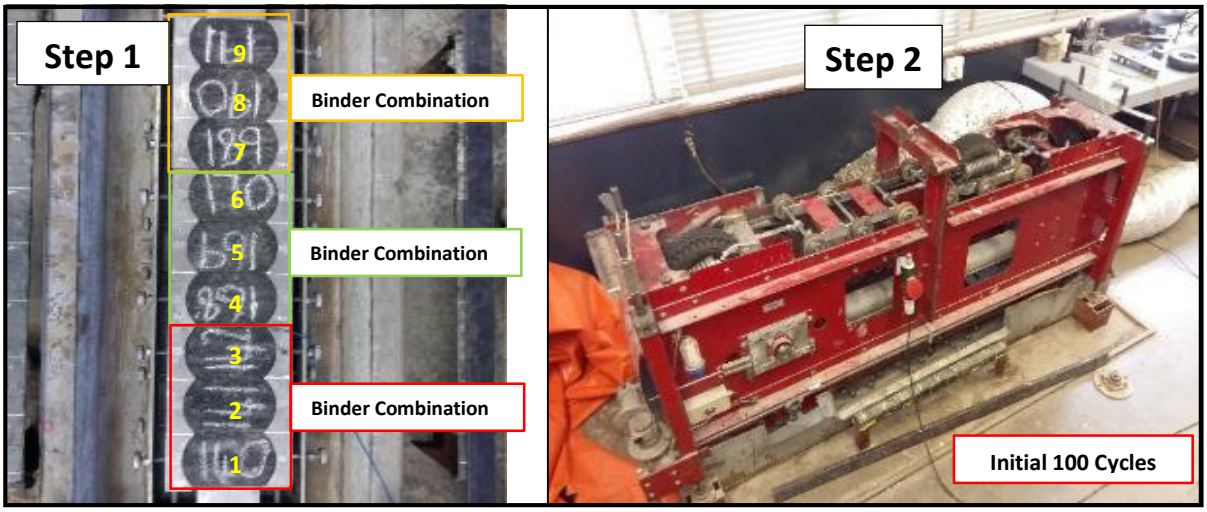

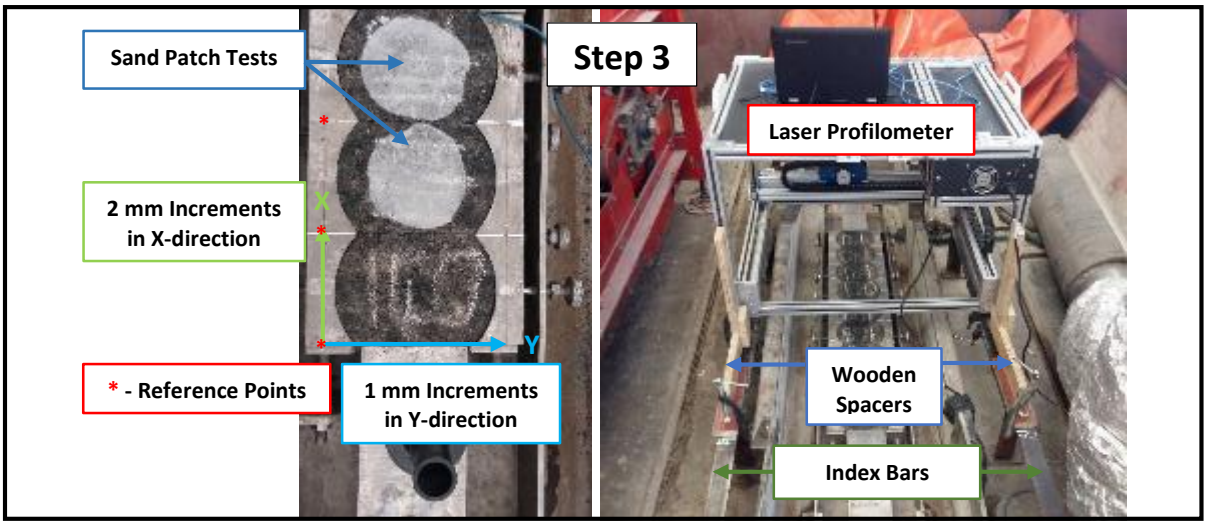

Note: This figure continuous on the next page.

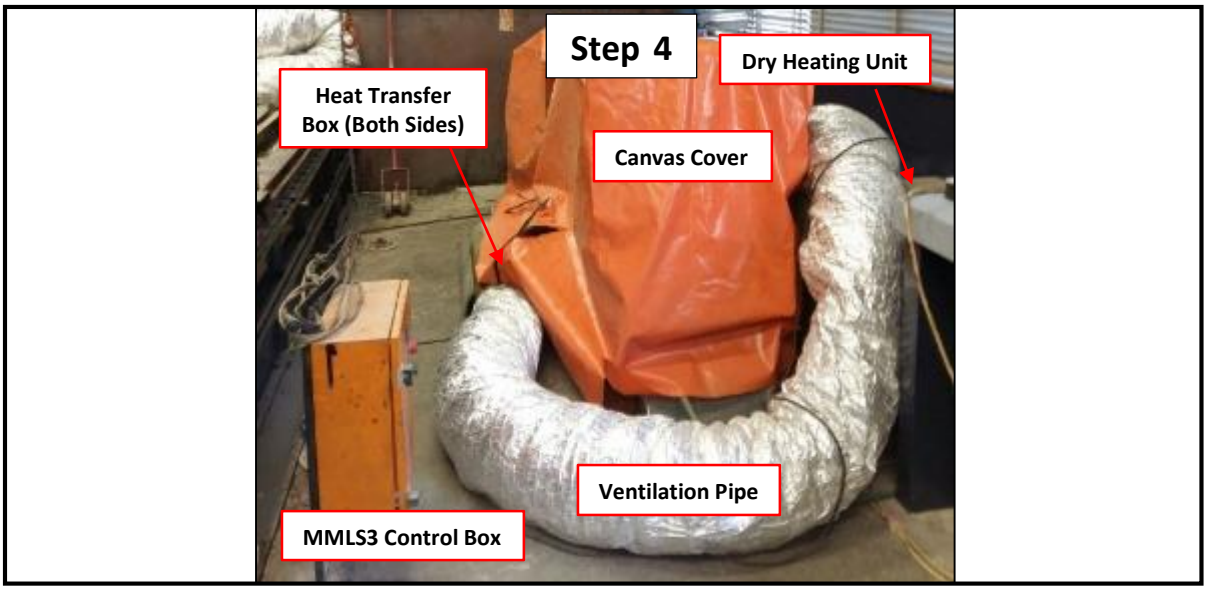

Figure 3. 12 - Test procedure: MMLS3 dry testing.

3.5.5.3 MMLS3: Wet Testing Condition

Under wet conditions, the MMLS3 trafficking was completed in the presence of grey water. Wet MMLS3 trafficking required a water heating unit (WHU) in order to heat the grey water and asphalt briquettes in the test bed. SANS 3001-PD1 in conjunction with the MMLS3 Supplementary Items Manual (2011) were used as guidelines to complete the wet MMLS3 trafficking.

The test procedure followed for wet MMLS3 trafficking is illustrated in Figure 3.13. The numbered steps below discuss the procedures followed as illustrated in Figure 3.13.

1. Asphalt briquettes were weighed before MMLS3 trafficking. Nine prepared asphalt briquettes were installed in a test bed and clamped together to prevent movement during trafficking (see *Appendix B* for details of the test bed). The asphalt briquettes were assigned a location number in the test bed as indicated. Similar to what was discussed in *Section 3.5.5.2*, it was decided to test three binder combinations in a single MMLS3 test by preparing only three asphalt briquettes per binder combination. This is illustrated in Figure 3.13. The MMLS3 was calibrated as discussed in *Section 3.5.5.1*.

2. The MML3 was placed on the test bed and levelled with its four adjustable legs. The legs were adjusted until the rubber stoppers on each bogie moved 10 mm away from the bogie frame to ensure the calibrated wheel load was exerted on the asphalt briquettes. An initial 100 cycles were completed to ensure samples were embedded in the test bed.

3. The MMLS3 was removed from the test bed and initial laser profilometer readings were completed. The surface of each asphalt briquette was measured individually. The laser profilometer was set to measure elevation (z-coordinate) readings at 1 mm increments in the y-direction until the total distance measured was equal to 170 mm. Once readings in the y-direction were completed, the laser profilometer was set to move in increments of 2 mm in the x-direction where a new line of elevation (z-coordinate) readings in the Y-direction were captured. Movement of the laser profilometer in the x-direction was repeated until the total distance measured was equal to 102 mm. This concept is illustrated in Figure 3.13. A reference point was selected for each of the nine asphalt briquettes from where profilometer readings were started. Correct alignment of the laser profilometer with the reference point was ensured by wooden spacers which were clamped to index bars with markings as indicated in Figure 3.13.

In addition to laser profilometer readings, sand patch tests were performed according to SANS 3001-BT11:2011. Sand patch tests were completed at locations 2, 3, 5, 6, 7 and 8 in the test bed. Due to the small surface area of each asphalt briquette the standard 50 ml volume glass beats that are suggested to perform this test, could not be used. A constant volume of 3 ml glass beats was therefore used to perform the sand patch tests. The test was executed as specified in the SANS document to determine the texture of the asphalt briquettes' surface.

4. The test bed is bolted to the floor and is located within a water bath. The water bath was filled with grey water having a concentration of 0.5% OMO® laundry detergent and 0.5% Sunlight® dishwashing liquid per 10 litres of clean water. The water bath was filled with grey water until a 1 to 2 mm film of water flowed on the surface of the asphalt briquettes in the test bed. Grey water in the water bath had to be heated to 40^{o}C and kept constant at this temperature during trafficking. Heating of the grey water was achieved through a WHU, which consisted of a 90-litre geyser with a temperature controller (see *Appendix B*). Heated grey water from the geyser flowed through a pipe to the water bath. Grey water from the water bath was recycled to the geyser with a water pump located in the bath. This assembly kept the temperature constant and ensured circulation of grey water in the water bath. A flow regulator was installed to regulate the water flow to the water heating unit.

Once the water temperature was constant the calibrated MMLS3 was placed on the test bed and levelled. The rubber stoppers of the MMLS3's bogie system was checked to be 10 mm away from the bogie frame to ensure that the correct load was transferred to the asphalt briquette's surface.

MMLS3 trafficking was stopped after the predetermined number of load cycle intervals was reached, to perform laser profilometer readings and sand patch tests. Table 3.9 summarise the load cycle intervals as suggested by SANS 3001-PD1. The time to complete each load cycle interval is also presented.

Table 3. 9 - Summary of load cycle intervals.

Load Cycle Interval	Time (@ 7200 cycles/hr)	Profilometer Readings	Sand Patch Test
0	0 min	•	•
2 500	21 min	•	
5 000	21 min	•	
10 000	42 min	•	
20 000	1 hr 23 min	•	
50 000	4 hr 10 min	•	•
100 000	6 hr 58 min	•	•

5. Step three and four was repeated until a total of 100 000 load cycles were achieved. The MMLS3 had to be calibrated after each load cycle interval before testing could continue. The profilometer readings were completed by lowering the grey water level in the water bath. Excess water was stored to ensure the grey water concentration remained constant. Asphalt briquettes were weight after MMLS3 trafficking to determine the material loss (stripping) caused by the grey water conditioning.

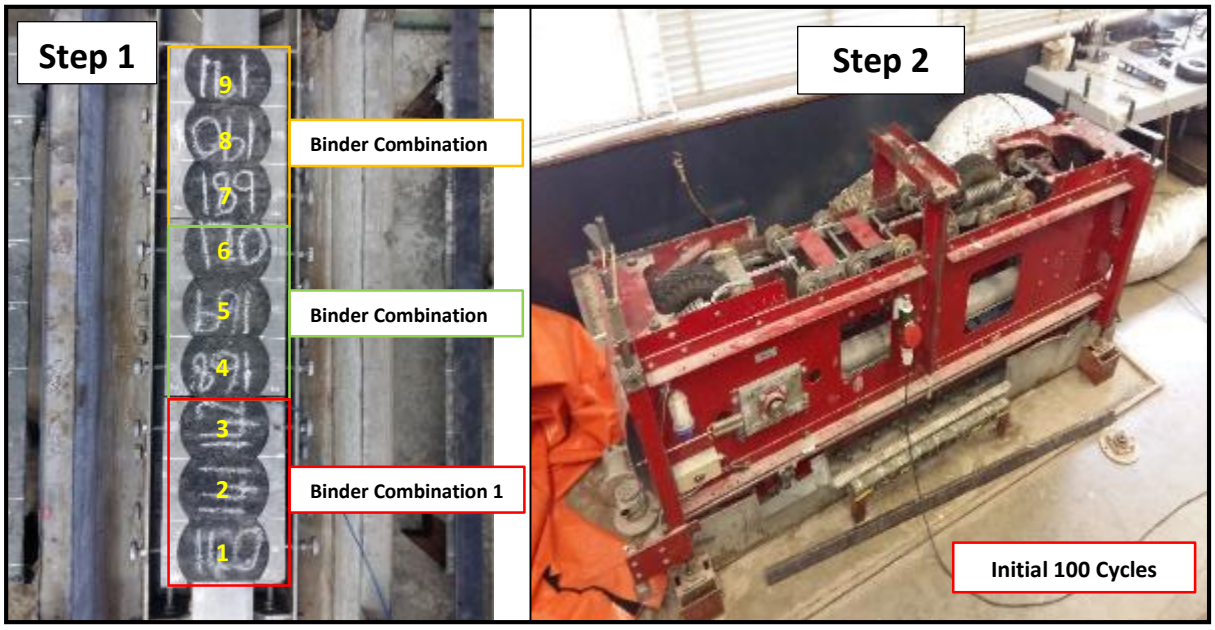

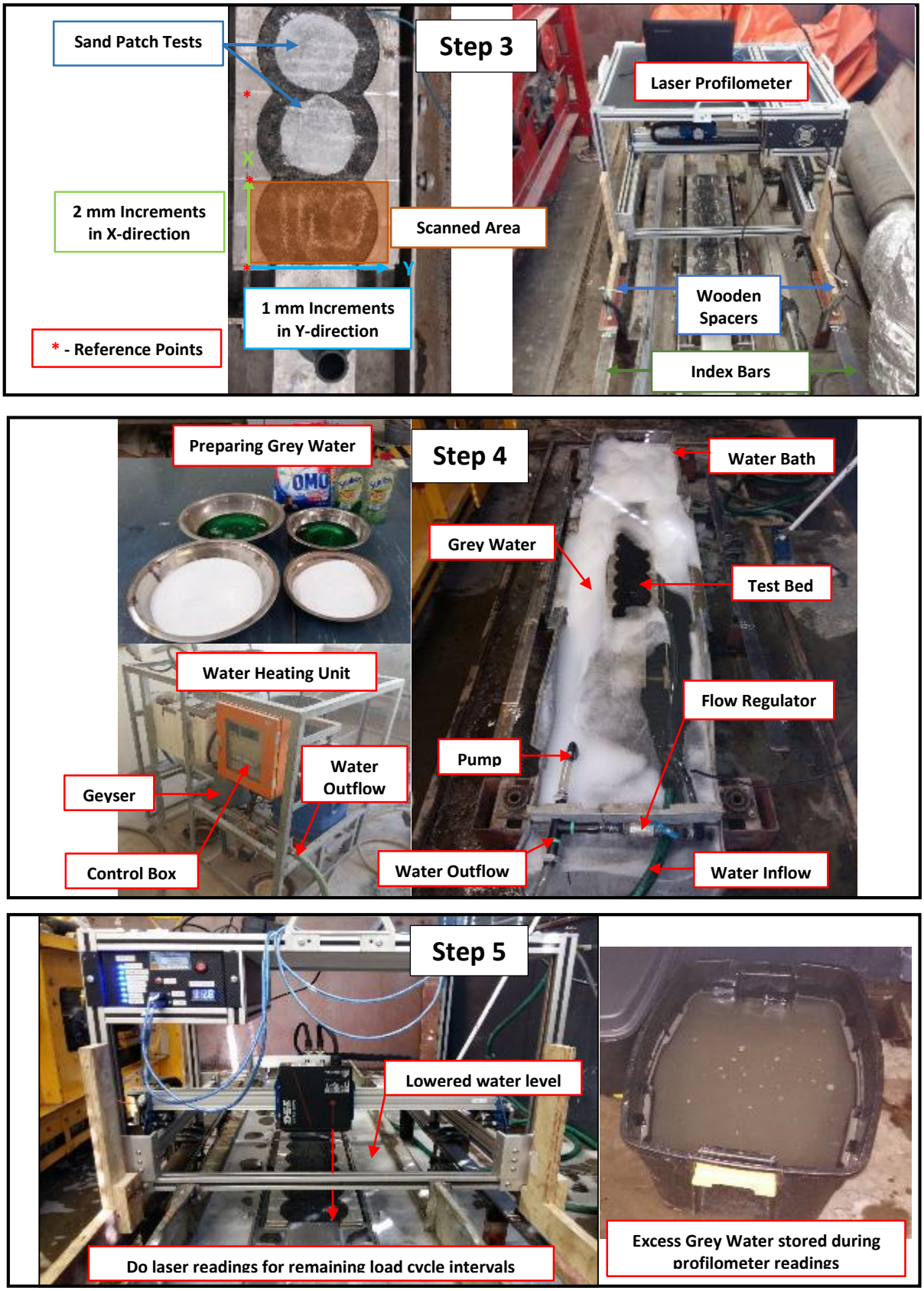

Figure 3. 13 - Test procedure: Wet MMLS3 testing.

3.5.6 PHASE 2: INDIRECT TENSILE STRENGTH TESTING

Dry (no water) and wet (grey water) trafficked asphalt briquettes were subjected to ITS testing. ITS tests were used to determine the effect grey water conditioning under traffic loading had on the performance of the asphalt mixtures. These tests were also conducted at 25°C with a loading rate of 50.8 mm/min. A summary of the average ITS results for asphalt mixtures subjected to no-conditioning and grey water conditioning is presented in Table 3.10.

Table 3. 10 - ITS results for Phase 2 of Grey Water study.

Gradation Type	Binder Type	ITS_{NC} (kPa)	ITS_{GW} (kPa)	TSR (%)
COLTO Medium	50/70 Penetration Grade Bitumen	879	716	82
COLTO Medium	SBS + Extra Lime	748	841	112
COLTO Medium	SBS + 1%Sasobit+Extra Lime	806	751	93
COLTO Medium	SBS + Polyamine + 1%Sasobit + Extra Lime	868	811	93
COLTO Medium	SBS + 1%Sasobit + 0.1%ZycoTherm + Extra Lime	683	628	92
COLTO Medium	EVA + Extra Lime	766	734	96
COLTO Medium	EVA + 1%Sasobit + Extra Lime	853	919	108
COLTO Medium	EVA + 1%Sasobit + 0.1%ZycoTherm + Extra Lime	1113	1063	96
COLTO Fine	50/70 Penetration Grade Bitumen	591	514	87
COLTO Fine	50/70 + 0.1%ZycoTherm	539	793	147
COLTO Fine	EVA + 1%Sasobit	925	835	90
COLTO Fine	EVA + 1%Sasobit + 0.1%ZycoTherm	654	566	87
CCC Fine	50/70 Penetration Grade Bitumen	854	738	86
CCC Fine	EVA + 1%Sasobit	894	698	78
Much Fine	50/70 + 0.07%ZycoTherm	876	985	112

Notes: NC - No-Conditioning; GW - Grey Water Conditioning; DNF - Did Not Finish

From Table 3.10 it follows that the calculated tensile strength ratios (TSR) represent the change in asphalt mixture strength as a result of grey water condition and traffic loading. ITS result for Phase 2 is discussed in detail in Chapter 5.

3.6 THEORETICAL ANALYSIS OF DATA CAPTURED DURING MMLS3 TRAFFICKING

3.6.1 LASER PROFILOMETER READINGS

Laser profilometer reading files were processed to extract data from the MMLS3 wheel path on the asphalt briquettes. The processed data provided information on the permanent deformation and texture of various asphalt mixtures that were tested.

3.6.1.1 Extracting data from wheel path

Each laser profilometer measurement produced a data file containing a set of x, y and z-coordinates. However, to evaluate the permanent deformation and texture, readings within the MMLS3 wheel path had to be extracted. During testing, specific measurements were taken to ensure that the correct

coordinates were extracted from these data files. Figure 3.14 illustrates the section from where data was needed to be extracted from each laser profilometer data file as well as the measurements required to ensure that the correct data was extracted.

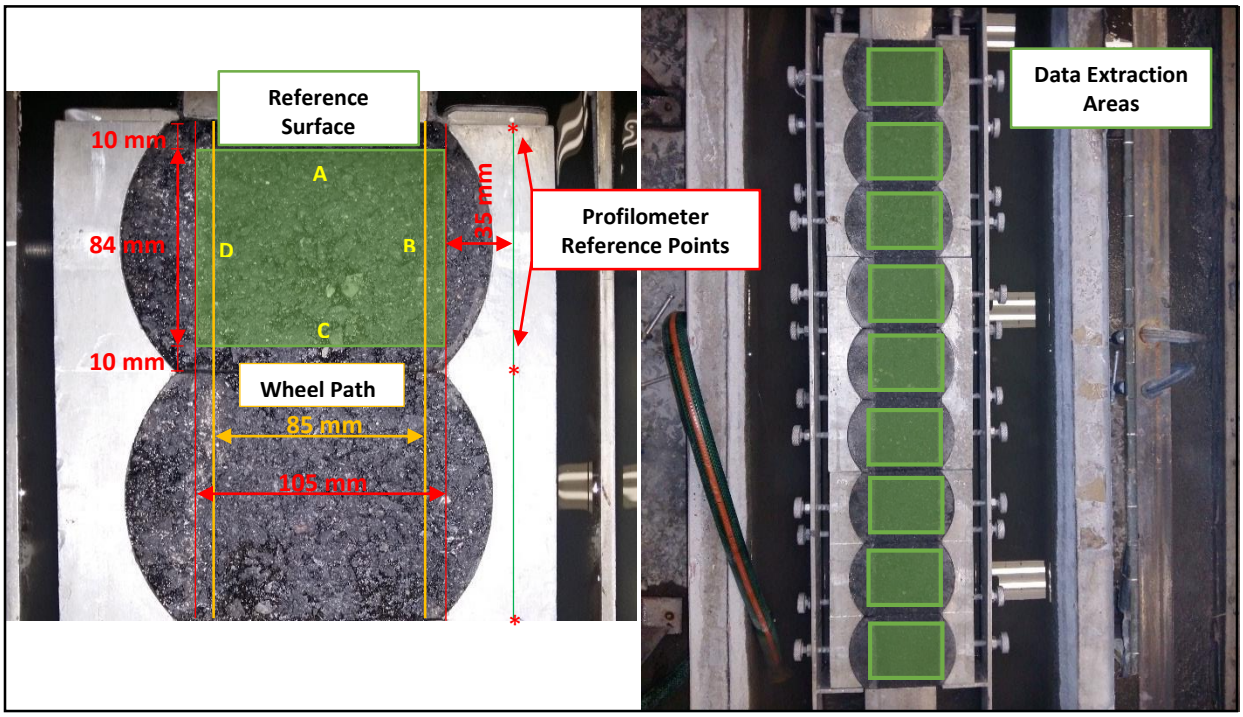

Figure 3. 14 - Illustration of how measurements were extracted from profilometer readings.

From Figure 3.14 it can be seen that the scanned area had to be reduced by 10 mm on sides A and C. It was reduced due defects at the transition joints between the asphalt briquettes that were caused by MMLS3 wheels. With the wheel path 85 mm wide, an additional 10 mm was added to this width on both sides B and D. This was done to produce a reference surface from which the permanent deformation was measured. With the measurements illustrated in Figure 3.14 known, the data file of each profilometer reading was processed to extract the data from the wheel path. Figure 3.15 illustrates the layout of a laser profilometer data file.

	A	B	C	D	E	F	G	H	I	J	K	L	M	N	O	P	Q	R	S	T
177	MN140-10000Axles																			
178	Sample 1 Description																			
179	Riaan																			
180	2/4/2016 9:10																			
181																				
182	100	38.1	38.27	37.91	37.72	37.92	38.02	37.82	37.99	37.66	37.87	37.69	37.85	37.88	38.1	38.23	38.01	38.06	38.11	37.92
183	101	38.1	38.27	37.91	37.72	37.92	38.02	37.82	37.99	37.66	37.87	37.69	37.85	37.88	38.1	38.23	38.01	38.06	38.11	37.92
184	102	37.94	38.02	37.86	37.9	37.67	37.91	37.89	37.99	38.06	37.98	37.98	38.09	38.17	37.77	38	37.97	38.17	38.02	38.26
185	103	38.31	37.95	37.98	38.16	38.11	38.15	37.98	38.02	38.23	37.82	38.28	38.12	38.37	38.23	38.15	37.79	37.76	37.86	38.05
186	104	37.89	38	38.07	38.18	38.29	38.22	38.08	38.22	38.3	38.11	38.13	38.15	38.07	38.07	38.57	38.46	38.29	38.09	38.28
187	105	38	37.95	38.23	37.95	37.84	37.96	38.1	38.18	38.15	38.26	38.2	37.93	38.1	38	37.97	38.38	37.75	37.99	38.06
188	106	38.2	38.01	38.02	38.07	37.94	38.12	38.09	38.13	37.99	38.01	38.26	38.41	38.32	38.3	38.18	38.05	38.19	38.35	38.18
189	107	38.01	38.25	38.19	38.21	38.21	38.15	38.31	38.09	38.05	38.09	38.19	38.13	38	38.12	38.43	38.2	38.1	38.45	38.09
190	108	38.15	38.04	38.19	38.2	38.05	38.1	38.26	38.36	37.89	38.25	38.28	38.27	38.09	38.21	38.2	38.41	38.71	38.32	38.33
191	109	38.02	38.28	38.16	38.1	38.2	38.05	37.84	38.31	38.27	38.27	38.1	38.05	38.39	38.3	38.3	38.32	38.35	38.57	38.56

Description

Columns represent movement in X-direction in 2 mm increments

Rows represent movement in Y-direction in 1 mm

Figure 3. 15 - Illustration of profilometer data file processing.

Each laser profilometer data file, as shown in Figure 5.15, was imported to Microsoft Excel. A data file description identifies the sample number, time and date, as well as the number of MMLS3 loads cycles at which the laser profilometer reading was completed. Column A represents the y-coordinates at which the elevation (z-coordinates) was measured. Measurements were started a 100 mm in the y-direction within the reference system of the laser profilometer. Each row in the spreadsheet represents a 1 mm increment in the y-direction. The laser profilometer was set to produce a total of 170 elevation (z-coordinate) measurements in the y-direction.

Columns B to T represents the movement of the laser profilometer in the x-direction. Each column consists of a set of elevation measurements (z-coordinates) as the profilometer moved in increments of 2 mm in the x-direction. A complete laser profilometer data file contains 51 columns representing the profilometer movement in the x-direction.

In order to extract the data from the wheel path of the profilometer data file, measurements as shown in Figure 3.14 were implemented to delete a specific number of columns and rows until the correct data was obtained. A single asphalt briquette had seven profilometer data files which is one file for each load cycle interval (see Table 3.8 and 3.9). Extraction of the wheel path data was completed for each of the seven profilometer data files per asphalt briquette subjected to MMLS3 trafficking. With the extracted data the permanent deformation and surface texture from 0 to 100 000 MMLS3 load cycles were evaluated.

3.6.1.2 Permanent Deformation

Data extracted from the seven laser profilometer data files per asphalt briquette was used to calculate the 95th percentile cross-sectional profile to evaluate the permanent deformation.

The 95th percentile cross-sectional profile calculation reduced the laser profilometer readings from a three-dimensional to a two-dimensional coordinate system (y and z-directions). A normal distribution was used to statistically calculate the 95th percentile elevation (z-coordinate) per y-coordinate using Equation 3.2.

Kurtosis and skewness tests were done on laser readings of one asphalt briquette per MMLS3 trafficking test completed in order to determine if a normal distribution applied. Asphalt briquettes were randomly selected on which kurtosis and skewness tests were completed. Kurtosis results ranged from 0.12 to 2.19. This indicated that the distribution shape of the data range, peaked from a lower to a higher value. Skewness results ranged from 0.13 to 0.99. This indicated that the skewness of data sets ranged from

being symmetric (Skewness < 0.5) to being moderately skew to the right (0.5 < Skewness < 1). In order to be consistent with statistical calculations, it was decided that a normal distribution will be used to perform 95th percentile cross-sectional profile calculations.

$$Z = \frac{X - \mu}{\frac{\sigma}{\sqrt{n}}} \qquad \textit{Equation 3.2}$$

where $Z = Confidence\ factor$
$X = Value\ at\ certain\ level\ of\ confidence$
$\mu = Sample\ Mean$
$\sigma = Sample\ standard\ deviation$
$n = Sample\ Size$

Elevation readings (z-coordinates) in the x-direction per y-coordinate were processed to a single reading representing the 95th percentile elevation for a given y-coordinate. A confidence factor (Z) of 1.96 was used they corresponded to a 95% level of confidence. This value was obtained from a standard normal distribution Z-table. Table 3.11 illustrates an example for calculating the 95th percentile elevation (z-coordinate) per y-coordinate.

Table 3. 11 - Example of calculating the 95th percentile elevation per Y-Coordinate.

Y-Coordinates	X-Coordinates							Equation 1.4 Parameters				
	1	2	3	…	40	41	42	N	μ	σ	Z	X
125	39.06	38.8	38.71	…	38.96	39.83	40.21	42	39.14	0.44	1.96	39.28
126	39.21	38.86	39.08	…	39	38.85	39.14	42	39.16	0.38	1.96	39.28
127	39.02	38.91	39.11	…	39.56	39.8	39	42	39.21	0.45	1.96	39.34
⋮	⋮	⋮	⋮	…	⋮	⋮	⋮	⋮	⋮	⋮	⋮	⋮
228	39.63	39.56	39.48	…	39.79	39.82	39.55	42	39.66	0.34	1.96	39.76
229	39.5	39.87	40.3	…	39.98	39.53	40.72	42	39.68	0.39	1.96	39.80
230	39.94	40.72	40.18	…	39.27	39.41	39.24	42	39.58	0.41	1.96	39.70

From Table 3.11 follows that the red column indicates the 95th percentile elevation (z-coordinate) per y-coordinate, calculated using Equation 3.2. This procedure was completed for the extracted 0, 2500, 5000, 10 000, 20 000, 50 000 and 100 000 MMLS3 load cycles as per the laser profilometer data files per asphalt briquette.

With the seven calculated 95th percentile cross-sectional profiles per asphalt briquette were established, they were further processed by following the steps below. SANS 3001-PD1 was used in setting up these steps.

1. It was required to establish a reference point to ensure each of the seven cross-sectional profiles started at the same elevation point. This was achieved by selecting a zero elevation for the first y-coordinate representing the reference point. This was achieved by subtracting all elevation values (z-coordinates) with the elevation value of the first y-coordinate of the cross-sectional profile. Step 1 in Figure 3.16 illustrates this procedure for a single cross-sectional profile.

2. After adjusting elevation values (z-coordinates) to a reference point, it was also required to perform adjustments for drifting. If the 95th percentile elevation value (z-coordinate) of the last y-coordinate of each cross-sectional profile was not equal to zero, it indicated that the cross-sectional profile was drifting. An angle was calculated between the elevation (z-coordinate) of the first y-coordinate and the elevation (z-coordinate) of the last y-coordinate. Using trigonometry it was possible to determine the elevation (z-coordinate) adjustment per y-coordinate required to ensure a zero elevation at the last y-coordinate of the profile. An example of this procedure is illustrated in Steps 2A and 2B in Figure 3.16.

3. The final step of processing included calculating a three-point running average. Each elevation value per Y-coordinate was replaced by an average of the point value itself and the proceeding and following point value (SANS 3001-PD1, 2016). This procedure smoothed the deformation curve and was completed for each of the seven 95th percentile cross-sectional profiles per asphalt briquette. After completing this procedure combined deformation curves were compiled, which illustrated the deformation of an asphalt briquette from 0 to 100 000 MMLS3 load cycles (See Figure 3.16).

4. The permanent deformation per load cycle interval was determined as the lowest point within the cross-sectional profile. Lastly, the permanent deformation results per cross-sectional profile were adjusted by subtracting it with the lowest point of the 0 MMLS3 load cycle profile which represented the reference point (See Figure 3.16).

The procedures as presented in Figure 3.16 were repeated for all asphalt briquettes subjected to MMLS3 trafficking.

Step 1

Y-Coordinate	95th Percentile Elevation (mm) (A)	Adjusted to Reference Point (mm) (B)
125	39.28	0
126	39.28	0
127	39.34	0.06
⋮	⋮	⋮
228	39.76	0.48
229	39.80	0.52
230	39.70	0.42

(A) – 39.28

Step 2A

Y-Coordinate	95th Percentile Elevation (mm) (A)	Adjusted to Reference Point (mm) (B)
125	39.28	0
126	39.28	0
127	39.34	0.06
⋮	⋮	⋮
228	39.76	0.48
229	39.80	0.52
230	39.70	0.42

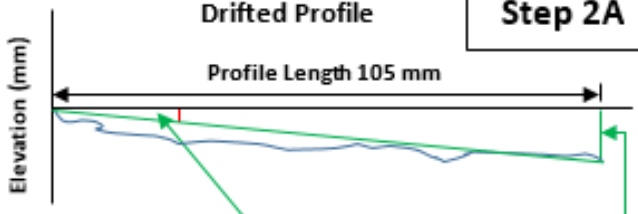

Angle = $\tan^{-1}(0.42/105) = 0.229°$

Difference in Elevation (0.42 – 0 = 0.42 mm)

Profile length (230 – 125) = 105 mm)

Step 2B

Adjustment per mm: tan(0.229) x 1 = 0.00399

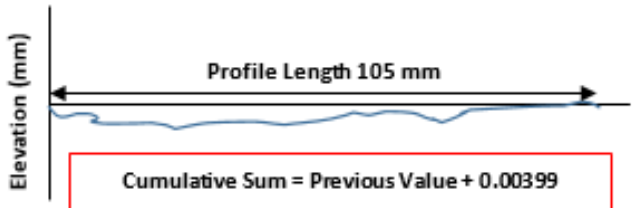

Cumulative Sum = Previous Value + 0.00399

(D) = (B) – (C)

Y-Coordinate	95th Percentile Elevation (mm) (A)	Adjusted to Reference Point (mm) (B)	Drift Adjustment (mm) (C)	Adjusted 95th Percentile Elevation (mm) (D)
125	39.28	0	0	0
126	39.28	0	0.00399	-0.0039
127	39.34	0.06	0.00799	0.052
⋮	⋮	⋮	⋮	⋮
228	39.76	0.48	0.411	0.069
229	39.80	0.52	0.415	0.105
230	39.70	0.42	0.42	0

Note: This figure continuous on the next page.

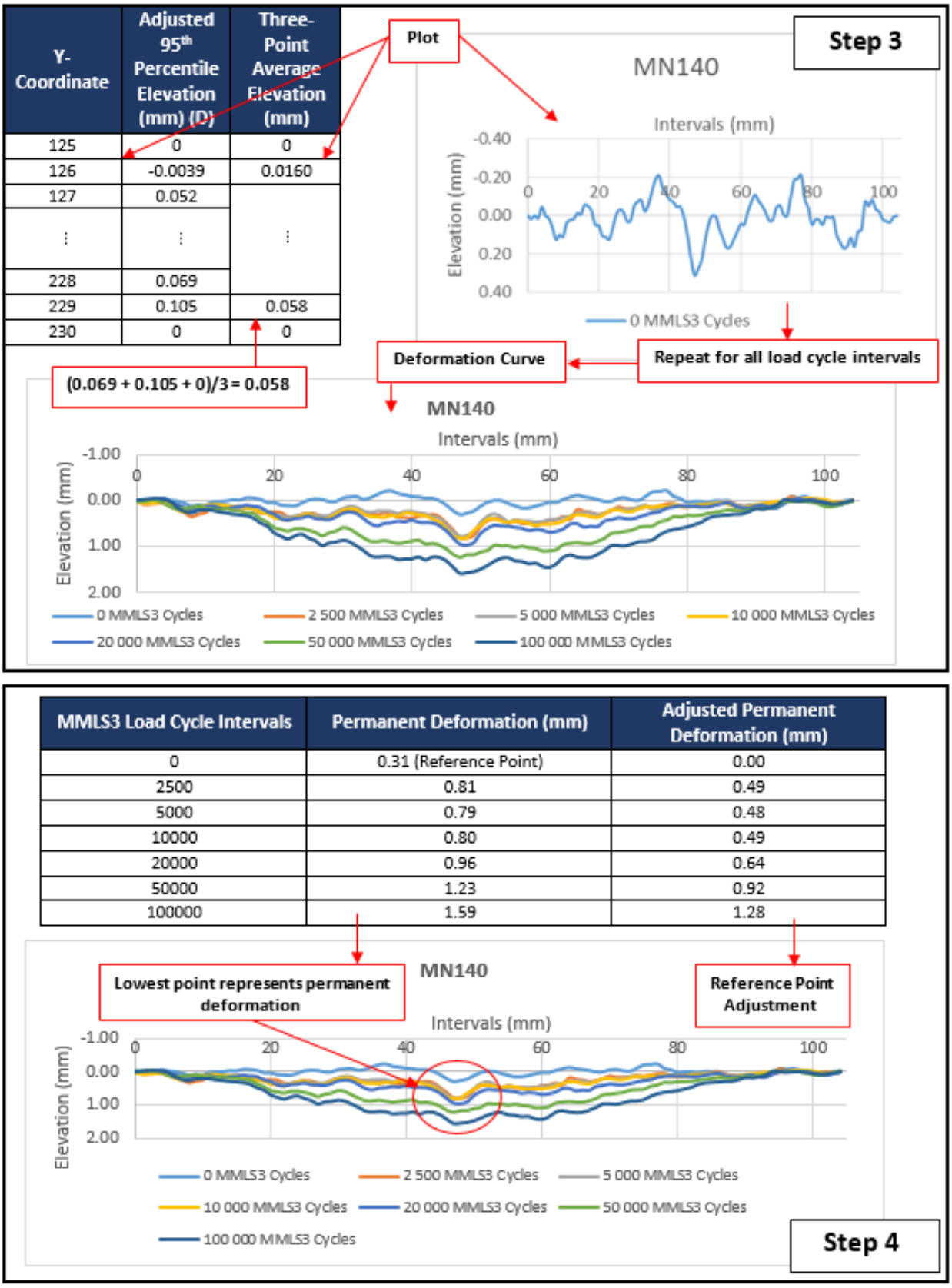

FIgure 3. 16 - Procedure for determining permanent deformation.

3.6.1.3 Texture analysis using laser profilometer readings

The texture of each asphalt briquette subjected to MMLS3 trafficking was analyzed at 0, 50 000 and 100 000 MMLS3 load cycles. The 95th percentile cross-sectional profile of each asphalt briquette was used during texture analysis, in accordance with the procedure discussed in *Section 3.6.1.2*. However, during texture analysis, it was not important to adjust the 95th percentile cross-sectional profiles to a reference point and for drifting as required for determining the permanent deformation.

Initially, texture analysis of the 95th percentile cross-sectional profiles were attempted using the trend line method that was developed for the old laser texture meter (LTM) at the University of Stellenbosch. The trend line method included plotting the LTM measured elevation values and cross-sectional intervals in Microsoft Excel. Thereafter, a second-degree polynomial trend line was added and a trend line equation was derived. With the trend line equation known, the elevation values per cross-sectional interval along the trend line were determined. The elevation values calculated using the trend line were then subtracted from the LTM measured elevation values per interval. Using the appropriate function in Microsoft Excel, the maximum difference between these two elevation values along the profile was determined which represented the texture depth of the asphalt briquette's surface. Figure 3.17 illustrates the trend line method.

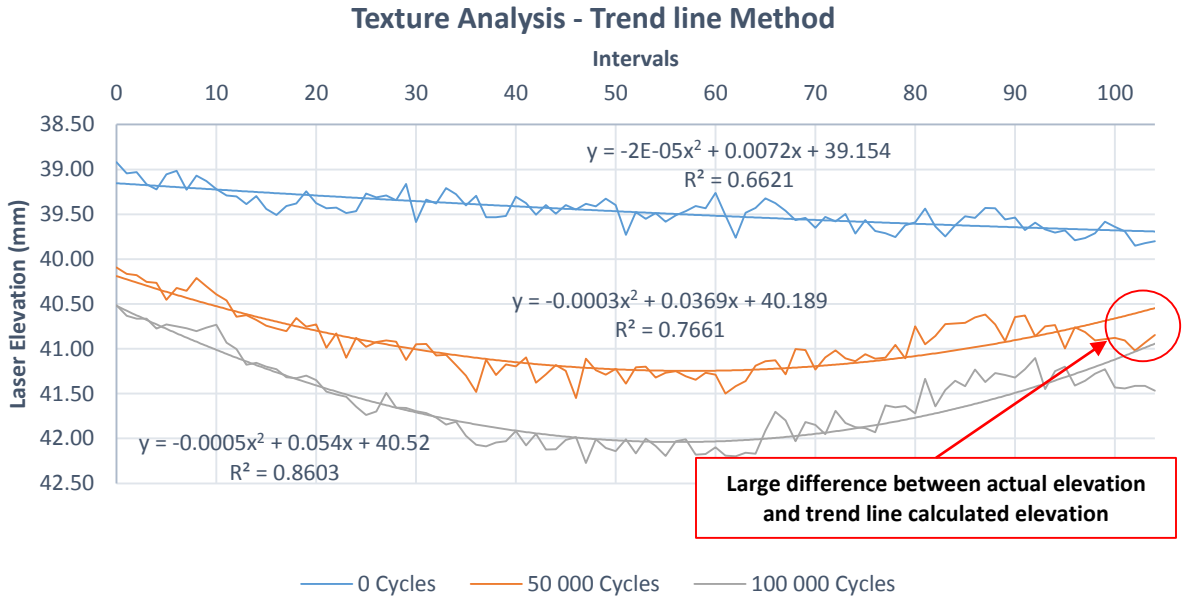

Figure 3. 17 - Illustration of texture analysis using the trend line method.

The trend line method did not produce accurate results at it did not move through the middle of the cross-sectional profile. Therefore, great differences between the trend line calculated elevation values and LTM measured elevation values occurred which were wrongfully interpreted as the texture depth. This problem is illustrated in Figure 3.17 with the red circle. The trend line method was consequently, abandoned and a different approach for analyzing the texture was developed.

The alternative solution for analyzing the texture of each asphalt briquette subjected to MMLS3 trafficking is illustrated in Figure 3.18. The Civil Designer® software package was used to import a survey file consisting of the x, y and z-coordinates of the 0, 50 000 and 100 000 MMLS3 cycles cross-sectional profiles of a single asphalt briquette in 'Survey mode'. The imported data showed as a series of points in Civil Designer®. By setting Civil Designer into 'CAD mode', a 'light weighted polyline' was selected from the 'Draw' options and used to connect the data points for each cross-sectional profile. Once all data points of each profile were connected, the light weighted polyline was continued by connecting all peak points on the cross-sectional profile. This approach is similar to the sand patch test as described in SANS 3001-BT11:2011. During the sand path test, glass beads are spread on the asphalt surface until peaks of the aggregate start to show. Only then the diameter of the distributed glass beats is measured.

In Civil Designer® the polyline formed a closed loop from which the area between the polylines could be determined. The area between the polylines was determined for the 0, 50 000 and 100 000 MMLS3 cycle's cross-sectional profiles from where an area ratio was determined instead of a texture depth. The area of the 0 MMLS3 load cycle cross-sectional profile represented the reference area and was given an area ratio of 1. The areas between the polylines for the 50 000 and 100 000 MMLS3 load cycles' cross-sectional profiles were divided with the area of the 0 MML3 load cycle cross-sectional profile to determine their area ratio. This procedure is illustrated in Figure 3.18.

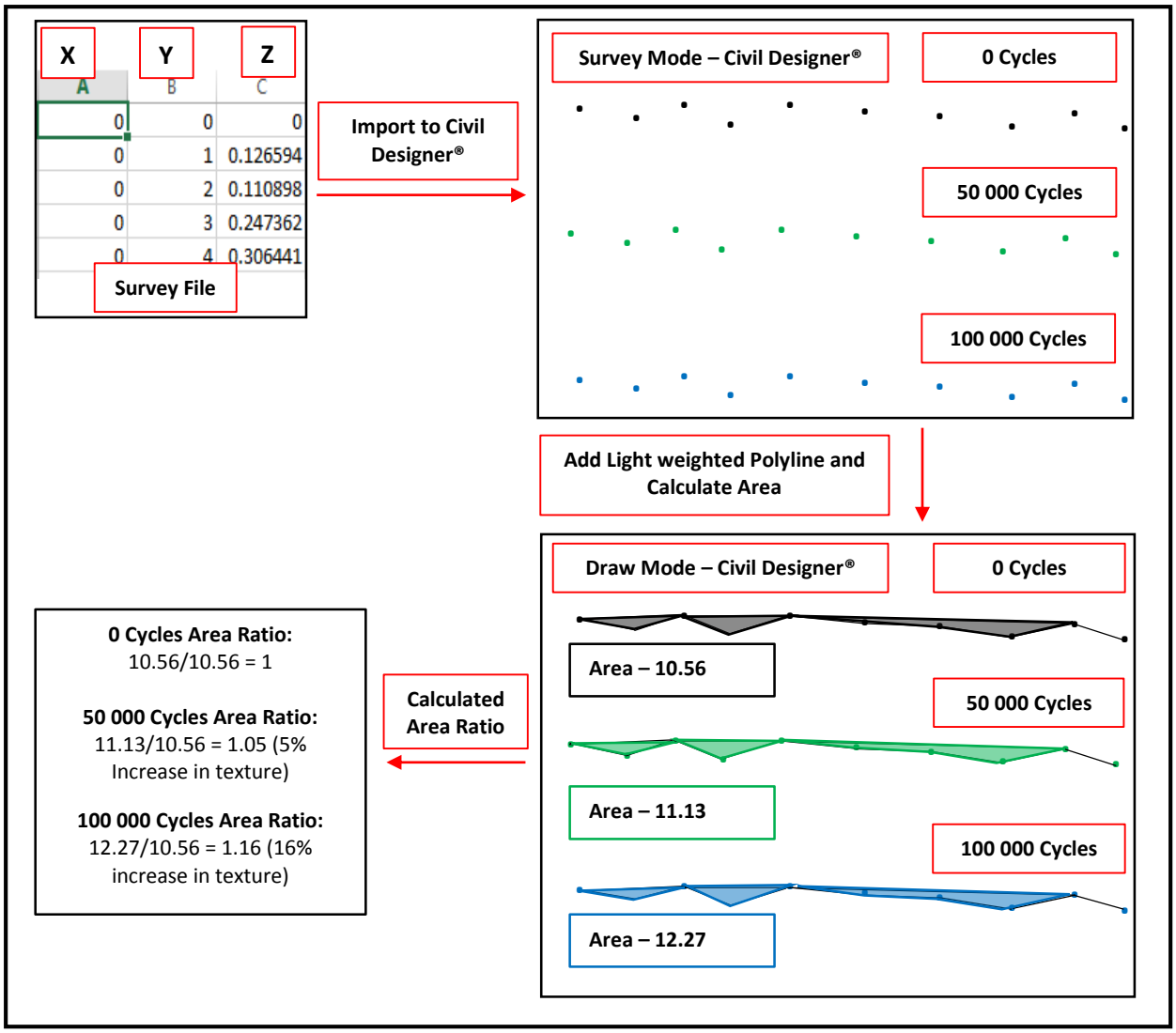

Figure 3. 18 - Analysis of texture in Civil Designer.

3.6.2 MATERIAL LOSS DATA

During MMLS3 trafficking asphalt briquettes subjected to dry (no water) and wet (grey water) trafficking were weighed before and after testing to determine the material loss (mass bitumen and aggregate). As indicated before, six asphalt briquettes were prepared per binder combination, with three being subjected to dry MMLS trafficking and the remaining three being subjected to wet MMLS trafficking. The material loss was determined for all six asphalt briquettes per binder combination after MMLS trafficking, where after the average material loss per binder combination was calculated.

The material loss calculated for the various binder combinations was small relative to the total mass of the asphalt briquettes. This was due to only a small section of the asphalt surface (wheel path) being subjected to loss of material during trafficking.

3.7 SUMMARY

The factors influencing the moisture susceptibility of asphalt mixtures formed the basis from which an experimental research methodology for improving the grey water susceptibility of asphalt mixtures was established. The research methodology consisted of a test matrix of two phases of laboratory work. In both phases 150 mm diameter asphalt briquettes with a height of 80 mm were prepared according to the asphalt mixture designs presented in the test matrix.

During Phase 1, asphalt briquettes were subjected to moisture inducing simulating test (MIST) conditioning after which indirect tensile strength (ITS) tests were performed to evaluate the influence of grey water on the performance of asphalt mixtures.

During Phase 2, asphalt briquettes were machined to fit in a test bed for laboratory scale model mobile load simulating (MMLS3) tests. Asphalt briquettes were subjected to dry and wet trafficking conditions. During wet trafficking conditions, the surface of asphalt briquettes was covered with a grey water concentrate. ITS tests were performed on the trafficked briquettes to evaluate the grey water susceptibility of asphalt mixtures presented in the test matrix.

Results obtained during execution of the experimental research methodology were processed to extract information of the retained strength, texture, permanent deformation and material loss after grey water conditioning. These results are presented in *Chapter 5*.

CHAPTER 4 – FINITE ELEMENT ANALYSIS RESEARCH METHODOLOGY (SECONDARY)

4.1 INTRODUCTION

A secondary research methodology was established to investigate the influence of an asphalt briquette's shape on the result of an indirect tensile strength (ITS) test. During execution of the primary research methodology, ITS tests were performed on 150 mm diameter asphalt briquettes. Reshaping of briquettes for MMLS3 testing require the machining-off of two opposing segments with parallel chords with the same mid-ordinates in order to fit into the test bed. The briquettes' shape before and after machining is shown in Figure 4.1.

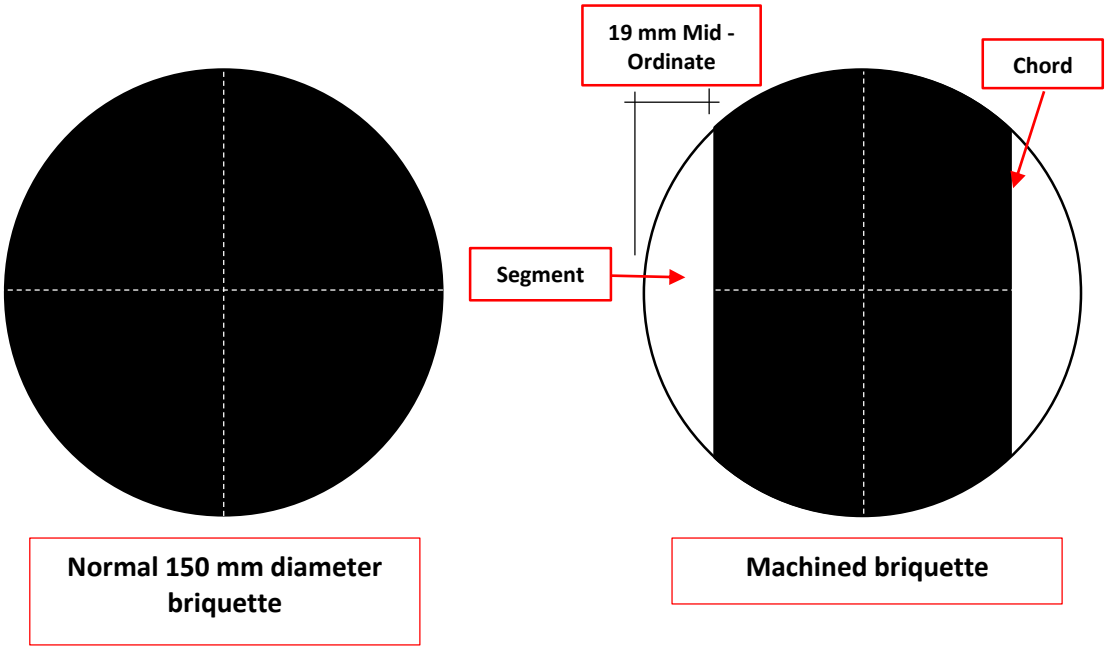

Figure 4. 1 - Difference between normal 150 mm diameter and machined briquette.

Investigating the influence of briquette's geometry on the ITS result was accomplished using Abaqus/CAE 6.14-1 finite element analysis software. The finite element analysis research methodology is based on the methodology devised by Walker (2013) during his research on: *Finite Element Analysis of Indirect Tensile Test*. The layout of the finite element analysis research methodology is presented in Figure 4.2.

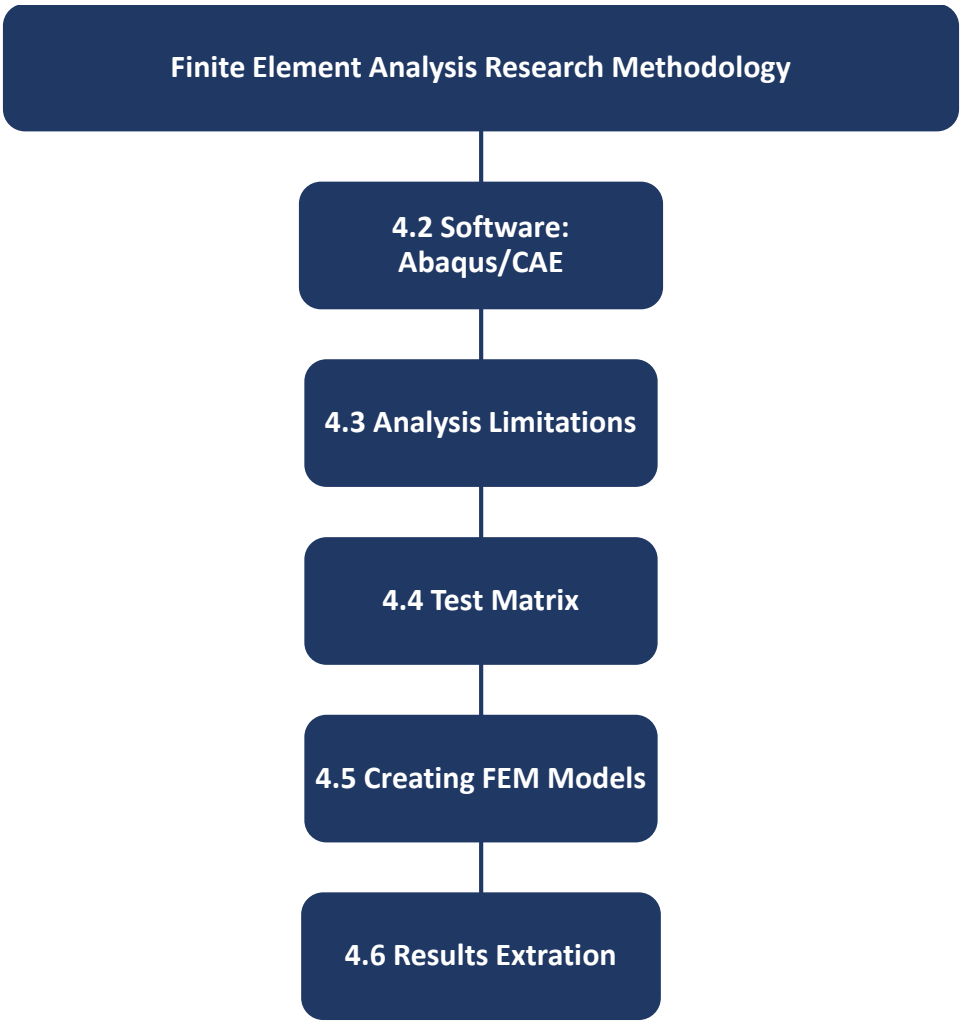

Figure 4. 2 - Layout of finite element analysis methodology.

4.2 SOFTWARE: ABAQUS/CAE

Abaqus/CAE is finite element analysis software that provides the user with the capability to create a model, assemble model components, analysis model components and visualise the processed finite element analysis results. The finite element analysis consists of three primary stages: Pre-processing, simulation and post-processing. These stages are linked to each other through files created by the finite element analysis software (Walker, 2013).

Figure 4.3 presents a flow diagram of the three stages of the finite element analysis. During each of the three stages of finite element analysis, the following actions are performed (Walker, 2013):

Stage 1 Pre-processing: Models are graphically created using Abaqus/CAE software. During this stage material characteristics, interaction between parts, boundary conditions and loading requirements are established.

Stage 2 Simulation: Numerical problems defined during the pre-processing stage are solved using Abaqus/ Standard or Abaqus/Explicit. Binary files (also referred to as output files) that contain the results of the numerical problems are created during this stage. These files are used during the post-processing stage. The simulation completion rate is dependent on the type of results required by the user. Stress and displacement simulations are time-consuming to produce results as they are influenced by the complexity of the simulation and the speed of the computer's processor.

Stage 3 Post-processing: The visualization module of Abaqus/CAE is used to evaluate the simulation results stored in the binary files during Stage 2. Results are displayed during the post-processing stage through colour contour plots, deformed shape plots and animations.

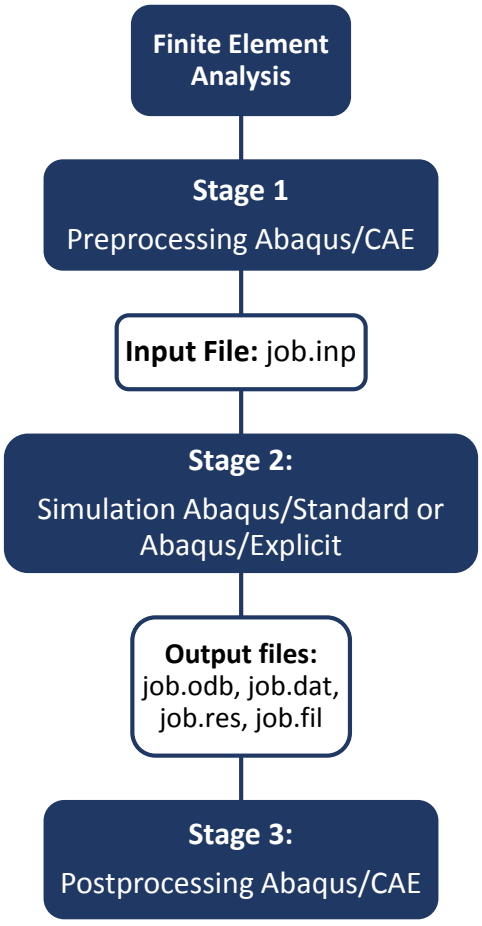

Figure 4. 3 - Flow diagram of finite element analysis stages adapted from Suvranu (2000).

The three stages of finite element analysis are performed through the simple interface provided by Abaqus/CAE. The user interacts with the Abaqus/CAE software via the main window which contains all the components required to successfully perform finite element analysis (Walker, 2013). The main window of Abaqus/CAE is illustrated in Figure 4.4.

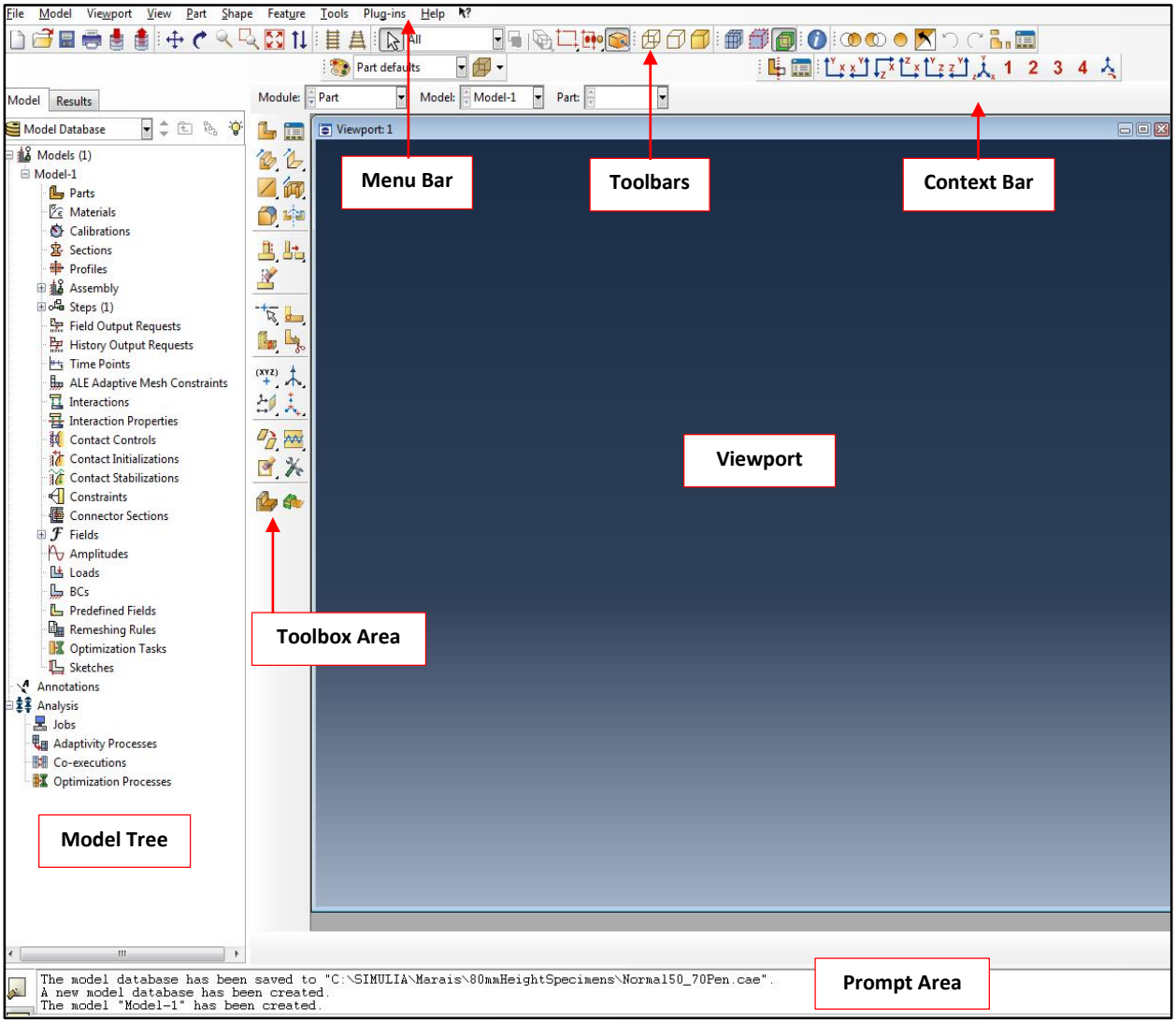

Figure 4. 4 - Main window of Abaqus/CAE.

The 'Model Tree' contains all information related to the model that is to be analysed with the finite element method. It not only provides a graphical overview of the model created but also presents the modules and objects contained in the model. Abaqus/CAE contains nine modules that require attention during the finite element analysis. These modules need to be completed in the sequence as shown in Table 4.1 (Walker, 2013).

Table 4. 1- Abaqus/CAE modules.

Number	Module	Description
1	Part	During this module, the geometry of the problem is sketched through the creation of individual parts.
2	Property	During this module, material properties are created and assigned to the part created in module 1.
3	Assembly	Individual parts created are assembled and an instance is created.
4	Step	Steps required for the analysis are created.
5	Interaction	Interaction points between parts are created.
6	Load	Loads applied to an instance are defined as well as boundary conditions.
7	Mesh	Elements and nodes are created and implemented on instances.
8	Job	Creating a job for analysis.
9	Visualization	View results after job execution.

Modules, as shown in Table 4.1, are discussed in more detail in *Appendix C*.

4.3 ANALYSIS LIMITATIONS

4.3.1 SOFTWARE LIMITATIONS

The Abaqus/CAE software used for finite element analysis during this study had a maximum capability of 100 000 elements for the meshing of instances. This capability was restricted by the Academic Teaching Abaqus Licence, which grants access for usage of the software. Large numbers of elements also jeopardise the computation time and was therefore limited to this version of Abaqus/CAE. These limitations identified restrict the ability of a finite element mesh to produce accurate results (Walker, 2013).

Input values such as for pressures are also rounded off in Abaqus, limiting the accuracy of the results produced during the finite element analysis (Walker, 2013).

4.3.2 MODEL LIMITATIONS

Asphalt exhibits viscoelastic material behaviour which is complex to simulate during the finite element analysis. The elastic component of asphalt's material behaviour is less complex as a linear relationship between stress and strain exists. However, the viscous component is time and temperature dependent which are complex variables. As a result, the finite element models developed during this study consisted of homogeneous and isotopic materials which exhibited linear-elastic behaviour. As only linear elastic finite element models were created, the viscous behaviour of asphalt materials was excluded which therefore limited true material behaviour. During linear-elastic material behaviour, no permanent strain develops during load application as the stresses in the material are limited to the elastic stress limit. During

finite element analysis, the user has the option to perform the analysis using linear or quadratic elements, which in turn determines the number of shape functions and nodes. Quadratic elements produce greater approximations and require more analysis time (Dean, n.d.). The finite element models created for this study therefore only considered linear elements.

4.4 TEST MATRIX

A test matrix was established for the finite element analysis research methodology and is presented in Table 4.2. Four variations in the asphalt briquette's dimensions of the mid-ordinate were selected to determine the influence of the reshaped briquettes on the indirect tensile strength (ITS) test. In addition, it was also decided to perform the finite element analysis with four resilient modulus variations, thus creating a total of 16 asphalt briquette combinations to analyse. Resilient modulus variations were determined after performing indirect tensile (ITT) tests. Execution of ITT tests is further discussed in Section 4.5.

Table 4. 2 - Test matrix for the finite element analysis research methodology.

Combination	Resilient Modulus (Mr)	Asphalt Briquette dimension
1	Mr_1 = 1230 MPa	**Normal Briquette:** - 150 mm diameter - Height 80 mm 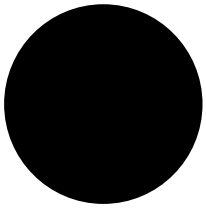
2	Mr_2= 1672 MPa	
3	Mr_3= 3074 MPa	
4	Mr_4= 4076 MPa	
5	Mr_1 = 1230 MPa	**10 mm Machined-Off Segments:** - 150 mm diameter (Original Dimension) - X = 10 mm - Height 80 mm 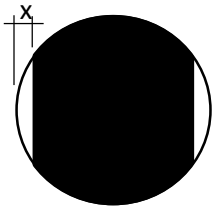
6	Mr_2= 1672 MPa	
7	Mr_3= 3074 MPa	
8	Mr_4= 4076 MPa	
9	Mr_1 = 1230 MPa	**15 mm Machined-Off Segments:** - 150 mm diameter (Original Dimension) - X = 15 mm - Height 80 mm 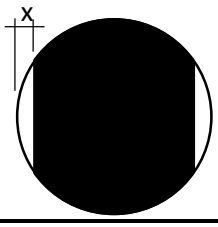
10	Mr_2= 1672 MPa	
11	Mr_3= 3074 MPa	
12	Mr_4= 4076 MPa	
13	Mr_1 = 1230 MPa	**19 mm Machined-Off Segments:** - 150 mm diameter (Original Dimension) - X = 19 mm (Test bed requirement for MMLS testing) - Height 80 mm 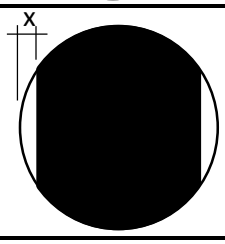
14	Mr_2= 1672 MPa	
15	Mr_3= 3074 MPa	
16	Mr_4= 4076 MPa	

4.5 INDIRECT TENSILE TEST (ITT): DETERMINING THE RESILIENT MODULUS

The COLTO medium 50/70 penetration graded binder combination, subjected to dry MMLS3 trafficking (see test matrix in Figure 3.5), was selected to determine the resilient modulus of the asphalt mixture under various temperature and load frequency conditions. The indirect tensile test (ITT) was used to determine the resilient modulus according to ASTM method D4123-83.

A materials testing system (MTS), similar to that described in *Appendix B*, was used to perform ITT tests. During ITT testing the asphalt briquettes were subjected to a repeated loading with a magnitude equal to 10% of maximum load to cause failure. A range of frequencies was selected to determine the asphalt's response during short and long loading periods. The repeatability of the applied load was determined through a Haversine wave with a specific frequency. Depending on the frequency, each Haversine wave had loading and resting periods with specific durations. Figure 4.5 illustrates the composition of a Haversine wave.

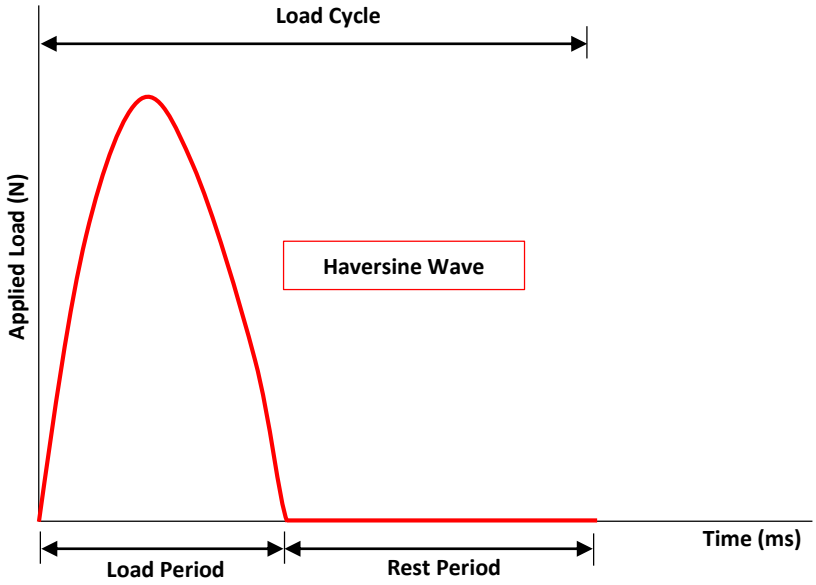

Figure 4. 5 - Haversine wave composition.

Table 4.3 summarizes the duration of the loading and rest periods per frequency selected to perform ITT tests. The asphalt's response during loading at various temperatures was also evaluated for the range of temperatures as shown. A total of 12 test combinations were performed to complete a single ITT test.

Furthermore, a total of three asphalt briquettes were used to perform ITT tests on this specific binder combination (i.e. COLTO medium 50/70 penetration grade).

Table 4. 3 - Summary of frequencies and temperatures selected for ITT test.

Frequencies and Temperatures				
Combination	Frequency (Hz)	Load Period (ms)	Rest Period (ms)	Temperature (°C)
1	1	1000	2000	10
2	2	500	1000	10
3	5	200	500	10
4	10	100	500	10
5	1	1000	2000	15
6	2	500	1000	15
7	5	200	500	15
8	10	100	500	15
9	1	1000	2000	25
10	2	500	1000	25
11	5	200	500	25
12	10	100	500	25

According to ASTM method D4123-82, specimens subjected to ITT testing should be 150 mm in diameter and at least 76 mm high. Asphalt briquettes prepared for MMLS3 trafficking were 150 mm in diameter and 80 mm in height. The dimensions of these asphalt briquettes, therefore, conformed to the specification. With the test combination in Table 4.3 known, asphalt briquettes were mounted in the MTS as illustrated in Figure 4.6. A jig was fixed to the asphalt briquette for the installation of two linear variable differential transducers (LVDT's) required for the measurement of the horizontal deformation during load applications. The horizontal deformation was required to calculate the resilient modulus after each applied load.

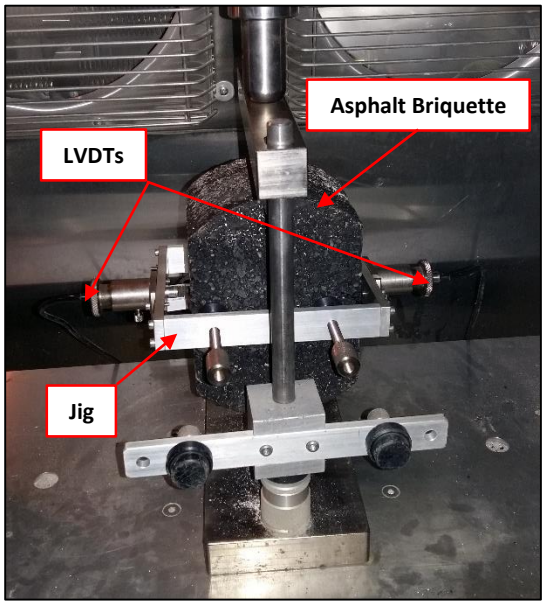

Figure 4. 6 - ITT test setup.

During testing the MTS's software automatically calculated the resilient modulus of an asphalt briquette after a load repetition was completed. This was required to determine the number of load cycles until a stable resilient modulus condition was produced. It was found that 200 load cycles produced a stable resilient modulus condition, which also conformed to the minimum required number of load cycles according to ASTM method D4123-83. The test method also required that a specimen was tested twice for its resilient modulus by turning it through 90° once the first test was completed. However, the

machined-off segments of the asphalt briquette subjected to MMLS3 trafficking limited ITT testing to one resilient modulus test per asphalt briquette per ITT test combination. According to ASTM method D4123-83, the resilient modulus is calculated using Equation 4.1.

$$E = \frac{P \times (v + 0.27)}{t \times \Delta H} \qquad \textit{Equation 4.1}$$

where $E = Total\ Resilient\ Modulus\ of\ Elasticity\ (MPa)$

$P = Applied\ Load\ (N)$

$v = Total\ Resilient\ Poisson's\ Ratio$

$\Delta H = Total\ Recoverable\ Horizontal\ Deformation\ (mm)$

$t = Asphalt\ briquette's\ Thickness\ (mm)$

A Poisson's ratio of 0.4 was selected for use in Equation 4.1, as this is representative of the average Poisson's ratio of asphalt subjected to cold and warm temperatures (SAPEM Chapter 2, 2014). The resilient modulus was calculated for each of the three asphalt briquettes per test combination as shown in Table 4.3. The average resilient modulus per test combination was then calculated and are these are shown in Table 4.4.

Table 4. 4 – Average resilient modulus results after ITT testing.

Binder Combination	Frequency (Hz)	Average Resilient Modulus (MPa)
Temperature (10°C)		
50/70 Penetration Grade Bitumen	1	6948
	2	8782
	5	11927
	10	14822
Temperature (15°C)		
50/70 Penetration Grade Bitumen	1	4080
	2	5506
	5	8428
	10	9800
Temperature (25°C)		
50/70 Penetration Grade Bitumen	1	1230
	2	1672
	5	3074
	10	4076

As indirect tensile strength (ITS) tests were performed at a temperature of 25°C during the execution of the primary experimental research methodology, the results for the resilient modulus as determined at this temperature were used as input values for Abaqus during the finite element analysis.

4.6 CREATING FINITE ELEMENT MODELS

The complete procedure followed to create and analyse the finite element models as described in Table 4.2, is not presented in this Chapter. This is due to the procedure being based on previous research done by Walker (2013) as described in *Appendix C*.

Four 3-dimensional linear-elastic finite element models, each with different shapes (see Table 4.2), were compiled by completing all Abaqus/CAE modules as presented in Table 4.1. The finite element model created and analysed for each shape, consisted of a quarter of the asphalt briquette. By using symmetric boundary conditions the remaining three quarters of each asphalt briquette were accounted for. The pressure load applied to the finite element model was equal to the average failure load for the 50/70 penetration grade binder combination subjected to dry MMLS3 trafficking. This failure load was determined after ITS testing. The stress and strain results along the x-, y- and z-axis were obtained to determine the influence of the machined-off segments. Figure 4.7 illustrates one of four 3-dimensional finite element models created and analysed in Abaqus/CAE.

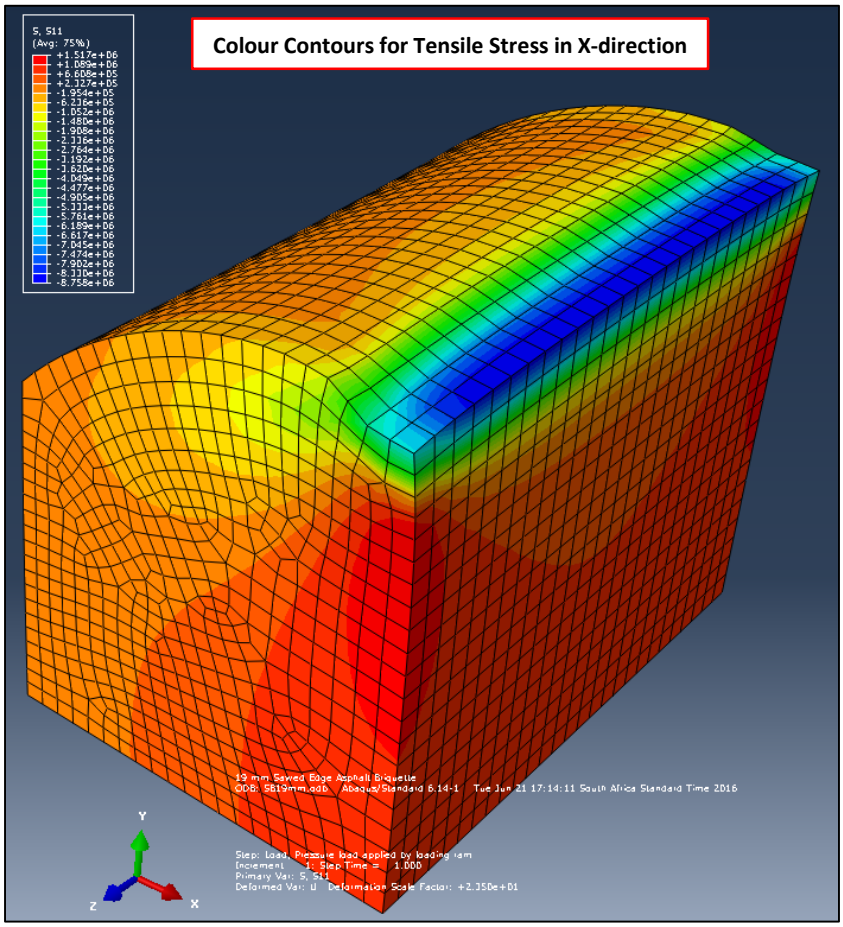

Figure 4. 7 - One of four finite element models created and analysed in Abaqus/CAE.

4.7 RESULTS EXTRACTION

Typical stress distributions along the x and y-axes, after ITS testing, are illustrated in Figure 4.8. From Figure 4.8 it follows that the distribution of stresses along the x-axis is influenced by the machined-off segments as the length is shortened over which tensile and compressive stresses can be distributed. It was expected that a redistribution of stresses will occur as a result of the foregoing and that this may influence the maximum tensile stress determined after ITS testing for asphalt briquettes with machined-off segments.

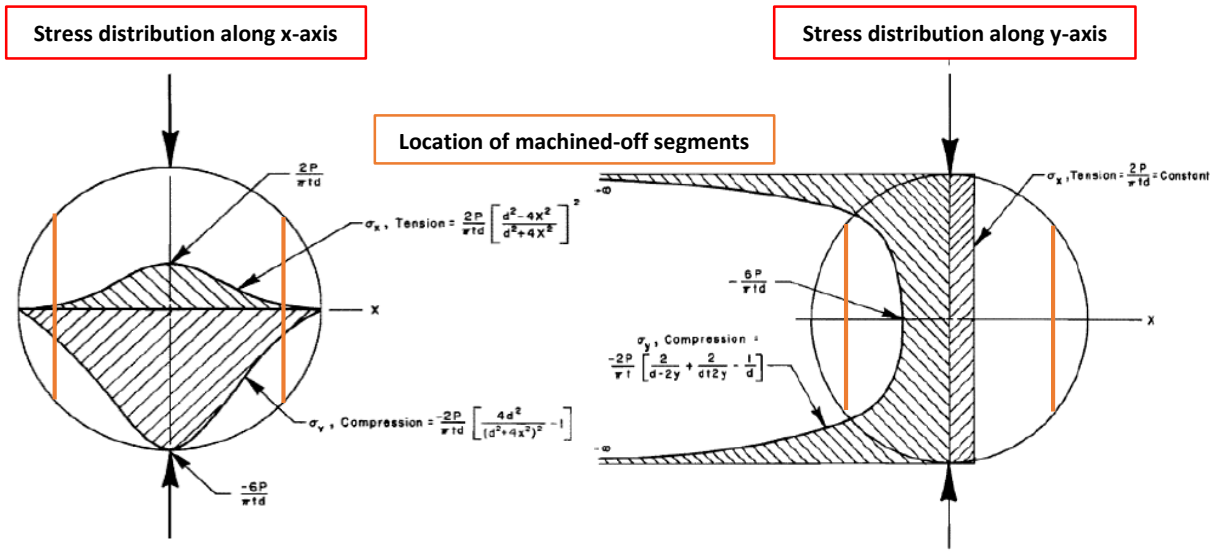

Figure 4. 8 - Distribution of stresses along x and y-axes during ITS testing (Hudson & Kennedy, 1968).

From Figure 4.8 it is clear that the distribution of compressive stresses along the y-axis should not be influenced by machined-off segments. However, this needs to be investigated in this research.

Based on Figure 4.8, the following stress results were obtained from the finite element models as developed for this study (See figure below for convention of block elements in finite element models):

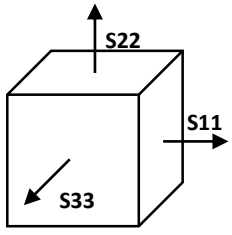

- S11 (Tensile stress on the x-plane in the x-direction) along the x-axis
- S11 (Tensile stress on the x-plane in the x-direction) along the y-axis
- S22 (Compressive stress on the y-plane in the y-direction) along the x-axis
- S22 (Compressive stress on the y-plane in the y-direction) along the y-axis

In addition, it was decided to investigate the distribution of the tensile stresses through the depth of the asphalt briquette. It must be noted that the tensile and compressive stresses S33 and S22 were not considered as the machined-off segments were not along the z-axis in the direction of these stresses. As a result of Hooke's law, it was also decided to investigate the strain along the x-axis in order to determine

the influence of a change in the resilient modules. Therefore, the following results were also extracted from the finite element models:

- S11 (Tensile stress on the z-plane in the z-direction) along the z-axis
- E11 (Tensile strain on the x-plane in the x-direction) along the x-axis

4.8 SUMMARY

The objective of this secondary research methodology was to investigate the effect of the geometry of 150 mm diameter asphalt briquettes on the outcome of ITS tests. Laboratory scale MMLS3 trafficking required the re-shaping of nine 150 mm diameter asphalt briquettes in order to fit in the test bed setup designed for the MLS system. Linear-elastic finite element analysis was assumed and four 3-dimensional asphalt briquette models were analysed in Abaqus/CAE software. Each of the four finite element models had different machined-off segments with a mid-ordinate ranging from 0 to 19 mm (see Table 4.2). The procedure for setting up the finite element models in Abaqus/CAE was based on the research methodology of Walker (2013).

ITT resilient modulus tests were performed on three COLTO medium asphalt briquettes with a 50/70 penetration grade binder. The resilient modulus of this mixture was determined at 25^{o}C and four loading rates according to ASTM method D4123-82. Different magnitudes of the resilient modulus were also included in the finite element analysis to investigate if a change in mixtures stiffness and briquette shape had an influence on the stress distribution within the asphalt briquette.

Stress and strain results were obtained along the x-, y- and z-axes and are presented in *Chapter 6*.

CHAPTER 5 - RESULTS AND INTERPRETATION: EXPERIMENTAL RESEARCH METHODOLOGY

5.1 INTRODUCTION

This Chapter contains the results obtained during execution of the primary experimental research methodology as presented in Chapter 3. Indirect tensile strength (ITS) testing, permanent deformation, texture and material loss of asphalt briquettes form the basis of results. These results are interpreted to conclude the laboratory findings for this study. The outline of this Chapter is illustrated in Figure 5.1.

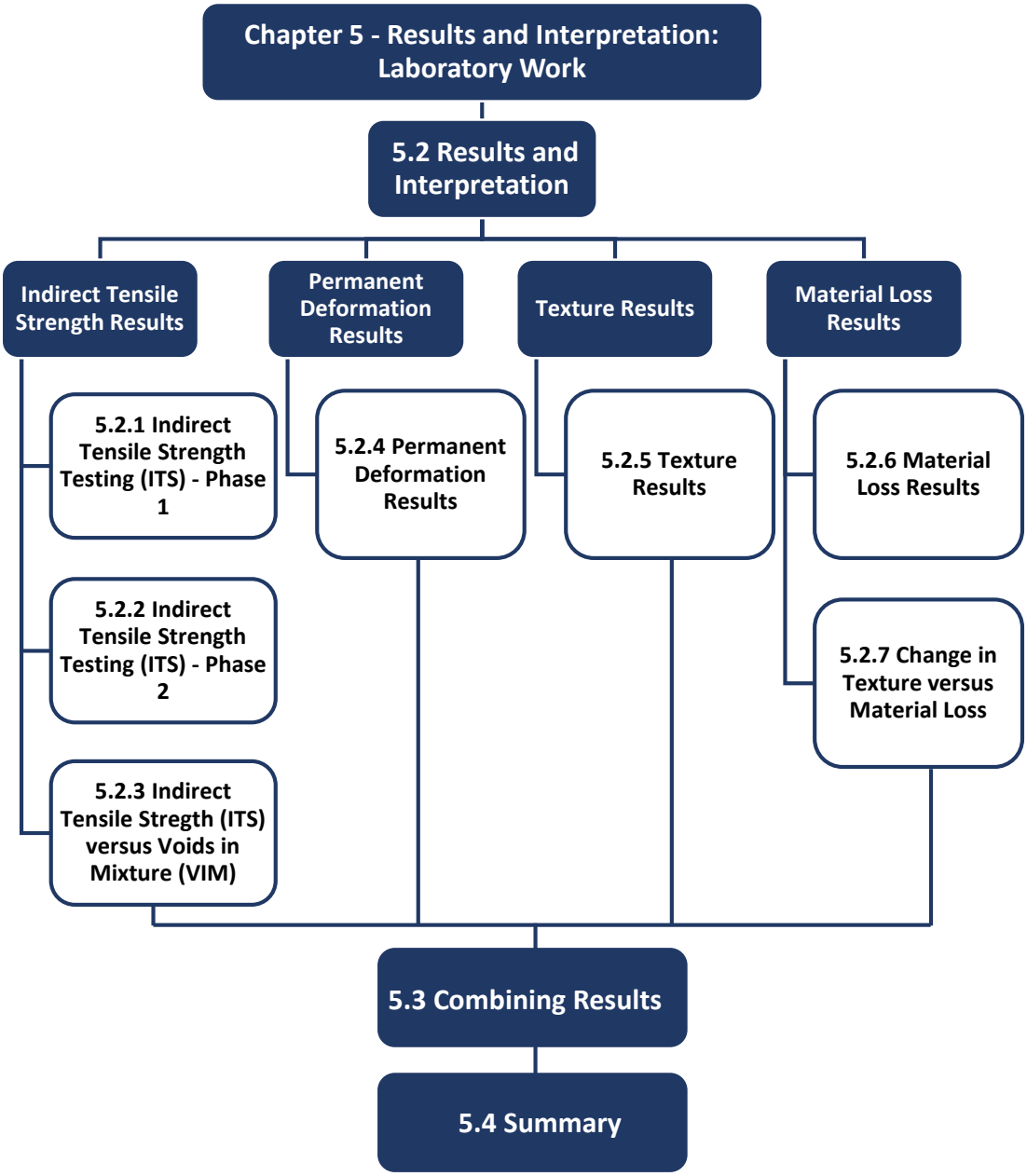

Figure 5. 1 - Layout of Chapter 5.

5.2 RESULTS AND INTERPRETATION

5.2.1 INDIRECT TENSILE STRENGTH TESTING (ITS) - PHASE 1

Phase 1 of this research methodology formed part of an initial investigation to determine the effect grey water had on the performance of various asphalt gradations and binder combinations. During this phase, asphalt briquettes were subjected to no conditioning, clean water conditioning and grey water conditioning using the MIST device (see *Appendix B*).

5.2.1.1 Mixture Strength and Stiffness

The ITS results for Phase 1 are shown in Figure 5.2. The COLTO specification requires a minimum indirect tensile strength of 800 kPa at a test temperature of 25°C for acceptable mixture strength and stiffness properties under a level 1 mix design.

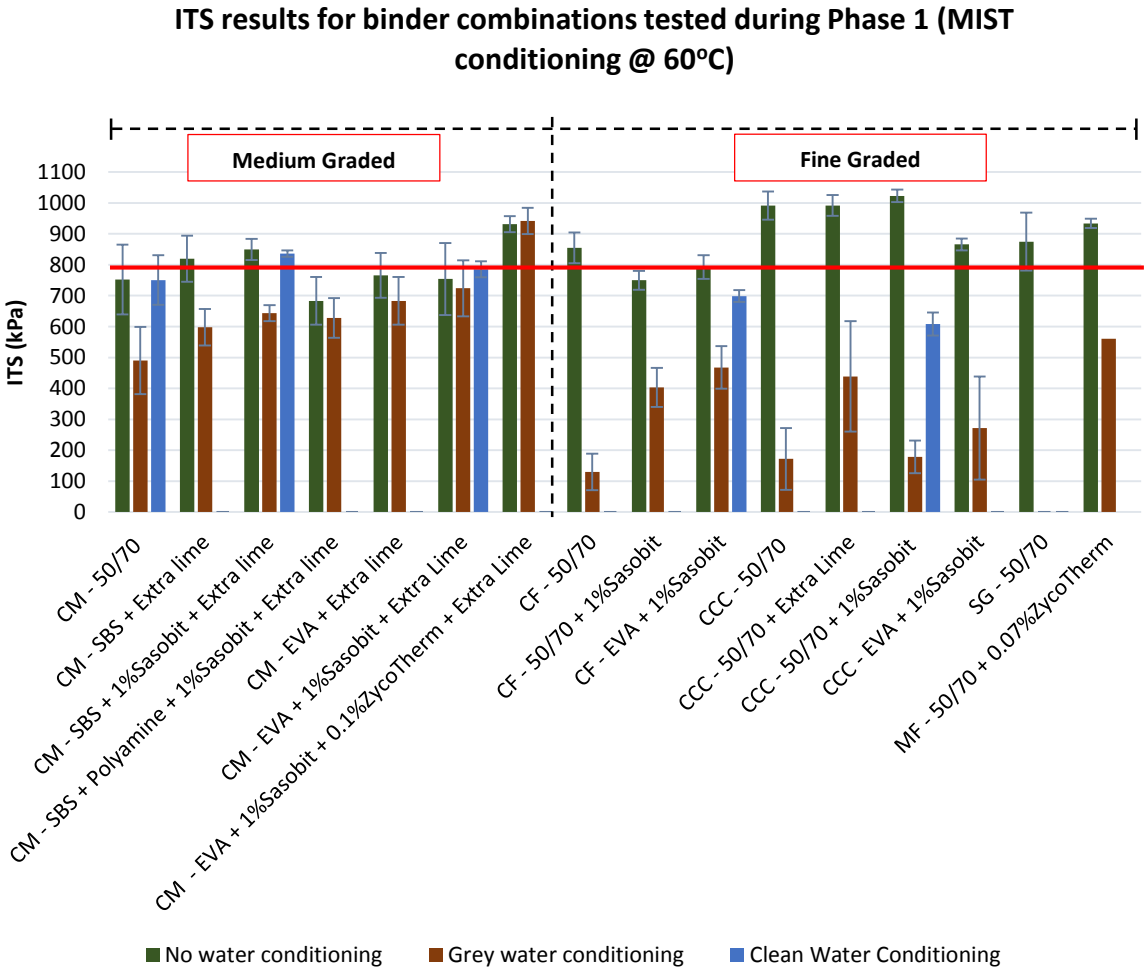

Notes: CM – COLTO Medium Graded; CF – COLTO Fine Graded; CCC – City of Cape Town Fine Graded; SG – Semi-Gap Graded; MF - Much Fine Grade

Figure 5. 2 - ITS results for binder combinations tested during Phase 1.

From Figure 5.2 follows that only three no water conditioned medium grade binder combination achieved an ITS result of greater than 800 kPa. These binder combinations were:

- SBS + Extra Lime
- SBS + 1% Sasobit® + Extra Lime
- EVA + 1% Sasobit® + 0.1% Zycotherm® + Extra Lime

The remaining no water conditioned medium graded binder combinations, except for the SBS plus polyamine plus 1% Sasobit plus extra lime, achieved ITS result of approximately 800 kPa as concluded from the standard deviation. According to Sabita Manual 35, the indirect tensile test assesses the strength and stiffness properties of the asphalt mixture. From Figure 5.2 follows that most no water conditioned medium graded binder combinations were in the proximity of the ITS requirements for strength and stiffness properties.

Clean water MIST conditioning was only completed as spot checks to compare with the damage caused by grey water conditioning. From Figure 5.2 follows that medium graded binder combinations, exposed to clean water MIST conditioning did not show significant changes in the indirect tensile strength as all results were in the proximity of 800 kPa. This indicates that clean water exposure do not have an influence on the strength and stiffness of these binder combinations. Based on the results of the medium graded 50/70 penetration grade binder combination, a lime content of 1%, as required for this mix design, was sufficient to provide mixture strength and stiffness under clean water conditions.

From Figure 5.2 follows that medium graded binder combinations exposed to grey water MIST conditioning indicated reduced ITS results. Research done by Ball et al (1999) investigated the permeability of chip-seals cores by mimicking pressures generated by vehicle tyres. Typical pressures that are generated by vehicle tyres reach up to 700 kPa. However, Ball et al (1999) found that a pressure of approximately 100 kPa may be sufficient to force water into the chip seal. They further concluded that water sometimes spread between the chip-seal layers instead of penetrating into the base layer. With this as background, it is apparent that the pressure of 150 kPa generated by the MIST device may be sufficient to force moisture into the mastic of asphalt briquettes located in the triaxial cell (see *Appendix B* for detail on the MIST device). Penetration of moisture may not have been significant for medium graded asphalt mixtures exposed to clean water, as indicated by ITS results. However, exposure to grey water may indicate that this phenomenon has occurred and was assisted by surfactants present in grey water. Only two binder combinations achieved or were in the proximity of the 800 kPa ITS specification. These binder combinations were:

- EVA + 1% Sasobit® + Extra Lime
- EVA + 1% Sasobit® + 0.1% ZycoTherm® + Extra Lime

It is apparent that the addition of Sasobit® wax was related to the strength and stiffness achieved by these asphalt mixtures. According to the *Technical Guideline 1* (TG1), F-T waxes allow lower compaction temperatures by reducing the viscosity of the bitumen. In addition, it also produces a binder with significantly higher stiffness during in-service temperatures when compared to conventional bitumen. MIST conditioning was done at 60°C, which is a good representation of typical in-service temperatures. The ability of Sasobit® wax to sustain higher stiffness during high in-service temperatures was reflected in ITS results. The 50/70 penetration grade binder combination indicated the highest reduction in strength and stiffness after exposure to grey water. This result substantiates the statement that the use of unconventional binder combinations are required to ensure that the required strength and stiffness are achieved under grey water conditions. SBS modified binder combinations also did not achieve the required asphalt strength and stiffness. However, the results indicated that the mixture strength and stiffness after grey water conditioning were higher than the 50/70 penetration grade binder combination. This can be attributed to either the addition of extra lime or the properties of the SBS modified binder, with both contributing to the strength and stiffness of the asphalt mixture.

From Figure 5.2 follows, that most fine graded asphalt mixtures achieved an ITS result of 800 kPa. The CCC fine asphalt mixtures, which are a standard fine continuous graded asphalt mixtures used by the City of Cape Town for surfacing of roads in informal settlements, achieved the highest strength and stiffness under no water conditions. From these results it are apparent that the CCC fine graded asphalt mixtures, due to their continuous grade, were more densely compacted after 100 gyrations which may be responsible for their significant strength and stiffness. The semi-gap and Much fine graded binder combinations also achieved significant mixture strength and stiffness under no water conditions. No significant variation in the ITS for penetration grade and modified binder combinations were observed for the CCC fine, semi-gap and Much graded asphalt mixtures. It was expected that the COLTO fine continuous graded binder combinations would achieve the greatest ITS results as their binder content was 6% when compared to 5.5% for other fine graded mixtures. In addition, a 1% lime content formed part of its mix design. According to Sabita Manual 35, active filler serves the purpose of acting as an extender for the binder in order to stiffen the mastic in the asphalt mixture, thereby improving the stability. Active filler is therefore essential to produce dense, cohesive, durable and resistance to water penetration in asphalt mixtures (Sabita Manual 35/TRH8, 2016).

ITS results indicated that fine graded asphalt mixtures, exposed to clean water MIST conditioning, did not achieve the 800 kPa specification. From this result it can be concluded that sufficient mixture strength and stiffness were not achieved by these mixtures after exposure to clean water conditioning. These results may be related to the penetration of moisture into the mastic of asphalt mixtures,

causing moisture damage as per the phenomenon discussed by Ball et al. (1999). Although the COLTO fine continuous graded asphalt mixture produced lower ITS results when compared to the CCC fine graded asphalt mixtures under no water conditioning, it is apparent that when exposed to clean water conditioning that COLTO fine continuous graded asphalt mixtures sustained greater ITS results. In this case, the ITS result is not necessarily related to the grading, but may be related to the binder combinations. The use of an EVA modified binder combination indicated greater resistance to clean water conditioning when compared to a 50/70 penetration grade bitumen. EVA forms a rigid three-dimensional network within the base binder, however, it does not necessarily improve the elastic recovery properties of the base binder, but provides a high stiffness (Asphalt Academy-TG1, 2007). ITS results reflected an improvement in the stiffness of the fine graded asphalt mixtures under clean water conditioning.

From Figure 5.2 follows that none of the fine graded asphalt mixture exposed to grey water conditioning achieved an ITS result of at least 800 kPa. Compared to medium graded asphalt mixtures, fine graded asphalt mixtures tend to be more susceptible to grey water related damage in their structures under similar test conditions. COLTO medium and fine graded 50/70 penetration grade binder combinations both require a 1% lime content in their mix designs. However, the COLTO fine graded mixture sustained greater damage after grey water exposure. Considering the variables of these two mixtures, the maximum nominal aggregate size may be related to the difference in mixture strength and stiffness. This is confirmed by the *Interim Guidelines for the design of Hot-Mix Asphalt (2001)*, which states that by increasing the nominal aggregate size, the stability of an asphalt mixture is generally increased. However, it reduces the workability of the mixture. This conclusion highlights the importance of the asphalt grading when the grey water resistance of asphalt is investigated. The COLTO fine continuous graded asphalt mixtures were the preferred fine graded asphalt to resist grey water exposure. A 1% lime content required for this asphalt gradation in combination with a binder modified with Sasobit® wax, may be related to this performance. Research indicated that the addition of lime has a chemical benefit to the moisture resistance of asphalt. A chemical reaction results in an ion exchange between the bitumen, aggregate and lime that improves the adhesion at the bitumen-aggregate interface (Robertson, 2000).

The performance of most CCC fine graded asphalt mixtures were poor in relation to COLTO fine continuous graded asphalt mixtures. Failures of the 50/70 penetration grade bitumen and 50/70 plus 1% Sasobit binder combination specimens were observed. However, it was possible to obtain ITS results. Semi-gap graded asphalt mixtures did not provide any mixture strength and stiffness after grey water exposure. MIST conditioning for this study was set for a duration of 6 hours and 2 minutes. The semi-gap graded asphalt mixture completely failed after 45 minutes of grey water conditioning. It

was interesting to notice that both the CCC fine and semi-gap graded asphalt mixtures had a natural sand fraction in its grading. During sample preparation it was found difficult to coat sand particles with bitumen, as this may have provided access for moisture to penetrate under a pressure of 150 kPa and cause loss of adhesion. This may indicate that the natural sand fraction should be avoided in mixtures designed with grey water resistance. However, MMLS3 testing may provide additional answers to this observation. Figures 5.3 illustrates severe cracking of the CCC fine 50/70 penetration grade and significant loss of adhesion by the CCC fine 50/70 plus 1% Sasobit® asphalt mixtures during grey water MIST conditioning. Poor coating of natural sand particles and complete failure of the semi-gap graded asphalt mixture are also illustrated in Figure 5.3.

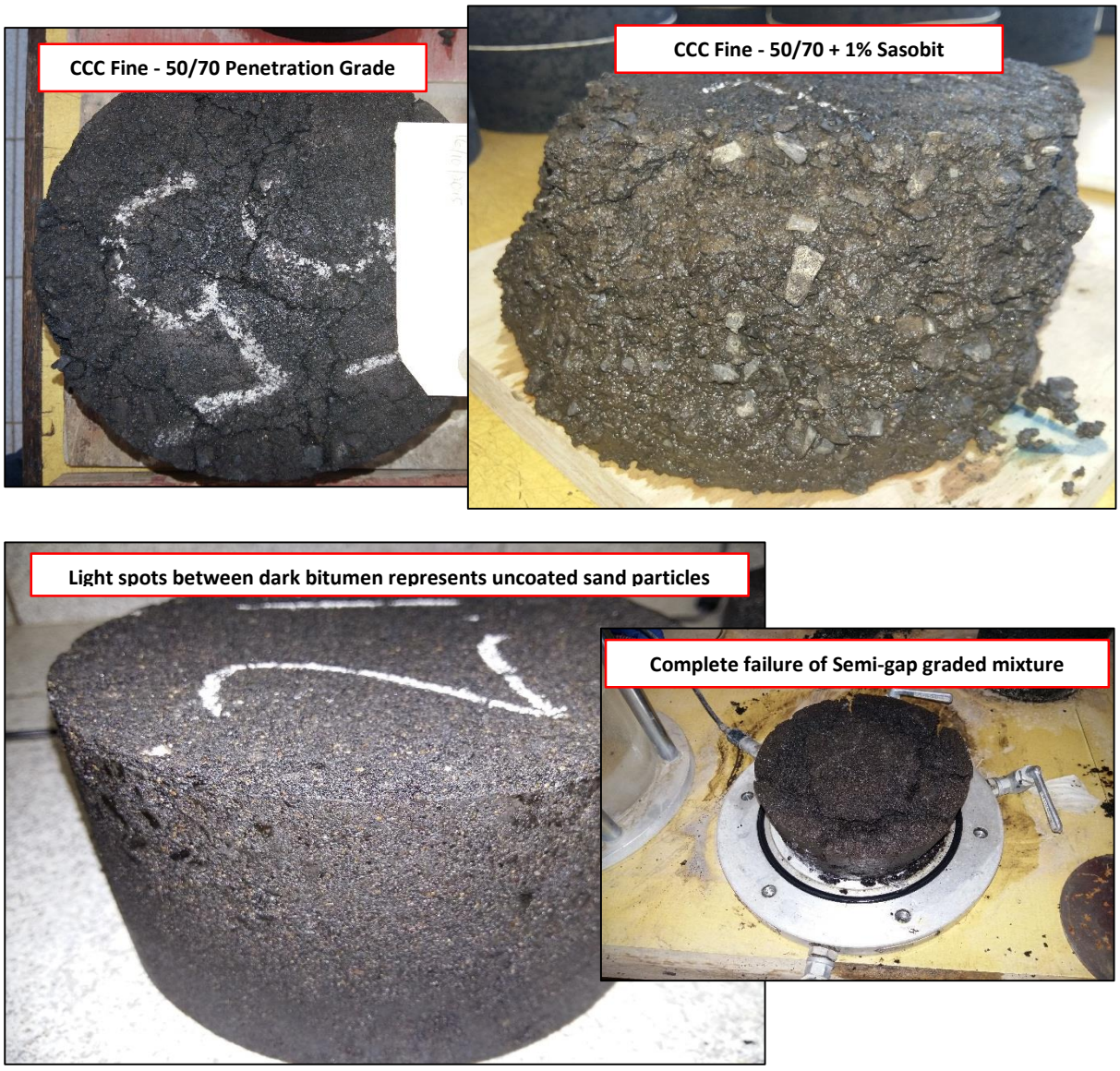

Figure 5. 3 - Failure of asphalt mixtures after grey water MIST conditioning.

The Much fine graded asphalt mixture also indicated signifcant mixture strength and stiffness. However, it should be noted that the ITS result in Figure 5.2 represents a sample size of one. Failure

of this asphalt mixture was also observed during grey water MIST conditioning. Failure of this mixture was related to the mixture properties, which is decussed in *Section 5.2.1.2.*

5.2.1.2 Moisture Suceptibility

According to Sabita Manual 35, the moisture susceptibility of asphalt mixtures is measured through a tensile strength ratio. The tensile strength ratio (TSR) represents the retained strength after an asphalt mixture was exposed to moisture conditioning. Sabita Manual 35 suggests the use of the Modified Lottman test (ASTM D4867 M) to determine the durability or TSR of asphalt mixtures after moisture exposure. However, conditioning performed on asphalt briquettes was approached different to the Modified Lottman test specification. Instead the MIST device was used for conditioning purposes. The Modified Lottman test specifies a minimum TSR of 80% for wearing courses to achieve acceptable moisture resistance under level 1 mix designs. This specification was also used in interpreting TSR results for this study. However, it should be noted that due to the uniqueness of this study, this specification may not be completely accurate in predicting the moisture susceptibility of asphalt mixtures exposed to grey water. This specification was set for asphalt mixtures exposed to moisture without the presence of surfactants. TSR results for Phase 1 are shown in Figure 5.4.

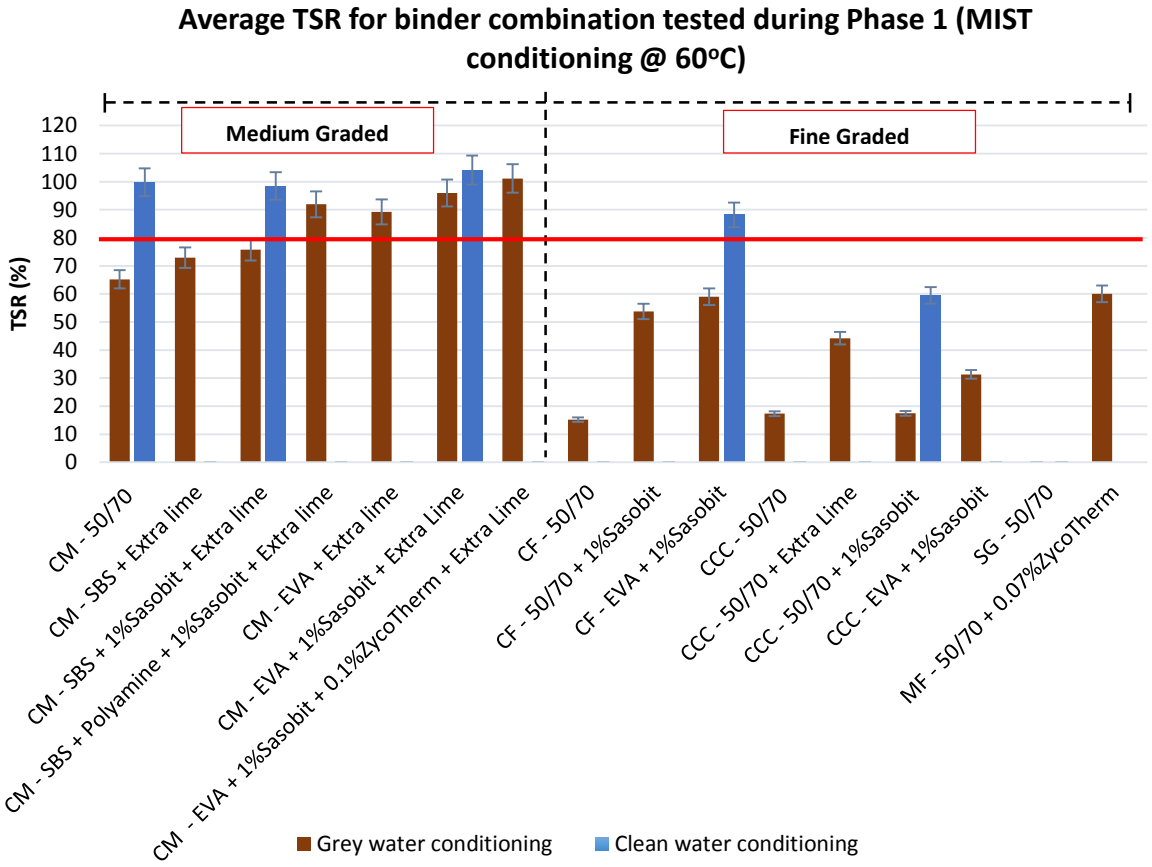

Notes: CM – COLTO Medium Graded; CF – COLTO Fine Graded; CCC – City of Cape Town Fine Graded; SG – Semi-Gap Graded; MF - Much Fine Graded

Figure 5. 4 - TSR for binder combinations tested during Phase 1.

From Figure 5.4 follows that clean water MIST conditioning of selected binder combinations did not cause as much moisture damage when compared to grey water MIST conditioning. All binder combinations subjected to clean water MIST conditioning indicated a greater retained strength compared to the retained strength after grey water MIST conditioning. This indicated that moisture was more easily forced into the asphalt briquettes under 150 kPa of pressure with the assistance of surfactants present in grey water as compared to clean water. It should be noted that the TSR results for one case of clean water conditioning was above 100%, which indicated that the retained strength was greater than obtained after no water conditioning. The most reasonable explanation to this result was mechanical problems experienced with the MIST device. The solenoid switches of the MIST device did not function properly during clean and grey water conditioning of some asphalt mixtures. This may have led to the generation of pressure pulses less than 150 kPa which may have resulted in insignificant damage to the asphalt mastic. However, conclusions from Figure 5.4 are in line with findings by Greyling et al. (2015(2)) and Petersen (2013), where damage to asphalt mixtures subjected to clean water conditioning was observed. However, the presence of surfactants significantly accelerates the rate of damage.

From Figure 5.4 it follows that the 50/70 penetration grade binder combinations showed the least retained strength for a given asphalt gradation. However, the medium graded 50/70 penetration grade asphalt mixture's TSR result was only 10% smaller when compared to most modified binder combinations tested for the COLTO medium gradation. Based on the Sabita Manual 35 TSR specification of 80%, the medium graded 50/70 penetrations grade asphalt mixture did not conform to the moisture resistance specification. This indicated that a modified binder is required to enhance the engineering properties of the COLTO medium graded asphalt to an acceptable level of grey water resistance.

It is also noted that medium graded asphalt mixtures retained greater strength when compared to the fine graded asphalt mixtures. The average void content of these gradations may be related to this behaviour. Figure 5.5 shows the average VIM for all asphalt gradations tested during Phase 1. From Figure 5.5 follows that the average VIM for the COLTO medium graded asphalt mixtures was less than 5%, whereas fine graded asphalt mixtures achieved VIM values of greater than 5%. This can be related to the difference in TSR results, as volumetric properties of the asphalt mixture are of great importance when it comes to improving grey water resistance. The foregoing was also concluded from the Literature Review in *Chapter 2.* Greyling et al. (2015(2)) concluded that the asphalt mixture's resistance to grey water is improved by increased compaction effort. Results on the average void content of asphalt mixtures may also provide an indication of the compactibility of mixtures tested during Phase 1. The red line in Figure 5.5 indicates the compaction specification of a gyratory

compacted specimen after a design number of 100 gyrations which is set by the Superpave mixture design method for a traffic class of 3 to less than 10 million equivalent standard axle loads (ESALs). From these results it can be concluded that the COLTO medium continuous graded asphalt mixtures were more compactible when compared to fine graded asphalt mixtures. The compactibility of asphalt mixtures is discussed in more detail in *Section 5.2.1.3*.

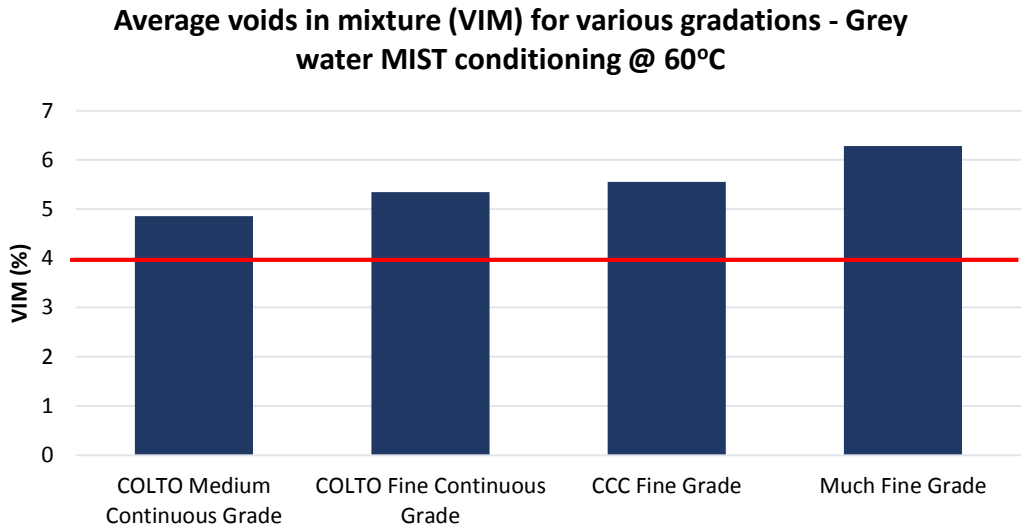

Figure 5. 5 - Average void in mixture for gradations tested during Phase 1.

Referring to research done by Ball et al. (1999) on the penetration of water through a chip-seal under the pressure of a vehicle tyre, penetration of water into the base course was significantly higher where voids in the chip-seal were present. This led to an increase in the moisture content of the base layer at such locations where shear and pothole failures soon followed. This highlights the importance of the surfacing layer to be water proof. In this case study it has been confirmed that the presence of surfactants in grey water significantly reduces the moisture resistance of an asphalt mixture. From Figure 5.5 follows that the void content of the COLTO medium continuous graded asphalt mixtures was less than the void content of fine graded asphalt mixtures. In addition to the void content, the 150 kPa generated in the MIST triaxial cell may be related to the TSR obtained by various mixtures. It is apparent that the higher the void content, the more easily water can be forced into the asphalt structure that interferes with the adhesive bond between the bitumen and aggregate.

From Figure 5.4 follows that the medium graded EVA plus 1% Sasobit® plus 0.1% ZycoTherm® plus extra lime binder combination retained most of its strength after grey water conditioning. However, this result may not be completely accurate as mechanical problems were experienced with the MIST device as previously explained. The SBS plus polyamine plus 1% Sasobit® plus extra lime and the EVA plus 1% Sasobit® plus extra lime medium graded binder combinations also showed good performance with a retained strength of greater than 90%. EVA plus 1% Sasobit® was the fine grade binder

combination that retained most of its strength after grey water conditioning. The significant performance of these mixtures can be related to the binder additives used. A combination of strength enhancing additives such as SBS and EVA, as well as adhesion improving additives such as polyamine and ZycoTherm®, assisted in achieving the higher retained strength in these mixtures.

The overall retained strength of CCC fine graded asphalt mixtures with binder additives, after grey water MIST conditioning, was less than that of the COLTO fine continuous graded asphalt mixtures with binder additives. As discussed in *Section 5.2.1.1*, the CCC fine gradation consisted of a sand fraction which was found difficult to coat with bitumen during the sample preparation stage. When exposed to moisture, poor coating of the aggregate surface was identified in the Literature Review as a factor causing significant loss of adhesion in the asphalt mixture. Uncoated aggregate surfaces provide easy access for the grey water to penetrate and cause significant loss of adhesion. Cases of significant loss of adhesion was observed during grey water MIST conditioning.

As already concluded in *Section 5.2.1.1*, the semi-gap graded asphalt mixture performed the poorest of all fine graded asphalt mixtures due to premature failure. This asphalt mixture did not provide any resistance to grey water conditioning. As a consequence, no TSR value was available for this mixture. This result contradicts findings by Briedenhann and Jenkins (2015), where they concluded that the semi-gap graded asphalt mixture showed potential to resist grey water due to its low void content. However, it should be noted that the semi-gap graded asphalt mixture used in this study had an extremely high natural sand content of 35%. The natural sand content of a laboratory prepared semi-gap graded asphalt mixture by Briedenhann and Jenkins (2015) was 15%. Briedenhann and Jenkins (2015) tested a variety of binder additives with the semi-gap graded asphalt mixture where ITS results, obtained at a temperature of 40°C, were compared with a continuous graded asphalt mixture. They concluded that the semi-gap graded asphalt mixture obtained a higher ITS result for 75% of the cases after grey water conditioning, to the lower void content of this mixture.

The Much fine graded asphalt mixture experienced similar problems as CCC fine and semi-gap graded asphalt mixtures. Premature failure of these mixtures was also observed. However, one asphalt briquette resisted grey water MIST conditioning and was subjected to ITS testing. The retained strength (Figure 5.4) and ITS (Figure 5.5) results obtained for this asphalt mixture are therefore only based on a single asphalt briquette. These results should therefore not be considered significant when compared to other tested asphalt mixtures. From Figure 5.5 it follows that the Much fine graded asphalt mixture had the highest void content of all gradations. This can possibly be related to the failure of this mixture as a result of grey water penetrating the voids and causing a loss of adhesion.

5.2.1.3 Permeability and Compactibility

It is apparent that the permeability of an asphalt mixture is dependent on the void content and migration of moisture as a result of vehicle tyre pressures (Ball, et al., 1999). Tests have shown that the permeability of asphalt layers is very low for void contents of less than 6%. However, between 6% and 7% permeability significantly increases. At void contents of 8% to 8.5% the asphalt layer becomes excessively permeable (Hainin, et al., 2003). It is most likely that permeability tests completed by Hainin et al. (2003) to investigate the permeability of an asphalt mixture versus the void content, were performed with water with no surfactant content and no exposure of asphalt mixtures to pressure pulses. Figure 5.6 shows the void content of binder combinations tested during Phase 1 of this study.

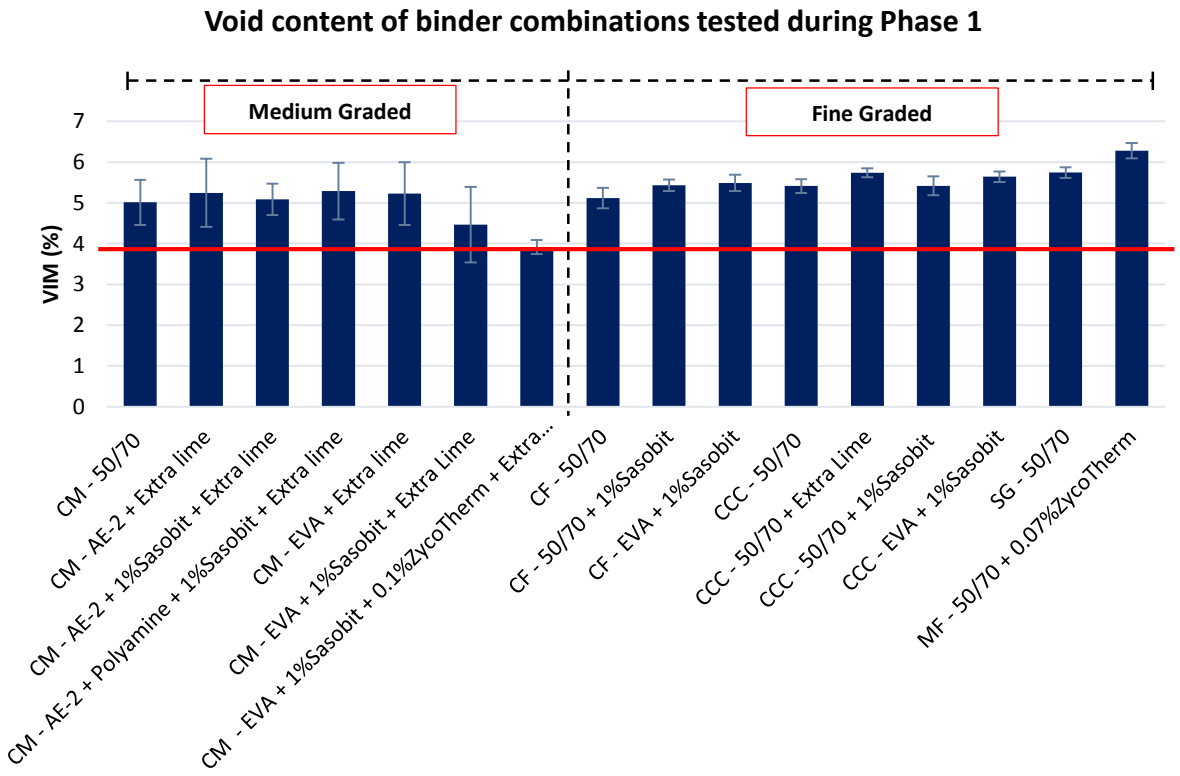

Notes: CM – COLTO Medium Graded; CF – COLTO Fine Graded; CCC – City of Cape Town Fine Graded; SG – Semi-Gap Graded; MF - Much Fine Graded

Figure 5. 6 - Void content of binder combinations tested during phase 1.

Permeability was investigated in terms of the void content limits as stated by Hainin et al (2003). In addition, the void content was also compared to the TSR results of Phase 1 to provide an indication of the permeability. A hypothesis was established which stated that an increase in the void content will lead to a reduction in the TSR result this being due to the penetration of grey water into the asphalt mixture under the 150 kPa induced by the MIST device.

From Figure 5.6 follows that, with the exception of the Much Fine graded asphalt mixture all binder combinations had a void content of less than 6%. Therefore, most asphalt mixtures tested during this Phase 1 should have low permeability according to Hainin et al (2003). It was interesting to notice that asphalt mixtures that failed under grey water MIST conditioning had void contents that ranged between 5.5% to 6%. This may indicate that a combination of surfactants and exposure to pressure pulses of 150 kPa may increase the permeability of asphalt mixtures which in turn leads to significant moisture damage and loss of adhesion (see Figure 5.3). Although TSR results were obtained for most asphalt mixtures that failed during Phase 1 (see Figure 5.3), it was interesting to notice that these mixtures were among mixtures with the highest void content. An asphalt mixture, such as the COLTO medium EVA plus 1% Sasobit® plus 0.1%ZycoTherm® plus extra lime, had a void content of 4% and achieved significant strength and stiffness after grey water MIST conditioning. These observations indicated that the hypothesis on the permeability of asphalt mixtures may be confirmed, although this was not the case for all asphalt mixtures tested during Phase 1. An ANOVA analysis was therefore performed to investigate this hypothesis statistically. See *Section 5.2.3* for the outcome of this analysis.

The void content of asphalt mixtures tested during Phase 1 also provided an indication of the compactibility of mixtures. Asphalt briquettes prepared during this phase were compacted to 100 gyrations using a gyratory compactor. Although different levels of compactions were not investigated during this study, results in Figure 5.6 indicate that the compactibility of fine graded asphalt mixtures were slightly less when compared to medium grade asphalt mixtures. For a similar binder combination, binder content and compaction effort, COLTO medium, CCC fine and Semi-gap graded 50/70 penetration grade binder combinations obtained different degrees of compaction. Therefore, compactibility of these mixtures was not necessarily related to the binder combinations, but rather to the packing of the aggregates during the compaction process. Compactibility of an asphalt mixture exposed to grey water is an important consideration. In this regard Briedenhann and Jenkins (2015) established that increasing the compaction effort may result in a 68% probability that grey water resistance will be improved.

5.2.2 INDIRECT TENSILE STRENGTH TESTING (ITS) - PHASE 2

ITS results for Phase 2 of the experimental research methodology were obtained after binder combinations, as shown in Figures 3.5 and 3.6, were subjected to dry (no water) and wet (grey water) MMLS3 trafficking. Thereafter, trafficked asphalt briquettes were subjected to ITS testing.

5.2.2.1 Mixture Strength and Stiffness

Similar to Phase 1, indirect tensile strength (ITS) results provided an indication of the mixture strength and stiffness under different levels of moisture exposure. During Phase 2, each asphalt briquette was exposed to no water and grey water conditioning at a temperature 40°C. In addition, conditioning included subjecting asphalt briquettes to 100 000 MMLS3 load cycles which provided information on the behaviour of various asphalt mixtures under traffic loading and grey water exposure. ITS results obtained during this phase were evaluated according to the minimum specification of 800 kPa at a test temperature of 25°C specified by COLTO.

From Figure 5.7 follows that some binder combinations from Phase 1 were selected for further testing in Phase 2 of this study. In addition, a binder modifier produced by Zydex Industries, known as ZycoTherm®, was introduced to test the grey water resistance of asphalt mixtures. Due to its performance in Phase 1, the EVA plus 1% Sasobit® plus extra lime binder combination was further modified by adding 0.1% ZycoTherm®. The SBS plus 1% Sasobit® plus extra lime and the 50/70 penetration grade binder combination binder combination were also modified with 0.1% ZycoTherm®. These newly modified binders were tested in COLTO medium and fine continuous graded asphalt mixtures as shown in Figure 5.7.

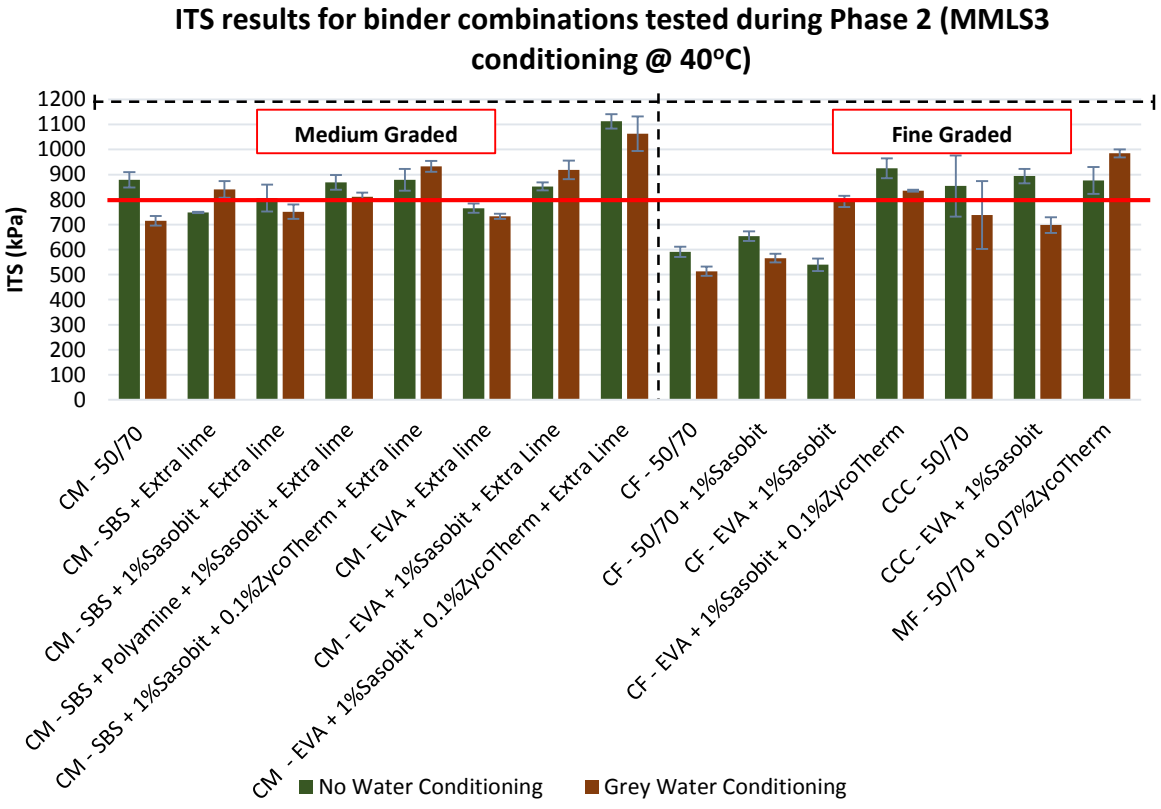

Notes: CM – COLTO Medium Graded; CF – COLTO Fine Graded; CCC – City of Cape Town Fine Graded; SG – Semi-Gap Graded; MF – Much Fine Graded

Figure 5. 7 - ITS results for binder combinations tested during Phase 2.

From Figure 5.7 follows that 75% of the medium graded binder combinations exposed to dry MMLS3 trafficking achieved ITS results of greater than 800 kPa. From these results it were concluded that the mixture strength and stiffness properties for most medium graded asphalt mixtures after dry MMLS3 trafficking were still acceptable in terms of the specification. In addition, 75% of the medium graded binder combinations exposed to wet MMLS3 trafficking also achieved ITS results of greater than 800 kPa. Therefore, mixture strength and stiffness properties for most medium graded binder combinations exposed to wet MMLS3 trafficking were approximately similar to asphalt mixtures exposed to dry MMLS3 trafficking. Medium graded binder combinations that showed significant mixture strength after grey water conditioning and 100 000 MMLS3 load cycles were:

- SBS + 1% Sasobit® + 0.1%ZycoTherm® + Extra Lime
- EVA + 1% Sasobit® + 0.1%ZycoTherm® + Extra Lime
- EVA + 1% Sasobit® + Extra Lime

Of note is that EVA binder additives are present in two of the three medium graded binder combinations identified with significant mixture strength after grey water conditioning. EVA is a binder additive that has been successfully used in areas of fuel spillages such as intersections (Asphalt Academy-TG1, 2007). Fuels, such as diesel types, are well known to dissolve asphalt and are commonly used in laboratories to recover aggregate from the asphalt in order to check the mixture grading. This provides an indication that EVA tends to increase the adhesion of the asphalt mixture when exposed to chemicals. This attribute of EVA helped to improve the strength and stiffness properties of the asphalt after grey water conditioning and trafficking. The addition of the binder additive ZycoTherm® in combination with EVA, further improved the mixture strength after grey water conditioning. The moisture repelling effect of the ZycoTherm® additive can be related to the improved mixture strength. In addition, EVA modified binders performed better than SBS modified binders, which in turn supports a similar conclusion made by Briedenhann and Jenkins (2015).

After wet MMLS3 trafficking, three binder combinations indicated that the mixture strength and stiffness properties were greater after wet MMLS3 trafficking when compared to dry MMLS3 trafficking. Although the void contents of asphalt mixtures after dry and wet MMLS3 trafficking were not determined, it is most likely that a greater ITS result after wet MMLS3 trafficking was related to densification of the asphalt mixture under the 700 kPa tyre pressure. Densification is the process where the density of the asphalt mixture increases as a result of traffic loading. This was supported by research done by Walubita (2000) which indicated that a relative increase in the density of asphalt mixtures occurred after MMLS3 trafficking and wetting. In addition, Briedenhann and Jenkins (2015) investigated the grey water resistance of asphalt mixtures under different levels of compaction, where in most cases higher ITS results were obtained for asphalt mixtures compacted to a higher degree.

From Figure 5.7 follows that most COLTO fine continuous graded asphalt mixtures failed to conform to the 800 kPa ITS specification after dry and wet MMLS3 trafficking. This was an unexpected result as these asphalt mixtures had a higher binder content of 6% when compared to 5.5% used for COLTO medium, CCC fine and Much Fine graded asphalt mixtures. Based on the Marshall stability and binder content relationship of the COLTO fine continuous graded asphalt mixture (see Appendix E), an increase in the binder content will lead to increased stability. However, this was not the case. The COLTO fine continuous graded binder combinations that showed the most significant mixture stength and stiffness after grey water conditioning and trafficking were:

- EVA + 1% Sasobit®
- EVA + 1% Sasobit® + 0.1%ZycoTherm®

The ITS result for dry MMLS3 trafficking of the COLTO fine continuous graded EVA plus 1% Sasobit binder combination indicated a lower mixture strength and stiffness when compared to the ITS results after wet MMLS3 trafficking. This result may be related to densification of the asphalt mixture under the MMLS3 wheel load. However, this cannot be confirmed as no density tests were completed after MMLS trafficking. ITS results indicated that the mixture strength and stiffness of the COLTO fine continuous graded asphalt mixture was even improved further with the addition of ZycoTherm® in combination with EVA. ZycoTherm® is an anti-stripping agent that chemically interacts between the bitumen and aggregate through surface charges which lead to improved moisture resistance.

From Figure 5.7 follows that in most cases binder combinations tested with CCC fine and Much fine graded asphalt mixtures satisfied the COLTO specification for ITS testing. The 50/70 penetration grade CCC fine graded binder combination achieved the greatest stability for this gradation. However, it was not significantly greater than the EVA plus 1% Sasobit® binder combination. The Much fine graded binder combination showed significant mixture stability after grey water conditioning and trafficking. However, this is not consistent with the results obtained during grey water MIST conditioning. Further investigation on the performance of this binder combination is required before it can be considered for improving the grey water resistance of asphalt.

5.2.2.2 Moisture Susceptibility

Similar as in Phase 1, a tensile strength ratio (TSR) was determined during Phase 2 for each binder combination to evaluate the retained strength after trafficking and grey water conditioning. The TSR results of binder combinations obtained after MMLS trafficking at 40°C were also compared with binder combinations that were grey water MIST conditioned at 60°C during Phase 1. No direct comparison between MMLS and MIST TSR results should be considered as these two test methods are

based on different principles. However, it was compared to investigate trends in results. Figure 5.8 shows these results.

From Figure 5.8 follows that the TSR results from Phase 2 for medium and fine graded asphalt mixtures did not show significant variation. The all gradations retained a TSR result greater than 80% after MMLS3 trafficking and grey water conditioning and thus conformed to the Sabita Manual 35 specification. This is an indication that under MMLS3 trafficking significant moisture susceptibility was achieved by asphalt mixtures. Comparing results after wet MMLS3 trafficking to results obtained after MIST conditioning, 75% of asphalt mixtures produced significantly different TSR results. Although the MIST and MMLS are different test procedures, it is apparent that temperature had a greater effect on the moisture susceptibility of asphalt mixtures compared to pressure. MIST conditioning was performed at 60°C and a pressure of 150 kPa, whereas MMLS trafficking was performed at 40°C and a tyre pressure of 700 kPa. However, at a temperature of 60°C more viscous behaviour of the asphalt mixture is expected which may relate to moisture penetrating the asphalt mastic more easily under a pressure of 150 kPa and cause damage compared to a temperature of 40°C.

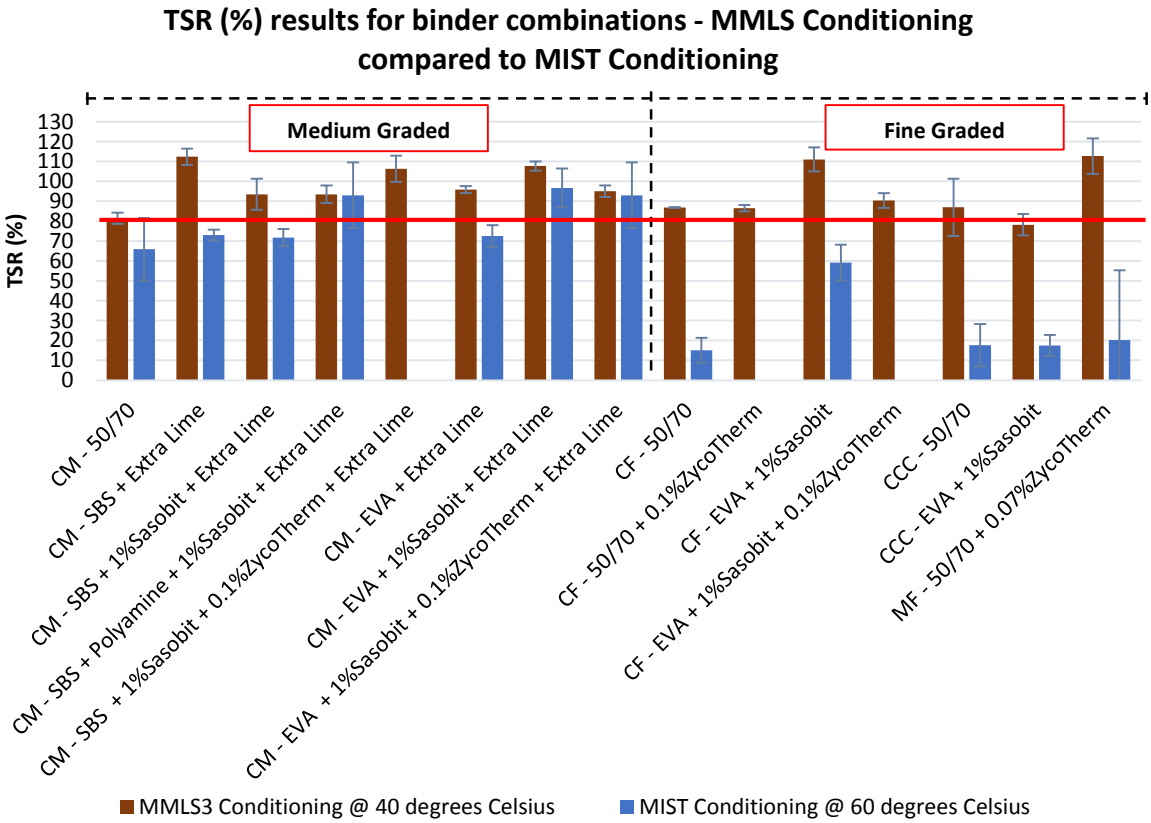

Notes: CM – COLTO Medium Graded; CF – COLTO Fine Graded; CCC – City of Cape Town Fine Graded; SG – Semi-Gap Graded; MF – Much Fine Graded

Figure 5. 8 - TSR (%) results for binder combinations tested during Phase 2.

The medium graded 50/70 penetration grade binder combination produced the lowest TSR result compared to medium graded modified binder combinations. However, similar to the TSR results of

Phase 1, the retained strength of the 50/70 penetration grade binder combination was only 12% less than the tested medium graded modified binder combinations. This indicates that the medium graded 50/70 penetration grade binder combination produced significant mixture strength which can be further improved upon with the addition of binder additives.

The SBS plus extra lime binder combination achieved the greatest retained strength for medium graded binder combinations. However, this result is questionable as compatibility problems were identified with SBS modified binders. During sample preparation, heating of SBS modified binders caused separation of the SBS polymer from the bitumen. This caused the formation of a thick layer of SBS polymer floating on top of the bitumen. An attempt was made by Colas to remix the SBS polymer into the bitumen using a high shear mixer. However, this problem was not resolved. Figure 5.9 illustrates the SBS compatibility problems identified and may cause this binder to be mistaken for a SBR (Styrene-Butadiene-Rubber) modified binder.

Figure 5. 9 - SBS compatibility problems.

SBS modified binder should be a homogenous, by mixing the SBS modifier and bitumen to a level where the separation between the two components is only microscopically visible (Asphalt Academy-TG1, 2007). The properties of the modified binder are dependent on the polymer characteristics, binder characteristics, mixing conditions and compatibility of the polymer with the binder. According to Becker et al. (2001), incompatible polymers lead to heterogeneous mixtures without cohesion or ductility as it affects the colloidal equilibrium of the binder. They further stated that sufficient compactibility between the polymer and binder is necessary to avoid separation during storage, pumping and the application of the binder. From this finding it is clear that the incompatibility problems encountered during Phase 2 with SBS modified binders were likely to produce questionable results.

From Figure 5.8 medium graded binder combinations that showed significant strength retention and with TSR results greater than 100% were:

- SBS + 1% Sasobit® + 0.1%ZycoTherm® + Extra Lime
- EVA + 1% Sasobit®+ Extra Lime

Densification of the asphalt mixtures under MMLS3 trafficking was related to and TSR result of greater than 100%. In addition, the performance of these binder combinations can be related to the binder additives used to improve grey water resistance.

From Figure 5.8 follows that the EVA plus 1% Sasobit® binder combination showed the most significant TSR result for COLTO fine graded binder combinations after MMLS trafficking and grey water conditioning. Sasobit wax lowers the compaction temperature of asphalt mixture, however, it still produce binders with high stiffness (Asphalt Academy-TG1, 2007). The polyethylene component of EVA is also responsible for improving the stiffness of the binder. The properties of these binder additives in combination with densification under MMLS3 trafficking was related to the strength retained by this binder combination. As for the CCC fine graded asphalt mixtures, the 50/70 penetration grade binder combination achieved the greatest TSR result. The Much fine graded binder combination also achieved a significant TSR result after MMLS trafficking and grey water conditioning. However, this result is not comparable with the conclusions made as part of Phase 1 experimental research methodology.

5.2.2.3 Permeability and Compactability

The permeability of asphalt mixtures prepared during Phase 2 was investigated through the average void content after compaction. Similar to Phase 1, asphalt mixtures were compacted to 100 gyrations using a gyratory compactor. Figure 5.10 showed the void content of binder combinations tested during Phase 2 of this study.

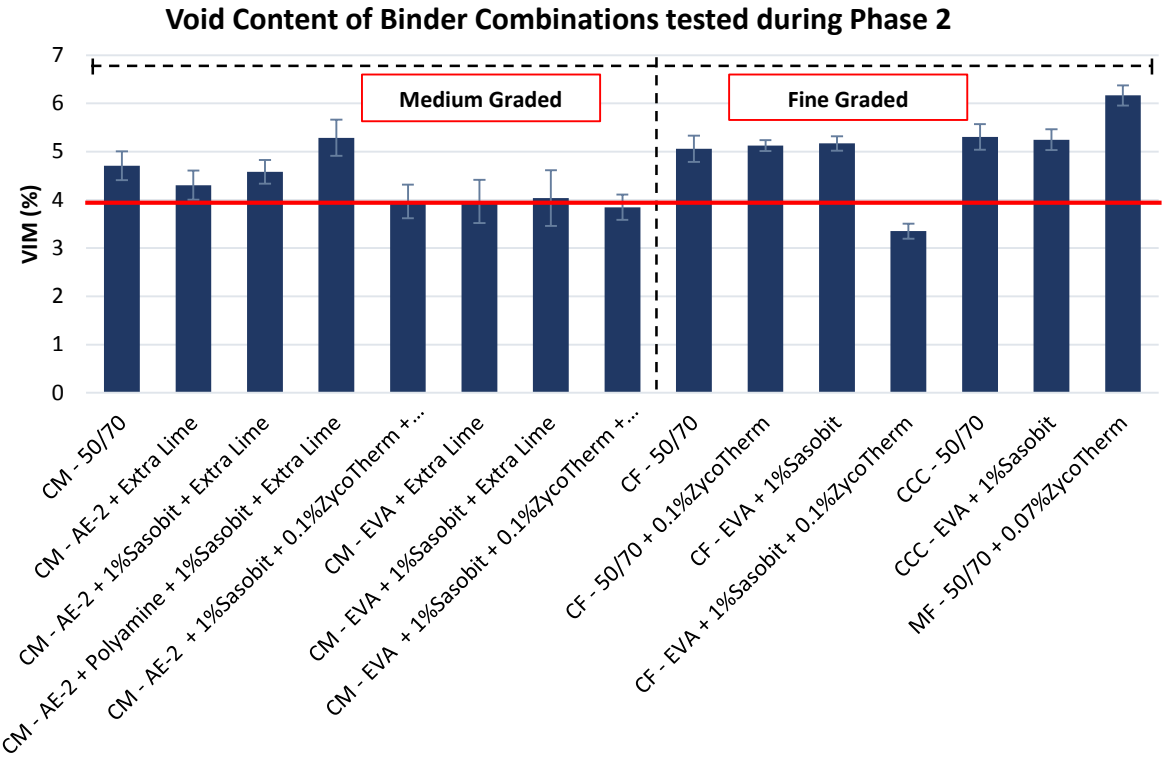

Notes: CM – COLTO Medium Graded; CF – COLTO Fine Graded; CCC – City of Cape Town Fine Graded; SG – Semi-Gap Graded; MF – Much Fine Graded

Figure 5. 10 - Void content of binder combinations tested during Phase 2.

Based on the void content limits stated by Hainin et al. (2003) asphalt mixtures tested during Phase 2 should have had low permeability. Similar as in Phase 1, the permeability was also investigated by comparing the void content and TSR results of Phase 2. The hypothesis was that an increase in the void content would lead to a reduction in the TSR result this being due to the penetration of grey water into the asphalt mixture by the 700 kPa tyre pressure of the MMLS3. This hypothesis was difficult to prove during Phase 2 as a possible trend between the void content and strength of the asphalt mixture was not easily established as in Phase 1. MMLS3 trafficking was completed at 40°C compared to MIST conditioning at 60°C. In addition, the tyre pressure of the MMLS3 was 700 kPa when compared to the 150 kPa pressure pulses produced by the MIST device. This may indicate that the permeability of asphalt mixture is more dependent on the conditioning temperature than the pressure exerted on asphalt surface. The visco-elastic material behaviour of the bitumen may also be related to this behaviour. As temperature increases, the consequent bitumen softening leads to greater viscous behaviour. Therefore, based on the results of Phases 1 and 2 at high temperatures, a smaller pressure may force grey water into the asphalt mixture more easily and thereby cause damage. The relationship between the void content and mixture strength was further investigated through an ANOVA analysis as presented in Section 5.2.3.

From Figure 5.10 follows that most fine graded asphalt mixtures have a void content between 5% and 5.5%. This is slightly less than what was observed during Phase 1, which indicates better compactibility during Phase 2. The Much fine graded asphalt mixture had a similar void content as determined during Phase 1. The COLTO fine graded EVA plus 1% Sasobit® plus 0.1% ZycoTherm® binder combination achieved a void content of 3.4%, which was significantly less than the COLTO Fine EVA plus 1% Sasobit® binder combination. This may indicate that the ZycoTherm® acts as a compaction agent providing better compactibility. The void contents of medium graded asphalt mixtures during Phase 2 were slightly less than those observed during Phase 1. Differences in the compactibility of asphalt mixtures during Phases 1 and 2 can be related to sample preparation. Based on the void contents of binder combinations tested during Phase 2, fine graded asphalt mixtures did were less compactible than medium graded asphalt mixtures, as also observed during Phase 1.

5.2.3 INDIRECT TENSILE STRENGTH (ITS) VERSUS VOIDS IN MIXTURE (VIM)

5.2.3.1 Analysis of Variance (ANOVA)

Analysis of variance (ANOVA) is a statistical method that uses a hypothesis test to determine whether two or more samples differ from one another. This method is mostly used for comparing the means of samples. However, it can also be used to test the equality of variance. ANOVA is also used in regression analysis to determine whether a relationship exists between a dependent variable Y and independent variable X (van As, 2008). This ANOVA method is presented in this *Section* to provide background for the establishment of linear relationships.

The ANOVA method requires calculating the sum of squares. The total sum of squares (SS_T) is made up of two additive components namely, the residual sum of squares (SS_R) and the error sum of squares (SS_E). Each sum of squares has degrees of freedom (df) associated with it. Dividing the sum of squares with the degrees of freedom calculates the total mean squares (MS_T), residual mean squares (MS_R) and error mean squares (MS_E) (van As, 2008). Figure 5.12 defines ANOVA parameters required for regression analysis.

Source of variation	Sum of squares	df	Mean squares
Regression	$SS_M = \Sigma (y(x_i) - m_Y)^2$	1	$MS_M = SS_M$
Error	$SS_E = \Sigma (y_i - y(x_i))^2$	n–2	$MS_E = SS_E/(n-2)$
Total	$SS_T = \Sigma (y_i - m_Y)^2$	n–1	$MS_T = SS_T/(n-1)$

n = sample size

Figure 5. 11 - ANOVA parameters for regression analysis (van As, 2008).

In order to establish a linear relationship, correlation analysis is required. Correlation analysis is used to determine the linearity of the relationship between the dependent variable Y and independent variable X. The determination coefficient (r^2) provides an indication of the linearity of the relationship

and is calculated using Equation 5.1. This coefficient range between $0 \leq r^2 \leq 1$. The closer this coefficient is to 1, the greater the linear relationship between the Y and X variables (van As, 2008). In other word, it is an indication of how close the regression is to the actual results. A determination coefficient of at least 0.7 is required to establish a significant relationship between variables

$$r^2 = \frac{SS_M}{SS_T} \qquad \textit{Equation 5.1}$$

A linear regression equation is defined as follow: y = b.x + a. The regression constants 'b' and 'a' represents the gradient and y-axis intercept of this linear relationship. A further test to determine whether a relationship between the Y and X variable exist is by performing a hypothesis test, based on ANOVA parameters, to determine whether the regression constant 'b' is equal or not equal to 0. In order to perform this calculation the standard error (SE) of the regression coefficient 'b' needs to be calculated using Equation 5.2 (van As, 2008).

$$SE^2 = \frac{MS_E}{\sum(X_i - \bar{X})^2} \qquad \textit{Equation 5.2}$$

The t-test is then used to determine the significance of the regression constant 'b', by performing the hypothesis test illustrated in Figure 5.13 (van As, 2008).

H_o	: b = 0
H_1	: b ≠ 0
Statistic	: t = |b|/SE
Accept H_o if	: $t \leq t_{1-\alpha/2,n-2}$

Figure 5. 12 - Requirements of hypothesis test for determining the significance of regression constant 'b'.

The constant $t_{1-\alpha/2,n-2}$ is determined from a table developed for the t-distribution. The t-distribution is used as it is better suited for statistical analysis of smaller samples sizes. If H_o of the hypothesis test is accepted, it indicates that no relationship between the dependent variable Y and independent variable X exists. If the hypothesis test is rejected, a relationship between the variables is established. However, the magnitude of the determination coefficient and the regression coefficient β should be investigated to determine the strength of the relationship.

In addition, a hypothesis test can be done to determine whether the regression constant 'an' is equal or not equal to zero. This can be used to determine whether the linear regression can be reduced to a line going through the origin (van As, 2008). The variance of the intercept ($S_{y(0)}$) is required to calculate the t-value to compare with the $t_{1-\alpha/2,n-2}$ constant. The variance of the intercept ($S_{y(0)}$) can be calculated using Equation 5.3.

$$S_{y(0)} = \sigma^2 \times \left(\frac{1}{n} + \frac{\bar{X}^2}{\sum(X_i - \bar{X})^2}\right) \qquad \textit{Equation 5.3}$$

With the variance of the intercept known, the hypothesis test, illustrated in Figure 5.14, can be performed (van As, 2008).

$$H_o \quad : a = 0$$
$$H_1 \quad : a \neq 0$$
$$Statistic \quad : t = |a|/s_{y(0)}$$
$$Accept\ H_o\ if \quad : t \leq t_{1-\alpha/2,n-2}$$

Figure 5. 13 - Requirements of a hypothesis test for determining the significance of regression constant 'a'.

Linear regression and ANOVA analysis during this study were done using the 'Data Analysis' add-in of Microsoft Excel. The 'Data Analysis' add-in compiles a report consisting of regression coefficients as well as the ANOVA parameters to determine the relationship between the dependent variable Y and independent variable X. These coefficients and parameters were obtained from the 'Data Analysis' report from where a summary table was created to establish the significance of the linear regression relationship. Therefore, when a relationship between two variables was investigated in this study, only the summary table is presented in this report.

5.2.3.2 ITS versus VIM Results

ITS results of binder combinations and gradations subjected to dry (no water) and wet (grey water) trafficking were also plotted versus the average VIM per binder combination. The purpose of this plot was to establish whether wet trafficking increased the rate at which asphalt mixtures losses its strength with an increase in the VIM of the mixture. These plots are illustrated in Figure 5.15.

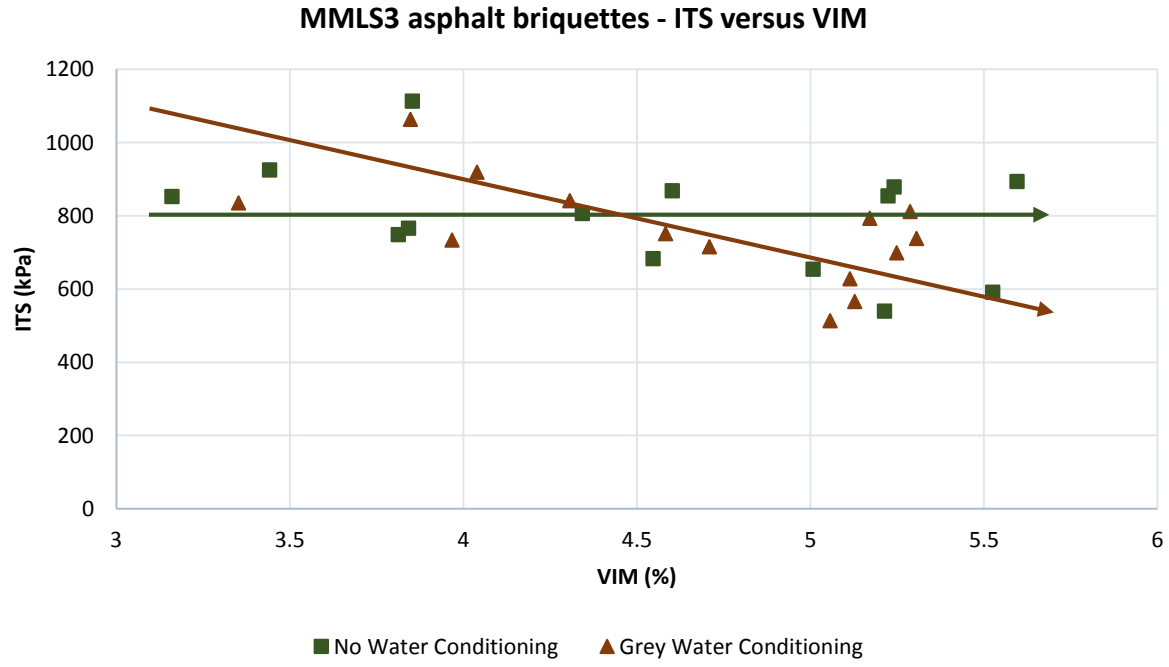

Figure 5. 14 - ITS versus VIM.

An ANOVA analysis was performed to establish whether a relationship between the ITS and VIM existed for both dry (no water) and wet (grey water) trafficked conditions. A summary of the ANOVA analysis is presented in Table 5.1.

Table 5. 1 - Summary of ANOVA analysis for ITS versus VIM.

MMLS3 ITS versus VIM ANOVA Summary		
ANOVA: Constants and Parameters	**Dry (No Water)**	**Wet (Grey Water)**
r^2 (Determination Coefficient)	0.16	0.36
a	1133.82	1368.93
b	-74.13	-131.44
$\Sigma(X-X_m)^2$	8.36	5.37
MS_{Error}	20269.09	13574.59
SE	49.250	50.283
α	0.05	0.05
n	14	14
$S_{y(0)}$	1.62	1.67
t_a	698.39	821.05
t_b	1.505	2.614
$t_{1-\alpha/2,\ n-2}$ (From t-Table)	2.179	2.179
Hypothesis Tests Results		
H_o (a = 0) $t_a \leq t_{1-\alpha/2,\ n-2}$	Reject	Reject
H_1 (a ≠ 0) $t_a > t_{1-\alpha/2,\ n-2}$	Accept	Accept
H_o (b = 0) $t_b \leq t_{1-\alpha/2,\ n-2}$	Accept	Reject
H_1 (b ≠ 0) $t_b > t_{1-\alpha/2,\ n-2}$	Reject	Accept

From Table 5.1 follows that the ANOVA analysis for dry traffic conditions indicated that the linearity (r^2) of the relationship between the ITS and VIM results is insignificant as it was less than 0.7. However, from the hypothesis tests, it was concluded that the regression constants 'b' is equal 0 and 'a' is not equal to 0. This indicates that the linear regression equation has no gradient, however, it intercepts the y-axis. Statistically, this means that under dry trafficked conditions an increase in the VIM does not influence the magnitude of the ITS results. An arrow-line (dark blue) was sketched in Figure 5.13 to illustrate this behaviour. This arrow-line is only for illustration purposes and should not be considered a trend line.

From Table 5.1 it also follows that the ANOVA analysis for wet traffic conditions indicated insignificant linearity with an r^2 closer to 0 instead of 0.7. However, the hypothesis tests indicated statistically that both regression coefficients 'b' and 'a' are not equal to 0. Based on the sign of the 'b' coefficient, which is negative, an indirect relation between the ITS and VIM results occurred under wet traffic conditions. Thus an increase in the VIM results caused a decrease in the strength of the asphalt mixture when

exposed to grey water and traffic. An arrow-line (light blue) was also sketched in Figure 5.13 to illustrate this behaviour. This arrow-line is only for illustration purposes and should not be considered a trend line.

From the ANOVA analysis, it can be concluded that no linear relationship exists between the ITS and VIM under dry traffic conditions. Therefore, as the VIM increase, no change in the ITS result is expected. Traffic alone did not influence the relationship between ITS and VIM, although a weak relationship between the ITS and VIM existed under wet traffic conditions. In this case, an increase in the VIM results decreased ITS result. In addition, it can be concluded that grey water increases the rate at which mixture looses strength with an increase in VIM. This conclusion is comparable with research done by Briedenhann and Jenkins (2015).

5.2.4 PERMANENT DEFORMATION RESULTS

5.2.4.1 Cumulative permanent deformation

Laser profilometer readings were processed as discussed in *Section 3.6.1* to determine the permanent deformation as a result of MMLS3 trafficking and grey water conditioning. The average cumulative deformation after 100 000 MMLS3 cycles per binder combination under dry (no water) and wet (grey water) MMLS3 trafficking was determined and is presented in Figure 5.15.

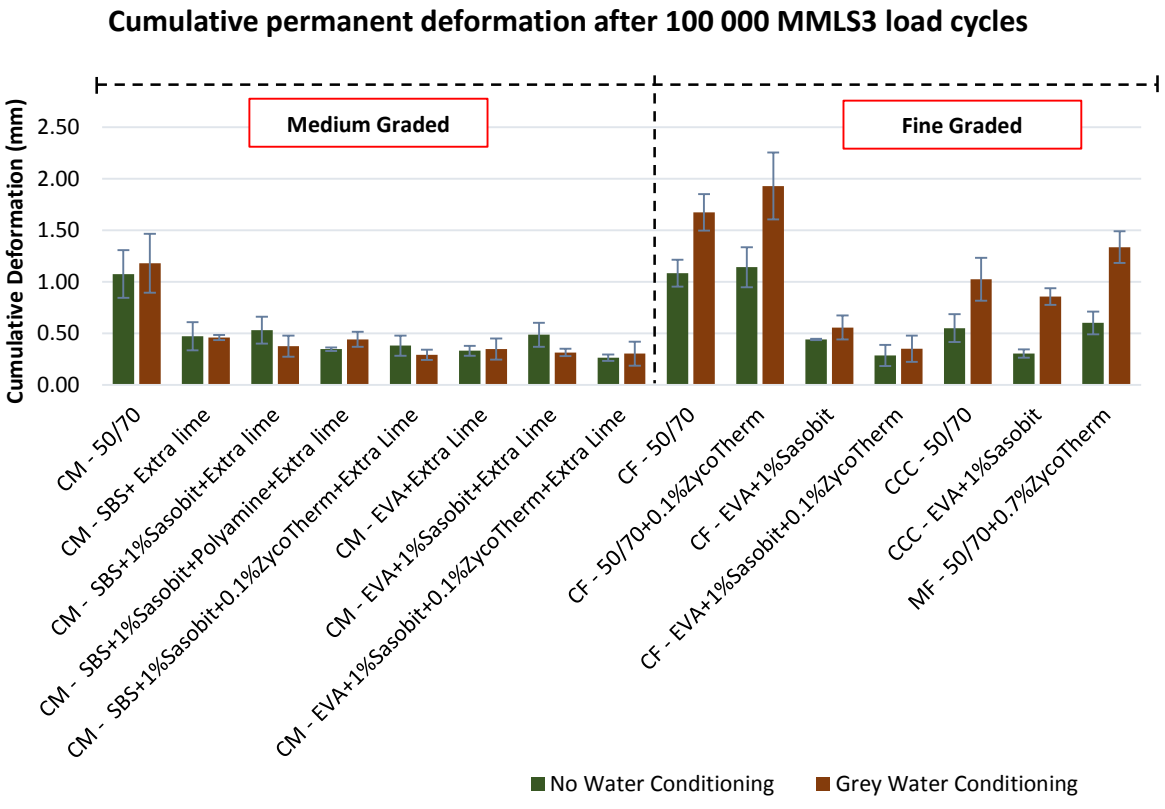

Notes: CM – COLTO Medium Graded; CF – COLTO Fine Graded; CCC – City of Cape Town Fine Graded; MF - Much Fine Graded

Figure 5. 15 - Cumulative permanent deformation after 100 000 MMLS3 load cycles.

Cumulative permanent deformation results for some asphalt briquettes installed in the first slot of the MLS test bed achieved greater deformation results when compared to briquettes in slots two and three (see Figure 3.12). During MMLS3 trafficking, it was observed that the clamping system of the test bed tended to push the asphalt briquette in the first slot upwards thus causing the surface of this briquette to be slightly elevated from the neighbouring asphalt briquette. The briquette in the first slot was first to receive contact with the wheels of the MMLS3. Load transfer to this briquette was greater due to its elevated surface. This produced an outlier as the cumulative permanent deformation result for the briquette in the first slot was significantly greater compared to the results of the briquettes fitted in slots two and three. The standard deviation of cumulative permanent deformation results was also high. It was therefore decided to reduce the sample size to two for binder combinations influenced by this occurrence. The binder combinations effected the most by this adjustment were:

- COLTO Medium: EVA + 1%Sasobit + 0.1%ZycoTherm + Extra Lime (Grey water conditioning)
- COLTO Fine: EVA + 1%Sasobit (No water conditioning)

From Figure 5.15 it follows that significantly greater resistance to permanent deformation was achieved by modified binder combinations consisting of EVA and SBS when compared to 50/70 penetration grade binder combinations. EVA and SBS are known to reduce the deformation by increasing the elastic limit of the binder as well as increasing the shear resistance and stiffness of the asphalt mixture (Asphalt Academy-TG1, 2007). In most cases, medium graded asphalt mixtures with modified binders tended to achieve greater resistance to permanent deformation compared to fine graded asphalt mixtures. Larger aggregate fractions present in medium graded asphalt mixtures contributed to greater stability and provided better dispersion of stresses induced by the MMLS3. Medium graded binder combinations that showed the lowest cumulative permanent deformations after wet traffic conditions were:

- SBS + 1% Sasobit® + 0.1% ZycoTherm® + Extra Lime
- EVA + 1% Sasobit® + Extra Lime
- EVA + 1% Sasobit® + 0.1% ZycoTherm® + Extra Lime

Of note is that two out of the three binder combinations contained EVA as a binder additive. Furthermore, the addition of ZycoTherm® in combination with EVA only slightly reduced the cumulative permanent deformation after wet trafficking. It was suspected that the EVA modifier had a greater contribution to the reduced cumulative permanent deformation than the ZycoTherm® binder additive.

Under wet trafficking, the presence of surfactants significantly increased the cumulative permanent deformation of most fine graded binder combinations. The fine graded binder combinations that showed the lowest cumulative permanent deformation after wet trafficking were:

- EVA + 1% Sasobit®
- EVA + 1% Sasobit® + 0.1% ZycoTherm®

Once again the binder additive EVA assisted in reducing the deformation by increasing the shear resistance of these binder combinations. Furthermore, the addition of ZycoTherm® in combination with EVA reduced the cumulative permanent deformation even more.

Based on the cumulative permanent deformation results of fine graded binder combinations ZycoTherm® is more effective when used in combination with EVA as opposed a virgin binder (50/70 penetration grade). This was especially the case for the cumulative permanent deformation after wet trafficking.

5.2.4.2 Rate of Permanent Deformation

Permanent deformation results were plotted versus the number of MMLS3 load cycles to establish deformation curves for all binder combination tested during Phase 2. From the deformation curves, it was concluded that two stages of deformation occurred as the 100 000 MMLS3 load cycles were applied. These stages differ from one another through the rate of deformation which is represented by the slope of the deformation curve. The first stage consists of a primary (initial) rate of deformation, whereas the second stage consists of a secondary rate of deformation. The primary rate of deformation is significantly higher than the secondary rate of deformation. In addition, depending on the binder combination, at a specific number of load cycles the primary rate changes to the secondary rate of deformation as illustrate by Figure 5.16.

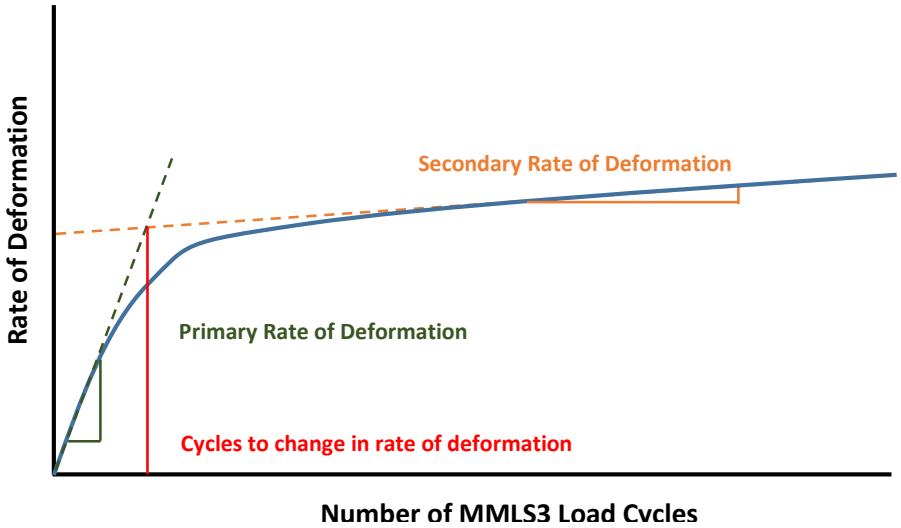

Figure 5. 16 - Deformation curve concept.

Based on the concept illustrated in Figure 5.16, the primary and secondary rates of deformation as well as the number of cycles to change the rate of deformation, were determined for each binder combination tested in Phase 2. The primary rate of deformation per binder combination is shown in Figure 5.17.

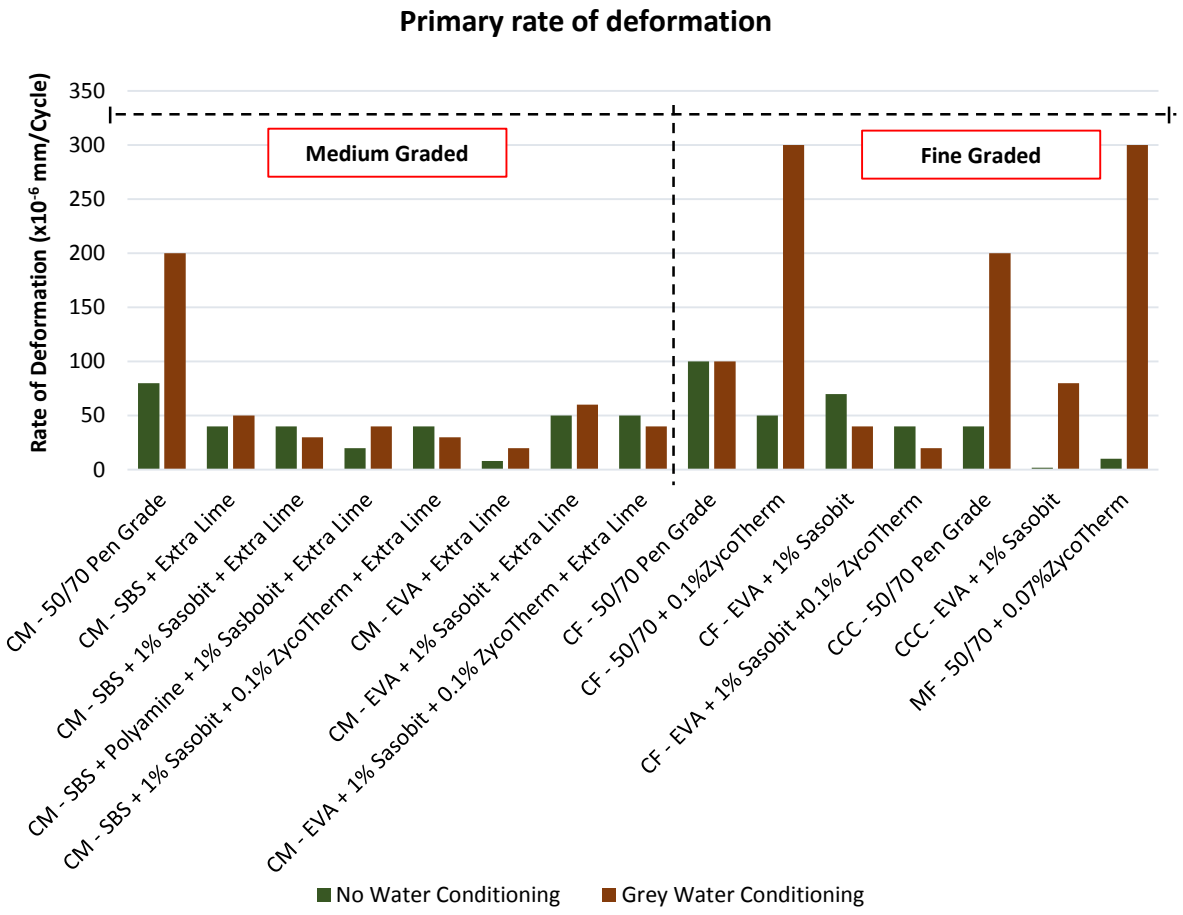

Notes: *CM – COLTO Medium Graded; CF – COLTO Fine Graded; CCC – City of Cape Town Fine Graded; MF - Much Fine Graded*

Figure 5. 17 - The primary rate of deformation.

From Figure 5.17 follows that binder combinations consisting of 50/70 penetration grade binder showed primary rates of deformation equal to and greater than 100 x 10^{-6} mm/cycle during wet (grey water) trafficking. This is significantly higher when compared to binder combinations consisting of EVA and SBS. From these results, it was also concluded that ZycoTherm® is more effective in combination with EVA or SBS than with a virgin binder (50/70 penetration grade). The attributes of these binder additives assisted significantly in reducing the primary rate of deformation.

Differences in the primary rate of deformation between medium graded modified binder combinations during wet trafficking were not significant. However, the EVA plus extra lime binder combination was an exception. The COLTO fine continuous graded EVA plus 1% Sasobit® plus 0.1% ZycoTherm® had the lowest primary rate of deformation of all fine grades. The binder additives used

in this mixture can be related to its performance. The grading of fine continuous mixtures may also relate to better performance due to better packing being usually achieved. The continuous grading is usually close to the 0.45 power line of the Nijboer chart, which results in better packing characteristics.

The secondary rate of deformation per binder combinations is shown in Figure 5.18.

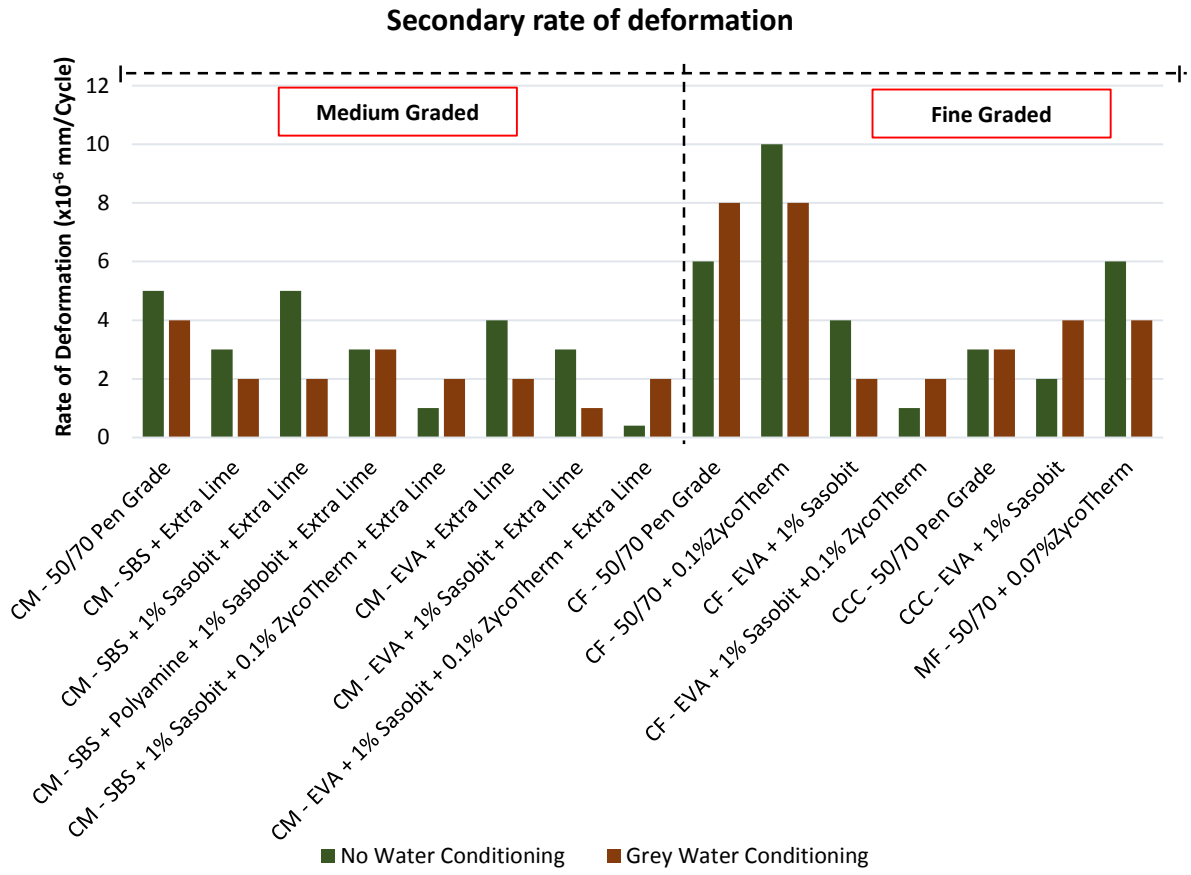

Notes: *CM – COLTO Medium Graded; CF – COLTO Fine Graded; CCC – City of Cape Town Fine Graded; MF - Much Fine Graded*

Figure 5. 18 - The secondary rate of deformation.

From Figure 5.18 follows that the secondary rate of deformation was significantly lower than the primary rate of deformation. Similar trends as in Figure 5.17 are present in Figure 5.18. In most cases, the binder combinations consisting of 50/70 penetration grade binder showed higher secondary rates of deformation after wet trafficking when compared to EVA and SBS modified binder combinations.

In most cases, the medium graded modified binder combinations subjected to wet trafficking did not show significant changes in the secondary rate of deformation. COLTO fine continuous graded EVA and Sasobit® modified binder combinations showed a significant reduction in the secondary rate of deformation after wet trafficking. The EVA and Sasobit® modifiers can be related to this performance.

Figure 5.19 shows the cycles to change the rate of deformation. In most cases, the change in the rate of deformation occurred within less than 10 000 MMLS3 cycles. In addition, no significant trend could be established between the cycles to change the rate of deformation and the type of conditioning (no water or grey water).

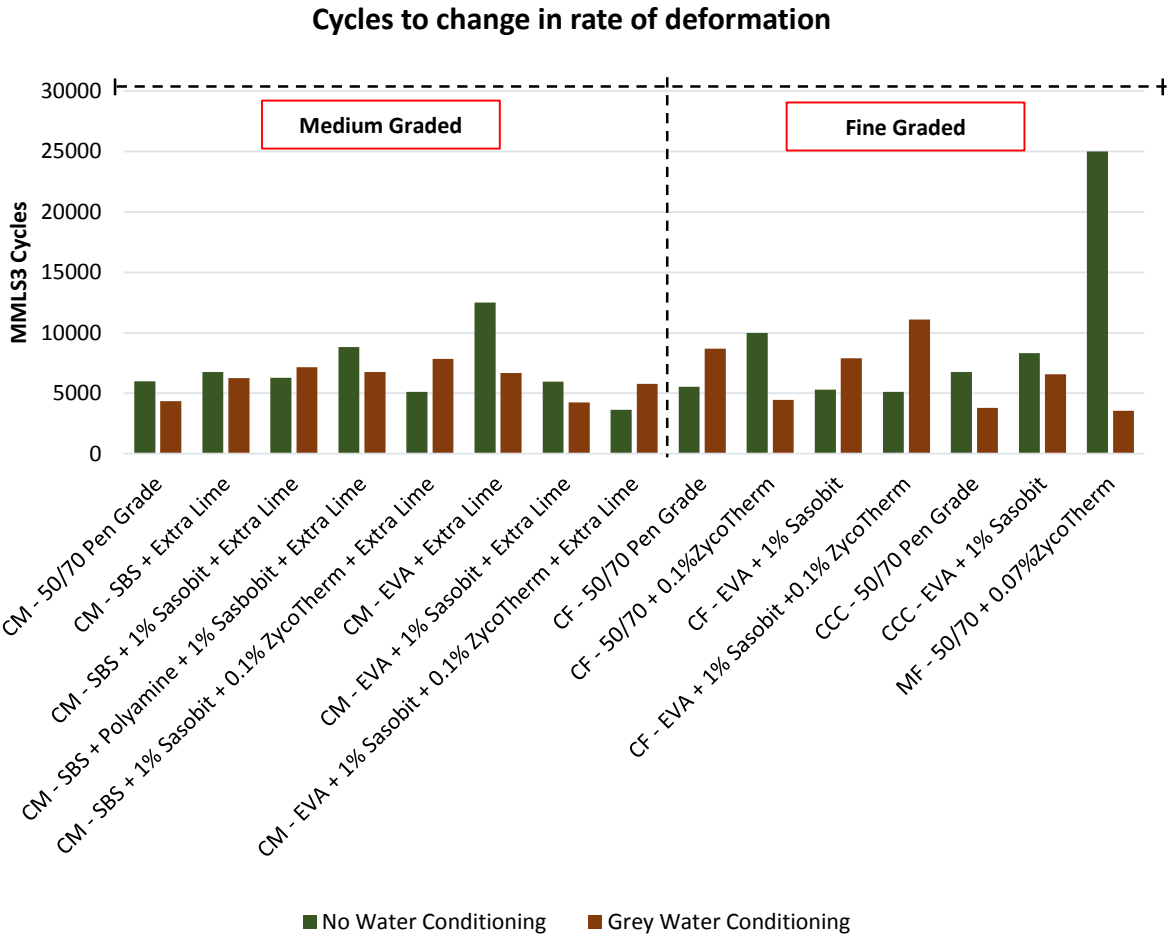

Notes: CM – COLTO Medium Graded; CF – COLTO Fine Graded; CCC – City of Cape Town Fine Graded; MF - Much Fine Graded

Figure 5. 19 - Cycles to change in rate of deformation.

5.2.4.3 ITS versus Rate of deformation

ITS results of wet trafficked binder combinations were plotted versus the primary and secondary rates of deformation. The purpose of this plot was to establish which rate of deformation significantly increased the rate at which asphalt mixtures looses their strength. The rates of deformation are related to the shear strength of an asphalt mixture and thus it was found interesting to related these variables to ITS results which provided an indication of the mixture strength as shown in Figure 5.20.

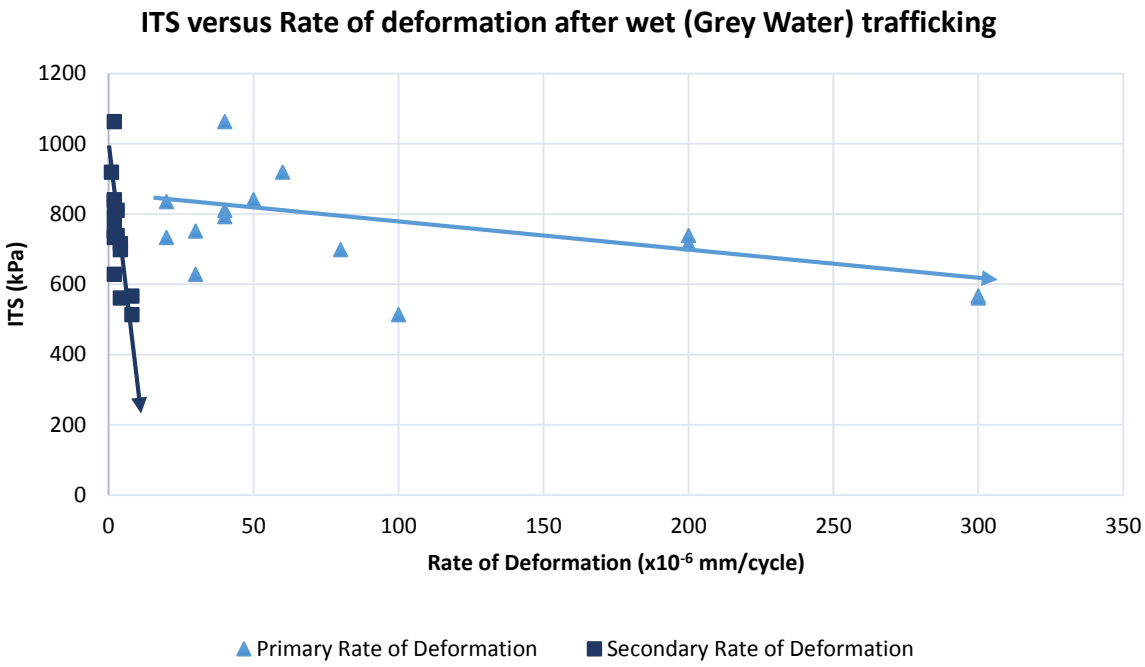

Figure 5. 20 - ITS versus the rate of deformation after wet trafficking.

An ANOVA analysis was performed to determine whether a relationship between the ITS and rate of deformation exists. The results of the ANOVA analysis are presented in Table 5.2.

Table 5. 2 - ITS versus the rate of deformation.

MMLS3 ITS versus Rate of Deformation		
ANOVA: Constants and Parameters	**ITS vs Primary Rate of Deformation**	**ITS vs Secondary Rate of Deformation**
r^2 (Determination Coefficient)	0.31	0.52
b	-0.81	-49.07
Σ(X-Xm)2	137893.33	62.93
MSError	15508.33	10795.74
SE	0.34	13.10
α	0.05	0.05
n	15	15
t	2.412	3.746
$t_{1-\alpha/2,\ n-2}$ (From t-Table)	2.16	2.16
Hypothesis Test		
Ho (b = 0) t ≤ t1-α/2, n-2	Reject	Reject
H1 (b ≠ 0) t > t1-α/2, n-2	Accept	Accept

From Table 5.2 it follows that the ANOVA analysis for the ITS versus the primary rate of deformation indicated a poor linearity (r^2) of 0.31 between the two variables. The hypothesis test statistically indicated that the regression coefficient 'b' is not equal to 0. Based on these results a relationship

between the ITS and primary rate of deformation exists. However, linearity indicated that this relationship is not significantly strong. Based on the sign of the regression coefficient 'b', which is negative, it can be concluded from the ANOVA analysis that an indirect behaviour between the ITS and primary rate of deformation exists. This behaviour indicates that as the primary rate of deformation increases the strength of the mixture decreases. This behaviour is indicated in Figure 5.19 with the arrow line (light blue). This arrow-line is for illustration purposes only and should not be considered a trend line.

From Table 5.2 it follows that the ANOVA analysis for the ITS versus the secondary rate of deformation indicated moderate linearity with the determination coefficient (r^2) being less than 0.7. The hypothesis test statistically proved that the regression coefficient 'b' is not equal to 0. It was therefore concluded, from these results that a relationship between the ITS and secondary rate of deformation exists but based on the linearity, this relationship is not strong enough to be considered significant. Based on the sign of the regression coefficient 'b', which is negative, an indirect behaviour exists between the ITS and secondary rate of deformation. Therefore, as the primary rate of deformation increases a decrease in the strength of the mixture occurs. This behaviour is indicated in Figure 5.19 with the arrow line (dark blue). This arrow-line is for illustration purposes only and should not be considered a trend line.

It must be noted that the regression coefficient 'b' for the ITS versus secondary rate of deformation is significantly greater when compared to the ITS versus primary rate of deformation. This indicates that the rate at which the ITS strength reduces is greater than the secondary rate of deformation. This is expected as it was concluded that for most binder combination the change in the rate of deformation occurred after 10 000 MMLS3 load cycles. For the remaining 90 000 MMLS3 cycles, the secondary rate of deformation increased damage already caused during the primary rate of deformation.

5.2.5 TEXTURE RESULTS

5.2.5.1 Retained Texture

The texture of each binder combination was analysed at 0, 50 000 and 100 000 MMLS3 load cycles using the procedure discussed in *Section 3.6.1.3*. An average texture ratio was calculated at these load cycle intervals to evaluate the change in texture as the MMLS3 load cycles were applied. The average texture ratios calculated after 0, 50 000 and 100 000 MMLS cycles for dry (no water) and wet (grey water) MMLS trafficking, were compared for each of the binder combinations. A percentage retained texture was calculated from the texture ratios for 50 000 and 100 000 MMLS3 load cycles per binder combination. This represented the percentage increase or decrease in texture as a result of grey water conditioning. These results are presented in Figure 5.21. From Figure 5.21 follows that the retained

texture after 0 MMLS3 cycles were 100% as it represents the reference texture before MMLS3 cycles were applied. Retained texture results greater or less than 100% represent an increase or decrease in the texture of binder combinations after grey water conditioning.

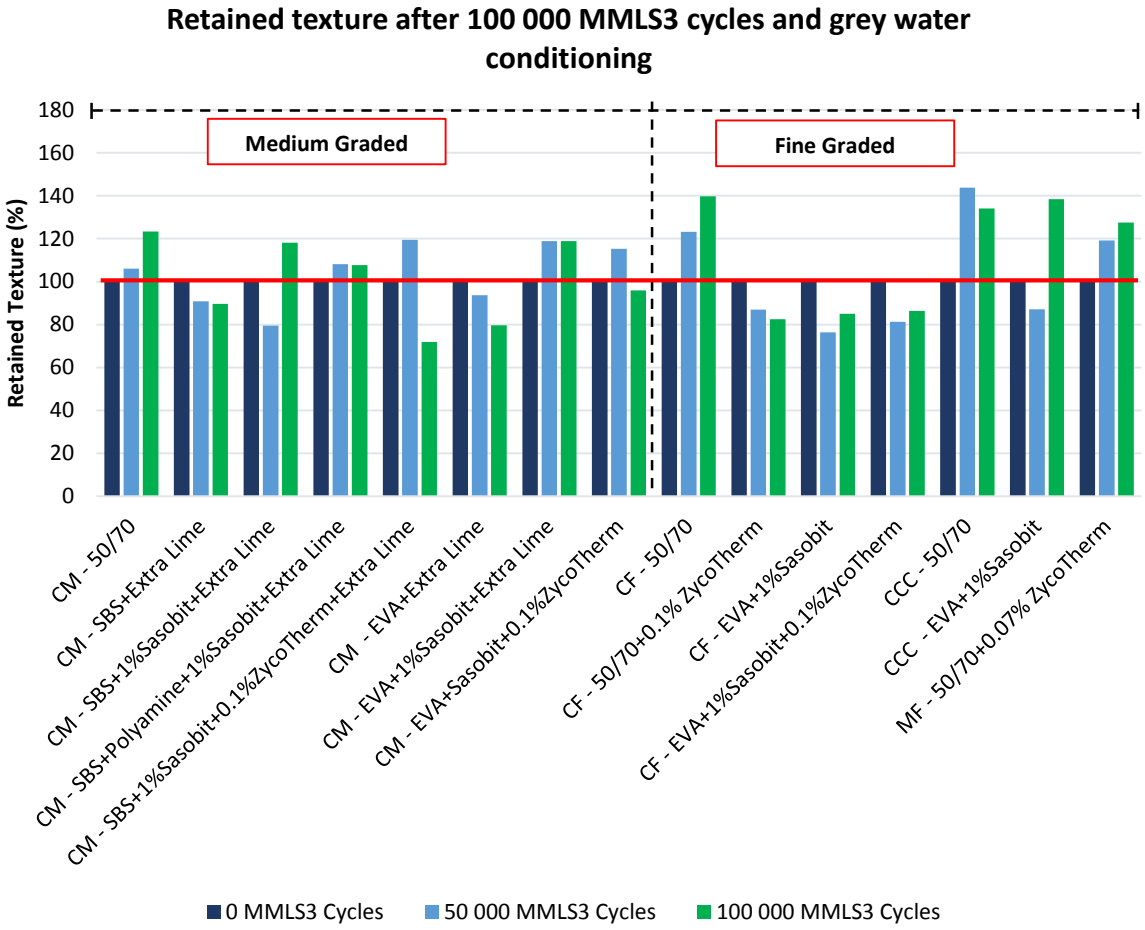

Notes: CM – COLTO Medium Graded; CF – COLTO Fine Graded; CCC – City of Cape Town Fine Graded; MF - Much Fine Graded

Figure 5. 21 - Retained texture after 100 000 MMLS3 cycles and grey water conditioning.

Four scenarios related to the texture are derived from Figure 5.21. These scenarios are:

- **Scenario 1**: The retained texture increases after 50 000 MMLS3 cycles. After 100 000 MMLS3 cycles, the retained texture is even greater than determined after 50 000 MMLS3 cycles. During this scenario, the increased texture may be related to the action of the MMLS3 wheels in combination with the surfactants present in grey water. The material is continuously washed from the asphalt briquette's surface causing increased texture for the duration of the MMLS test.
- **Scenario 2**: The retained texture increases after 50 000 MMLS3 cycles. After 100 000 MMLS3 cycles, the retained texture is less than determined after 50 000 MMLS3 cycles. During this scenario, the increase in texture after 50 000 MMLS3 cycles may be related to Scenario 1. After 100 000 MMLS3 cycles, the surfactants in the grey water did not react with the bitumen-

aggregate bond, causing no material loss. Instead, the wheels of the MMLS3 smoothed the texture of surface after 100 000 MMLS3 cycles.

- **Scenario 3**: The retained texture decreases after 50 000 MMLS3 cycles. After 100 000 MMLS3 cycles, the retained texture is greater than determined after 50 000 MMLS3 cycles. During this scenario, the decrease in texture after 50 000 MMLS3 cycles may be related to the smoothening action of the MMLS3 wheels. After 100 000 MMLS3 cycles, the surfactants in the grey water react with the bitumen-aggregate bond causing material loss. The material washed from the asphalt briquette's surface due to the grey water and action of the MMLS3 wheels produces a surface with increased texture.
- **Scenario 4**: The retained texture decreases after 50 000 MMLS3 cycles. After 100 000 MMLS3 cycles, the retained texture is even less than determined after 50 000 MMLS3 cycles. During this scenario, the increased texture may be related to no reaction between the surfactants present in grey water and the bitumen-aggregate bond. Material loss is expected to be low as the smoothening action of the MMLS3 wheels performs the dominant role.

Table 5.3 summarises the scenarios identified for each binder combination presented in Figure 5.21.

Table 5. 3 - Texture scenario identified for each binder combination in Figure 7.7.

Asphalt Gradation	Binder Type	Scenario Identified
COLTO Medium	50/70	1
COLTO Medium	SBS + Extra Lime	4
COLTO Medium	SBS + 1% Sasobit® + Extra Lime	3
COLTO Medium	SBS + Polyamine + 1% Sasobit® + Extra Lime	4
COLTO Medium	SBS + 1% Sasobit® + 0.1% ZycoTherm® Extra Lime	2
COLTO Medium	EVA + Extra Lime	4
COLTO Medium	EVA + 1% Sasobit® + Extra Lime	1
COLTO Medium	EVA + 1% Sasobit® + 0.1% ZycoTherm® Extra Lime	2
COLTO Fine	50/70	1
COLTO Fine	50/70 + 0.1%ZycoTherm®	4
COLTO Fine	EVA + 1%Sasobit®	3
COLTO Fine	EVA + 1% Sasobit® + 0.1% ZycoTherm®	3
CCC	50/70	2
CCC	EVA + 1%Sasobit®	3
Much Fine	50/70 + 0.07%ZycoTherm®	1

5.2.5.2 Laser profilometer texture results versus Sand Patch Test

Sand patch tests were conducted during MMLS trafficking according to SANS 3001-BT11:2011. The sand patch test results were used to validate the texture results obtained from the laser profilometer measurements.

Sand patch test was done at 0, 50 000 and 100 000 MMLS3 load cycle intervals on two asphalt briquettes per binder combination. The texture depth was determined as established from SANS 3001-BT11:2011. Thereafter a texture ratio was determined at each of the mentioned MMLS3 load cycle intervals. The texture ratios for 50 000 and 100 000 MMLS3 load cycles were determined by dividing its texture depth results with the 0 MMLS3 load cycle texture depth result, of which the texture ratio of the latter was equal to 1.

A relationship between the laser profilometer (also referred to as LTM) and the sand patch test was investigated for various asphalt gradations used during this study. Only the 50 000 and 100 000 MMLS3 cycles texture ratios were used for investigating this relationship. Figure 5.22 illustrates the relationship between the laser profilometer (LTM) and sand patch test.

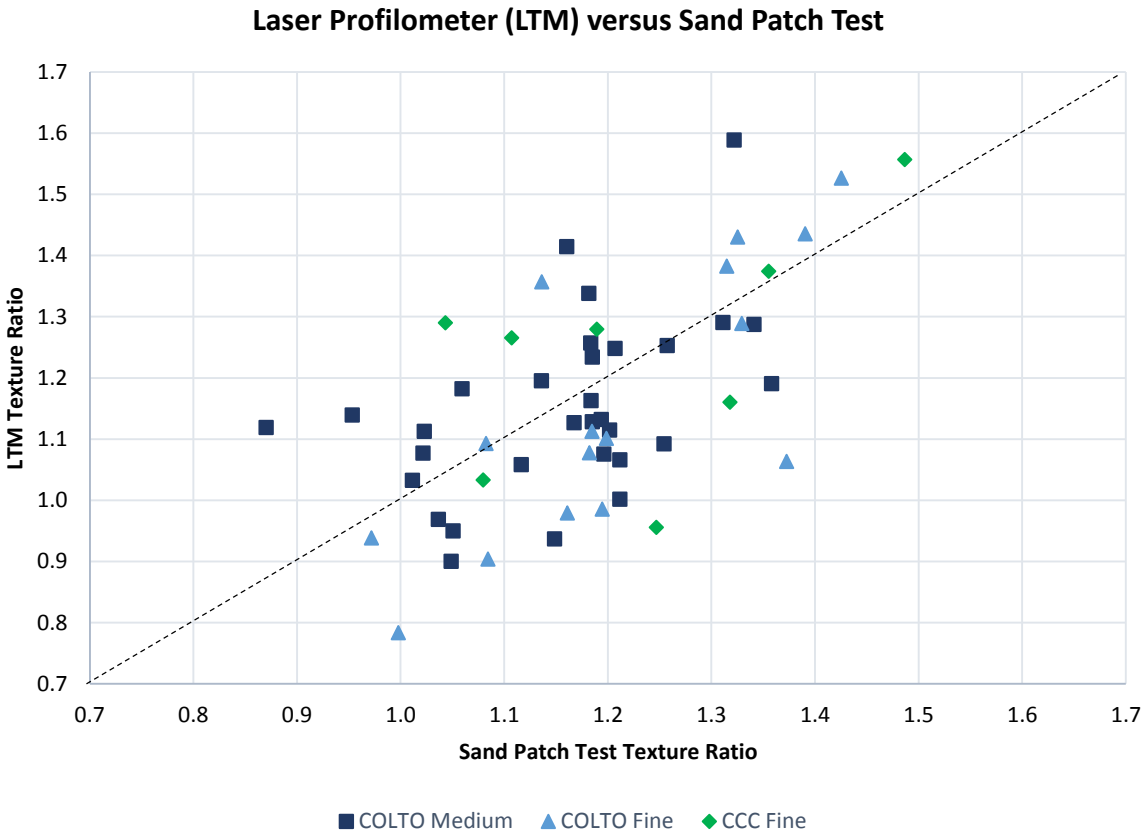

Figure 5. 22 - LTM versus sand patch test.

An ANOVA analysis was performed to statistically determine whether a relationship between the laser profilometer and the sand patch test texture measurements for various gradations existed. Table 5.4 summarises the results of the ANOVA analysis.

Table 5. 4 - ANOVA analysis for laser profilometer and sand patch test measurements.

Laser Profilometer texture ratio's versus Sand Patch Test texture ratio's				
ANOVA: Constants and Parameters	**COLTO Medium Graded**	**COLTO Fine Graded**	**CCC Fine Graded**	**Gradations Combined**
r^2 (Determination Coefficient)	0.330	0.606	0.258	0.391
b	0.854	1.245	0.631	0.916
$\Sigma(X-X_m)^2$	0.444	0.287	0.164	0.937
MS_{Error}	0.022	0.021	0.031	0.023
SE	0.222	0.268	0.437	0.155
α	0.05	0.05	0.05	0.05
n	32	16	8	56
t	3.846	4.645	1.443	5.890
t1-α/2, n-2 (From t-Table)	2.042	2.145	2.447	2.015
Hypothesis Test				
H_o (b = 0) $t \leq t_{1-\alpha/2, n-2}$	Reject	Reject	Accept	Reject
H_1 (b ≠ 0) $t > t_{1-\alpha/2, n-2}$	Accept	Accept	Reject	Accept

From Table 5.4 follows that the determination coefficient (r^2) from the ANOVA analysis indicated an insignificant linearity between the laser profilometer and the texture of the sand patch test's texture results for the medium and CCC fine gradations. In both cases, the determination coefficient was less than 0.7. The determination coefficient for the relationship between the laser profilometer and the texture of the sand patch test results for the COLTO fine continuous graded was also less than 0.7. This indicates a moderate linearity between the two variables. Combining the laser profilometer and sand patch test results of all gradations, the determination coefficient was also less 0.7. Therefore, by combining results also produced an insignificant linearity between the laser profilometer and sand patch test texture results.

In addition, a hypothesis test was performed on the texture ratios of the laser profilometer and sand path test for each gradation. The objective of the hypothesis test was to establish if a relationship between two sets of texture rations existed. This was achieved by testing if the regression coefficient 'b' of the linear regression equation was equal to 0 or not. The hypothesis test indicated the regression coefficient 'b' for laser profilometer and sand patch test texture ratios of the COLTO medium and fine graded were not equal to 0. This indicates that a relationship between the laser profilometer and sand patch test for these gradations exists. However, based on the determination coefficient the linearity of this relationship is not significantly strong. The hypothesis test indicated that the regression coefficient 'b' for the CCC fine graded texture results is equal to 0. Thus no significant relationship between the laser profilometer and sand patch test results exists. Performing the hypothesis test on the combined texture ratios of the laser profilometer and sand patch test all gradations indicated that

the regression coefficient ‘b’ was not equal to 0. Thus a relationship between the combined texture results of the laser profilometer and sand patch test exists but the linearity of this relationship it is not significantly strong.

It should be noted that the regression coefficient is positive for all ANOVA analysis on texture results per gradation. Therefore, in cases where the regression coefficient ‘b’ was statistically proven not to be equal to 0, direct behaviour between the laser profilometer and sand patch test texture results occurred. Thus, the sand patch test texture ratio increased with an increase of the laser profilometer's texture ratio.

Although a significant relationship between the laser profilometer and sand patch test texture ratios was not established, Figure 5.22 illustrates that texture results are scattered around the 45^{o} line. Therefore, statistically determined texture ratio results of the laser profilometer and sand patch test will not produce significant relationships.

5.2.6 MATERIAL LOSS RESULTS

Asphalt briquettes subjected to dry (no water) and wet (grey water) MMLS3 trafficking were weighed before and after testing to determine the material loss of binder and aggregate. The material loss provides an indication of how the surfactants reacted with the bitumen-aggregate bond that caused a loss of adhesion. The action of the MMLS3 wheel also contributed to removing loose material from the asphalt briquettes surface. The material loss results were relatively small. However, it should be noted that only one surface of the asphalt briquette is subjected to the action of the MMLS3 wheel and a large part of the asphalt briquette is not in direct contact with the wheels of the MMLS3. Therefore, the percentage change in the material loss after dry and wet MMLS3 trafficking was calculated. This result provided information on the sensitivity of binder combinations to ravel once exposed to grey water and traffic conditions. Figure 5.23 shows the change in material loss after dry and wet MMLS3 trafficking. In most cases, signs of material loss were observed between 0 and 20 000 MMLS3 load cycles under wet conditions.

From Figure 5.23 follows that the 50/70 penetration grade binder combinations showed a significant increase in material loss after exposure to grey water and trafficking compared to modified binder combinations. This indicated that the 50/70 penetration graded binder combinations were more sensitive to ravelling. This conclusion was also formulated from visual inspection data from Mew Way.

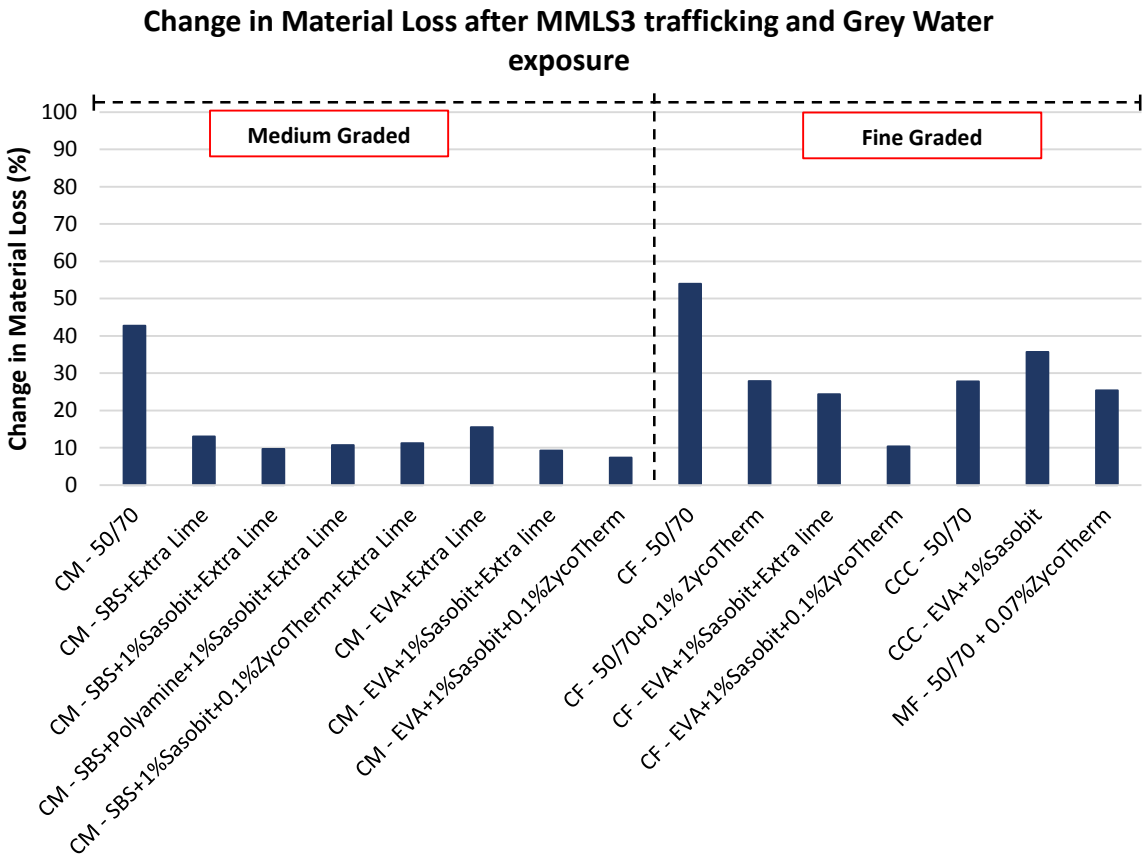

Notes: CM – COLTO Medium Graded; CF – COLTO Fine Graded; CCC – City of Cape Town Fine Graded; MF - Much Fine Graded

Figure 5. 23 – Change in the material Loss after 100 000 MMLS3 cycles.

The change in the material loss of medium graded EVA and SBS modified binder combinations did not significantly differ from one another. However, the addition of ZycoTherm® to EVA and SBS modified binders caused less material loss. The nanotechnology of ZycoTherm® was related to this behaviour as it chemically established a stronger bond between the aggregate and bitumen. As these bonds are chemically formed they are not easily broken by the presence of grey water. Medium graded binder combinations that showed the lowest change in the material loss were:

- SBS + 1% Sasobit® + 0.1% ZycoTherm® + Extra Lime
- EVA + 1% Sasobit® + 0.01% ZycoTherm® + Extra Lime

The material loss results also indicated that ZycoTherm® in combination with an EVA and SBS modified binder provided better adhesion when compared to using ZycoTherm® with a virgin binder (50/70 penetration grade have.

From Figure 5.23 follows that the COLTO fine EVA plus 1% Sasobit plus 0.1% ZycoTherm® showed the least increase in the material loss of all fine grade asphalt binder combinations. Once again the

additives of this binder combination improved the adhesion of the asphalt, thus providing better resistance to grey water trafficking when compared to other modified binders used with fine asphalt gradations.

5.2.7 CHANGE IN TEXTURE VERSUS MATERIALS LOSS

A relationship between the change in texture and the material loss after grey water conditioning and 100 000 MMLS3 load cycles was investigated. The purpose of this relationship was to establish if the material loss is related to the texture retained after wet trafficking. This relationship was investigated for medium and fine graded asphalt mixtures. It should be noted that the change in texture and material loss results for COLTO fine continuous, CCC fine and Much fine graded asphalt mixtures were combined to form results for fine graded mixtures. Figure 5.24 illustrates the relationship between the change in texture and material loss for medium and fine graded asphalt mixtures.

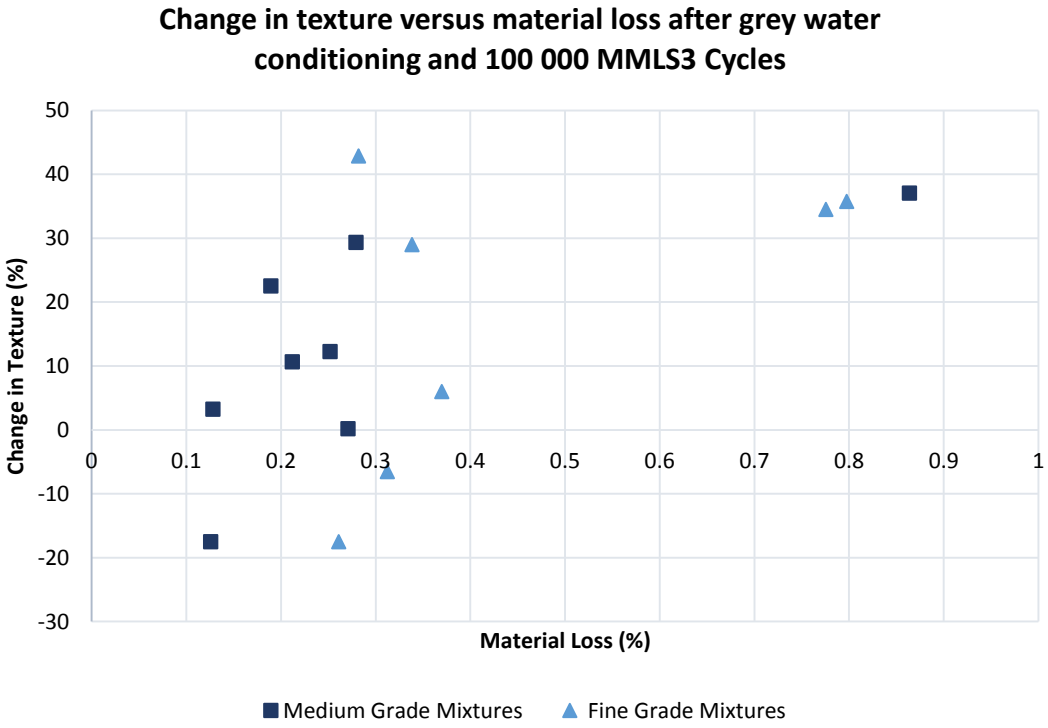

Figure 5. 24 - Change in texture versus material moss after wet trafficking.

An ANOVA analysis was performed to determine whether a relationship between the texture and material loss exists. The ANOVA analysis was separately completed for medium and fine graded mixtures. It was also completed for combined medium and fine graded mixture results. Table 5.5 summarises the ANOVA analysis.

Table 5. 5 - Change in texture versus material loss after wet trafficking.

Change in Texture versus Material Loss			
ANOVA: Constants and Parameters	**Medium Graded**	**Fine Graded**	**Gradations Combined**
r^2 (Determination Coefficient	0.46	0.39	0.35
b	49.24	275.70	48.85
$\Sigma(X-X_m)^2$	0.401	0.017	18.39
MS_{Error}	192.92	409.90	278.16
SE	21.94	155.59	18.39
α	0.05	0.05	0.05
n	8	7	15
t	2.244	1.772	2.656
$t_{1-\alpha/2,\ n-2}$ (From t-Table)	2.447	4.303	2.16
Hypothesis Test			
H_o (b = 0) $t \leq t_{1-\alpha/2,\ n-2}$	Accept	Accept	Reject
H_1 (b ≠ 0) $t > t_{1-\alpha/2,\ n-2}$	Reject	Reject	Accept

From Table 5.5 follows that the ANOVA analysis indicated determination coefficients of less than 0.7 for medium and fine graded mixtures. This result indicates that an insignificant linearity exists between the change in texture and material loss for these gradations. Combining the change in texture and material loss results for medium and fine graded mixture also produced determination coefficients of less than 0.7.

A hypothesis test was also performed per gradation to determine if a relationship between these variables existed. The hypothesis test, which was performed on the regression coefficient 'b', indicated for both medium and fine graded mixtures the regression coefficient 'b' was equal to 0. From this result, it can be concluded that no linear relationship between the change in texture and material loss exists, for medium and fine graded mixtures. From Table 5.5 follows that the hypothesis test was also performed on the variables. The hypothesis test indicated the regression coefficient 'b' is not equal to 0. Therefore, the combined result indicated that a relationship between the change in texture and material loss existed although not significant. Based on the sign of the regression coefficient 'b', which is positive, direct behaviour between variables occurred. Thus, increased with an increase in material loss the change in texture.

The three outliers, in Figure 5.24 represent the change in texture and material loss results for 50/70 penetration grade binder combinations. These binder combinations experience significant material losses when compared to modified binder combinations. Therefore, these outliers do not represent faulty results and cannot be removed from the sample. As these outliers are significantly separated

from the rest of the results, it produced insignificant relationships between the change in texture and material loss.

5.3 COMBINING RESULTS

Results presented were combined to determine an effective grey water resistance asphalt mixture for high and low volume roads. For this study high volume roads refer to a road such as Mew Way, which is a main collector road to which internal roads of the informal settlement connect. Low volume roads refer to the internal roads of the informal settlement. The thickness of an asphalt layer is determined by the maximum aggregate size, which is one third of the layer thickness. The medium graded asphalt mixture tested during this study had a maximum stone size of 14 mm, which translates to a minimum layer thickness of 42 mm. This layer thickness is greater than 30 mm, which indicates the layer will serve a structural purpose (SAPEM Chapter 2, 2014). Therefore, a medium graded asphalt mixture will be suitable for high volume roads as the asphalt layer need to contribute to the structural capacity of these roads. For a low volume road, a fine graded asphalt mixture will be suitable. Fine graded asphalt mixtures tested during this study had a maximum aggregate size of 10 mm, which translates to a minimum layer thickness of 30 mm. The asphalt layer of a low volume road does not necessarily contribute to the structural capacity of the pavement, but serve a functional purpose.

A rating criteria was developed to combine results for Phases 1 and 2 of the experimental research methodology. This rating criteria was used to determine the two most effective grey water resistant asphalt mixtures for high and low volume roads. The variables considered in setting up the rating criteria were:

- Indirect Tensile Strength (ITS) after wet MMLS3 trafficking (kPa)
- Tensile Stress Ratio (TSR) after wet MMLS3 trafficking (%)
- Cumulative Permanent Deformation after dry (no water) trafficking (mm)
- Cumulative Permanent Deformation after wet (grey water) trafficking (mm)
- Change in material Loss after 100 000 MMLS3 cycles and grey water conditioning (%)

The variables selected for setting up the rating criteria considers the strength, stiffness, moisture susceptibility, shear resistance and ravelling of asphalt mixtures when exposed to grey water conditioning.

5.3.1 RATING OF ITS AND TSR RESULTS FOR PHASES 1 AND 2

Indirect tensile strength (ITS) and the tensile strength ratio (TSR) provide information on the strength, stiffness and moisture susceptibility of an asphalt mixture. COLTO specification states an ITS result of 800 kPa at a temperature of 25^{o}C to ensure the strength and stiffness, whereas a TSR result of 80% is

required to ensure the moisture susceptibility of an asphalt mixture is sufficient. This was used to calculate the percentage difference or deviation between the actual laboratory ITS or TSR results obtained and COLTO specification. Equations 5.4 and 5.5 were used to perform this calculation.

$$\%\ Difference\ in\ ITS = \frac{ITS_{Lab} - 800}{800} \times 100 \qquad \textit{Equation 5.4}$$

$$\%\ Difference\ in\ TSR = \frac{TSR_{Lab} - 80}{80} \times 100 \qquad \textit{Equation 5.5}$$

Based on this calculation the ITS and TSR results for binder combinations of medium and fine graded asphalt mixtures were rated accordingly. Table 5.6 shows the calculation based on Equations 5.4 and 5.5 and the rating of binder combinations tested during Phase 1 for medium graded asphalt mixtures.

Table 5. 6 - Rating of ITS and TSR results for medium graded binder combinations during Phase 1 of this study.

MIST - Phase 1						
Grading and Binder Combinations	**ITS (kPa)**	**% Difference between COLTO Specification (800 kPa) and Actual ITS**	**TSR (%)**	**% Difference between COLTO Specification (80%) and Actual TSR**	**Rating of ITS**	**Rating of TSR**
CM - 50/70	490	-38.7	65.19	-14.81	7	7
CM – SBS + Extra Lime	598	-25.2	72.97	-7.03	6	6
CM – SBS + 1%Sasobit + Extra Lime	643	-19.6	75.73	-4.27	4	5
CM – SBS + Polyamine + 1%Sasobit + Extra Lime	628	-21.5	91.94	11.94	5	3
CM – SBS + 1%Sasobit + 0.1%ZycoTherm + Extra Lime	-	-	-	-	-	-
CM – EVA + Extra Lime	683	-14.6	89.20	9.20	3	4
CM – EVA + 1%Sasobit + Extra lime	724	-9.5	96.00	16.00	2	2
CM – EVA + 1%Sasobit + 0.1%ZycoTherm	942	17.7	101.13	21.13	1	1

From Table 5.6 follows that the percentage difference between the ITS or TSR and COLTO specification were given a rating that ranged from 1 to 7. The highest positive percentage difference was given a rating of 1 whereas the highest negative percentage difference was given a rating of 7. A similar process was followed for fine graded asphalt mixtures tested during Phase 1. This process of rating ITS and TSR results was also completed for medium and fine graded asphalt mixtures tested during Phase 2 of this study.

5.3.2 CUMULATIVE PERMANENT DEFORMATION AND MATERIAL LOSS RESULTS

Cumulative permanent deformation after dry and wet MMLS3 trafficking was also included in the rating criteria for binder combinations. These results provided information on the shear resistance of binder combinations when exposed to no water and grey water trafficking. Material loss results

provided information on the sensitivity of binder combinations to ravelling once exposed to grey water conditioning. Both cumulative permanent deformation and material loss results were only applicable to Phase 2 of this study. Table 5.7 shows the rating of cumulative permanent deformation and material loss results for medium graded binder combinations.

Table 5. 7 - Rating of cumulative permanent deformation and material loss results for medium graded binder combinations.

MMLS - Phase 2						
Grading and Binder Combinations	**Cumulative Rutting Dry (mm)**	**Cumulative Rutting Wet (mm)**	**Material Loss (%)**	**Rating (Rutting Dry)**	**Rating (Rutting Wet)**	**Rating Material Loss**
CM - 50/70	1.08	1.18	4.75	8	8	8
CM – SBS + Extra Lime	0.47	0.46	13.00	5	7	6
CM – SBS + 1%Sasobit + Extra Lime	0.53	0.38	9.70	7	5	3
CM – SBS + Polyamine + 1%Sasobit + Extra Lime	0.35	0.44	10.69	3	6	4
CM – SBS + 1%Sasobit + 0.1%ZycoTherm + Extra Lime	0.38	0.29	11.25	4	1	5
CM – EVA + Extra Lime	0.33	0.35	15.50	2	4	7
CM – EVA + 1%Sasobit + Extra lime	0.49	0.31	9.27	6	3	2
CM – EVA + 1%Sasobit + 0.1%ZycoTherm	0.26	0.30	7.33	1	2	1

From Table 5.7 follows that the binder combination with the highest cumulative permanent deformation was given a rating of 8, whereas the binder combination with the lowest cumulative permanent deformation was given a rating of 1. A similar procedure was followed for rating the change in material loss of binder combinations when exposed to grey water conditioning. The binder combination with lowest change in material loss was given a rating of 1, which indicated this binder combination was the least sensitive to ravelling after grey water exposure. The binder combination with the highest change in material loss was given a rating of 7, which indicated this binder combination was the most sensitive to ravelling after grey water exposure. Rating of the cumulative permanent deformation and change in material loss was also completed for the fine graded binder combinations tested during Phase 2.

5.3.3 RESULTS OF RATING CRITERIA

Tables 5.8 and 5.9 summarise the rating of binder combinations for medium and fine graded asphalt mixtures tested during Phases 1 and 2. From these tables follow that an average rating was calculated for Phases 1 and 2, which also represents the final rating. This mean all variables used for the setting up of the rating criteria have an equal contribution to the final rating. A weighted contribution of variables to the total rating was not considered as all variables considered in setting up this rating criteria share equal importance to ensure the durability of an asphalt mixture.

Table 5. 8 - Rating of medium graded binder combinations.

Medium Graded Asphalt Mixtures																
Gradings and Binder Combinations	MIST Conditioning- Phase 1					MMLS Trafficking - Phase 2										
	ITS (kPa)	TSR (%)	Rating ITS	Rating TSR	Average Rating	ITS (kPa)	TSR (%)	Cumulative Rutting Dry (mm)	Cumulative Rutting Wet (mm)	Material Loss (%)	Rating ITS	Rating TSR	Rutting Dry	Rutting Wet	Rating Material Loss	Average Rating
CM - 50/70	490	65	7	7	7	716	81	1.08	1.18	42.8	8	8	8	8	8	8.0
CM – SBS + Extra Lime	598	73	6	6	6	841	112	0.47	0.46	13.0	4	1	5	7	6	4.6
CM – SBS + 1%Sasobit + Extra Lime	643	76	4	5	4.5	751	94	0.53	0.38	9.7	6	6	7	5	3	5.4
CM – SBS + Polyamine + 1%Sasobit + Extra Lime	628	92	5	3	4	811	93	0.35	0.44	10.7	5	7	3	6	4	5.0
CM – SBS + 1%Sasobit + 0.1%ZycoTherm + Extra Lime	-	-	-	-	-	933	106	0.38	0.29	11.3	2	3	4	1	5	3.0
CM – EVA + Extra Lime	683	89	3	4	3.5	734	96	0.33	0.35	15.5	7	4	2	4	7	4.8
CM – EVA + 1%Sasobit + Extra lime	724	96	2	2	2	919	108	0.49	0.31	9.3	3	2	6	3	2	3.2
CM – EVA + 1%Sasobit + 0.1%ZycoTherm	942	101	1	1	1	1063	95	0.26	0.30	7.3	1	5	1	2	1	2.0

Notes: CM – COLTO Medium Graded

Table 5. 9 - Rating of fine graded binder combinations.

Fine Graded Asphalt Mixtures																
Gradings and Binder Combinations	MIST Conditioning - Phase 1					MMLS Trafficking- Phase 2										
	ITS (kPa)	TSR (%)	Rating ITS	Rating TSR	Average Rating	ITS (kPa)	TSR (%)	Cumulative Rutting Dry (mm)	Cumulative Rutting Wet (mm)	Material Loss (%)	Rating ITS	Rating TSR	Rutting Dry	Rutting Wet	Rating Material Loss	Average Rating
CF - 50/70	130	15	8	8	8	514	87	1.08	1.67	54.0	7	5	6	6	7	6.2
CF - 50/70 + 1%Sasobit	403	54	4	3	3.5	-	-	-	-		-	-	-	-	-	-
CF - 50/70 + 0.1%ZycoTherm	-	-	-	-	-	566	87	1.14	1.93	27.8	6	6	7	7	5	6.2
CF – EVA + 1%Sasobit	468	59	2	2	2.0	793	111	0.44	0.56	24.4	3	2	3	2	2	2.4
CF – EVA + 1%Sasobit + 0.1%ZycoTherm	-	-	-	-	-	835	90	0.28	0.35	10.3	2	3	1	1	1	1.6
CCC - 50/70	172	17	7	7	7.0	738	87	0.55	1.03	27.8	4	4	4	4	4	4.0
CCC - 50/70 + Extra Lime	438	44	3	4	3.5	-	-	-	-	-	-	-	-	-	-	-
CCC - 50/70 + 1%Sasobit	179	17	6	6	6	-	-	-	-	-	-	-	-	-	-	-
CCC – EVA + 1%Sasobit	271	31	5	5	5	698	78	0.30	0.86	35.7	5	7	2	3	6	4.6
SG - 50/70	0	0	9	9	9	-	-	-	-	-	-	-	-	-	-	-
MF - 50/70 + 0.07%ZycoTherm	561	60	1	1	1	985	113	0.60	1.34	25.4	1	1	5	5	3	3.0

Notes: CF – COLTO Fine Graded; CCC – City of Cape Town Fine Graded; SG – Semi-Gap Graded; MF - Much Fine Graded

From Table 5.8 follows that the three **medium graded binder combinations** that showed the most effective grey water resistance after **Phase 1** were:

- EVA + 1% Sasobit® + 0.1% ZycoTherm® + Extra Lime
- EVA + 1% Sasobit® + Extra Lime
- EVA + Extra Lime

The **three medium graded binder combinations** that showed the most effective grey water resistance after **Phase 2** were:

- EVA + 1% Sasobit® + 0.1% ZycoTherm® + Extra Lime
- SBS + 1% Sasobit® + 0.1% ZycoTherm® + Extra Lime
- EVA + 1% Sasobit® + Extra Lime

The results of the rating criteria indicated that the EVA modified binder were more successful in improve the grey water resistance of medium graded asphalt mixtures compared to the 50/70 penetration grade bitumen and SBS modified binder. Although the SBS plus 1% Sasobit® plus 0.1% ZycoTherm® and extra lime binder combination was not tested during Phase 1, most SBS modified binder combinations that were tested during Phase 1 achieved lower ITS and TSR result compared to EVA modified binder combinations. This makes it uncertain that the addition of ZycoTherm® to a SBS modified binder, would contribute to a significant increase in the mixture strength, stiffness and moisture susceptibility and to outperform EVA modified binder combinations.

The addition of ZycoTherm® to a EVA modified binder consisting of 1% Sasobit did indicated significant mixture strength, stiffness and moisture susceptibility after MIST conditioning during Phase 1. However, its contribution to resist permanent deformation, which was tested during Phase 2, is still unclear. A similar conclusion was made for a binder combinations consisting of a SBS modified binder plus 1% Sasobit. It is most likely that the shear resistance of asphalt mixtures consisting of these binder combinations is improved by the SBS and EVA modifier and not necessarily by the ZycoTherm® additive.

Based on the rating criteria results of Phases 1 and 2, and conclusions the **medium graded EVA plus 1% Sasobit® plus extra lime binder combination** was suggested as the first choice binder combination for improving the grey water resistance of asphalt in areas with high volume traffic. The rating criteria result indicated that the SBS and EVA modified binder combinations with 1% Sasobit, 0.1% ZycoTherm® and extra lime have significant resistance to grey water, however these binder combinations should be used with caution as the contribution of the ZycoTherm® to the performance of an asphalt mixture is not

completely clear from laboratory results. A larger number of asphalt specimens consisting of these binder combinations must be tested to improve the confidence in these binder combination. Therefore, based on the results of Phases 1 and 2, and the rating criteria the medium graded **EVA plus extra lime binder combination** was suggested as a second choice for improving the grey water resistance of an asphalt mixture.

From Table 5.9 follows that the **four fine graded binder combinations** that showed the most effective grey water resistance after **Phase 1** were:

- 50/70 penetration grade bitumen + 0.07% ZycoTherm® (Much Fine graded)
- EVA + 1% Sasobit® (COLTO fine continuously graded)
- 50/70 penetration grade bitumen + 1% Sasobit® (COLTO fine continuously graded)
- 50/70 penetration grade bitumen + Extra Lime (City of Cape Town Fine graded)

The **three fine graded binder combinations** that showed the most effective grey water resistance after **Phase 2** were:

- EVA + 1% Sasobit® + 0.1% ZycoTherm® (COLTO fine continuously graded)
- EVA + 1% Sasobit® (COLTO fine continuously graded)
- 50/70 penetration grade bitumen + 0.07% ZycoTherm® (Much Fine graded)

The results of the rating criteria indicated that the Much fine graded 50/70 penetration grade binder combination was the best performing fine graded mixture tested during Phase 1. However, ITS and TSR results were based on an insufficient sample size due to failure of this asphalt mixture during MIST conditioning. This gradation and binder combination was also rated third best performing asphalt mixture during Phase 2. This result was also questionable as this gradation and binder combination had poor shear resistance which lead to significant permanent deformation after 100 000 MMLS3 load cycles. This asphalt mixture did show significant mixture strength and stiffness after grey water MMLS3 trafficking. Based on these conclusions, the performance of this asphalt mixture under grey water exposure in practice is questionable.

The COLTO fine continuously graded 50/70 plus 1% Sasobit® binder combination was rated third best in terms of its TSR, which indicated that its moisture susceptibility was third best of all fine graded asphalt mixtures tested during Phase 1. Its mixture strength and stiffness after grey water MIST conditioning was rated fourth best of all fine graded asphalt mixtures tested during Phase 1. However, the COLTO fine continuously graded EVA plus 1% Sasobit binder combination out performed this binder combination,

therefore it was not tested during Phase 1. The shear resistance of the 50/70 plus 1% Sasobit® binder combination is therefore unknown, which makes it unclear if this binder combination will perform satisfactory in practice.

The City of Cape Town (CCC) fine graded 50/70 plus extra lime also indicated significant mixture strength, stiffness and moisture susceptibility during. However, this asphalt gradation had a natural sand fraction in its grading which was related to numerous failures observed during MIST conditioning for different binder combinations. From these failures it was concluded that a natural sand fraction may not be suitable for improving the grey water resistance of asphalt. Therefore, the CCC fine graded 50/70 penetration graded and EVA plus 1% Sasobit® binder combinations were the only binder combinations selected for testing during Phase 2, in order to compare with similar binder combinations used in difference asphalt gradations.

Based on the results of Phase 1 and the rating criteria the COLTO fine continuously graded EVA plus 1% Sasobit® binder combination performed the best of all fine graded asphalt mixtures tested in terms of mixture strength, stiffness and moisture susceptibility after grey water MIST conditioning. This binder combination also performed second best during Phase 2 with significant mixture strength, stiffness, moisture susceptibility and shear resistance under grey water exposure and trafficking. In addition, its resistance to ravelling was also significant. During Phase 2 the COLTO fine continuously graded EVA plus 1% Sasobit® plus 0.1% ZycoTherm® binder combination outperformed this binder combination in terms of shear strength and resistance to ravelling. However, the EVA plus 1% Sasobit® plus 0.1% ZycoTherm® binder combination was not tested during Phase 1 and the contribution of the ZycoTherm® to this performance of this binder combination was not completely certain.

Based on the results of Phases 1 and 2, and the rating criteria the **first choice** fine graded binder combination for improving the grey water resistance of asphalt used for low volume roads was the **COLTO fine continuously graded EVA plus 1% Sasobit® binder combination**. As a **second choice** the **COLTO fine continuously graded EVA plus 0.1% ZycoTherm® binder combination** was suggested to improve the grey water resistance of asphalt used for low volume roads. However, this binder combination should be used with caution and it is recommended to increase the test sample size to improve the confidence in the performance of this binder combination.

5.4 SUMMARY

Indirect tensile strength (ITS), permanent deformation, texture and material loss formed the basis of the results and interpretation of this study. These results provided an indication of the effect grey water had on the performance of asphalt mixtures. In addition, it also provided information on the performance of asphalt mixtures under wet (grey water) MMLS3 trafficking. Only a conclusion on the outcomes of this chapter is presented whilst conclusions related to the results are discussed in detail in *Chapter 8*.

The strength of asphalt mixtures after grey water MIST conditioning and MMLS3 trafficking were investigated from ITS test results. Tensile strength ratio's (TSR) were also calculated to determine the percentage retained strength of asphalt mixtures after grey water MIST conditioning and MMLS3 trafficking. From these results, conclusions were made related to grading, binder additives and volumetric properties of grey water resistant asphalt mixtures.

Permanent deformation results were processed to determine the cumulative permanent deformation and rates of deformation for binder combination tested during Phase 2 of this study. From these results, it was possible to determine which gradings and binder combinations had the greatest resistance to permanent deformation after wet MMLS3 trafficking. An ANOVA analysis was performed between the ITS results of binder combinations subjected the grey water MMLS3 trafficking and rates of deformation. The purpose of this analysis was to determine the effect of different rates of deformation on the strength of the asphalt mixture.

Laser profilometer texture results were processed to determine the retained texture of binder combinations after grey water MMLS3 trafficking. The laser profilometer texture ratios were also compared with the sand patch test texture ratios to investigated the effectiveness of the Civil Designer® method develop to determine the texture from laser profilometer measurements. An ANOVA analysis was performed to determine the relationship between the laser profilometer texture ratios and sand patch texture ratios.

Material loss results provided information on the loss of bitumen and aggregate from the surface of the asphalt briquettes after grey water MMLS3 trafficking. This provided an indication of asphalt mixtures under grey water exposure and trafficking. An ANOVA analysis was performed to determine the relationship between changes in texture versus the material loss. The purpose was to establish if the material loss contributes significantly to the texture of the asphalt after grey water MMLS3 trafficking.

Results from Phases 1 and 2 of the experimental research methodology were combined to establish a rating criteria to rate the grey water resistance of binder combination tested during this phase. An average total rating was calculated per binder combination tested during Phases 1 and 2 after which two effective grey water resistant asphalt mixtures for high and low volume roads were selected.

CHAPTER 6 – RESULTS AND INTERPRETATION: FINITE ELEMENT ANALYSIS METHODOLOGY

6.1 INTRODUCTION

This Chapter reports on the results obtained from the finite element models developed as part of the research methodology. A conclusion is provided on the interpretation of results that are related to the effect on the indirect tensile strength (ITS) as caused by a reshaped 150 mm diameter asphalt briquette of which two opposite segments have been machined-off (see Chapter 4). The terminology "shaping" or "shaped", preceded or proceeded by the dimension of the mid-ordinate in mm or the word "briquette" will be used further in this report to refer to a circular briquette that underwent this machined modification.

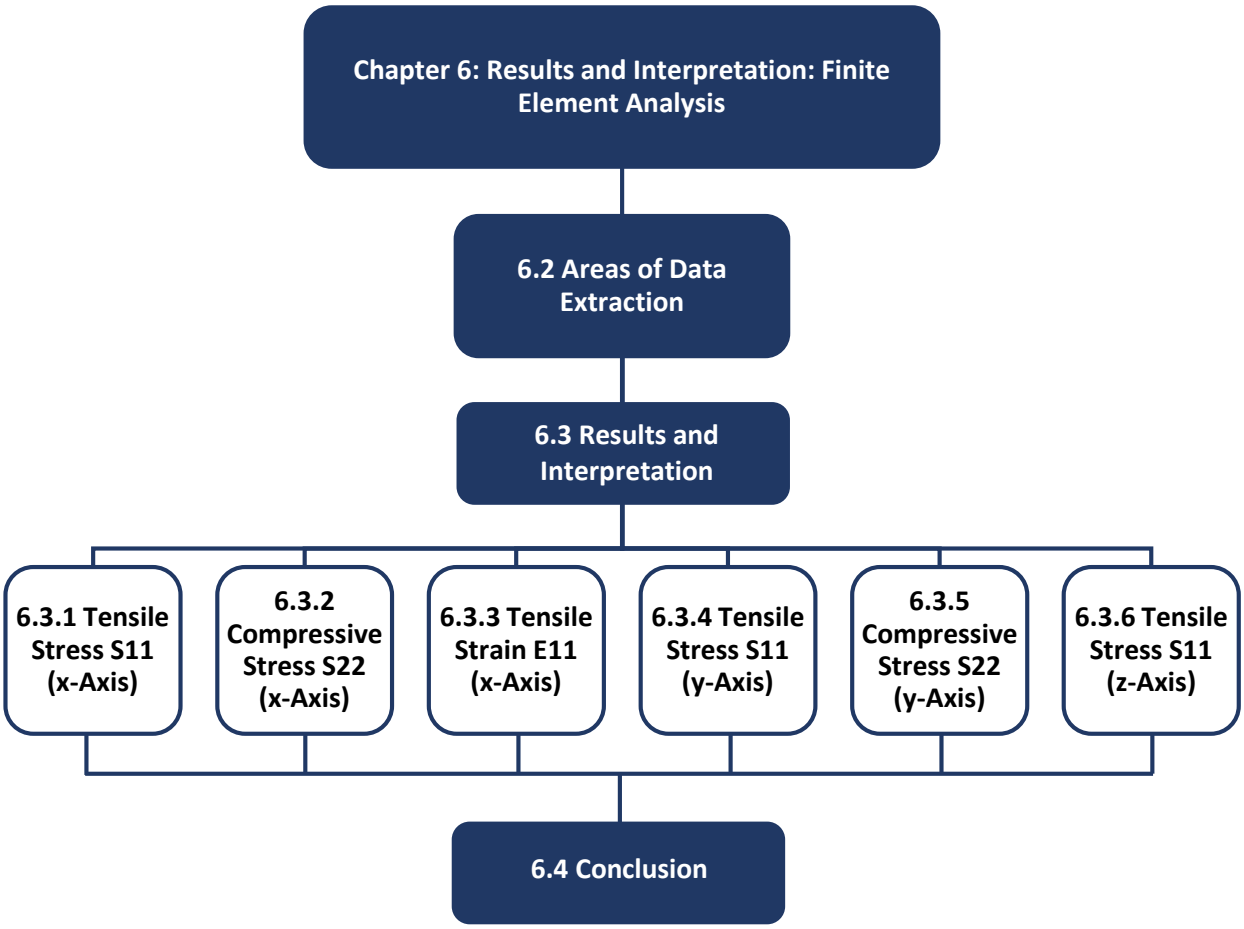

Figure 6. 1 - Layout of result and interpretation of finite element analysis research methodology.

6.2 AREAS OF DATA EXTRACTION

Stress and strain results were obtained from specific locations known as 'Paths' as shown in, see *Appendix C*. The purpose of this Section is to visually illustrate these 'Paths' and the three directions in which stresses and strains act. This visualisation is illustrated in Figure 6.2.

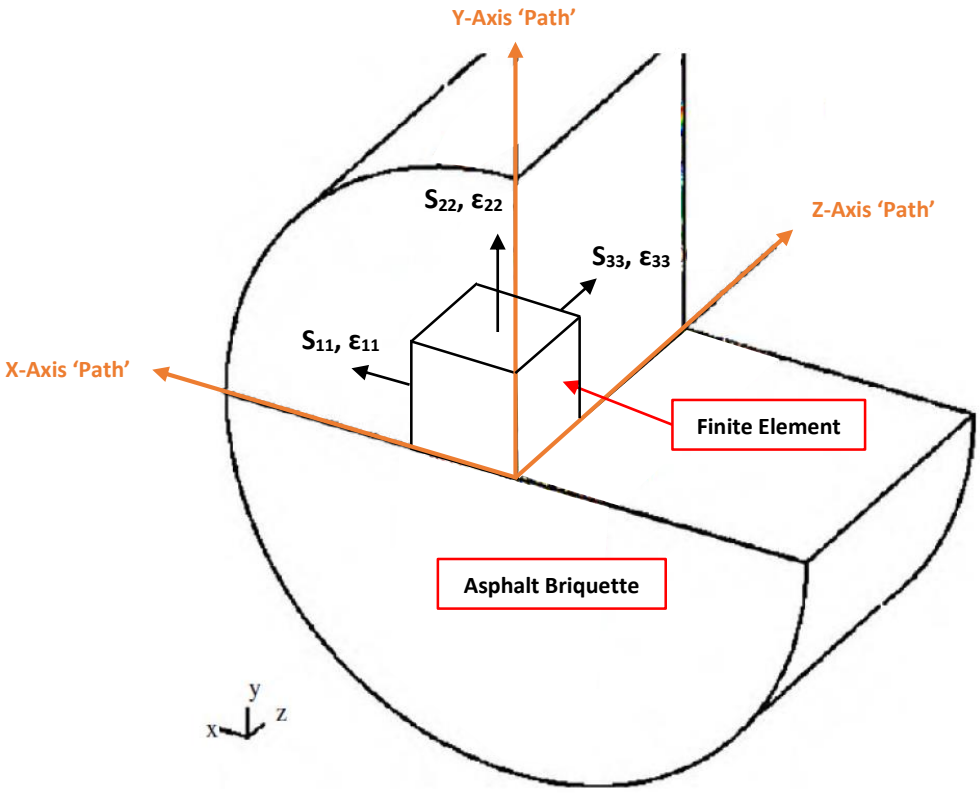

Figure 6. 2 - Illustration of 'Paths' as well as stress and strain directions for finite element.

The stress locations identified as significant for investigating the influence of MMLS3 prepared asphalt briquettes of which opposite segment have been machined-off, were:

- Tensile stress S11 along the x-axis
- Compressive stress S22 along the x-axis
- Tensile stress S11 along the y-axis
- Compressive S22 along the y-axis

The tensile stress S11 at the centre of the briquette along the z-axis was investigated to determine the influence of re-shaping through the depth of an asphalt briquette. The influence of re-shaping on the resilient modulus was also investigated through the tensile strain E11 along the x-axis. Results and interpretation of these stress and strain results are shown in *Section 6.3*.

6.3 RESULTS AND INTERPRETATION

6.3.1 TENSILE STRESS S11 (X-AXIS)

Tensile stress along the x-axis is represented by the stress S11 in Abaqus/CAE (see Figure 6.2). This indicates the tensile stress of which the distribution maximum occurs at the centre of the asphalt briquette. The maximum tensile stress represents the tensile stress determined after completion of indirect tensile strength (ITS) test. Typically the tensile stress decreases in a parabolic shape to a minimum at the outer circumference of a normal (not reshaped) asphalt briquette as illustrated in Figure 6.3.

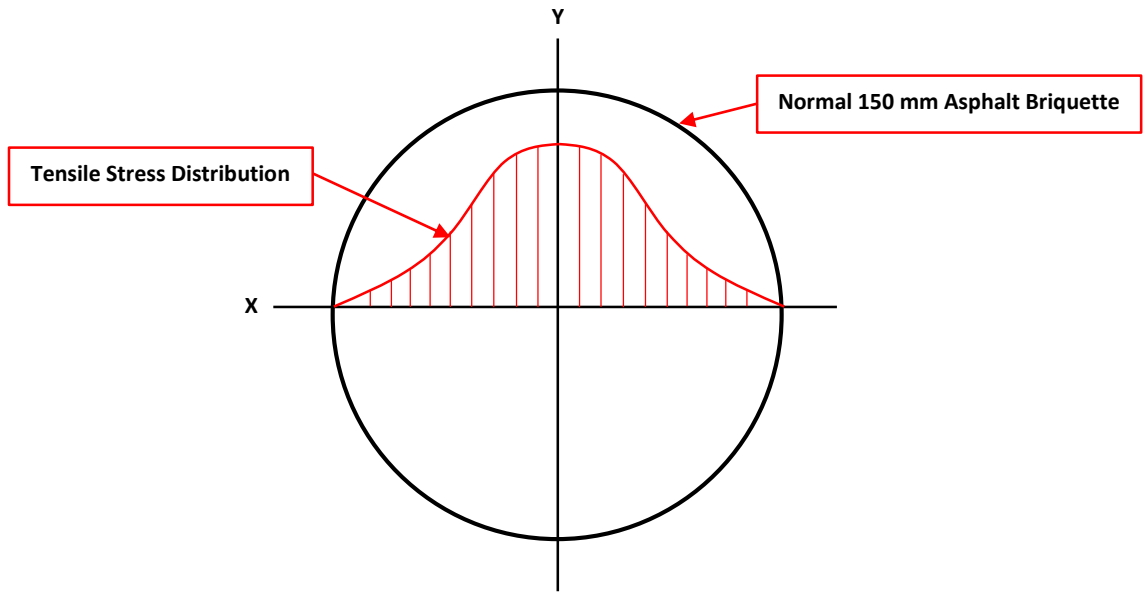

Figure 6. 3 - Typical tensile stress distribution along the x-axis during ITS test.

Tensile stress S11 results were extracted from the finite element models for four different conditioning with the following mid-ordinate dimension: (Normal), 10 mm, 15 mm and 19 mm (MMLS3 prepared briquettes). In addition, tensile stress S11 results were extracted for four variations in the asphalt mixture's resilient modulus (see Table 4.2). However, it was found that a change in the resilient modulus did not influence the tensile stress distribution and its magnitude at the centre of asphalt briquette. More results on the effect of a change in resilient modulus are presented in *Section 6.3.3*. Figure 6.4 illustrates the distribution and magnitude of tensile stresses obtained for the four different machined-off segment mid-ordinate dimensions.

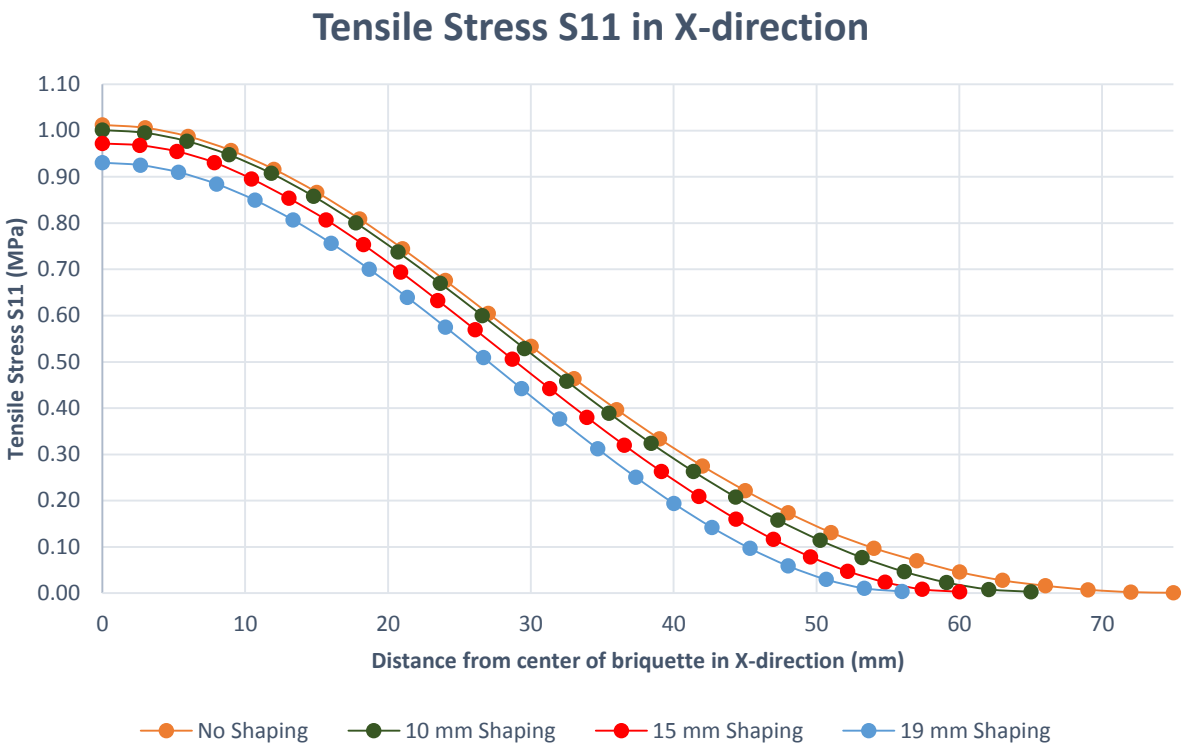

Figure 6. 4 - Tensile stress S11 for various dimensions of the machined-off segment mid-ordinates and resilient modulus.

From Figure 6.4 follows that the shape of the tensile stress distribution along the x-axis for the various machined-off segment mid-ordinate dimensions remained consistent with the shape illustrated in Figure 6.3. However, it is clear that an increase in the dimension of the mid-ordinates resulted in a decrease in the maximum tensile stress measured at the centre of the asphalt briquette. It can also be concluded that the machined-off segments cause a redistribution of the tensile stresses. It can be visually concluded from the graphs shown in Figure 6.4 that tensile stress decreases with an increase in the mid-ordinate dimension of the machine-off briquette segments.

As indicated the maximum tensile stress at the centre of the asphalt briquette equal the ITS of the asphalt mixture. The percentage change in the maximum tensile stress S11 at the centre of the briquette with a change in the dimension of the machined-off segments mid-ordinate, produced the relationship as shown in Figure 6.5. It should be noted that a change in the resilient modulus of the asphalt mixture did not affect this relationship. From Figure 6.5, follows that the maximum tensile stress at the centre of the briquette can be expected to reduce by 8% for a machined-off segment mid-ordinate of 19 mm. A significant change

in the maximum tensile stress can be therefore expected for MMLS3 prepared asphalt briquettes subjected to ITS testing.

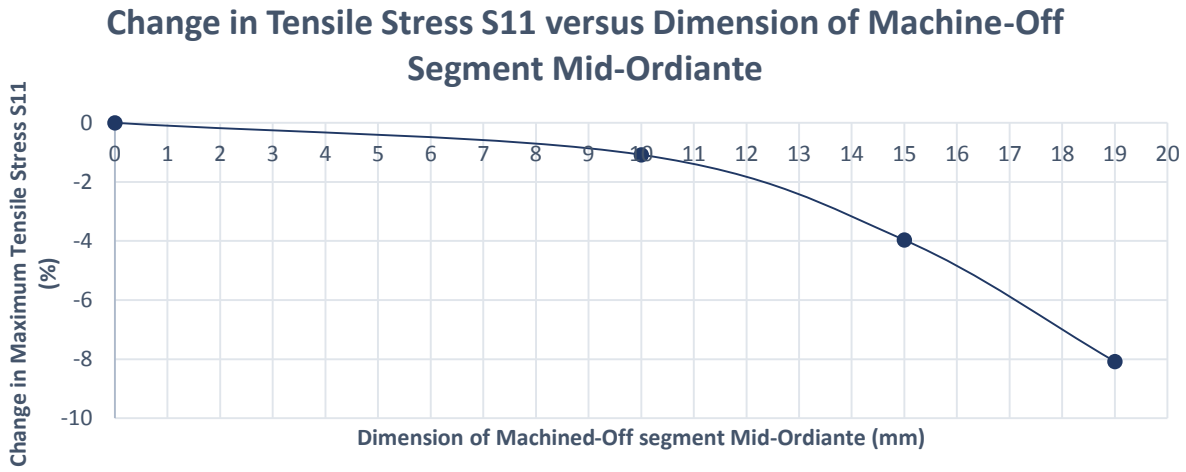

Figure 6. 5 - Change in Tensile Stress S11 versus dimension of machined-off segment mid-ordinate.

From these results the standard ITS equation as shown in Equation 6.1, may have to be adjusted for MMLS3 prepared asphalt briquettes to accommodate for the influence of briquette re-shaping on the ITS result. For further details on the ITS equation see *Appendix B*.

$$ITS = \frac{2 \times P}{\pi \times t \times D} \qquad \textit{Equation 6.1}$$

Actual laboratory ITS test results obtained during this study were compared with the maximum tensile stress S11 results as obtained from the finite element model 19 mm machined-off segment mid-ordinate. Table 6.1 summarises the comparisons of the results for the COLTO medium 50/70 penetration grade MMLS prepared asphalt briquettes.

Table 6. 1 - Finite element model compared with laboratory ITS results.

Finite Element Model*		Laboratory ITS test**	Percentage Difference Between Results (%)
Resilient Modulus (MPa)	Maximum Tensile Stress S11 (kPa)	Maximum Tensile Stress (kPa)	
1230	931	879	5.6
1672	931		5.6
3074	931		5.6
4076	931		5.6

Notes: * - Finite element model results for various resilient modulus inputs.
** - Laboratory ITS results on 50/70 penetration grade MMLS prepared asphalt briquettes.

From Table 6.1 follows that the maximum tensile stress S11 results did not show any changes in its magnitude due to changes in the resilient modulus of the asphalt mixture during finite element analysis as a result of Hooke's law. This indicates the resilient modulus may rather have an influence on the tensile strain along the x-axis.

From Table 6.1 follows that the percentage difference between the maximum tensile stresses determined through finite element analysis and laboratory ITS testing was 5.6%. This result indicates that the linear-elastic finite element model produces results moderately comparable with the results obtained through laboratory ITS testing. It is expected, that by incorporating the viscous component of the asphalt materials' behaviour and the quadratic element, the finite element model will produce results even more comparable.

6.3.2 COMPRESSIVE STRESS S22 (X-AXIS)

Compressive stresses along the x-axis were also investigated during the finite element analysis. Due to the machined-off segments being located along the x-axis, it was expected that a change in the compressive stress S22 (see Figure 6.2) should occur. A typical compressive stress distribution along the x-axis during ITS testing is illustrated in Figure 6.6. The maximum compressive stress occurs at the centre of the asphalt briquette as a result of the MTS loading ram and gradually decreases to zero towards the outer circumference of asphalt briquette.

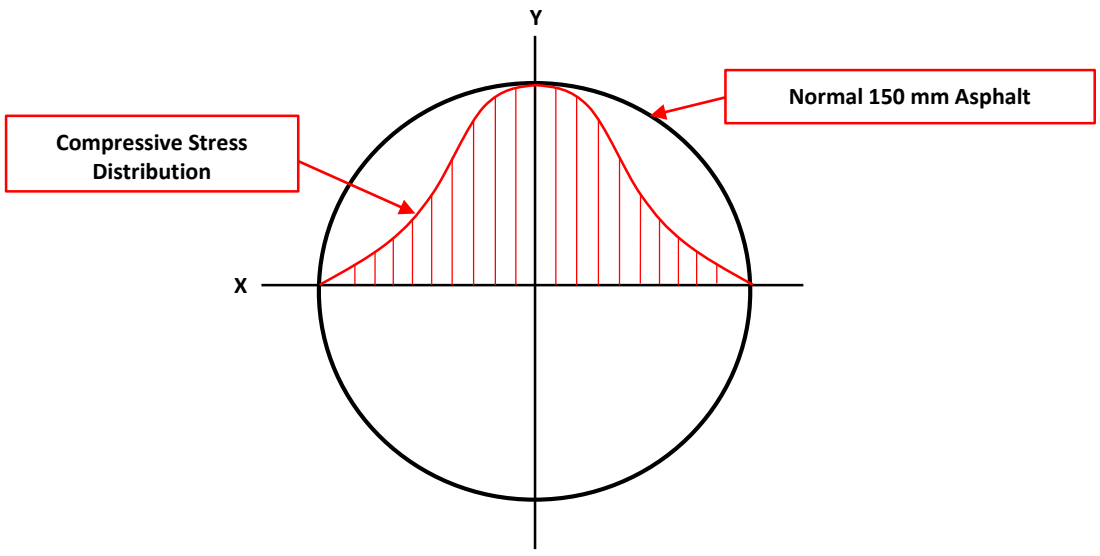

Figure 6. 6 - Distribution of compressive stresses along the x-axis.

Finite element analysis of the compressive stress S22 along the x-axis was completed for various dimensions of the machined-off segment mid-ordinate and resilient modulus inputs. The analysis showed changes in the resilient modulus of the material did not affect the magnitude of the compressive stress S22. The compressive stress S22 results for various dimensions of the machined-off segment mid-ordinate is illustrated in Figure 6.7.

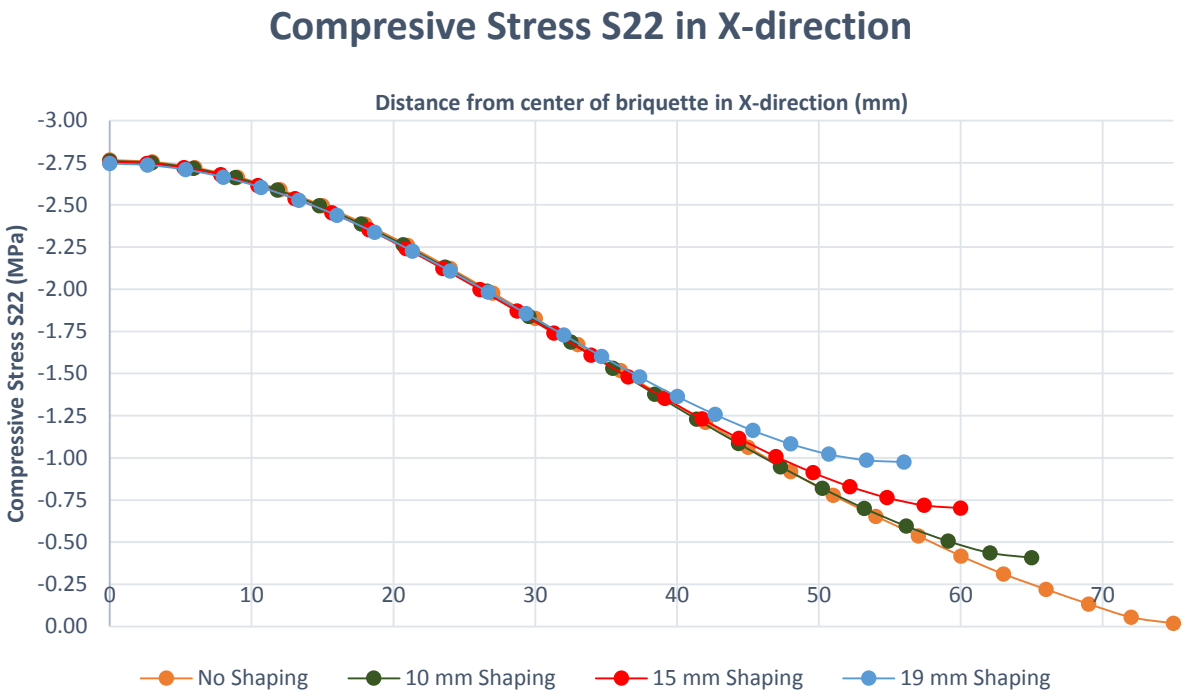

Figure 6. 7 - Compressive stress S22 results along x-axis for various dimensions of the machined-off segment mid-ordinate and resilient modulus.

From Figure 6.7 follows that the maximum compressive stress S22 did not show any change in its magnitude for various dimensions of the machined-off segment mid-ordinate. However, distribution of compressive stresses along the x-axis seemed to be influenced by the re-shaped briquette form as the shape of curves in Figure 6.7 deviate from the typical distribution illustrated in Figure 6.6. From these results it can be concluded that the conventional equation for determining the maximum compressive stress during ITS testing does not have to be adjusted for the influence of the briquette's machined-off segments.

From Figure 6.7 follows that an increase in compressive stress at the outer circumference of the briquette is experienced with an increase in the dimension of the machined-off segments mid-ordinate. For the same load applied, a greater compressive stress, therefore, needs to be absorbed by the material at the

outer circumference of the asphalt briquette as the dimension of the machined-off segments mid-ordinate increases. However, the compressive stress condition at the edge of the asphalt briquette is seldom of significance when it comes to calculating important stress conditions during ITS testing.

6.3.3 TENSILE STRAIN E11 (X-AXIS)

It was previously observed that a change in the resilient modulus of the material for the various re-shaped conditions did not influence the magnitude and distribution of the tensile and compressive stresses. Figure 6.8 provides an illustration of this occurrence which was encountered during analysis of the tensile stress S11 along the x-axis. It should be noted that similar results were produced for other stress conditions.

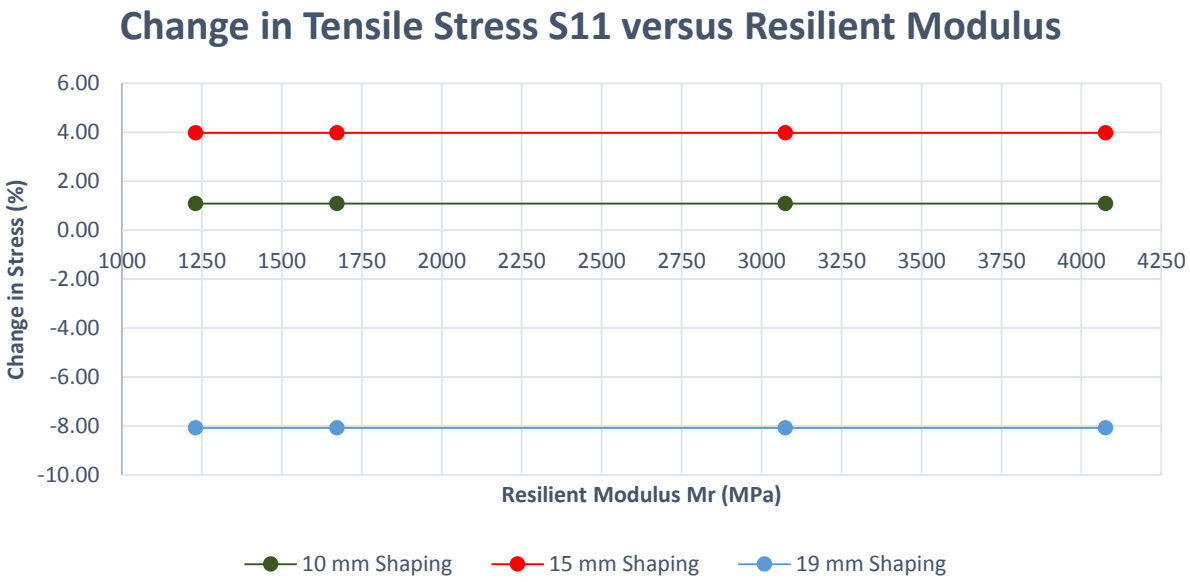

Figure 6. 8 - Change in tensile stress S11 versus resilient modulus.

Figure 6.8 illustrates the change in the maximum tensile stress S11 at the centre of the briquette along the x-axis for various resilient modulus inputs and machined-off segments mid-ordinate conditions. A constant relationship between the change in tensile stress S11 and the resilient modulus was established for the various machined-off segments mid-ordinate conditions. This indicates that a change in the resilient modulus has no influence on the magnitude of maximum tensile stresses at the centre of the asphalt briquette. Instead, this result indicates that the tensile strain E11 along the x-axis is expected to change for various resilient modulus inputs. This was confirmed by the finite element analysis that a relationship exists between the maximum tensile strain E11 at the centre of the asphalt briquette and resilient modulus. This relationship is illustrated in Figure 6.9.

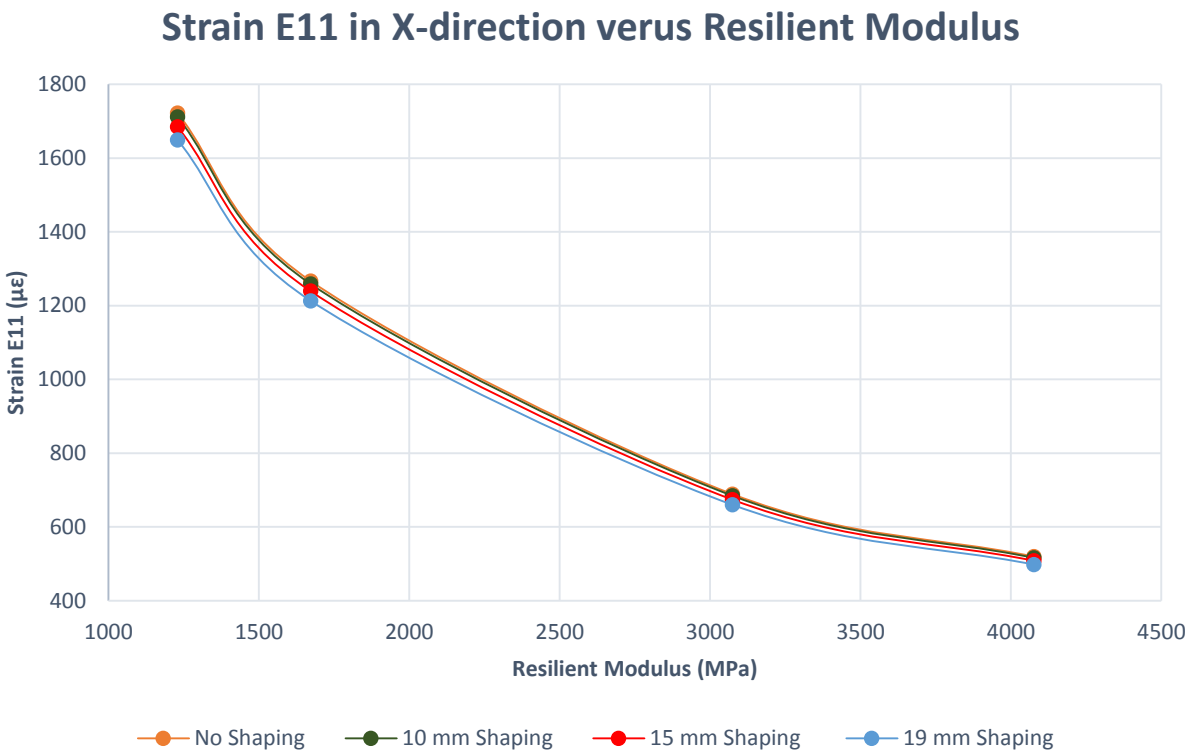

Figure 6. 9 - Tensile Strain E11 along x-axis versus resilient modulus.

From Figure 6.9 follows that an increase in the resilient modulus results in a decrease in the tensile strain E11 at centre of the asphalt briquette. The foregoing stress-strain relationship for a constant stress confirmed Hook's law, as shown in Equation 6.2, for strain along the x-axis for a 3-dimensional stress condition, is confirmed.

$$\varepsilon_x = \frac{1}{E}(\sigma_x - \nu(\sigma_y + \sigma_z) \qquad \textit{Equation 6.2}$$

From Figure 6.9, follows that as the dimension of the mid-ordinate of the machined-off segments increases a slight decrease in the tensile strain E11 are experienced. However, this decrease in tensile strain is not as severe as experienced with the tensile stress S11 and was therefore not considered as significant.

6.3.4 TENSILE STRESS S11 (Y-AXIS)

A typical tensile stress distribution along the y-axis during ITS testing is illustrated in Figure 6.10. The tensile stress along this axis remained constant in magnitude throughout the diameter of the briquette.

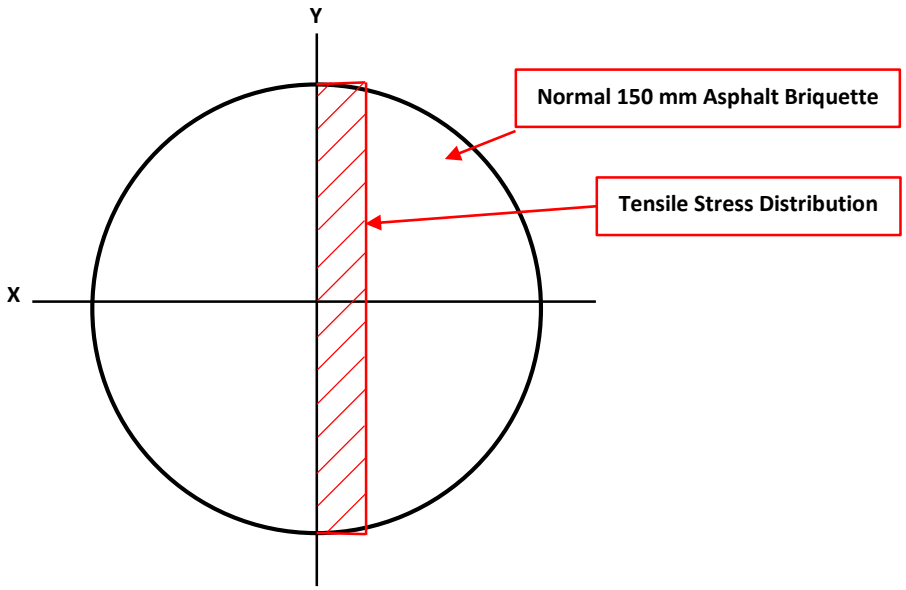

Figure 6. 10 - Tensile and compressive stress distribution along y-axis.

Investigation of the tensile stress S11 along the y-axis, with finite element models, indicated that a change in the resilient modulus had no change in the magnitude of the stress. The tensile stress S11 was investigated for various dimensions of shaping. Figure 6.11 illustrates the results of this investigation.

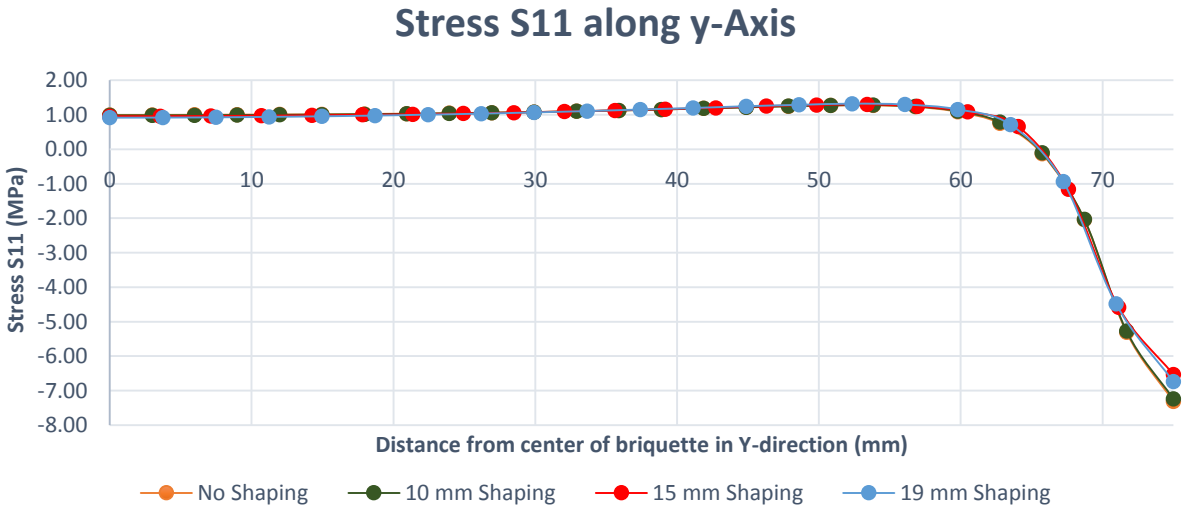

Figure 6. 11 - Tensile Stress S11 along Y-axis

From Figure 6.11 follows that a constant tensile stress is exhibited from the centre of the asphalt briquette up to a distance of 60 mm along the y-axis. Thereafter the stress condition changed to compression for the remaining distance to the outer circumference of the asphalt briquette. This change in stress condition

may be the result of distortion caused by load transfer between the loading ram of the MTS and the asphalt briquette.

From Figure 6.11 follows that the dimension of shaping had no significant influence on the stress condition and its magnitude.

6.3.5 COMPRESSIVE STRESS S22 (Y-AXIS)

A typical compressive stress distribution along the y-axis during ITS testing is illustrated in Figure 6.12. The maximum compressive stress occurs at the outer circumference of the asphalt briquette due to direct contact with the loading ram of the MTS.

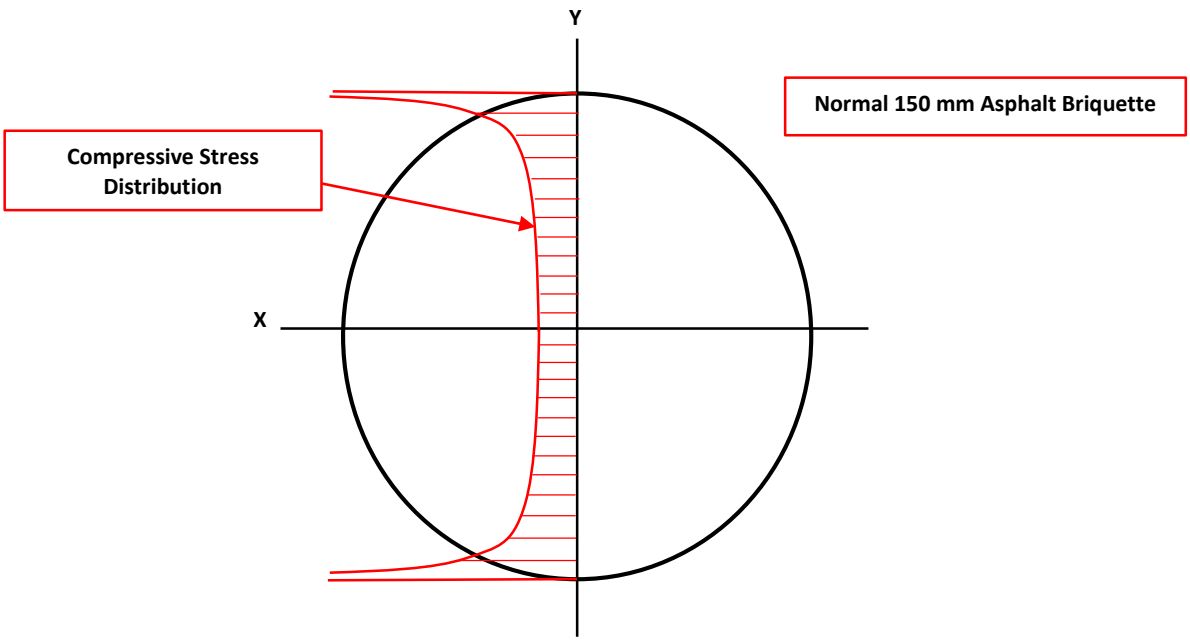

Figure 6. 12 - Compressive stress distribution along y-axis.

The compressive stress S22 results along the y-axis were obtained from finite element models and is illustrated in Figure 6.13. Changes in the resilient modulus once again had no influence the magnitude of the compressive stress S22 along the y-axis.

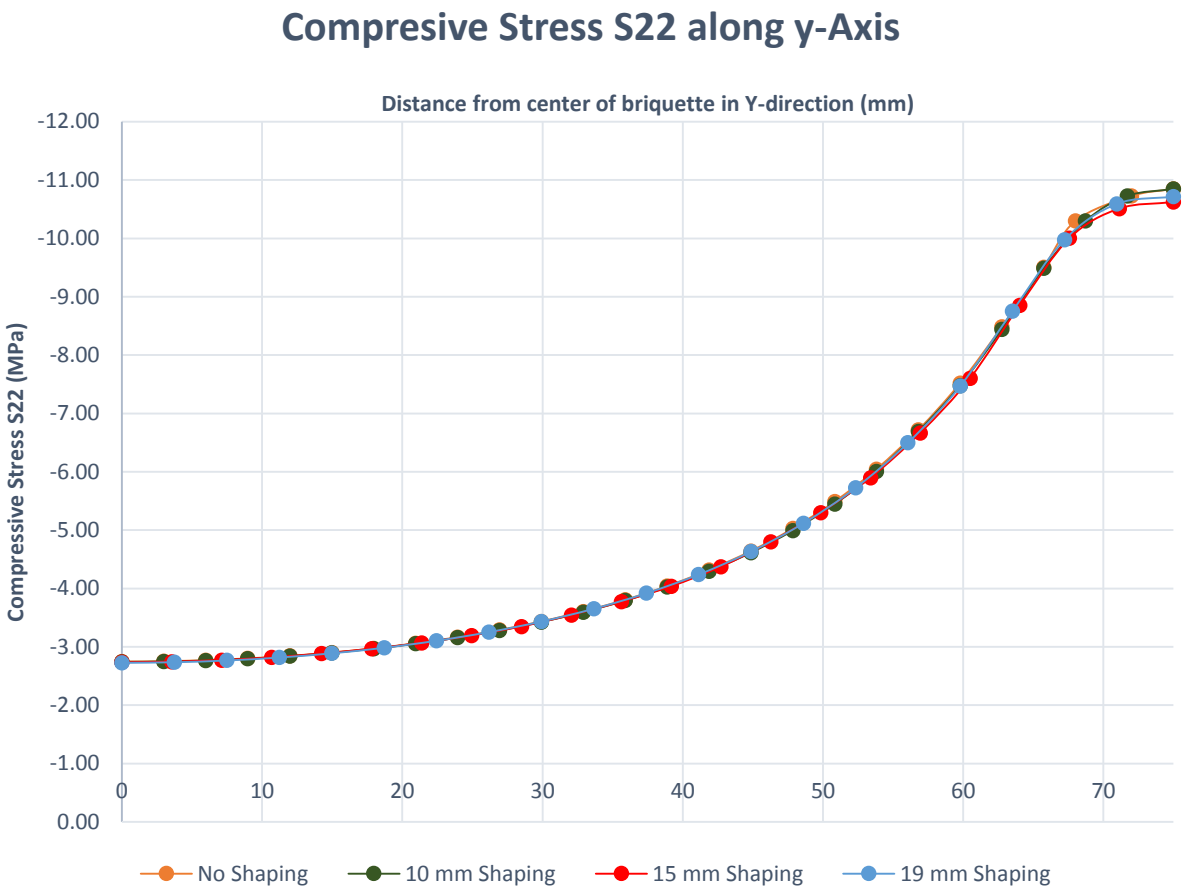

Figure 6. 13 - Compressive stress S22 along the y-axis.

From Figure 6.13 follows that the distribution of the compressive stress along the y-axis was fairly comparable to the typical distribution illustrated in Figure 6.13. As expected, the maximum compressive stress S22 was equal to the pressure load applied to the asphalt briquette. The compressive stress S22 exponentially decreases from a maximum to a minimum towards the centre of the asphalt briquette. It can also be concluded that the compressive stress S22 was not influenced by the dimension of the reshaping.

6.3.6 TENSILE STRESS S11 (Z-AXIS)

The tensile stress S11 at the centre of the asphalt briquette along the z-axis was also investigated to determine whether a change in dimension of shaping influenced the tensile stress magnitude and distribution through the depth of the asphalt briquette. The results of this investigation are illustrated in Figure 6.14.

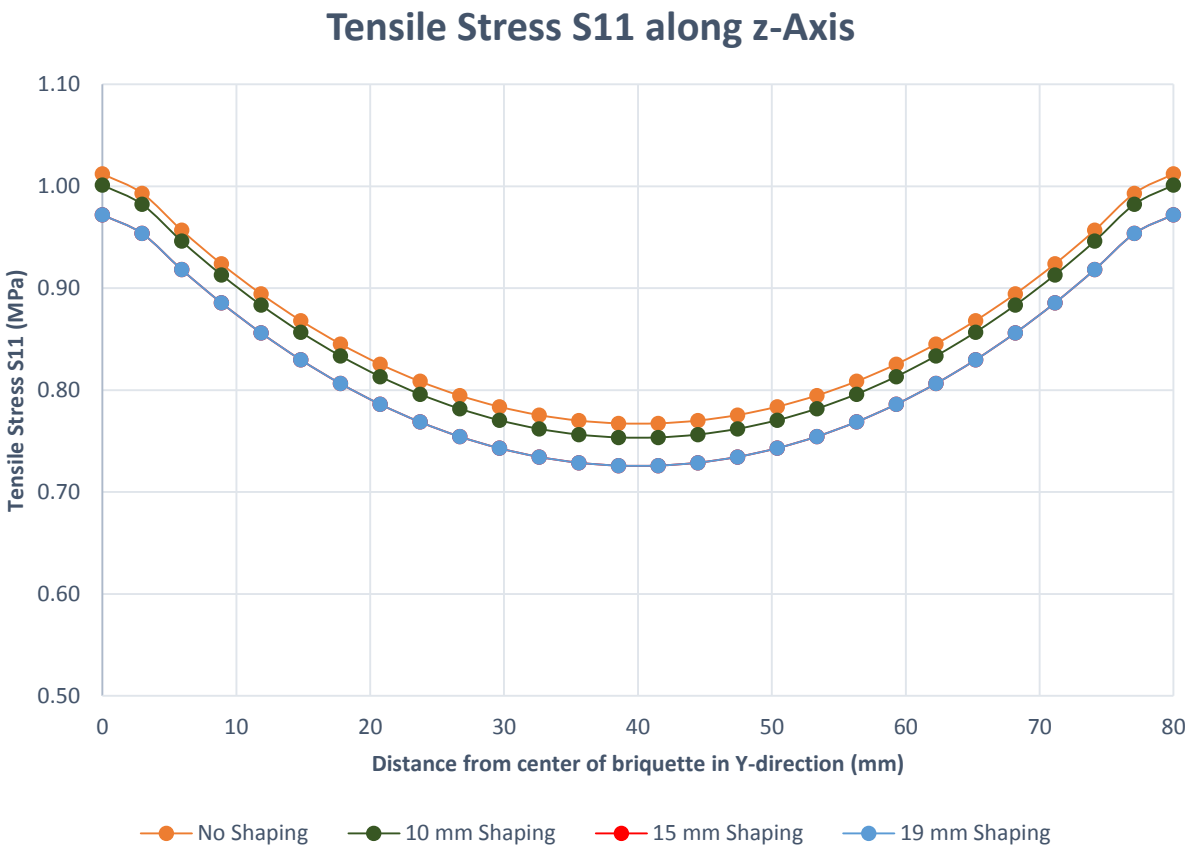

Figure 6. 14 - Tensile stress S11 along the z-axis at the centre of the asphalt briquette.

From Figure 6.14 follows that the tensile stress S11 achieved its maximum at a depth of 0 mm and 80 mm. The minimum tensile stress occurred at the centre of the asphalt briquette. A machined-off segment with a mid-ordinate of 15 mm and 19 mm seemed to have a slight influence on the distribution of the tensile stress S11. However, this influence could be considered insignificant. Therefore, it can be concluded that a change in the dimension of shaping had no significant influence on the tensile stress S11 along the z-axis throughout the depth of the asphalt briquette.

6.4 SUMMARY

Tensile and compressive stress results were obtained from four 3-dimensional finite element models and analysed to determine the effect of machined-off segments on the indirect tensile strength of asphalt mixtures. This investigation was initiated after ITS tests were performed on MMLS3 prepared asphalt briquettes, which required machining-off two segments, with a mid-ordinate of 19 mm, on the asphalt briquette to fit in the MLS test bed setup.

The linear-elastic finite element models were moderately comparable to the actual behaviour of the asphalt briquettes when subjected to ITS testing. The comparative difference of 5.6% for the indirect tensile strength was determined by finite element models and actual laboratory ITS testing. It is expected, that greater approximations to the actual behaviour of the asphalt briquette under ITS testing will be achieved if the viscous component of the asphalt material's behaviour and the quadratic element are included in the finite element models.

The linear-elastic finite element models indicated a reduction in the indirect tensile stress of the asphalt mixture of up to 8% that can be expected when MMLS3 prepared asphalt briquettes are subjected to ITS testing. As the machined-off segments with a 19 mm mid-ordinate fell within the area of a typical ITS tensile stress distribution along the x-axis, a redistribution of these stresses occurred (See Figure 6.3 and 6.4). It should be noted that the shape of the tensile stress distribution along the x-axis remained the same, whilst the maximum tensile stress occurred at the centre and the minimum at the outer circumference of the asphalt briquette.

Compressive stresses along the x-axis were not significantly influenced by the presence of the machined-off segments of a typical MMLS3 prepared asphalt briquette. The maximum compressive stress along the x-axis had not shown any sign of influence by the presence of machined-off segments. However, the minimum compressive stress increased with an increase in the dimension of the machined-off segments. Only the maximum compressive stress along the x-axis was considered important as it provides information on the crushing of the asphalt. Compressive stresses along the y-axis were not influenced by the presence of the machined-off segments. The machined-off segments did not fall within the typical compressive stress distribution area along the y-axis (see Figure 6.12) and was subsequently not influenced by the presence of it.

The finite element models analysed the effect of changes in the resilient modulus and it was found that it had no influence on the distribution and magnitude of compressive and tensile stresses. However, an increase in the resilient modulus led to a decrease in the strain magnitude. This correlate with Hook's law for a 3-dimensional stress condition. Research done by Walker (2013) also investigated the influence of changes in the material stiffness on the indirect tensile strength using finite element analysis. During his research, he also concluded that a change in the materials stiffness had a negligible effect on the stress (Walker, 2013).

CHAPTER 7 – CONCLUSIONS AND RECOMMENDATIONS

7.1 INTRODUCTION

A summary of the primary and secondary objective for this study is presented in this Chapter. In addition, the findings, conclusions and recommendations derived from a literature study, laboratory work and finite element modelling are also presented.

7.2 SUMMARY, FINDINGS, CONCLUSIONS AND RESEARCH RECOMMENDATIONS

7.2.1 PRIMARY OBJECTIVES

The primary objective of this study was to identify gradings and binder combinations for improving the grey water resistance of asphalt. The primary objective was achieved by completing three sub-objectives, discussed in Chapter 1.

7.2.1.1 Sub-Objective 1: Asphalt composition and mechanism of moisture failure

An extensive literature review was compiled to provide knowledge and understanding of the composition and properties of asphalt mixtures. Mechanisms of moisture failure related to asphalt surfacing were identified which highlighted key areas for improving the grey water resistance of asphalt. In order to improve the grey water resistance of an asphalt mixture, literature on the moisture susceptibility of asphalt formed the basis to identify areas for improvement in grey water resistance. Four key areas were identified to improve the moisture susceptibility of asphalt:

- Volumetric Properties
- Aggregate Properties
- Bitumen Properties
- Compaction

Previous research on the grey water resistance of asphalt completed by the University of Stellenbosch investigated these key areas and found reducing the VIM of asphalt mixtures and increasing the compaction effort resulted in greater grey water resistance. It was also found that modified binders significantly improved the grey water resistance of asphalt mixtures. This research provided the starting point for identifying gradings and binder combination for improving the grey water resistance of asphalt.

7.2.1.2 Sub-Objective 2: Setting up an extensive research methodology

An experimental research methodology was set up which consisted of two phases. Phase 1 consisted of subjecting selected asphalt grading and binder combinations to clean and grey water MIST conditioning. Five gradations and several binder combinations formed part of this phase. Gradings tested during this phase included: COLTO medium continuous graded, COLTO fine continuous graded, City of Cape Town (CCC) fine graded, semi-gap graded and Much fine graded. Binder combinations consisted of penetration grade binders as well as modified binders. Binder additives used included SBS, EVA, polyamine, Sasobit® and ZycoTherm®. After MIST conditioning asphalt briquettes were subjected to ITS testing to identify variables that influence the grey water susceptibility of asphalt mixtures.

Phase 2 consisted of laboratory scale dry (no water) and wet (grey water) MMLS3 trafficking of selected grading and binder combinations. Four gradations and several binder combinations formed part of this phase. Gradings tested during this phase included: COLTO medium continuous graded, COLTO fine continuous graded, City of Cape Town (CCC) fine graded, semi-gap graded and Much fine graded. Similar as in Phase 1, binder combinations consisted of virgin and modified binders. Binder additives used in Phase 2 were the same as in Phase 1. During Phase 2 results related to the permanent deformation, texture, material loss and mixture strength after dry and wet MMLS3 trafficking were captured for further analysis.

7.2.1.3 Sub-Objective 3: Conclude findings of this study

Tensile Strength Ratio (TSR) and Indirect Tensile Strength (ITS)

Tensile strength ratios (TSR) were calculated from ITS results to establish the strength retained by asphalt mixtures after clean and grey water MIST conditioning. From these results, it was concluded that grey water significantly decreased that the retained strength of asphalt when compared to clean water. This is associated to the surfactants in grey water which accelerate damage caused by moisture in asphalt. This finding was similar as Briedenhann and Jenkins (2015) identified.

TSR results also indicated that medium graded asphalt tended to retain greater strength after grey water MIST conditioning when compared to fine graded asphalt. This was related to the larger maximum aggregate size present in medium graded asphalt, which created greater strength and stiffness in the asphalt mixture when compared to fine graded asphalt. In addition, a natural sand fraction formed part of the City of Cape Town fine and semi-gap graded asphalt mixtures which was related to several premature failures during grey water MIST conditioning. Sand particles was found difficult to properly

coat with bitumen during sample preparation, which may have provided access for grey water to penetrate and cause significant damage.

In most cases, modified binder combinations significantly increased the grey water resistance of asphalt mixtures when compared to virgin binder combinations. ITS results indicated that binder additives, EVA and ZycoTherm®, increased the strength of asphalt after grey water MIST conditioning.

Trends from tensile strength ratios (TSR) of asphalt mixtures subjected to dry and wet MMLS3 trafficking, were not comparable to the results from MIST conditioning. MMLS3 trafficking was performed at 40°C and 100 000 load cycles with a tyre pressure of 700 kPa, whereas MIST conditioning was performed at 60°C with pressure pulses of 150 kPa. Although direct comparison between the two test methods was not made, it seemed that MIST conditioning caused more severe damage to the asphalt when compared to MMLS3 trafficking. Research done by Ball et al (1999) indicated that a pressure of 100 kPa is sufficient to force water through a chip seal and cause significant damage to the seal and base layer. Based on the research of Ball et al. (1999), it was suspected that temperature may also have a significant influence on the magnitude of the pressure and the penetration of water into an asphalt mixture. In most cases, ITS results after grey water MIST conditioning were also lower than results obtained after grey water MMLS3 trafficking. The visco-elastic behaviour of asphalt was related to this observation as MIST conditioning at 60°C softens the bitumen more than MMLS trafficking at 40°C. Therefore, a lower pressure of 150 kPa at a high temperature forces water much easier into the asphalt mixture and causes significant damage compared to a pressure of 700 kPa at a lower temperature.

The relationship between the ITS and VIM of asphalt mixtures, subjected to dry (no water) and wet (grey water) MMLS3 trafficking, was investigated through ANOVA analysis. Although a significant relationship was not established, regression coefficients indicated that ITS results for no water conditioning did not change with as increase in VIM. ITS results for grey water conditioning tended to decrease with an increase in VIM. This behaviour was related to grey water penetrating voids in the asphalt that caused a loss of adhesion.

Permanent deformation

Cumulative permanent deformation results, after dry and wet MMLS3 trafficking, indicated that EVA and SBS modified binders significantly improved an asphalt mixtures resistance to permanent deformation when compared to penetration grade binders. The adding of Sasobit® and ZycoTherm® to EVA and SBS modified binders significantly reduced the cumulative permanent deformation of COLTO medium and fine

continuous graded asphalt mixtures. However, the contribution of the ZycoTherm® to the improved permanent deformation result was not clear and it was suspected that the EVA and SBS binder additives contributed the most to reduce the permanent deformation. EVA and SBS modified binders are known to increase the elastic limit and stiffness of asphalt mixtures, providing greater resistance to deformation. In addition, it was observed that ZycoTherm®, in combination with a penetration grade binder, increased the cumulative permanent deformation.

Deformation curves, which plotted the permanent deformation versus MMLS3 load cycles, indicated that two rates of deformation occurred when 100 000 MMLS3 load cycles are applied. A primary rate of deformation occurred from 0 to 10 000 MMLS3 load cycles, whereas a secondary rate of deformation occurred from 10 000 to 100 000 MMLS3 load cycles. The primary rate of deformation was significantly higher than the secondary rate of deformation. Primary and secondary rates of deformation results confirmed that EVA and SBS modified binder combinations significantly reduced the deformation of asphalt mixtures.

An ANOVA analysis was performed to establish if a relationship between the ITS and two rates of deformation for grey water MMLS3 trafficking existed. Although an insignificant trend was established, a hypothesis test indicated that the regression coefficient ‘b’ was not equal to zero and had a negative sign. This indicated that the strength of the asphalt mixture tended to reduce with an increase in the primary and secondary rate of deformation.

Texture and Material Loss

Texture results obtained from laser profilometer measurements and sand patch tests had not provided significant trends. However, an ANOVA analysis was performed to establish a relationship between laser profilometer results and sand patch tests results. The purpose of this relationship was to validate the Civil Designer® texture analysis method developed during this study. Although this relationship was insignificant a hypothesis test indicated that the regression coefficient ‘b’ was not equal to 0 and had a positive sign. This indicated as the laser profilometer measured texture increase so does the sand patch test measured texture. As the sand path test is accepted by SANS, further refinement of the Civil Designer® texture analysis method is required to achieve a greater relationship.

Material loss results indicated a significant increase in the material loss for fine graded asphalt mixtures than for medium graded asphalt mixtures after grey water MMLS3 trafficking. The change in material loss

for modified binder combinations were less than penetration grade binder combinations after grey water MMLS3 trafficking.

Combining Results and Rating Criteria

A rating criteria was developed to combine ITS, TSR, permanent deformation and material loss results for determining the most effective grey water resistance asphalt mixture for high and low volume roads. In this study high volume roads refer to collector roads such as Mew Way, into which the internal roads of the informal settlement connect. In this study low volume roads refer to the internal roads of the informal settlement. The rating criteria was used to rate each grading and binder combination based on results obtained during Phases 1 and 2 of the experimental research methodology. For high volume roads the asphalt layer must have a structural contribution to pavement structure, which is achieved when the layer thickness is greater than 30 mm. The layer thickness is determined by the maximum aggregate size of an asphalt mixture, of which the latter is equal to one third of the layer thickness. This translates to a minimum layer thickness of 42 mm for the medium graded asphalt mixture tested during this study. Therefore, medium graded asphalt mixtures may provide a suitable grey water susceptible asphalt mixture for high volume roads this being due to the structural contribution of the layer and a larger 14 mm maximum stone size that contributes to greater strength and stiffness. Fine graded asphalt mixtures may provide a solution for low volume internal roads, having a layer thicknesses of less than 30 mm. Fine graded mixtures tested during this study had a maximum stone size of 10 mm, which translates to a layer thickness of 30 mm. Thin asphalt layers are more cost effective and should satisfy the functional requirements of the pavement.

Based on the rating criteria the following **medium graded** asphalt binder combinations showed significant grey water resistance:

- SBS + 1%Sasobit® + 0.1%ZycoTherm® + Extra Lime (COLTO Medium Continuous Graded)
- EVA + 1%Sasobit® + 0.1%ZycoTherm® + Extra Lime (COLTO Medium Continuous Graded)
- EVA + 1%Sasobit® + Extra Lime (COLTO Medium Continuous Graded)
- EVA + Extra Lime (COLTO Medium Continuous Graded)

The contribution of the ZycoTherm to the performance of asphalt mixtures was not completely clear. It is therefore recommended that the sample size of the above-mentioned binder combinations consisting of this binder additive, should be increased. The following medium graded binder combinations are therefore suggested to improve the grey water resistance of asphalt:

- EVA + 1%Sasobit® + Extra Lime (COLTO Medium Continuous Graded)
- EVA + Extra Lime (COLTO Medium Continuous Graded)

Based on the rating criteria the following **fine graded** asphalt binder combinations showed significant grey water resistance:

- EVA +1%Sasobit® (COLTO Fine Continuous Graded)
- EVA + 1%Sasobit® +0.1%ZycoTherm® (COLTO Fine Continuous Graded)

For the COLTO fine continuously graded asphalt mixtures, the ZycoTherm® binder additive indicated improved mixture strength, stiffness, shear resistance and resistance to ravelling. However, it was recommended as a second choice binder combination for improving the grey water resistance of asphalt for low volume roads. It is therefore suggested to increase the sample size of this binder combination to determine whether the improved properties continue to follow a trend.

7.3 SECONDARY OBJECTIVES

The secondary objective of this study was to determine the influence of machined-off segments with two parallel chords and each having a 19 mm mid-ordinate on a 150 mm diameter asphalt briquette subjected to indirect tensile strength (ITS) testing. Asphalt briquettes with this geometry are typically prepared for laboratory scale MMLS3 trafficking. Finite element analysis was used to investigate this objective.

Linear elastic finite element analysis of various briquette shape conditions and resilient modulus inputs indicated that a change in resilient modulus did not influence the distribution and magnitude of stresses in asphalt briquettes due to the applied load during ITS testing. Instead, an increase in the resilient modulus resulted in a decrease in strain results along the axis under investigation. This conformed to Hooke's law for determining the strain of a 3-dimensional stress condition.

With the stress results constant with a change in resilient modulus, the finite element analysis indicated that the tensile stress S11 along the x-axis was significantly influenced by a change in the dimension of the briquette shape. Trends indicated that the maximum tensile stress at the centre of the asphalt briquette decreases with an increase in the dimension of the briquette shape. Asphalt briquettes with 19 mm shaping, typically prepared for laboratory scale MMLS trafficking, may produce an indirect tensile strength (ITS) result up to 8% lower compared to briquettes with no shaping. Finite element analysis also indicated that compressive stresses along the y and z-axis were not influenced by the presence of a briquette shape.

Only linear-elastic material behaviour was modelled during the finite element analysis. Viscous material behaviour, which is typically exhibited by bituminous materials, may have a further influenced the results produced by finite element models. Factors for adjusting ITS results of shaped asphalt briquettes should, therefore, be used with caution.

7.4 RECOMMENDATIONS FOR FUTURE RESEARCH

The following recommendations are made for further research on the grey water resistance of asphalt:

- The effect of the grey water concentrate on the performance of asphalt should be investigated. During this study, a constant concentrate of grey water was assumed. Variation in the concentration of surfactants in grey water is a variable related to premature failure of asphalt surfacing. In addition, MMLS3 trafficking should be done at a temperature of 60^{o}C.
- The grey water resistance through surface energy and adhesion theories such as developed by Cheng et al. (2002) should be further investigated in order to relate laboratory results with theories developed to investigate the bitumen-aggregate bond strength.
- The Civil Designer® texture analysis method used to evaluate the texture during this study was a two-dimensional approach. A three-dimensional approach to evaluate the texture may provide results with greater accuracy when compare with sand patch test results. More refinement of this method is required to produce accurate results.
- Trail section data should be compared with laboratory results.
- Test the chemical effects of ZycoTherm® to determine its true contribution to the performance of asphalt mixtures. Increase the sample size of EVA and SBS binder combinations, consisting of ZycoTherm® to determine whether improved mixture properties follow a continuous trend.

The following recommendation is made for further research on the geometry of ITS specimens through finite element analysis:

- Include more material properties in the finite element models to simulate viscous material behaviour. Once correct material behaviour is achieved, adjustment factors can be developed to account for shaping when conducting ITS tests on laboratory scale MMLS briquettes.

8. BIBLIOGRAPHY

1. Abrahams, M., 2015. *Towards the development of a standard test protocol: Application of the MMLS3 for evaulating the performance of surfacing seals.,* Stellenbosch: University of Stellenbosch.

2. American Cleaning Institute, 2016. *Soaps and Detergents: Chemistry.* [Online] Available at: http://www.cleaninginstitute.org/clean_living/soaps__detergents_chemistry.aspx [Accessed 2016 January 11].

3. Anderson, D., 1987. Guideline for Use of Dust in Hot Mix Asphalt Concrete Mixtures. *Association of Asphalt Paving Technologists,* Volume 56, p. 492.

4. Asphalt Academy-TG1, 2007. *Technical Guideline 1: The use of Modified Bituminous Binders in Road Construction.* 2 ed. Pretoria: Asphalt Academy.

5. ASTM International, 2012. *Standard Test Method for Indirect Tensile (IDT) Strength of Bituminous Mixtures,* Pennsylvania: ASTM International.

6. Ball, G., Logan, T. & Patrick, J., 1999. *Flushing processes in chip-seals: Effect of water,* Wellington: Transfund New Zealand Research Report 156.

7. Briedenhann, R. & Jenkins, K., 2015. *Testing the grey water resistance of popular bitumen modifiers,* Stellenbosch: University of Stellenbosch, CAPSA.

8. Brovold, F. & Majidzadeh, K., 1968. *State of the art: Effect of water on bitumen-aggregate mixtures,* Washington D.C.: TRB.

9. California Department of Transport, 2000. *Method of test for moisture vapour susceptibility of bituminous mixtures,* California: California Department of Transportation.

10. Castan, M., 1968. Rising of Binder to the SUrface of an Open-Grade Bituminos Mix. *Bulletin de liaison des laboratories routiers,* Volume 33, pp. 77-84.

11. Chadbourn, B., 2000. *The Effects of Voids in Mineral Aggregate (VMA) on Hot-Mix Asphalt Pavements,* Minnesota: Minnesota Department of Transport.

12. Cheng, D., Little, D., Lytton, L. & Holste, J., 2002. Surface Energy Measurement of Asphalt and its application to predicting Fatigue and Healing in Asphalt Mixtures. *Journal of the Transport Research Board,* Issue 1810, pp. 44-53.

13. Colas, 2012(1). *Elastomer Modified Bitumen: Product Data Sheet,* Cape Town: Colas.

14. Colas, 2012(2). *Ficher Tropsch Wax Modified Bitumen,* Cape Town: Colas.

15. Colas, 2012(3). *Plastomer Modified Binder: Product Data Sheet,* Cape Town: Colas.

16. Colas, 2012(4). *ColAmin: Adhesion/Anti-stripping agent,* Cape Town: Colas.

17. Colas, 2013(1). *50/70 Penetration grade bitumen: Product data sheet,* Cape Town: Colas.

18. Curtis, C., Clapp, D., Jeon, Y. & Kiggundu, B., 1998. Absorption of Model Asphalt Functionalities AC-20 and Oxidzed Asphalts on Aggregate Surface. *Association of Asphalt Paving Technologists,* Volume 67, p. 125.

19. De Sombre, R., Newcomb D.E., Chadbourn, B. & Voller, V., 1998. Parameters to Define the Laboratroy Compaction Temperature Range of Hot-Mix Asphalt. *Association of Asphalt Paving Technologists,* Volume 67, p. 125.

20. Dean, J., n.d. *Introduction to the Finite Element Method: Lecture 2,* Cambridge: University of Cambridge: Department of Materials Science and Metallurgy.

21. Dictionary.com, 2015. *Dictionary.com.* [Online] Available at: http://dictionary.reference.com/browse/blackwater[Accessed 11 August 2015].

22. Diversey, 2011. *Material Safety Data Sheet,* Sturtevant: Diversey.

23. Douries, W., 2004. *Factors Influencing Asphalt Compactibility and Its Relation to Asphalt Rutting Performance,* Stellenbosch: University of Stellenbosch.

24. Draft Protocol Guideline, 2008. *DGP 1 - Method for evaluation of permanent defromation and susceptibility to moisture damage of bituminous road paving mixtures using the Model Mobile Load Simulator (MMLS3),* s.l.: s.n.

25. Epps J., 2000. *NCHRP Report 444: Compatibility of a test for Moisture-Induced Damage with Superpave Volumetric Mix Design,* Washington D.C.: National Research Council.

26. Eriksson, E., Auffarth, K., Henze, M. & Ledin, A., 2002. *Characteristics of grey water,* Lyngby: Technical University of Denmark.

27. Fromm, H., 1974. *The Mechanisms of Apshalt Stripping from Aggregate Surfaces.* Chicago, Assosiation of Apshalt Paving Technologists.

28. Goode, F., 1959. Use of Immersion Compression Test in Evaluation and Designng Bituminious PAving Mixtures. *ASM STP,* Volume 252, pp. 113-126.

29. Greyling, A., 2012. *Development of a Standard Test Method for Determining the Bitumen Bond Strength of Emulsions-A South African Perspective,* Stellenbosch: University of Stellenbosch.

30. Greyling, A., 2015. *Grey Water Resistance Asphalt Study Volume 2: Situation Report,* Cape Town: Grey Water Asphalt Research Group.

31. Greyling, A., van Zyl, G. & Jenkins, K., 2015 (1). *Grey water resistant asphalt study Volume 3: Literature review report,* Cape Town: BVi Consulting Engineers.

32. Greyling, A., van Zyl, G., Jenkins, K. & Bowker, I., 2015 (2). *The development of grey water resistant asphalt,* Stellenbosch: University of Stellenbosch, CAPSA.

33. Hainin, M., Cooley, L. & Prowell, B., 2003. *An Investigation of Factors Influencing Permeability of SuperPave Mixes,* Auburn: National Center for Asphalt Technology.

34. Hudson, W. & Kennedy, T., 1968. *An Indirect Tensile Test for Stabilized Materials,* Austin: Center for Highway Research/University of Texas.

35. Hughes, R., Lamb, D. & Pordes, O., 1960. Adhesion in bitumen Macadam. *Journal of Applied Chemistry,* Volume 10.

36. Hugo, F., Epps, A. & Smit, A. d. F., 1999. *A Case study of model APT in the field,* Reno: International Conference on Accelerated Pavement Testing.

37. Hugo, F. et al., 2004. *Distress of hot mix asphalt on the NCAT test track due to accelerated wet trafficking with the MMLS3,* Minneapolis: Second International APT Conference.

38. Hugo, F. & Steyn, W., 2015. *A Synthesis of Application of the MLS as an Innovative System for Evaulating Performance of Asphalt Materials in Pavement Engineering.* Stellenbosch, Univeristy of Stellenbosch/Pretoria.

39. Hunter, R., 1994. *Bituminous Mixtures in road contruction.* London: Thomas Telford Services Ltd.

40. Hunter, R. & et al., 2000. *Asphalts in Road Construction,* London: Thomas Telford.

41. Hunter, R., Self, A. & Read, J., 2015. *The Shell Bitumen Handbook.* 6th ed. London: ICE publishing.

42. Jenkins, K. & Twagira, M., 2008. *Updating Bituminous Stabilized Material Guidelines-Task 11 Durability: Ageing of bituminous binder,* s.l.: Technical Memorandum.

43. Jenkins, K. & Twagira, M., 2009. *Moisture damage on bituminous stabilized materials using a MIST device,* Stellenbosch: University of Stellenbosch.

44. Jeon, Y. & Curtis, W., 1990. *A Literature Review of the Absorption of Asphalt Functionalities on Aggregate Surfacees,* Washington D.C.: Strategic Highway Research Program.

45. Kandhal, P., Lubold Jr, C. & Roberts, F., 1989. *Water Damage to Asphalt Overlays: Case Histories.* Alabama: National Centre for Asphalt Technologies.

46. Kemp, M., 2006. *Concept to Reality - MLS10,* Stellenbosch: University of Stellenbosch.

47. Kiggundu, B. & Roberts, F., 1988. *The Success/Failure of Methods used to Predict the stripping potential in the performance of Bituminous Pavement Mixtures,* s.l.: Submitted to TRB.

48. Kim, Y., Little, D. & Lytton, R., 2002. *Fatigue and Healing Characterization of Asphalt Mixtures.* s.l.:American Society of Civil Engineers.

49. King, G., 2003. Influence of Asphalt Grade and polymer concentration of the high temperature perofmance of polymer modified asphalt. *Association of Asphalt Paving Technologists,* Volume 61, p. 28.

50. Little, D. & Jones IV, D., 2003. *Moisture Sensitivity of Asphalt Pavements Topic 2: Chemical and Mechanical Processes of Moisture Damage in Hot-Mix Apshalt Pavements,* San Diego: Transporation Research Board of the National Academies.

51. Maupin, . G., 1982. *The use of Anti-Stripping Additives in Virginia,* Kansas City: Association of Asphalt PAving Technologists.

52. Milne, T., 2004. *Towards a performance related design method for bitumen and modified road seal binders,* Stellenbosch: Dissertation (PHD) University of Stellenbosch.

53. MMLS3 Operator's Manual, 2012. *MLS: MMLS3 Operator's Manual,* Stellenbosch: MLS Test Systems Pty Ltd.

54. MMLS3 Supplementary Items, 2011. *MLS: MMLS3 Supplementary Items,* Stellenbosch: MLS Test Systems Pty Ltd.

55. Petersen, H., 2013. *Investigating the effect of grey water on various bitumen asphalt grades,* Cape Town: s.n.

56. Petersen, J., Plancher, H. & Harnsberger, P., 1987. *Lime Treatement of Asphalt-Final Report,* s.l.: National Lime Association.

57. Plancher, H., Dorrence, S. & Petersen, J., 1977. *Identification of Chemical Types in Asphalts strongly absorbed at the Asphalt–Aggregate Interface and their relative displacementby water,* Chicago: Association of Apshalt Paving Technologists.

58. Porubszky, I. et al., 1969. Bitumen Adhesion to Stones. *Chimie, physique et applications partiques des agents de surface: compte-rendus du 5eme Congres International se la Detergence,* Volume 2, pp. 713-725.

59. Prowell, B. & Hurley, G., 2005. *Evaluation of Sasobit for use in warm mix asphalt,* Auburn: National Center for Asphalt Technology.

60. Raab, C., Partl, M., Jenkins, K. & Hugo, F., 2005. *Determiniation of Rutting and Water Susceptibility of Selected Pavement Materials Using MMLS3,* Norway: Bearing Capacity Conference Trondheim CRA'05.

61. Read, J. & Whiteoak, D., 2003. *The Shell Bitumen Handbook.* Fifth Edition ed. London: Thomas Telford Publishing.

62. Rice, J., 1958. Relationship of Aggregate Characteristics to the Effect of Water on Bituminous Paving Mixtures. *Symposium on Effect of Water on Bituminous Paving Mixtures,* Volume ASTM 240, pp. 17-34.

63. Roberts, F. et al., 1991. *HMA Materials, Mixture Design and Construction.* 1st ed. Maryland: NAPA Research and Education Foundation.

64. Robertson, R., 2000. *Chemical properties of Aphalts and Their Effects on Pavement Perfromace,* Washington D.C.: National Research Council.

65. Ruth, B., 1984. *Evaluation and Prevention of Water Damage to Apshalt Pavement Materials.* Philadelphia: American Society for Testing and Materials.

66. Sabita Manual 35/TRH8, 2016. *Design and Use of Asphalt in Road Pavements.* 1st ed. Cape Town: Sabita.

67. Sabita Manual 35/TRH8, 2016. *Design and Use of Asphalt in Road Pavements.* 1st ed. Cape Town: Sabita.

68. SANS 2001-BT11, 2011. *Part BT11: Texture depth measurement for the desing of surfacing seals,* Pretoria: SABS Standards Division.

69. SANS 3001-PD1, 2016. *Part PD1: Determination of permanent defromation and moisture sensitivity in asphalt mixes with the MMLS3.* Pretoria: SABS Standards Division.

70. SANS 4001-BT1, 2014. *Penetration Grade Bitumen,* Pretoria: SABS.

71. SAPEM Chapter 2, 2014. *Pavement Composition and Behaviour,* Pretoria: SANRAL.

72. SAPEM Chapter 4, 2014. *Standards.* 2nd ed. Pretoria: SANRAL.

73. SAPEM Chapter 8, 2014. *Material Sources,* Pretoria: SANRAL.

74. SAPEM Chapter 9, 2014. *Utilisation of Materials and Design.* 2 ed. Pretoria: SANRAL.

75. Schmidt, R. & Graf, P., 1972. The effect of water on the resilient modulus of apshalt treated mixtes. *Association of Asphalt Paving Technologists,* Volume 41, pp. 118-162.

76. Scott, J., 1978. Adhesion and Disbonding Mechanisms of Aspahlt used in Highway Construction and Maintenance. *Assosiation of Aspahlt Paving Technologists,* Volume 47, pp. 19-48.

77. Singh, H. & Jain, P., 1997. Bitumen quality and manufacturing processes - Past and present technological status. *Indian Journal of Chemical Technology,* Volume 4, pp. 259-276.

78. Soenen, H., 2015. *A review on fatigue cracking and asphalt,* International: NYNAS Petroleum.

79. Solaimanian, M., Harvey, J., Tahmoressi, M. & Tandon, V., 2003. *Test Methods to Predict Moisture Sensitivety of Hot-Mix Asphalt Pavements,* California: Moisture Sensitivity of Asphalt Pavements: A National Seminar.

80. Solaimanian, M. & Kennedy, T., 2000. *Research Report 4909-1F: Precision of the Moisture Susceptinility Test Methods Tex 531-C,* Austin: Center for Transportation Research.

81. Suvranu, D., 2000. *MANE 4240/CVL 4240: Introduction to Finite Elements,* s.l.: s.n.

82. Tarrer, A. & Wagh, V., 1991. *The Effect of the Physical and Chemical Characteristics of Aggregate on Bonding,* Washington D.C.: National Research Council.

83. Taute, A., Verhaeghe, B. & Visser, A., 2001. *Interim Guidelines for the Design of Hot-Mix Asphalt in South Africa,* Pretoria: SANRAL, CSIR, SABITA.

84. Terrel, R. & Al-Swailmi, S., 1994. *Water sensitivity of Asphalt-Aggregate Mixes: Test Selection,* Washington D.C.: National Research Council.

85. Terrel, R. & Shute, J., 1989. *Report on water sensitivity,* Washington D.C.: National Research Council.

86. TRH 21, 1996. *Hot Mix Recycling,* Pretoria: CSIR.

87. TRH 9, 1992. *Pavement Managment Systems: Standard Visual Assessment Manual for Flexible Pavements,* Pretoria: Department of Transport.

88. Unilever, 2015. *Unilever Product Information.* [Online] Available at: ttp://pioti.unilever.com/ pioti/en/p1.asp [Accessed 17 January 2016].

89. van As, S., 2008. *Applied Statistics for Civil Engineers,* South Africa: s.n.

90. Walker, P., 2013. *Finite Element Analysis of Indirect Tensile Test,* Stellenbosch: University of Stellenbosch.

91. Walubita, L., 2000. *MSc.Eng Thesis: Accelerated Testing of an Asphalt Pavement with the Third-Scale Model Mobile Load Simulator,* Stellenbosch: Stellenbosch Univeristy.

92. Walubita, L., Hugo, F., Epps, M. & Martin, A., 2002. Indirect tensile fatigue perfromance of asphalt after MMLS trafficking under different environmental conditions. *South African Institution of Civil Engineering,* 44(3).

93. WesTrack Forensic Team, 2001. *Superpave mixture design guideline,* Washington, DC: Federal Highway Administation.

94. Williams, T. & Miknis, F., 1998. The effect of antistrip treatments on asphalt-aggregate systems: An environmental scannin electron microscope study. *Journal of Elastomer and Plastics,* Volume 30.

95. Zydex Industries, 2015(1). *Anti-Stripping performance of ZycoTherm with Grey Water binders compared,* Vadodana: Zydex Industries.

96. Zydex Industries, 2015(2). *Zycotherm: 3C Nanotechnology,* Vadodara: Zydex Industries.

APPENDIX A – MATERIALS

A.1 INTRODUCTION

In Appendix A the materials used for the production of HMA are be discussed. The outline of this chapter consists of an overview of the following materials: bitumen and aggregate. Under bitumen, bitumen production and types. In addition, sources and the use of aggregate for HMA production as well as the sources of active filler available in South Africa, are discussed.

A.2 BITUMEN

A.2.1 PRODUCTION OF BITUMEN AND AVAILIBILITY IN SOUTH AFRICA

Bitumen is produced from crude oil through a process known as vacuum distillation. The vacuum distillation process is illustrated in Figure A.1.

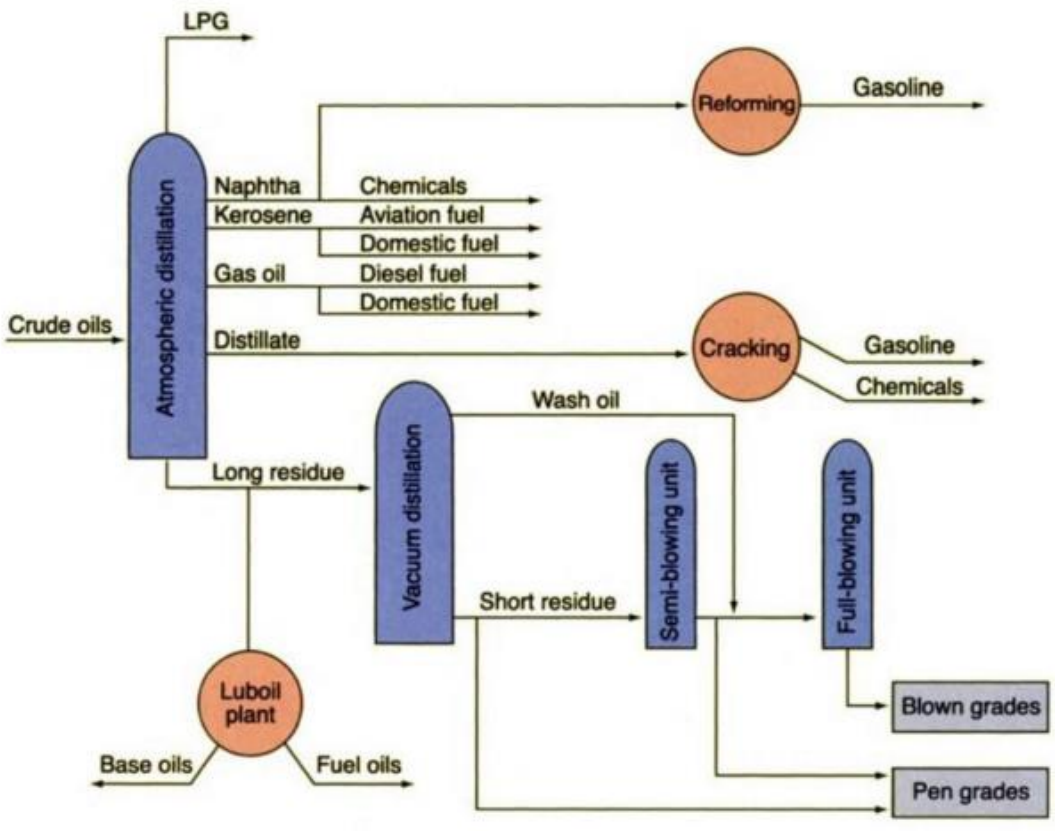

Figure A. 1 - Production of bitumen through vacuum distillation (Read & Whiteoak, 2003).

During vacuum distillation, the crude oil is pumped into a furnace that heats it up to 315°C. As the crude oil is heated, it is injected into an atmospheric tower where lower boiling point products, such as kerosene

and petroleum oil, are extracted. The heavy crude oil constituents are located at the bottom of the atmospheric tower from where it is pumped into a vacuum tower at 357 to 400°C and a pressure of 1.33 kPa to 20 kPa. The pressure maintained is dependent on the type of crude oil being processed. The crude oil residue at the bottom of the vacuum tower is bitumen and consists of Asphaltenes and Maltenes broader groups, which determines the composition and properties of the bitumen. At most refineries an air blowing tower is part of the bitumen production process as the bitumen in the vacuum tower may not have the required properties for asphalt production. Bitumen is therefore pumped into an air blowing tower to produce bitumen with the correct properties. The bitumen is extracted from the air blowing tower by selecting an appropriate residue length or cut point (Singh & Jain, 1997).

As established in the literature review, the exact composition of bitumen is difficult to determine, as it is influenced by the crude oil it is refined from. However, bitumen is divided into broader groups known as insoluble Asphaltenes and soluble Maltenes. The Maltenes broader group is further divided into resins, aromatics and saturates. It has also been established that by increasing the aromatics, saturates and resins content in the bitumen, the rheological properties such as viscosity and shear susceptibility are influenced. In the roads industry various types of bitumen products are used. These products include penetration grade bitumen, cut back bitumen, modified binders, bitumen emulsion and precoating base fluids. However in asphalt production, penetration grade bitumen and modified binders are the most common bitumen products used.

In South Africa, bitumen is produced at refineries located in Cape Town, Sasolburg and Durban. Crude oils are refined at these refineries to produce petroleum products, diesel and petrol. Only 2.5% of a barrel of crude oil represents bitumen (Greyling, 2012). The biggest user of bitumen in South Africa is the roads industry, which contributes to 70% of bitumen use in the country. However, a lack of bitumen supply in South Africa has been experienced since 2012 as local refineries are not able to produce the correct grade of bitumen for the roads industry. This is due to the aging of local refineries and unscheduled shutdowns. Local asphalt suppliers are therefore, being forced to import the required grade of bitumen from Singapore at a cost of 20% more than local supply, when no shortages are experienced.

A.2.2 PENETRATION GRADE BITUMEN AND SUPPLY IN SOUTH AFRICA

Penetration grade bitumen is refined and blended for use in road construction. It is manufactured through either vacuum distillation or blending of two base binders. In the latter case, base binders refer to two different penetration grade bitumen types. South African penetration grade bitumen specifications are

provided in SANS 4001-BT1. Table A.1 was extracted from SANS 4001-BT1 and summarizes the South African specifications for penetration grade bitumen.

Table A. 1 - SANS 4001-BT1 specification for South African penetration grade bitumen.

1	2	3	4	5	6	7
Property	**Penetration Grade**					
	10/20	**15/25**	**35/50**	**50/70**	**70/100**	**150/200**
	Requirements					
Penetration at 25°C/100g/5s, 1/10 mm	10-20	15-25	35-50	50-70	70-100	150-200
Softening point (ring and ball) °C	58-78	55-71	49-59	46-56	42-51	36-43
Minimum viscosity at 60°C, Pa.s	700	550	220	120	75	30
Viscosity at 135°C, mPa.s	≥750	≥650	270-700	220-500	150-400	120-300
Performance when subjected to the rolling thin film oven test:						
a) Mass change, % by mass fraction, max).	-	0.5	0.3	0.3	0.3	0.3
b) Viscosity at 60°C, % of original, max.	-	-	300	300	300	300
c) Softening point (ring and ball), °C, min	-	57	52	48	44	37
d) Increase in softening point, °C, max.	10	8	7	7	7	7
e) Retained penetration, % of original, min.	-	55	60	50	50	50
Spot test, % xylene, max.	-	-	30	30	30	30

The type of penetration grade bitumen selected for asphalt production is determined by two performance grade (PG) binder zones. The PG 58 zone includes provinces such as the Western Cape, Eastern Cape, most parts of KwaZulu-Natal, eastern parts of the Free State, Gauteng, parts of Limpopo and Mpumalanga. The PG 64 zone covers the remaining parts of the country, which includes the Northern Cape and North West. These zones are based on the average maximum asphalt temperature over a 7-day period. Bitumen selection for asphalt production is also determined from traffic volume categories and vehicle speed. Once

the PG binder zone, traffic volume and vehicle speed have been established, the appropriate binder to conform to these requirements is selected from SANS 4001-BT1 (Sabita Manual 35/TRH8, 2016).

The most common type of bitumen used for the production of asphalt for low volume roads is 50/70. In Cape Town, Colas is a local supplier of 50/70 penetration grade bitumen. Colas provide the following SANS 4001-BT1 specifications as shown in Table A.2, for 50/70 penetration grade bitumen before and after ageing.

Table A. 2 - 50/70 Penetration grade bitumen properties (Colas, 2013(1)).

50/70 Binder Properties	Requirements		Test Method
	Min	Max	
Before Ageing			
Penetration @ 25°C/100g/5s, 1/10 mm	50	70	EN 1426
Softening point, °C	46	56	ASTM D 36
Dynamic Viscosity @ 60°C, Pa.s	140	-	ASTM D 4402
Dynamic Viscosity @ 135°C, Pa.s	0.22	0.45	ASTM D 4402
After Ageing (RTFO)			
Mass change % m/m	-	0.3	ASTM D 2872
Softening Point, °C	-	300	ASTM D 36
Increase in softening point, °C	48	-	ASTM D 36
Retained Penetration, % of original	55	-	EN 1426
Spot Test, % xylene	-	30	AASHTO T102

A temperature-viscosity relationship is established for penetration grade bitumen, which implicates a softening gradually softens as it is heated and a hardening as it cools down. Therefore, high in-service temperatures penetration grade bitumen exhibits Newtonian fluid behaviour. The mixing temperature of 50/70 penetration grade bitumen varies from 150 to 160°C, with compaction temperatures for asphalt mixtures varying from 135 to 145°C (Colas, 2013(1)).

A.2.3 MODIFIED BINDERS AND SUPPLY IN SOUTH AFRICA

Modified binders are common to use in the production of asphalt. In the literature review it was established that the modification of bitumen may improve certain properties of the bitumen. These properties improve the durability and performance of asphalt mixtures. Modified binders are produced from a base binder and in most cases is 70/100 penetration grade bitumen. Colas in Cape Town is a supplier of modified binders and established the following SANS 4001-BT1 specification as shown in Table A.3 for 70/100 penetration grade bitumen

Table A. 3 - 70/100 Penetration grade bitumen properties (Colas, 2013(2)).

70/100 Binder Properties	Requirements		Test Method
	Min	Max	
Before Ageing			
Penetration @ 25°C/100g/5s, 1/10 mm	70	100	EN 1426
Softening point, °C	42	51	ASTM D 36
Dynamic Viscosity @ 60°C, Pa.s	75	-	ASTM D 4402
Dynamic Viscosity @ 135°C, Pa.s	0.15	0.40	ASTM D 4402
After Ageing (RTFOT)			
Mass change % m/m	-	0.3	ASTM D 2872
Softening Point, °C	-	300	ASTM D 36
Increase in softening point, °C	44	-	ASTM D 36
Retained Penetration, % of original	50	-	EN 1426
Spot Test, % xylene	-	30	AASHTO T102

Similar to 50/70 penetration grade bitumen, 70/100 also exhibits Newtonian fluid behaviour at high in-service temperatures. The mixing and compaction temperature for modified 70/100 penetration grade bitumen is dependent on the type of modifier used. The rheological properties of unmodified binders are uncomplicated to determine, however, the rheological properties of modified binders are complex. Therefore in-service performance of modified binders are difficult to determine as the rheological properties of the bitumen is not only determined by the crude oil source, but also by the type of modifier used in the modification process (Asphalt Academy-TG1, 2007).

Modified binders are classified as homogenous or non-homogenous. Homogenous binders consist of blending the bitumen and polymers to a point where the distinctive phases of the bitumen and polymers cannot be detected on a microscopic level. Therefore, the modified binder acts as a single-phase material. Examples of homogenous binders include EVA, SBR, SBS and amine modified binders. Non-homogenous binders are identified by having two distinctive and detectible material phases consisting of the bitumen and the modifier. The properties of a non-homogenous binder are dependent on the stage at which tests are performed on the modified binder. An example of a non-homogenous binder is bitumen rubber (Asphalt Academy-TG1, 2007).

In South Africa a classification system has developed for modified binders. This classification system is derived from the application of the modified binder, the type of binder, type of modifier used and the level of modification. Table A.4 summarises this modified binder classification system.

Table A. 4 - South African modified binder classification system (Asphalt Academy-TG1, 2007).

Classification System	Classification Description
Application of Modified Binder	S - Seal A - Asphalt C - Crack Sealant
Type of Binder (Letter follows after application of modified binder letter has been established.)	C - Refers to Emulsion (Cold applied) No letter is established for hot-application
Type of Modifier (Letter follows after type of binder letter has been established.)	E - Elastomer P - Plastomer R - Rubber H - Hydrocarbon
Level of Modification (Letter follows after type of modifier letter has been established.)	The level of modification is either 1 or 2 and determines the softening point of the binder. A level of modification equal to 2 produces a binder which have a higher softening point compared to a level of modification equal to 1.
Additional code (Letter follows after level of modification has been established.)	The letter "t" should be added if the binder is not permitted the use of cutter or flux.
An Example: A-E2	A - Asphalt application E - Elastomer type modifier 2 - Higher softening point than A-E1

From Table A.4 it follows that various types of modified binders are produced in South Africa which are dependent on the type of application. Table A.5 presents typical modified binder types specifically produced for used in HMA production.

Table A. 5 - Modified binders used in HMA production in South Africa (Asphalt Academy-TG1, 2007).

Modified binder type	Classification
Styrene-Butadiene-Rubber (SBR)	A-E1
Styrene-Butadiene-Styrene (SBS)	A-E2
Ethylene-Vinyl-Acetate (EVA)	A-P1
Natural Hydrocarbons	A-H1
Aliphatic Synthetic Wax	A-H2
Bitumen Rubber	A-R1

It was established from the literature review that modified binders consisting of SBS, Fisher-Tropsch (F-T) waxes, EVA and amine anti-stripping agents are of interest when it comes to the moisture susceptibility of an asphalt mixture. These modified binders are discussed in sections that follow.

A.2.3.1 Styrene-Butadiene-Styrene (SBS) modified bitumen

Styrene-Butadiene-Styrene (SBS) is a block co-polymer used for the modification of bitumen properties. SBS can be classified as a radial or linear co-polymer, however, radial block co-polymer binders achieve higher softening points and viscosity when compared to linear block co-polymer binders. The maltenes of the bitumen, which is a broader group of the bitumen composition, absorb the SBS during modification. High dosage levels of SBS, ranging from 4% to 6%, cause continuous molecular networks to form within the maltenes of the bitumen, which makes up the majority of the bitumen volume. However, low dosages of 3% to 4% cause fragmented networks to form within the maltenes of the bitumen. The continuous networks result in an increase in the viscosity and softening point of the bitumen (Asphalt Academy-TG1, 2007).

The molecular networks formed by the SBS within the bitumen are responsible for an increase in the elastic behavior of the bitumen. This property of the bitumen improves its resistance to deformation. The elastic recovery of the bitumen is proportional to the SBS content. An increase in the SBS content will result in an increase in the elastic recovery after deformation. With an increase in the elastic recovery, the cohesion strength of the asphalt mixture will also increase. Increased resistance to deformation and cohesion improves the ability of the asphalt mixture to resist crack formation (Asphalt Academy-TG1, 2007). The properties of SBS modified binders are shown in Table A.6.

Table A. 6 - Properties of SBS modified bitumen produced in South Africa (Colas, 2012(1)).

Binder Properties	AE-1 Requirements		AE-2 Requirements		Test Method
	Min	Max	Min	Max	
Before Ageing					
Softening Point, °C	55	65	65	85	MB-17
Dynamic Viscosity @ 165°C, Pa.s	-	0.6	-	0.6	MB-18
Elastic Recovery @ 15°C, %	50	-	60	-	MB-4
Flash Point, °C	230	-	230	-	ASTM D93
Stability (R&B dif @ 160°C), °C	-	5	-	5	MB-6
After Ageing (RTFOT)					
Mass change %	-	1.0	-	1.0	MB-3
Elastic Recovery @ 15°C	50	-	60	-	MB-4

The mixing temperature for SBS modified asphalt mixtures ranges from 160 to 170°C, which is higher than for unmodified asphalt mixtures. The compaction temperature for SBS modified asphalt mixtures ranges from 140 to 150°C (Colas, 2012(1)).

At low temperatures the flexibility of the SBS modified bitumen is greater than unmodified binders, which will decrease the formation and progression of cracks (Asphalt Academy-TG1, 2007). Cracks formed in the bitumen mastic cause moisture ingress and loss of adhesion at the bitumen-aggregate interface. SBS modified bitumen increases the ability of the asphalt mixture to resist cracking, therefore it can be of significance when producing a grey-water resistant asphalt mixture.

A.2.3.2 Fisher-Tropsch (F-T) waxes

F-T waxes originate from the coal gasification process and consist of long carbon iso-alkane or alkane chains. These chains consist of 40 to 100 carbon atoms and are significantly longer when compared to the 20 to 40 carbon atom waxes produced from crude oils. F-T waxes improve the flow of the bitumen by reducing the viscosity of the modified binder during mixing and compaction of HMA. This is achieved without having a negative effect on the bitumen properties at low temperatures. Reducing the viscosity improves the ability of the bitumen to completely coat the aggregate surface. The softening point of F-T wax modified binders is also increased, whereas the penetration is decreased at in-service temperatures less than 80°C. Therefore, these modified binders produce asphalt mixtures that are more susceptible to deformation at higher temperatures (Asphalt Academy-TG1, 2007). Colas in Cape Town is a supplier of F-T wax modified binders and provide the following binder properties as shown in Table A.7.

Table A. 7 - Properties of F-T wax modified binder produced in South Africa (Colas, 2012(2)).

F-T Wax Modified Binder Properties	Requirements		Test Method
	Min	Max	
Softening point, °C	70	90	ASTM D 36
Dynamic Viscosity @ 165°C, Pa.s	-	0.30	ASTM D 4402
Stability @ 160°C	-	5	MB-6
Flash point, °C	230	-	ASTM D 93
After Ageing (RTFOT)			
Difference in softening point, °C	-2	+8	ASTM D 6
Mass change, %	-	1.0	MB-3

The mixing temperature of F-T wax modified asphalt mixtures ranges from 110 to 120°C, which is lower than unmodified asphalt mixtures. The compaction temperature of F-T wax modified asphalt mixture range from 100 to 110°C (Colas, 2012(2)).

Sasobit® wax is an F-T wax modifier produced by Sasol. Sasobit® wax melts at a temperature of approximately 102^{0}C, whilst dissolving completely at 120^{0}C. In its melted state, Sasobit® wax produces a crystalline network structure within the bitumen which provides more stability. Sasobit® wax can be used as a cross-linking agent with an elastomer, such as SBS, to produce a more viscous and flexible modified binder. Sasol recommends a Sasobit® wax content of 0.8% to 3% per binder mass (Prowell & Hurley, 2005, p. 2).

Research done by Hurley and Powell (2005) included moisture sensitivity tests on asphalt mixtures with Sasobit® wax modified binder. They concluded that the use of Sasobit® wax, combined with an anti-stripping agent, improved the moisture sensitivity of asphalt mixtures produced from granite aggregates. Their research also showed that Sasobit® wax reduces the air void content of asphalt mixtures when compacted using the gyratory compactor. They also concluded that lower compaction temperatures for asphalt mixtures with Sasobit® wax modified binder were achieved. Lower indirect tensile strength (ITS) results for asphalt mixtures containing Sasobit® wax modified binder were also achieved when compared to control asphalt mixtures. Hurley and Powell (2005) also suggested that decreased ITS results might be linked to the anti-ageing properties of Sasobit® wax as observed during binder testing.

Sasobit® wax modified binder may increase the grey water resistance of an asphalt mixture by reducing the permeability of the mixture. This is due to a reduced air void content that may be achieved during compaction. The use of Sasobit® wax, in conjunction with an elastomer, may improve more than one engineering property of an asphalt mixture.

A.2.3.3 Ethylene Vinyl Acetate (EVA) modifier (Homogenous)

Ethylene-Vinyl-Acetate (EVA) modifier consists of two ethylene monomers and vinyl-acetate. EVA is a polymeric plastomer consisting of polyethylene crystalline and vinyl-acetate molecules that form amorphous chains. The polyethylene is responsible for providing the stiffness to the modified binder, whereas the crystalline produces cohesion (Asphalt Academy-TG1, 2007).

EVA improves the ability of HMA to resist permanent deformation when compared to unmodified binders. It also aims to increase the workability, which is significantly better when compared to SBS modified binders. EVA provides thermal cracking resistance at low temperatures. EVA modified binders also

improve the elastic behavior, ageing and cohesion properties of HMA. Due to its stability when heated and its slow rate of deterioration, the durability of EVA modified bitumen is better than SBS modified bitumen (Asphalt Academy-TG1, 2007). Colas in Cape Town is a supplier of EVA modified binders and provide the following binder properties as shown in Table A.8.

Table A. 8 - Properties of EVA modified binder produced in South Africa (Colas, 2012(3))

EVA Modified Binder Properties	Requirements		Test Method
	Min	Max	
Softening point, °C	63	73	ASTM D 36
Dynamic Viscosity @ 165°C, Pa.s	-	0.30	ASTM D 4402
Elastic Recovery @ 15°C, %	30	-	MB-4
Stability @ 160°C	-	5	MB-6
Flash point, °C	230	-	ASTM D 93
After Ageing (RTFOT)			
Difference in softening point, °C	-2	+8	ASTM D 6
Mass change, %	-	1.0	MB-3

The mixing temperature for EVA modified asphalt mixtures ranges from 160 to 170°C, which is greater than for unmodified asphalt mixtures. The compaction temperature for EVA modified asphalt mixtures ranges from 140 to 150°C (Colas, 2012(3)).

Increased workability is the result of a less viscous binder at mixing temperatures, which improves the ability of the bitumen to coat the aggregate surface and provides resistance to disbonding. A less viscous binder also significantly influences on the compactibility of an asphalt mixture as it acts as a lubricant during compaction. EVA modified binders have proven successful in areas subjected to fuel spillages (Asphalt Academy-TG1, 2007). This is significant as it is well known that refined oil base products, such as turpentine and diesel fuel, can easily remove bitumen stains.

EVA modified binders may offer a solution to improve the grey water resistance of asphalt mixtures. Improved compactibility of asphalt mixtures can produce an impermeable material more susceptible to moisture. Resistance to deformation reduces crack formation within the bitumen mastic, therefore improving the moisture susceptibility of an asphalt mixture.

A.2.3.4 Amine Anti-Stripping Agent

Colas in Cape Town is a supplier of amine anti-stripping modified binders. This modified binder improves bitumen-aggregate adhesion. By means of strong electrochemical bonds (Colas, 2012(4)).

The amine component has a molecular structure consisting of a polar end group and a non-polar hydrocarbon chain. The non-polar hydrocarbon chain shares similar properties as bitumen and therefore forms part of the molecular structure of the bitumen. The polar end group has a charge opposite to that of the aggregate surface, therefore producing an electrochemical bond with the aggregate surface. It also displaces any water during the formation of this bond and is also resistant to moisture ingress (Colas, 2012(4)).

Information on the properties of amine modified binders are not provided by Colas. However, anti-stripping agents significantly improve the adhesive properties of the bitumen by making asphalt mixtures more susceptible to moisture. Therefore, amine modified binders may offer a solution to improve the grey water resistance of an asphalt mixture.

A.3 AGGREGATE

In HMA production, aggregates refers to the crushed stone used during the mixing process. In dense graded asphalt mixtures the aggregate represents 95% of the asphalt mixture by mass and 85% of its volume. In the literature review it has been established that aggregates have a dominant effect on the bitumen-aggregate bond. Therefore, the adhesive properties of an asphalt mixture are significantly influenced by the selection of an appropriate aggregate. Aggregates used in HMA production are divided into three sizes namely: coarse, fine and filler material (Sabita Manual 35/TRH8, 2016).

- **Coarse Aggregates** – Coarse aggregates refer to aggregate with a particle size of greater than the 5 mm sieve. Crushed rock is an example of a coarse aggregate.
- **Fine Aggregates** – Fine aggregates refer to aggregate with a particle size of less than the 5 mm sieve and greater than the 0.075 mm sieve. This type of aggregate includes mined sand, natural sand, crushed sand and selected river gravel.
- **Filler Material** – Filler materials refer to material with a particle size of less than the 0.075 mm sieve.

A.3.1 SOURCES OF AGGREGATES

Aggregates are found in either natural, processed or manufactured forms. Natural formed aggregates, also known as natural aggregates, are mined Aeolian and glacial deposits in riverbeds and do not require any further processing to be used in the production of asphalt. Natural gravel and sand are the most common natural aggregates to be used in asphalt production. Aeolian deposits consist of rounded

particles and are beneficial as it improves the workability of an asphalt mixture. However, it compromises the ability of the asphalt mixture to resist permanent deformation (Sabita Manual 35/TRH8, 2016).

Processed aggregates are sourced by blasting in quarries, where it is also crushed and screened before use in asphalt production. The aim of these processes are aimed to achieve certain aggregate characteristics which improve the performance of asphalt mixtures. Figure A.2 illustrates a quarry operation for the mining and processing of road construction aggregates. In HMA production aggregates should be cubic and angular in shape, as then promote the adhesive bond between the bitumen and aggregate. It has been established that flat and elongated aggregate particles compromise the performance of an asphalt mixture. Therefore, processes are used to control the shape and texture of the aggregates (Sabita Manual 35/TRH8, 2016).

Figure A. 2 - Quarry operation for producing processed aggregates (SAPEM Chapter 8, 2014).

Manufactured aggregates refer to by-products from industrial processes such as steel making or reclaimed asphalt. Slag aggregates are produce as a by-product of the steel making process and are used in the production of asphalt with improved stripping resistance of asphalt mixture by aiding binder coating. These produces a durable asphalt mixture especially in high moisture regions. Figure A.3 illustrates steel slag in its molten form being dumped to cool down. After cooling, the steel slag is crushed and screened to produce slag aggregates. Slag aggregates have high levels of absorption, therefore the binder content of an asphalt mixture consisting of these aggregates is usually increased to prevent partial coating of aggregates.

Figure A. 3 - Steel slag being dumped to cool.

Reclaimed asphalt is a manufactured aggregate that is milled from existing roads for stockpiling and re-use later in road construction. However, in its stockpiled form care must be taken during grading sampling

due to segregation of stockpile materials being common to occur. The TRH 21 (2009) manual provides guidelines for processing reclaimed asphalt (Sabita Manual 35/TRH8, 2016).

A.3.2 AGGREGATES USED IN HMA PRODUCTION IN SOUTH AFRICA

The availability of aggregates is an important consideration during the design process of HMA mixtures. In South Africa various types of aggregates are used in the production of asphalt, however the availability of aggregates is dependent on the location. Table A.9 represents the type of aggregates in relation to its availability in South Africa.

Table A. 9 - Type of aggregate in relation to availability in South Africa as adapted from Sabita Manual (2014).

Aggregate types	Province in South Africa								
	Western Cape	Northern Cape	Eastern Cape	Free State	North West	Gauteng	KwaZulu-Natal	Mpumalanga	Limpopo
Andesite					•	•			
Dolerite		•	•	•		•	•	•	
Granite		•				•	•	•	•
Hornfels	•								
Norite					•			•	•
Quartzite	•		•		•	•	•		
Tillite		•					•		

A.3.3 FILLER MATERIAL

Filler material is used in the production of HMA to produce dense asphalt mixtures with improved cohesion and moisture susceptibility. As established in the literature review, filler material is categorised as inert or active fillers. However, active fillers have shown to have the most significant influence on the moisture susceptibility of an asphalt mixture. In HMA production filler material serves the purpose of stiffening the bitumen mastic, which in turn controls the stability of the asphalt. Filler material also serves as void-filling material, which can be used for adjusting the volumetric properties and the grading of an asphalt mixture. Table A.10 shows active and inert filler materials availability in South Africa and their associated characteristics.

Table A. 10 – Active and inert filler material availability in South Africa (Sabita Manual 35/TRH8, 2016).

Type of Active Filler	Characteristics of Active Filler
Hydrate Lime (Active Filler)	• Improves adhesive properties of an asphalt mixture. • Reduce hardening of bitumen through oxidation, therefore improve the durability of an asphalt mixture. • Lime has a high surface area and low bulk density, therefore it stiffens the bitumen mastic (Stiffness should be controlled as compactibility problems may be experienced.) • Relatively expensive.
Portland Cement (Active Filler)	• Relatively expensive. • Stiffens the asphalt mixture, due to high surface area. (Stiffness of mixture should be controlled as compactibility problems may be experienced).
Baghouse Fines (Inert Filler)	• Variability in the characteristics of baghouse fines are common. • Some sources may affect the durability of asphalt mixtures. • Not suitable for asphalt mixtures with sensitive binder contents.
Limestone Dust (Inert Filler)	• Manufacture in a controlled environment therefore it conform to a specific grading requirement. • Cost effective. • Inert filler; however, the pH-value of limestone dust reduces the moisture susceptibility of an asphalt mixture.
Fly Ash (Non-active Filler)	• Variability in the characteristics of fly ash are common. • Relatively expensive. • Low bulk density.

A.4 SUMMARY

In this Appendix the material components in the production of HMA were discussed. In addition, the following aspects were also highlighted: the benefits of using modified binders, the identification of binder modifiers suitable for improving the grey water susceptibility of asphalt mixtures and factors related to the sourcing of aggregates and filler material.

APPENDIX B – EQUIPMENT AND TEST METHODS

B.1 INTRODUCTION

In Appendix B the equipment and test methods applicable to this research are discussed. The discussion focuses on the properties of the applicable equipment, whilst Standard test protocols and methods are not presented in detail.

B.2 COMPACTION AND VOLUMETRIC PROPERTIES

B.2.1 GYRATORY COMPACTOR

The gyratory compactor was developed for the Superpave mix design method and to replace the aging Marshall hammer. Figure B.1 illustrates the gyratory compactor used for compacting asphalt briquettes. During compaction the asphalt mixture is placed in a preheated mould and compacted by applying a 600 kPa vertical pressure while the mould rotates at a tilted angle. The mould rotates at 30 rpm and is tilted at a specified angle of 1.25°. This tilted rotational action is also referred to as a kneading action which simulates the action of field rollers (Douries, 2004).

Figure B. 1 - Gyratory compactor and mould.

Prior to compaction, the on board computer of the gyratory compactor requires the bulk relative density of the asphalt mixture. During compaction the densification of an asphalt mixture is measured by recording the briquette height after each gyration. Using the bulk relative density and recorded briquette heights, the change in density ($\%G_{mm}$) is calculated against the number of gyrations. This calculation provides an indication of the compactibility of the asphalt mixture (Douries, 2004).

The Superpave mix design method established three levels of compaction for the gyratory compactor. These levels determine the number of gyrations required to simulate the compaction of an asphalt mixture at a specific time during its design life. The three levels of compaction are as follow (Douries, 2004):

- **$N_{Initial}$ –** The number of gyrations required to simulate the compaction of an asphalt mixture during field rolling. Superpave specifies that the VIM content of an asphalt mixture should be at least 11% after $N_{Initial}$ number of gyrations.
- **N_{Design} –** The number of gyrations required to simulate the compaction of an asphalt mixture at the end of its design life. The design life is determined from the expected amount of traffic. The Superpave criteria specifies that the VIM content should be equal to 4% after N_{Design} number of gyrations.
- **N_{Max} –** The number of gyrations required to simulate the compaction of an asphalt mixture during extreme stress conditions. Superpave criteria specifies that the VIM content should not be less than 2% after N_{Max} number of gyrations.

The Marshall hammer is still the most common compaction method used in South Africa. However, it has been established that the gyratory compactor simulates field compaction more realistically, due to its kneading action applied during compaction.

B.2.2 VOLUMETRIC PROPERTIES

The volumetric properties applicable to this research are shown in Table B.1. The standard test methods for determining the density and volumetric parameters used in the volumetric analysis of an asphalt mixture are also shown.

Table B. 1 - Volumetric properties applicable to research.

Symbol or Calculation	Description	Test method
MVD	Max theoretical relative density (kg/m^3)	SANS 3001-AS11
BD_{Mix}	Bulk relative density (kg/m^3)	SANS 3001-AS10
BD_A	Bulk relative density of total aggregate (kg/m^3)	SANS 3001-AG20 SANS 3001-AG21
M_B	Mass of binder in the mixture (g)	SANS 3001-AS11
M_A	Mass of aggregate in mixture (g)	SANS 3001-AS11
$\boldsymbol{P_B} = 100 \times \left(\frac{M_B}{M_A + M_B}\right)$	Percentage binder in mixture (%)	-
$\boldsymbol{VIM} = \frac{(MVD - BD_{Mix})}{MVD} \times 100$	Voids in the Mix (%)	-
$\boldsymbol{VMA} = 100 - \frac{(100 - P_B) \times MVD}{BD_A}$	Voids in Mineral Aggregate (%)	-
$\boldsymbol{V_{BEF}} = VMA - VIM$	Volume of effective binder (%)	-
$\boldsymbol{VFB} = 100 \times \left(\frac{V_{BEF}}{VMA}\right)$	Voids filled with binder (%)	-

Table B.1 shows only the most important volumetric properties which determine whether the asphalt mixture conforms to specification. A detailed list of how to determine all density and volume parameters for the volumetric analysis is presented in Sabita Manual (2014).

B.3 MOISTURE INDUCING SIMULATING TEST (MIST)

The University of Stellenbosch developed a MIST device to simulate field pulsing conditions caused by repeated traffic loads. The MIST device was originally developed to evaluate the effect of pulsing conditions on the moisture susceptibility of BSMs. However, Jenkins and Twagira (2009) suggested that a similar test procedure may be used to evaluate the moisture susceptibility of HMA and cement treated materials (CTM). Ultimately the MIST device can be used to condition asphalt briquettes on a laboratory scale as if they were subjected to pore pressures induced by traffic loads. The test procedure includes saturating a material specimen in a tri-axial pressure cell while moisture is being pulsed into the specimen. After MIST conditioning the material specimen is subjected to loading using a materials testing system (MTS). The results from the MTS are used to evaluate the moisture susceptibility of the material (Jenkins & Twagira, 2009). The MIST device setup is illustrated in Figure B.2.

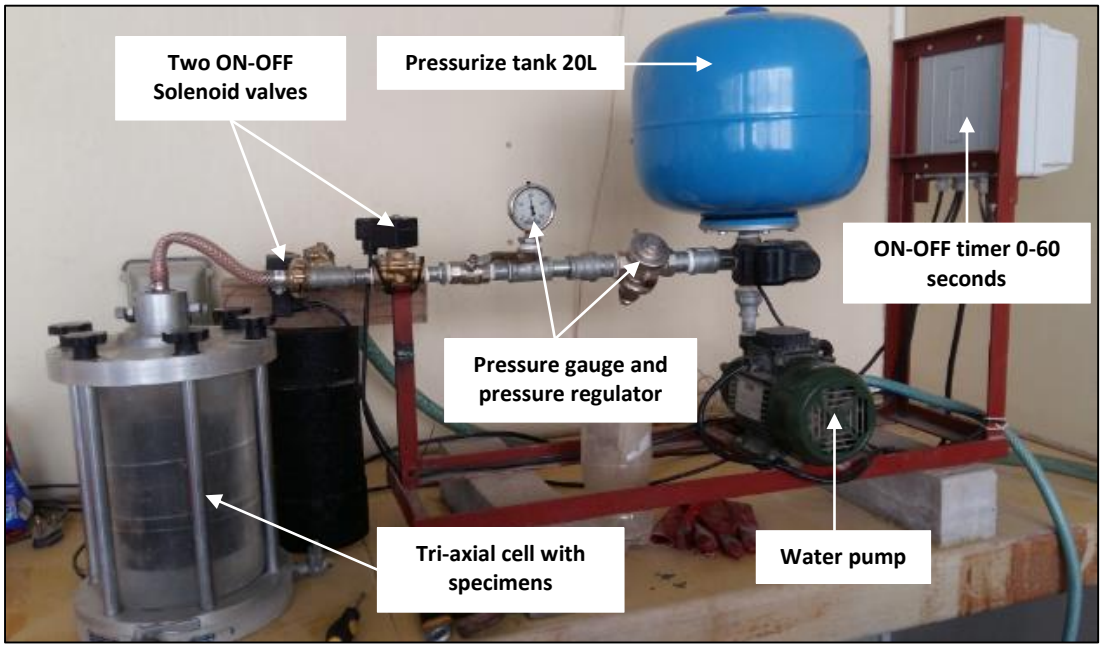

Figure B. 2 - MIST device setup adapted from Jenkins and Twagira (2009).

Material specimens are sealed in the tri-axial cell by fixing the six screws at the top of the cell. Once the cell is sealed, the water pump is switched on to pressurize the 20 litre tank. The pulsing water pressure in the tri-axle cell is set to 140 kPa and is regulated with the pressure gauge and pressure regulator. The

pressure magnitude selected is based on a study done in New Zealand (2005), which indicated that the hydraulic pressure created by vehicles traveling at 80 km/h on a sealed surface has a magnitude of 140 kPa. The ON-OFF timer is set to open the first solenoid valve for 0.54 seconds to pressurize the tri-axial cell with the second valve remaining closed. After 0.54 seconds the first solenoid valve closes and the second valve opens for 1.40 seconds to relieve the pressure in the tri-axial cell (Jenkins & Twagira, 2009).

B.4 ACCELERATED PAVEMENT TESTING (APT)

Third-scale mobile model load simulator (MMLS) tests can done in laboratory on nine asphalt briquettes installed in a test bed. The MMLS3 is used to evaluate the resistance to permanent deformation and moisture susceptibility of asphalt mixtures. Environmental conditions can be simulated by using the supplementary items, such as the water heating unit (WHU) and dry heating unit (DHU), which are part of the MLS-system. In the following sections the capabilities of the MMLS3 are discussed as well as calibration of the machine. A brief discussion on the test bed, WHU and DHU are also presented.

B.4.1 MMLS3 CAPABILITIES

The MMLS3 consists of four single wheels, each with a diameter of 300 mm and a width of 80 mm. These wheels are fixed to a bogie system and can produce a total of 7200 real load repetitions per hour at a maximum speed of 2.5 m/s. The MMLS3 is controlled from a box equipped with a motor controller to adjust the trafficking speed and two wheel load counters for the number of load repetitions. The tyre pressure of the four single wheels is usually set to 700 kPa. However, tests have been performed with tyre pressures of up to 850 kPa. The wheel load can range from 1.9 kN to 2.7 kN depending on the test requirements. The MMLS3 is capable of lateral wandering which is not used during the test bed setup (MMLS3 Operator's Manual, 2012).

B.4.2 MMLS3 CALIBRATION - SETTING THE WHEEL LOAD

The tyre pressure of the four wheels of the MMLS3 must be inflated to the correct pressure before calibration of the wheel load is done. Milne (2004) explained that the MMLS3 produces a wheel contact area which is one ninth ($\frac{1}{3} \times \frac{1}{3} = \frac{1}{9}$) of the contact area produced by an E80 tyre. Therefore, the wheel load and contact area of the MMLS3 translates to an approximate scale factor of 1 to 9 with the tyre pressure translating to a 1:1 scale factor. The wheel load of the MMLS3 is set to 2.1 kN as this load magnitude represents the load transferred to the pavement structure by a single wheel of a dual wheel configuration on an standard equivalent 80 kN axle.

The wheel load of the MMLS3 is controlled by an intricate bogie system consisting of the wheel, two rubber stoppers and adjustable suspension springs. The MMLS3 consists of a four bogie system as illustrated in Figure B.3. The suspension springs are calibrated to produce the correct wheel load. Calibration of the bogie springs are done using a calibration unit provided with the MLS-system.

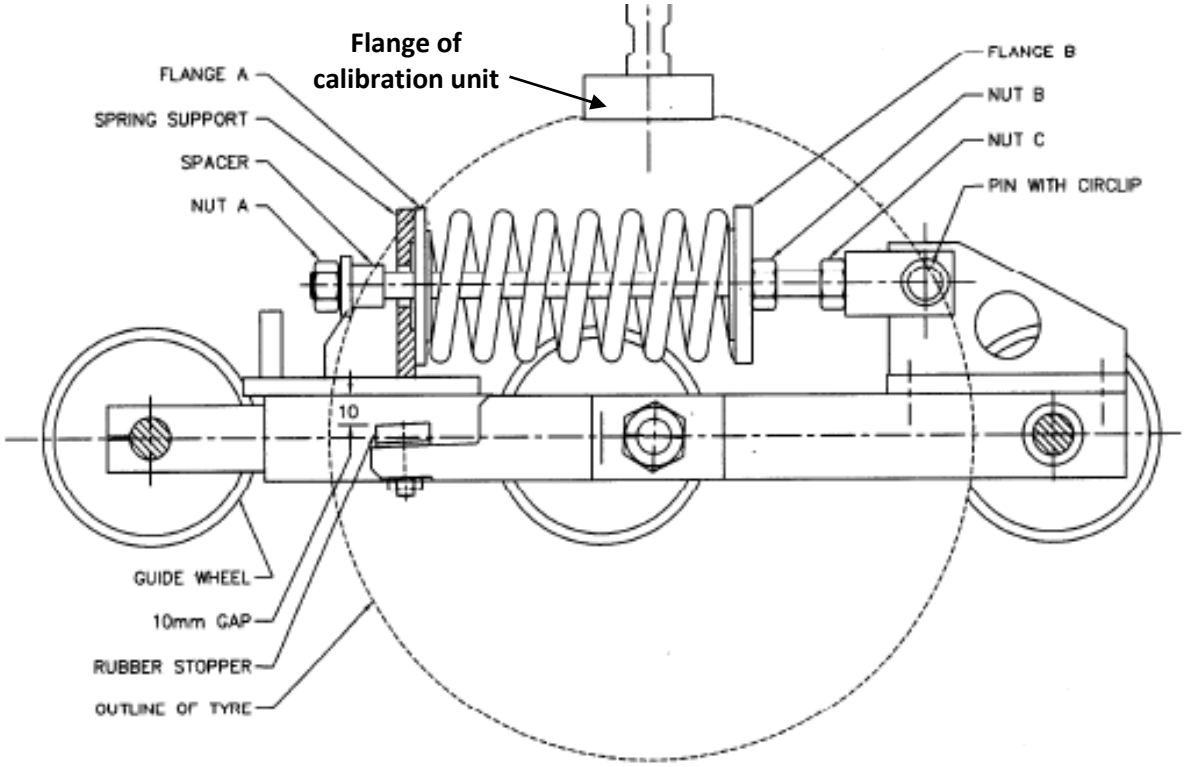

Figure B. 3 - MMLS3 bogie system (MMLS3 Operator's Manual, 2012).

Figure B.3 also illustrates the calibration unit fixed with two bolts to the channel beam on top of the MMLS3,. Calibration is done by moving each bogie system so that the wheel is directly below the flange of the calibration unit. The bogie system must be fixed with a clamp to prevent it from moving while the crank of the calibration unit is turned and the flange moves down. A pressure is exerted on the bogie system as the flange moves down. This causes the rubber stopper to move away from the frame of the bogie system. The crank of the calibration unit should be turned until the gap between the bogie frame and rubber stopper is 10 mm. A digital screen on the calibration unit displays the magnitude of the load exerted on the wheel. The suspension springs must be adjusted if the wheel load is less or greater than 2.1 kN for a 10 mm gap between the bogie frame and rubber stopper.

If the wheel load is less than 2.1 kN, it can be increased by compressing the suspension springs. This is achieved by loosening locknut B as well as using a spacer and locknut A as illustrated in Figure B.3. Locknut A is tightened and the suspension spring is lifted out of place. Rotating the suspension spring in a clockwise

direction will compress it. A similar procedure is followed if the wheel load be greater than 2.1 kN as discussed. However, the suspension spring must be loosened by rotating it counter-clockwise. Once this process is completed the length of the suspension springs must be measured. The length of the suspension springs may at most differ by 2 mm. After the length of the suspension springs is measured the wheel load must be tested with the calibration unit. This process is repeated for all bogie systems until the correct wheel load is achieved and corresponds to a 10 mm gap between the bogie frame and the rubber stopper (Abrahams, 2015).

The MMLS3 must be placed on the test bed and levelled by adjusting the four legs of the machine. It is important that the machine is placed correctly on the test bed as load transfer is dependent thereof. When the wheel is on the material surface to be tested, the gap between the bogie frame and rubber stopper must be 10 mm. If this is not the case, the legs of the machine must be adjusted until a 10 mm gap is achieved.

B.4.3 TEST BED, WATER HEATING UNIT (WHU) AND DRY HEATING UNIT (DHU)

The test bed forms part of the MLS-system and provides space for nine 150 mm diameter machined asphalt briquettes or field cores to be trafficked under wet or dry conditions with the MMLS3. By using a dual blade saw the samples are machined to specific dimensions as illustrated in Figure B.4. The distance of between the blades of the saw is 105 mm to ensure a perfect fit in the test bed. The asphalt briquettes or field cores are fixed to the test bed with a clamping system. Only samples with a thickness between 25 mm and 100 mm can be tested in the test bed. The test bed is installed inside a water bath with an inlet, an outlet and a drain valve as illustrated in Figure B.5. The water bath is used during wet tests. The test bed and water bath is bolted to the floor to prevent it from moving during trafficking (MMLS3 Operator's Manual, 2012).

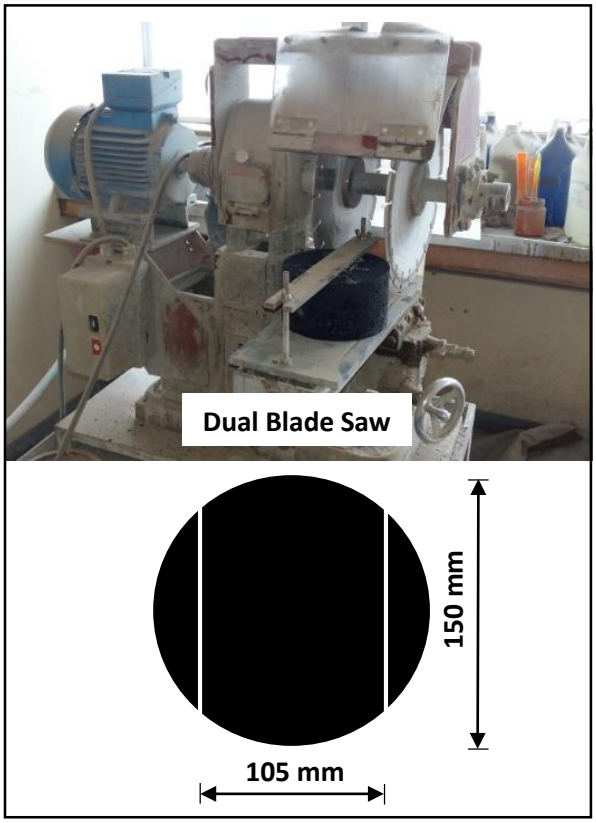

Figure B. 4 - Dimension requirements for specimens to fit in test bed.

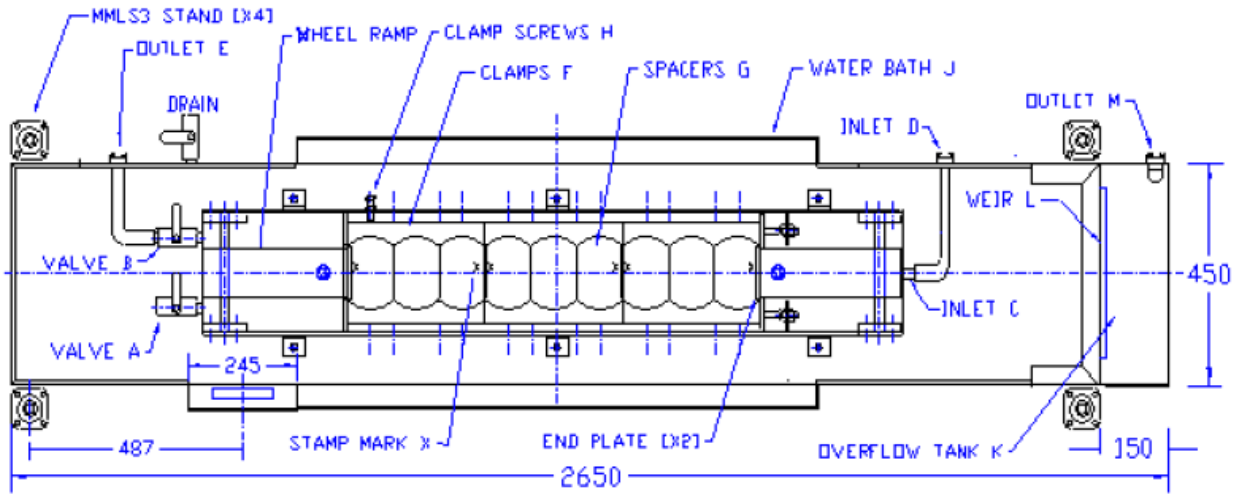

Figure B. 6 - Schematics of the test bed and water bath (MMLS3 Supplementary Items, 2011).

The water heating unit (WHU) is used to circulate heated water in the water bath during trafficking. The unit consists of a control box, storage tank, geyser tank, pump and control valves as illustrated in Figure B.6. The control box consists of an automatic temperature control unit and switches to control the heating elements. The WHU can achieve a maximum temperature of 90°C. A safety mechanism switches the WHU off, when the water reaches a temperature of greater than 90°C. During wet tests the WHU is connected to inlet D, as illustrated in Figure B.5, to feed heated water through the test bed. Water exits the test bed at valves A and B into the water bath. A pipe from outlet M is connected to the pump of the WHU to extract water from the water bath. The water is pumped to the geyser tank where it is reheated and fed to inlet D. The control valves (see Figure B.6) of the WHU are used to maintain a steady water flow rate from the WHU to the test bed. The flow rate is considered steady if the pump of the WHU extracts water fast enough from the over flow tank of the water bath (see Figure B.6) to maintain a 1 to 2 mm thick water film is maintained on the surface of the briquettes. The temperature of the asphalt briquettes

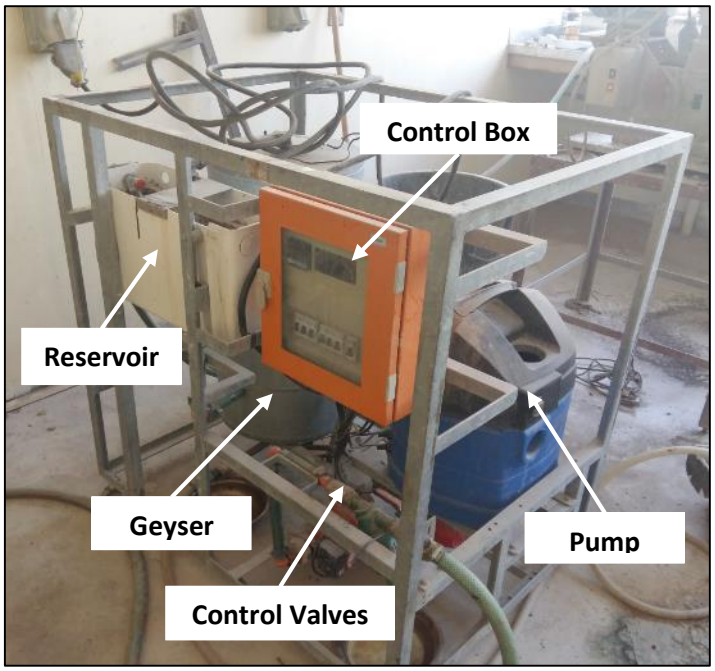

Figure B. 5 - Water heating unit (WHU).

or field cores is monitored by a thermocouple installed between positions 3 and 4 of the test bed. The thermocouple is connected to the temperature control unit, which displays the temperature of the briquettes or field cores during trafficking (MMLS3 Supplementary Items, 2011).

The dry heating unit (DHU) is used to heat the surface of the asphalt briquettes or field cores in the test bed during dry testing. The DHU consists of a control panel, two way air valve, heat exchange box and a blower fan. The control panel consist of an automatic temperature control unit and switches to regulate the heater and blower fan. During dry testing the MMLS3 is placed onto the test bed and covered with a canvas blanket. The blanket helps to keep the surface temperature of the asphalt briquettes constant during trafficking (MMLS3 Supplementary Items, 2011). Heated air produced by the DHU is blown by the blower fan into ventilation pipes to the 'spreader boxes'. The 'spreader box' distributes the heated air evenly over the surface of the briquettes. The two way air valve in the DHU changes the direction of air flow during trafficking. During trafficking the temperature of the briquettes is monitored by the thermocouple installed between briquettes 3 and 4. The thermocouple is connected to the temperature control unit, on the control panel of the DHU. Once the required surface temperature is measured by the thermocouple, the temperature control unit regulates the heaters of the DHU by on- and off-switches to maintain a constant temperature.

B.5 INDIRECT TENSILE STRENGTH (ITS) TESTING

The indirect tensile strength (ITS) test was developed to estimate the potential rutting and cracking performance of asphalt mixtures. It is also used to evaluate the moisture susceptibility of asphalt mixtures to determine the potential moisture damage in the field. The ITS test device consists of electronic load cell and loading device which is fitted into the test chamber of a materials testing system (MTS) (ASTM International, 2012).

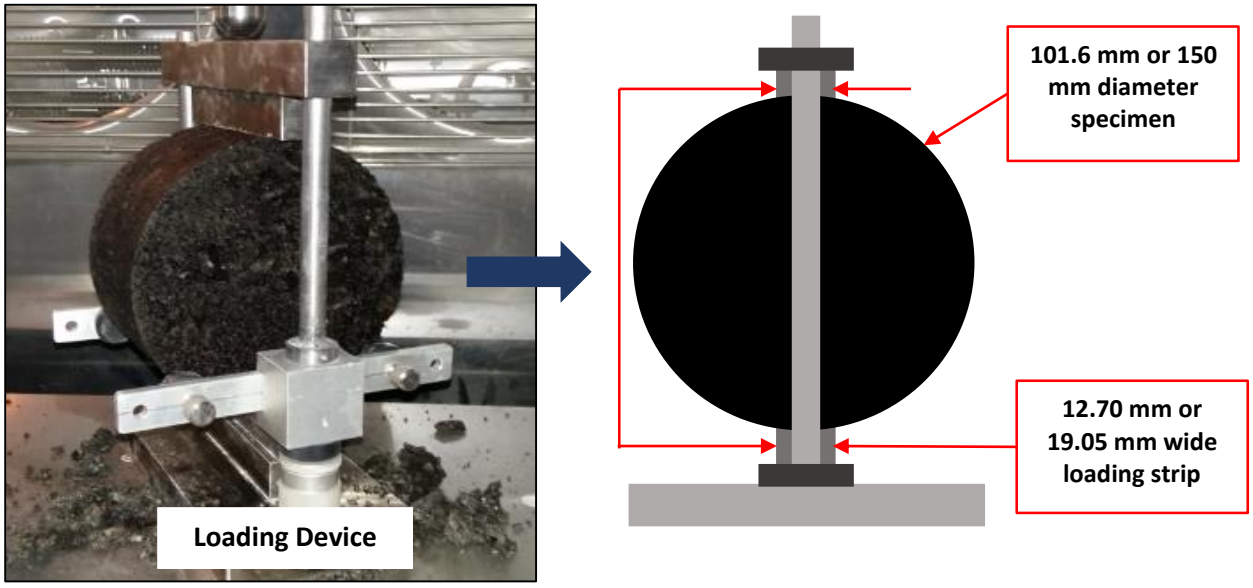

Figure B. 7 - ITS loading device.

An electronic load cell, fixed to a hydraulic or mechanical motor, applies a vertical compressive load at a controlled rate of deformation to the loading device. The loading device is fitted with loading strips to accommodate the material specimen during testing as illustrated in Figure B.7.

The load applied to and the deformation of the material specimen is constantly measured during the test. The loading strips have a concave shape with a radius equal to the nominal radius of the material specimen. Two material specimen sizes have been established for the ITS test as illustrated in Figure B.8. A material specimen with a nominal diameter equal to 101.6 mm has a minimum height requirement of 50.8 mm, whilst, a material specimen with a nominal diameter equal to 150 mm has a minimum height requirement of 75 mm. The loading strips must be 12.70 mm wide when testing a material specimen with a nominal diameter equal to 101.6 mm. When testing a material specimen with a nominal diameter equal to 150 mm, the loading strips should be 19.05 mm wide (ASTM International, 2012).

When the moisture susceptibility of asphalt mixtures is investigated, six 150 mm diameter asphalt briquettes from the same asphalt mixture are prepared. The asphalt briquettes are separated into two groups of three. One group of asphalt briquettes receives moisture-conditioning while the other is left unconditioned. After conditioning the indirect tensile strength of unconditioned and moisture-conditioned asphalt briquettes is measured using the ITS test device. Prior to testing the test temperature and displacement rate is set. ITS tests can be conducted at various temperatures and displacement rate. However, a test temperature of 25^{o}C and a loading rate of 50.8 mm/min is recommended (ASTM

International, 2012). During testing the maximum load that each asphalt briquette resists before failure is determined by the ITS test device and is recorded. Equation B.1 is then used to determine the indirect tensile strength of each asphalt briquette.

$$ITS = \frac{2 \times P}{\pi \times t \times D} \qquad \textit{Equation B.1}$$

where: *ITS* = *Indirect Tensile Strength (MPa)*

P = *Maximum applied load (N)*

t = *Thickness of specimen (mm)*

D = *Nominal diameter of specimen (mm)*

The ITS test results are used to calculate a tensile strength ratio (TSR), which is a ratio of the average indirect tensile strength of the unconditioned asphalt briquettes divided by the average indirect tensile strength of the conditioned asphalt briquettes. AASHTO method T283 suggests that a TSR of 80% is required for the asphalt mixture to satisfy moisture susceptibility specification.

B.6 SUMMARY

In this Appendix the test methods related to this study were identified and discussed. This Appendix also focused on the capabilities of equipment identified for executing test procedures, the operation of these equipment and the extraction of results.

APPENDIX C – CREATING THE FINITE ELEMENT MODEL

C.1 CREATING FINITE ELEMENT MODELS

In this Appendix the compilation of the finite element models in Abaqus/CAE according to the test matrix as presented in Table 6.2 of *Chapter 6*, is discussed. The Abaqus/CAE modules that are presented in the following Sections were required to complete the objectives of this study. As Abaqus/CAE does not have a fixed unit system a decision was taken to use SI units (kg, m, N, Pa) for setting up the finite element.

C.1.1 PART MODULE

From the 'Model Tree' in Abaqus/CAE's main window, the 'Parts' module was selected to create a part as illustrated in Figure C.1. A dialog box containing the properties of the part was used to assign a name, the modelling space, part type, base feature and approximate size of the part drawing area. The settings as illustrated in Figure C.1 were selected to create a part representing a quarter of a 150 mm diameter asphalt briquette.

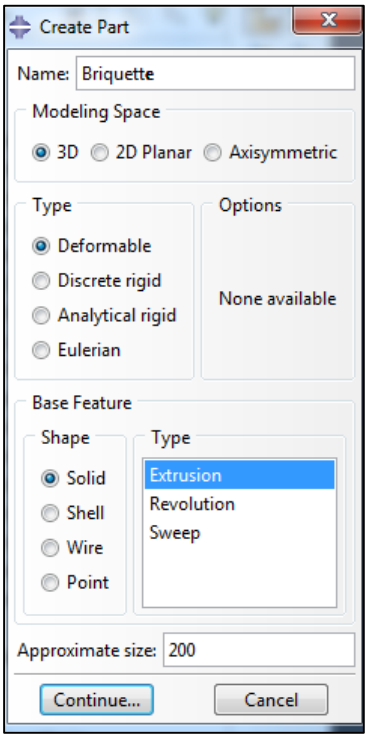

Figure C. 1 - Create as part.

As only a quarter of an asphalt briquette was subjected to finite element analysis, symmetric boundary conditions were used to account for the remaining three quarters of the asphalt briquette. This approach provided a method for analysis and visualisation of results. Using drawing tools, the quarter asphalt briquette part was created for each test combination using the dimensions presented in Table 6.2. Figure

C.2 illustrate drawings of the normal and the 19 mm shaped asphalt briquette parts in Abaqus/CAE. After completing drawings of the parts, the 'Done' option was selected in the 'Prompt Area' of the main window. Once the 'Done' option was selected Abaqus/CAE requested the depth of the part as illustrated in Figure C.2. A depth of 80 mm was selected, as this depth represents the actual height of asphalt briquettes prepared for this study.

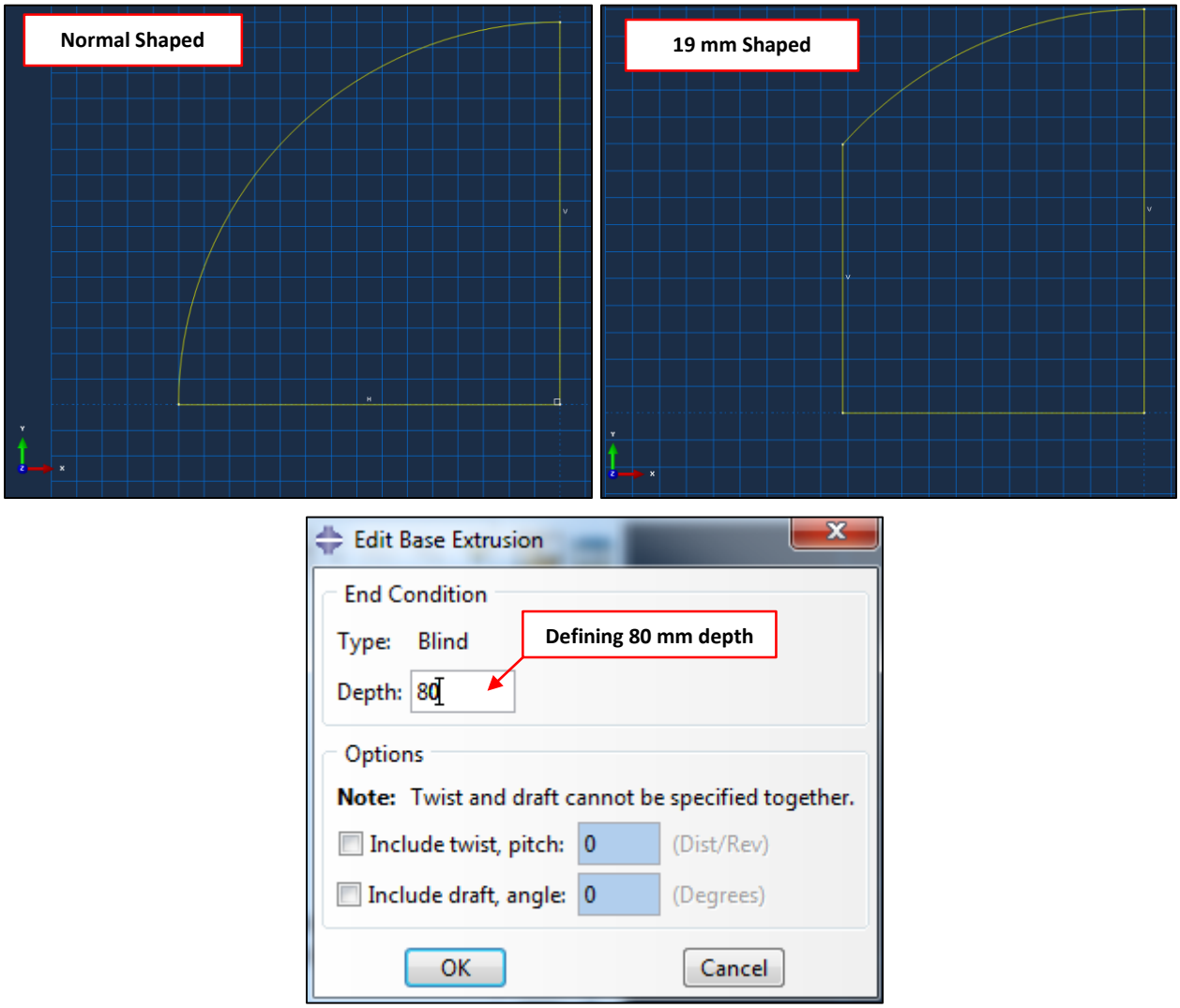

Figure C. 2 - Drawings of normal and 19 mm shaping of asphalt briquette parts.

In addition, it was required to apply a partition on the top face of the asphalt briquette for the pressure load applied by the loading ram of the MTS. The partition was created by selecting 'Create Partition' in the 'Toolbox Area' of the 'Part' module. A screen appeared as presented in Figure C.3, where the user was required to define the type and method of partitioning. The inputs as shown in Figure C.3 was used. Once

the inputs were defined, the area to be partitioned was selected and the 'Done' option selected in the 'Prompt Area', as illustrated in Figure C.3.

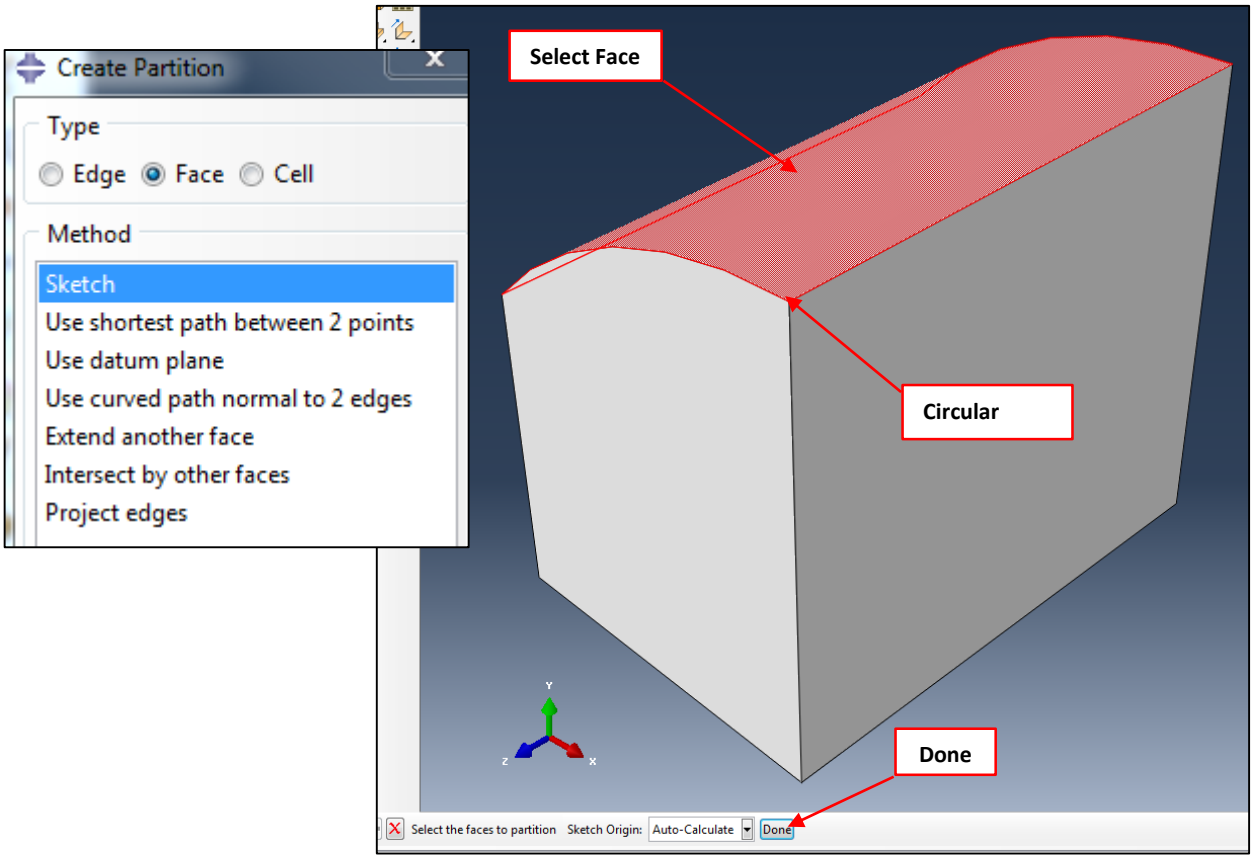

Figure C. 3 - Creating a partition.

Additional actions required the users attention after the 'Done' option was selected. Once the front face of the asphalt briquette was selected, the following question appeared: "How do you want to specify the projection distance?". The 'Through All' option was selected followed by a statement: "Arrows shows the projection direction" and selection of the 'Ok' option. There after the circular edge of the part was selected to create a partition.

Once the circular edge was selected, the asphalt briquette opened in a drawing area illustrated in Figure C.4, where the partition was drawn. The width of the partition was 9.525 mm, which represented half the width of the loading strip required for ITS testing of a 150 mm diameter asphalt briquettes, in according with ASTM method D4123-82.

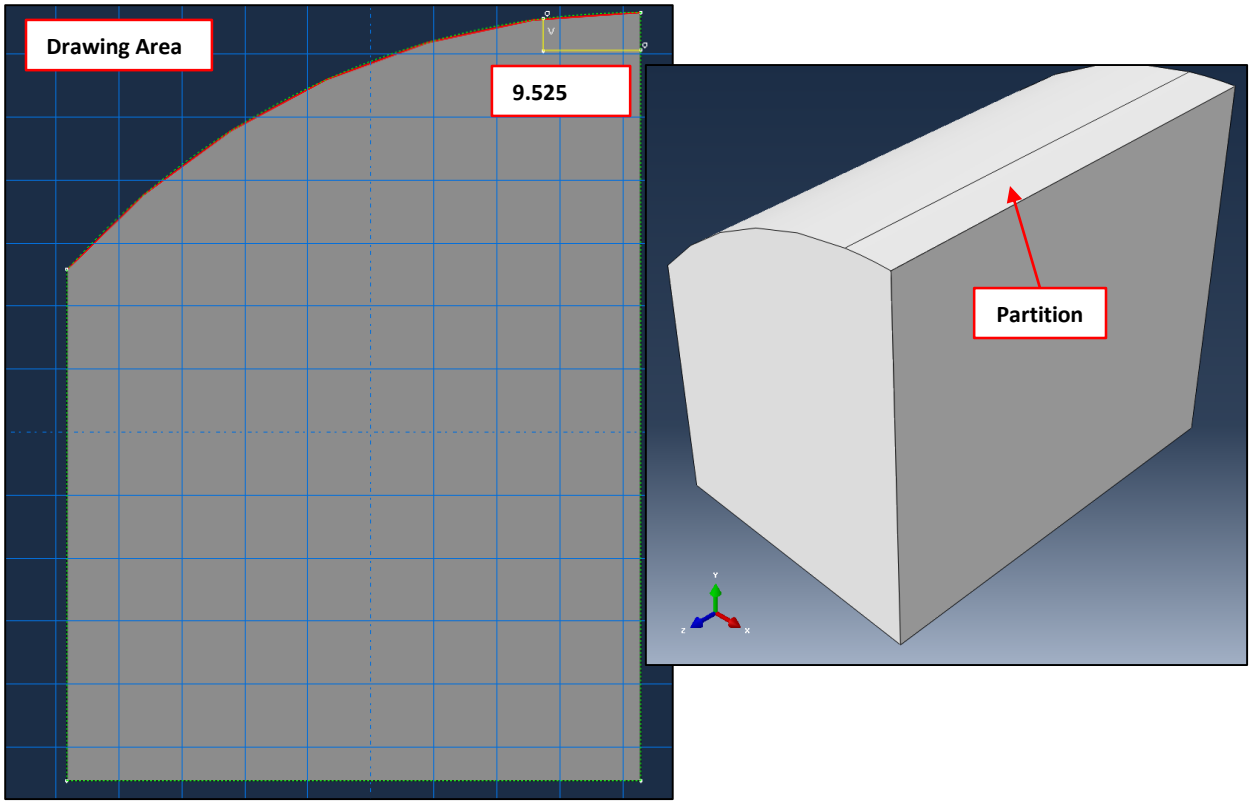

Figure C. 4 - Drawing partition.

C.1.2 PROPERTY MODULE

Under the 'Property' module in the 'Model Tree' asphalt material properties were created and assigned to the quarter asphalt briquette as created in the Part module. The asphalt material properties required input values for density, Young's modulus and the Poisson's ratio, as only linear elastic material behaviour was assumed. A density of 2 486 kg/m^3 was used as this value represented the maximum theoretical density of a 50/70 penetration grade binder combination. Various Young's modulus values, as presented in Table 6.2, were used in setting up the material properties. A Poisson's ratio of 0.4 was assumed for asphalt in accordance with SAPEM Chapter 2. Figure C.5 illustrates the steps taken to create asphalt material properties.

After creating the material properties, these properties were assigned to the quarter asphalt briquette by creating a material section. 'Create Section' was selected in the 'Toolbox Area' of the property module. The section properties were defined and selected as shown in Figure C.5. It must be note that the 'Plane stress/strain thickness' option was ticked and a thickness of 80 mm entered. The created section was next assigned to the asphalt briquette part by selecting 'Assign Section' in the 'Toolbox Area' under the 'Property' module.

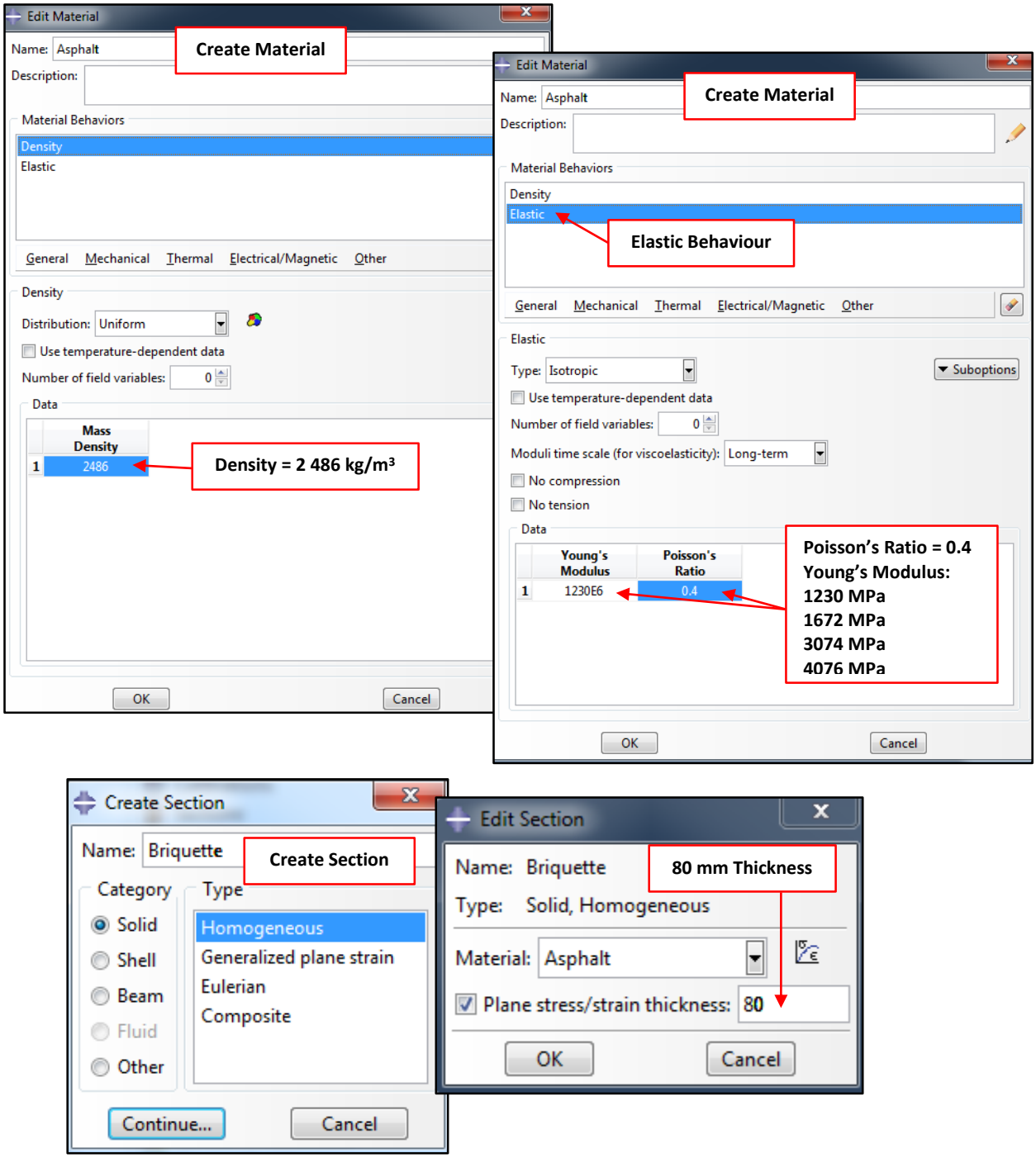

Figure C. 5 - Creating asphalt material and section properties.

C.1.3 ASSEMBLY MODULE

The 'Assembly' module was used to assemble the quarter asphalt briquette part created in the 'Part' module. Assembly was accomplished by selecting 'Instance Part' in the 'Toolbox Area' under the

'Assembly' module. An 'Instance Type' was required where the 'Dependent (mesh on part)' option was chosen and 'Ok' selected as illustrated in Figure C.6.

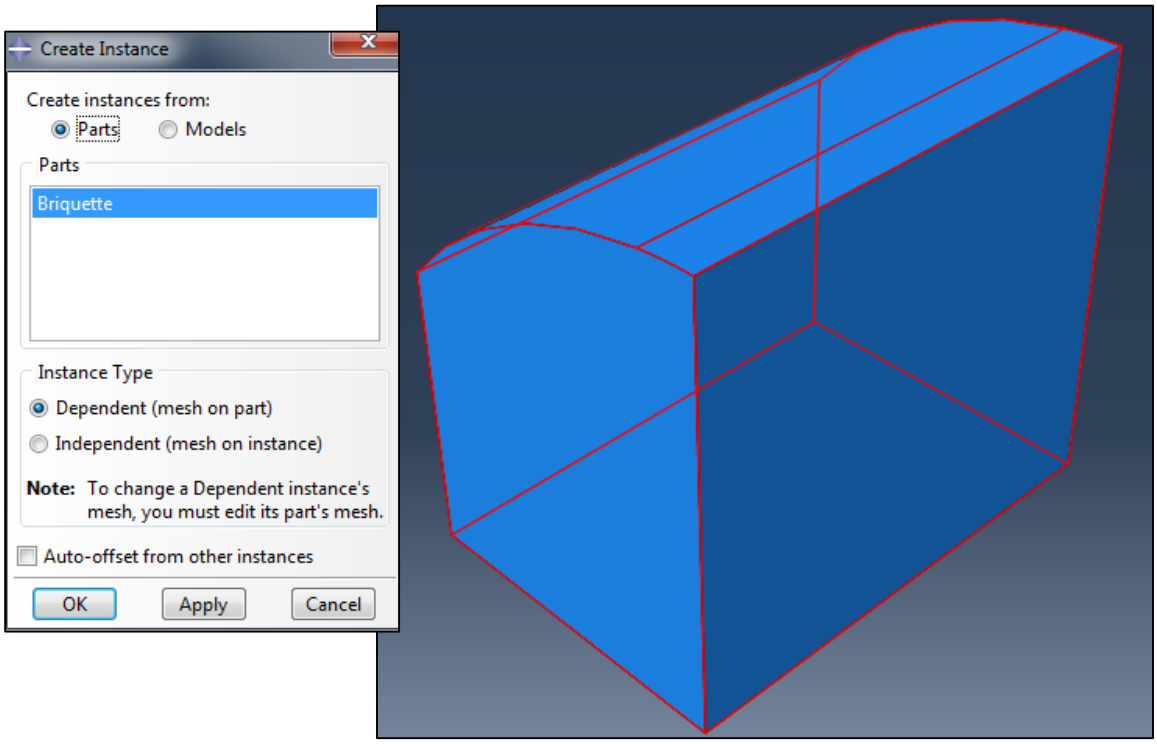

Figure C. 6 - Assemble part.

C.1.4 STEP MODULE

The 'Step' module provided the user with the ability to create the type of analysis required for the finite element analysis. It was required to create individual steps for the boundary conditions and loads applied to the assembled part. By default a step is created by Abaqus/CAE with the name 'Initial'. This step was used to apply boundary conditions to the assembled part. An additional step was created to accommodate the load applied to the assembled part. In the 'Toolbox Area' of the 'Step' module, 'Create Step' was selected and a dialog as presented in Figure C.7 appeared.

The 'Create Step' screen required from the user to define the input values of the new step to be created. The inputs as shown in Figure C.7 were selected. The 'Static, General' procedure was selected as the finite element analysis only considered linear elastic material behaviour.

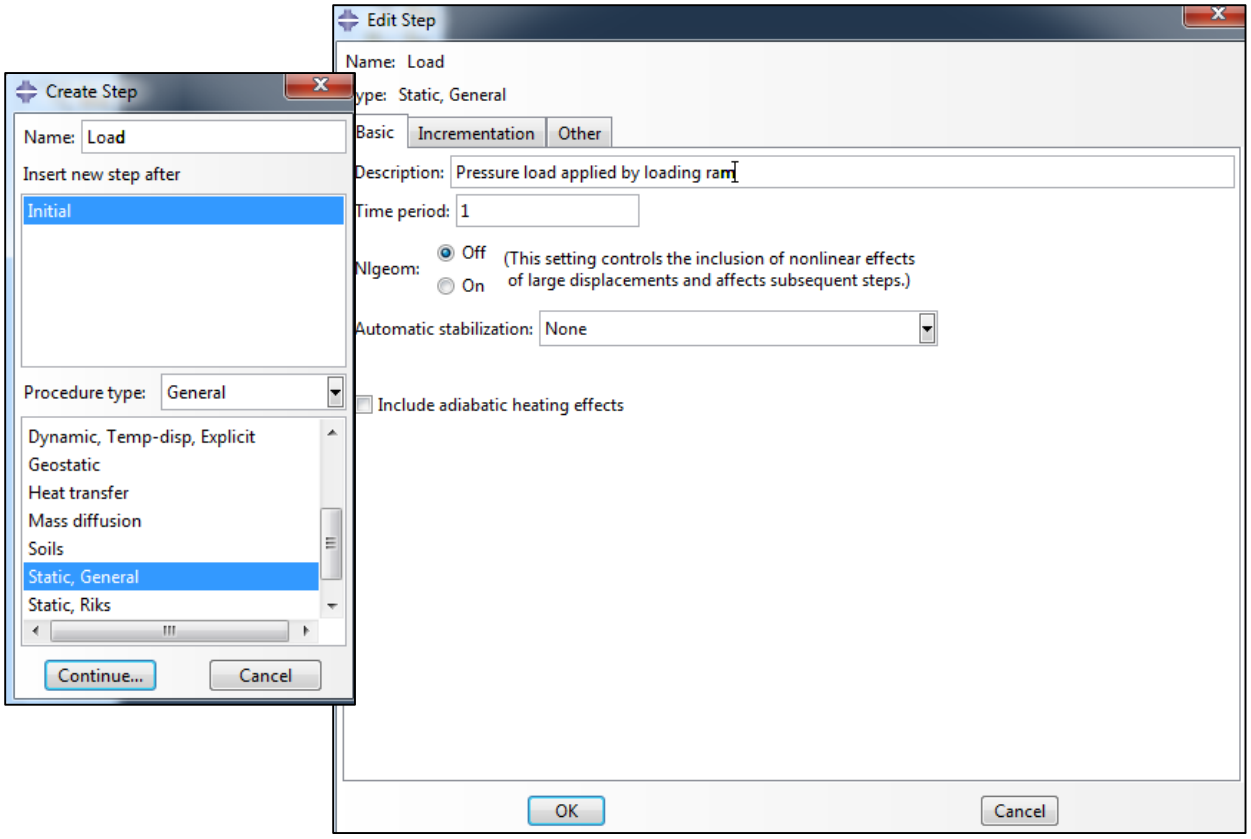

Figure C. 7 - Creating load step.

C.1.5 LOAD MODULE

The 'Load' module allowed the user to define loads and boundary conditions applied to the assembled part. As only a quarter of an asphalt briquette was analysed, symmetric boundary conditions were used to account for the remaining three quarters of the asphalt briquette. Boundary conditions were added by selecting 'Create boundary Condition' in the 'Toolbox Area' under the 'Load' module. From Figure C.8 follows that the Y-symmetric boundary condition was applied to the bottom plane of the assembled part. This boundary conditions assumed displacement in the y-direction (U2), rotation around the x-axis (UR1) and rotation around the z-axis (UR3) is equal to zero. A similar procedure was followed to apply boundary conditions to the right plane of the assembled part. From Figure C.8 follows that X-symmetry was applied to the right plane, thus restricting displacement in the x-direction (U1), rotation around the y-axis (UR2) and rotation around the z-axis (UR3) to zero.

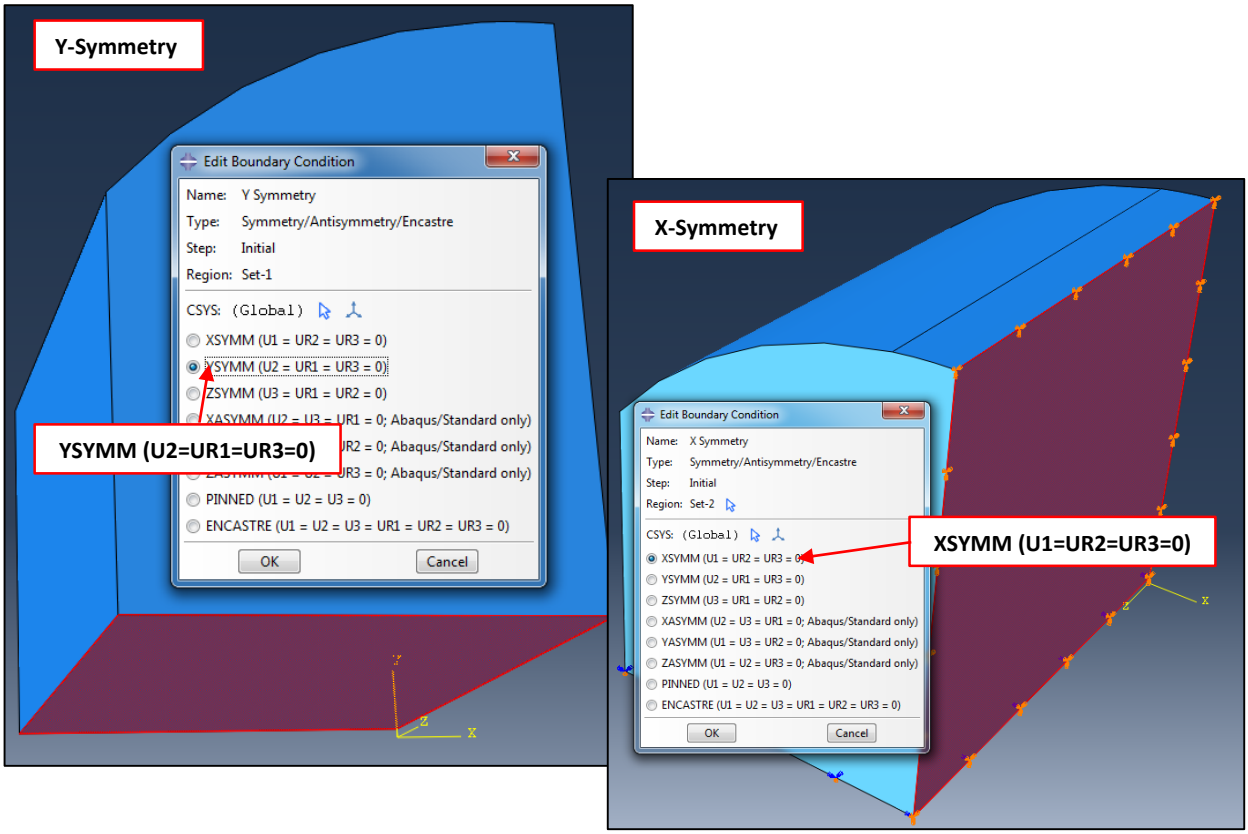

Figure C. 8 - Applying boundary conditions.

A pressure load was applied to the assembled part. However, before the load was created it was required to determine its magnitude. After executing ITS tests on the 50/70 penetration grade binder combination prepared for dry MMLS trafficking, an average failure load of 16.4 kN was calculated. It was required next to determine the partitioned area on the assembled part. The force (F) and area (A) results were used to calculate pressure load magnitude. Equations 6.1 to 6.4 were used for this calculation.

$$Pressure = \frac{Force}{Area} \qquad \textit{Equation C.1}$$

$$Area = \ Specimen\ Height\ \times Arc\ Length \qquad \textit{Equation C.2}$$

$$Arc\ Length = \frac{\theta}{360} \times 2 \times \pi \times Radius\ of\ Briquette \qquad \textit{Equation C.3}$$

$$\theta = \ \tan^{-1}\left(\frac{Half\ Width\ of\ Loading\ Strip}{Radius\ of\ Briquette}\right) \qquad \textit{Equation C.4}$$

Applying these equations the following results, as shown in Table C.1, were obtained.

Table C. 1 - Calculating the pressure load magnitude.

50/70 pen grade Briquette Pressure Load		
Depth	0.08	m
Half Loading Strip Width	0.009525	m
Radius	0.075	m
θ	7.24	
Arc length	0.00947428	m
Area	0.000757942	mm^2
Force	205079.17	N/m
Force Applied	8203.17	N
Pressure Load	10822941.63	N/m^2

With the pressure load known, it was applied to the assembled part by selecting 'Create Load' in the 'Toolbox Area' under the 'Load' module dialog appeared as illustrated in Figure C.9. From Figure C.9 follows that the 'Pressure Load' option was selected and the magnitude 10822941.63 N/m^2 entered.

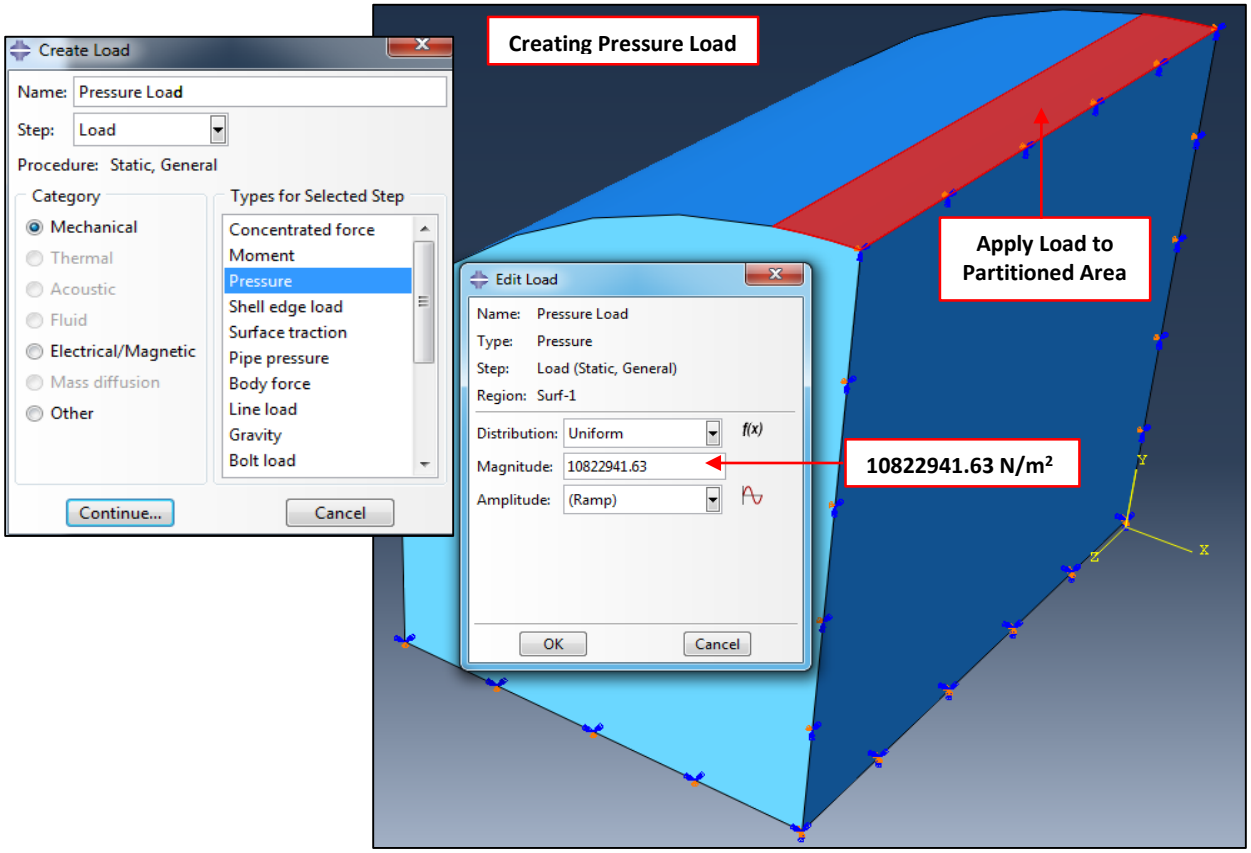

Figure C. 9 - Creating pressure load.

C.1.6 MESH MODULE

The 'Mesh' module controlled the properties of the mesh applied to the assembled part. In this module the mesh size, shape and type of elements are set. The assembled part was meshed, using the 'Seed Part Instance' option for the 'Toolbox Area' under the 'Mesh Module'. A dialog appeared as illustrated in Figure C.10, where the 'approximate element global size' was set. Walker (2013) conducted a sensitivity analysis on element size and found a size of 3 mm provided consistent results and quick simulation time. Therefore, an 'approximate global size' of 3 was used. In addition, the element shape was set by selecting the 'Assign Mesh Controls' option in the 'Toolbox Area' under the 'Mesh' module. From Figure C.10 follows that the element shape selected was the 'Hex' option as this represented an eight node brick element. The 'Sweep Technique' was also selected as illustrated in Figure C.10.

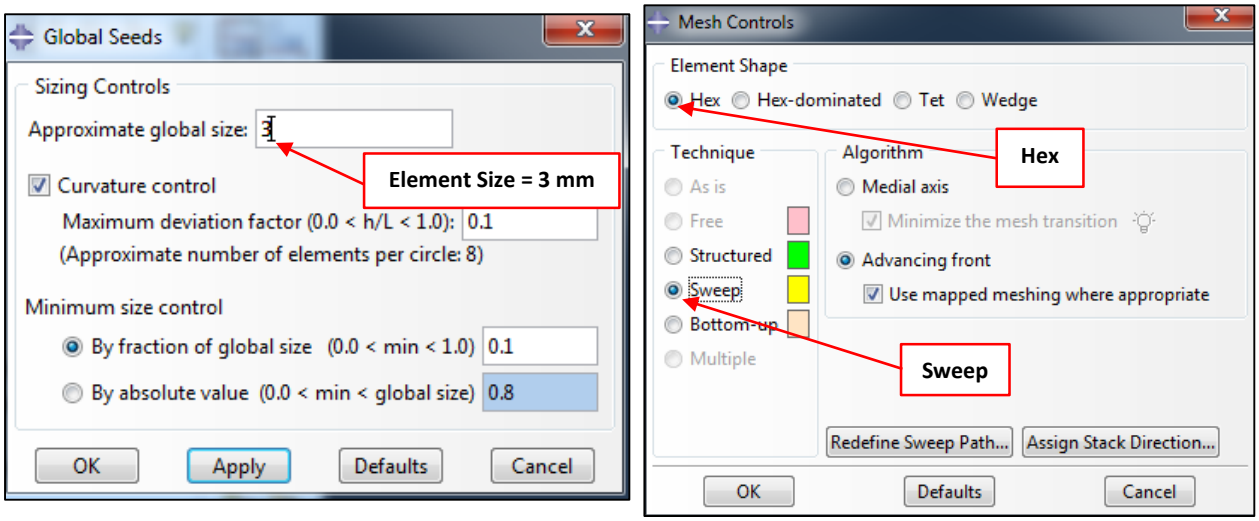

Figure C. 10 - Global seeds and mesh controls.

The 'Assign Element Type' option in the 'Toolbox Area' was selected to set the element type options. A dialog box appeared as illustrated in Figure C.11. Under the 'Element Library' heading the 'Standard' option was selected. The 'Linear' option was selected under the 'Geometric Order' as a linear finite element analysis was executed on the assembled part. The default setting was used for the remaining options. Finally, the assembled part was meshed as illustrated in Figure C.11, by selecting the 'Mesh Part' option in the 'Toolbox' area under the 'Mesh' module.

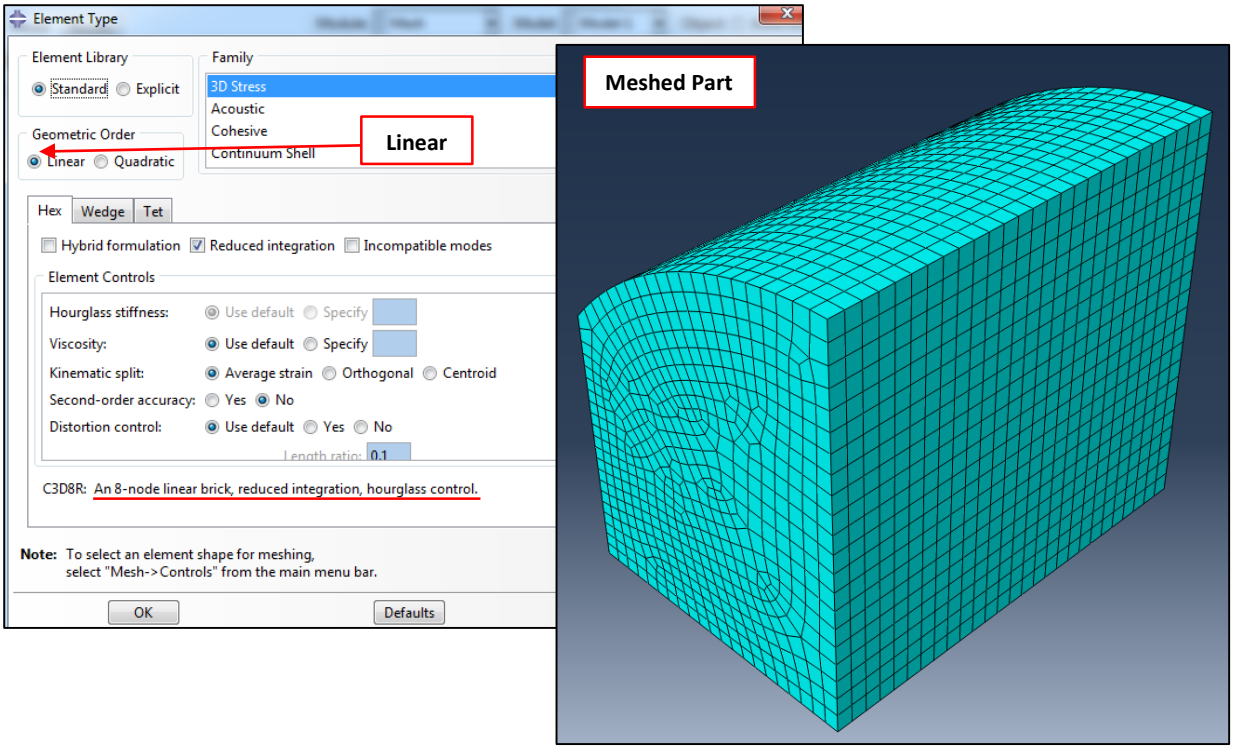

Figure C. 11 - Select element type.

C.1.7 JOB MODULE

The 'Job' module was used to submit the meshed part for analysis. The 'Create Job' option in the 'Toolbox Area' under the 'Job' module was selected. A screen appeared as illustrated in Figure C.12, where the job name and description were defined.

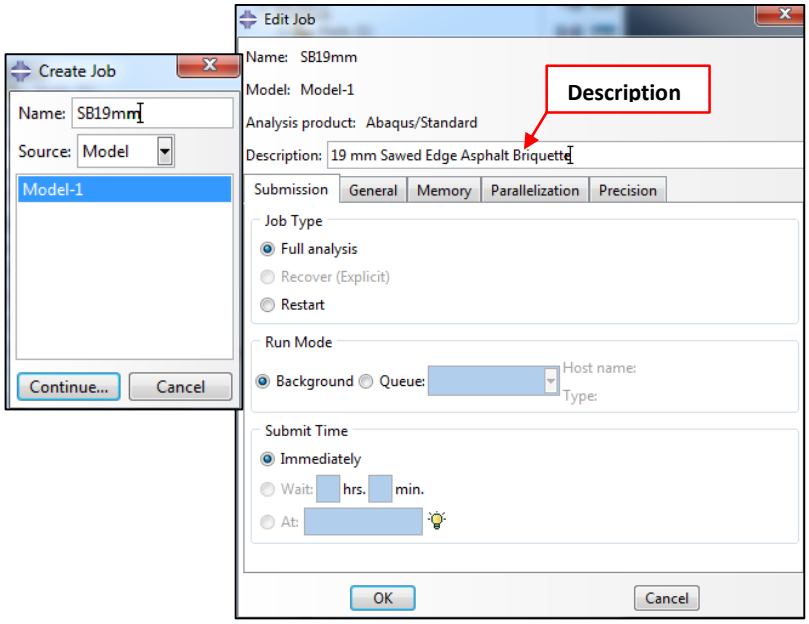

Figure C. 12 - Create Job.

C.1.8 VISUALIZATION MODULE

The 'Visualization' module was used to view deformation of the meshed part after analysis. In this module the stresses and strains or displacements could be visualized by plotting the contours as illustrated in Figure C.13.

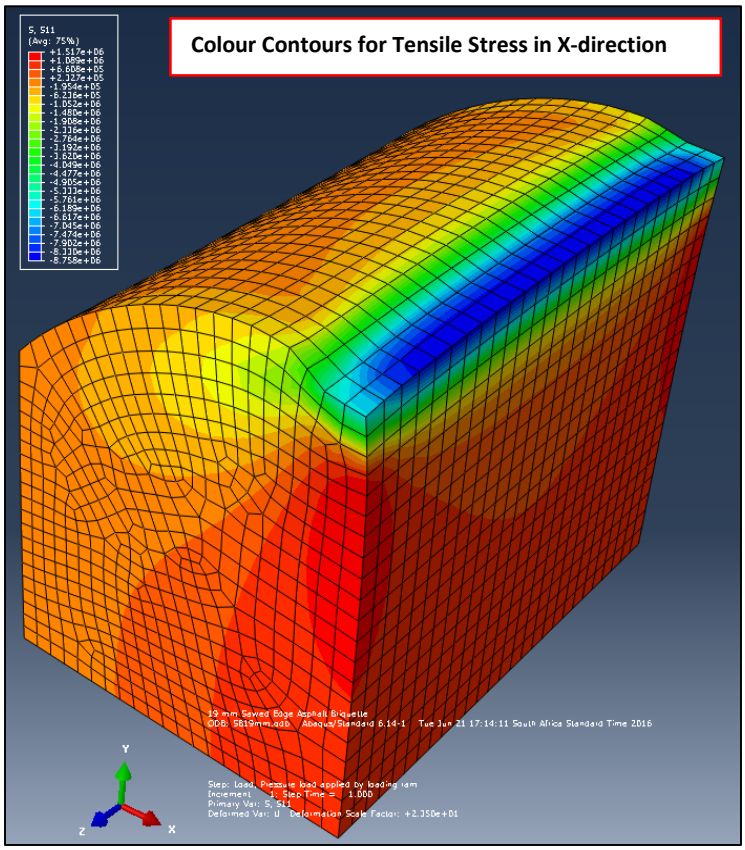

Figure C. 13 - Colour contours of stress S11.

In addition, results related to the stresses and strains or displacement could also be extracted from the analysed part by creating a specific path. Figure C.14 illustrates the creation of a path. By selecting 'Path' in the 'Model Tree' under the 'Results' tab, the option was given to create a 'Path' by defining its name and type. By selecting 'Continue' option, a secondary dialog box appeared that required for the creation of the node labels 'Path'. The 'Add Before' option was selected and the starting node of the 'Path' was selected. A similar procedure was followed for selecting the end node of the 'Path', by selecting the 'Add After' option. 'Paths' were created to extract data in the x, y and z-directions as illustrated in Figure C.14.

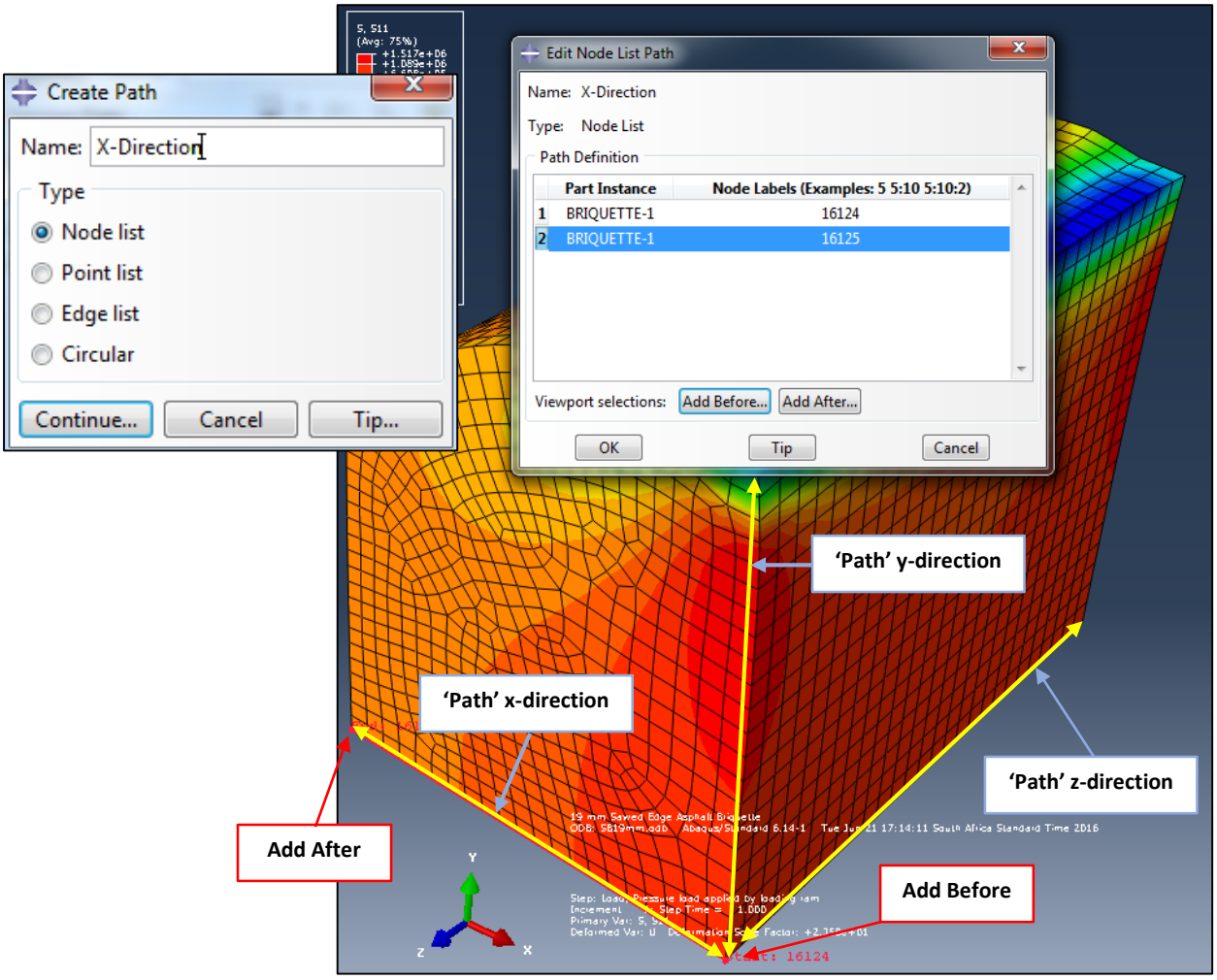

Figure C. 14 - Creating a 'Path'.

Once the 'Paths' were created, they were used to extract data from the analysed part by selecting the 'XY Data' option in the 'Module Tree'. From Figure C.15 follows that the 'Create XY Data' dialog box appeared when the 'Path' source option and 'Continue' were selected. A secondary 'XY Data from Path' dialog appeared and the 'Path' was defined. Under the 'Model Shape' heading, the deformed option was selected. The 'Include Intersections' box was selected to include all nodes along the 'Path' under consideration.

From Figure C.15 follows that the 'Field Output' box was selected. A 'Field Output' dialog box appeared from where the user selected the 'Output Variable' and its 'Component' according to the type of data required. In the example in Figure C.15, under the 'Component' heading, S11 (On the x-plane in the x-direction), S22 (on the y-plane in the y-direction) and S33 (on the z-plane in the z-direction) represent the principal stresses.

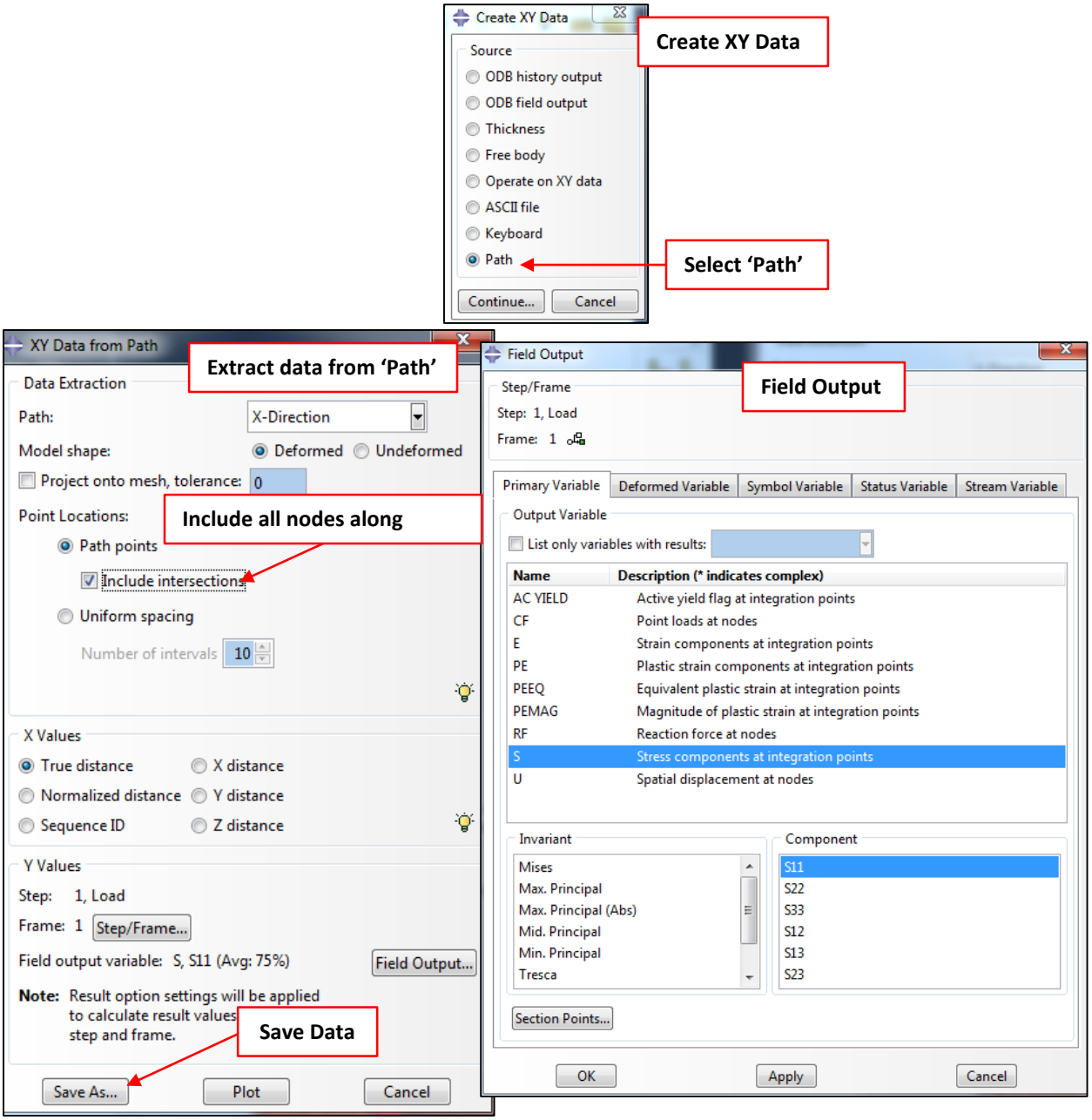

Figure C. 15 - Create data from 'Path'.

Extracted data was saved to be exported to Microsoft Excel by selecting the 'Save As' option from the 'XY Data from Path' dialog (see Figure C.15). The data was saved under a name defining the part type (NB-Normal Briquette, SB-Sawed Briquette), the stress or strain under consideration (S11, S22, S33 or E11) and the name of the 'Path' (X, Y or Z) as illustrated in Figure C.16. Next the 'Report' and 'XY' options under the 'Main Bar' were selected and the 'Report XY data' dialog appeared (see Figure C.16). Under the 'XY Data' tab, the file to be extracted was selected. Moving to the 'Setup' tab, the saved file directory was selected and a file name assigned.

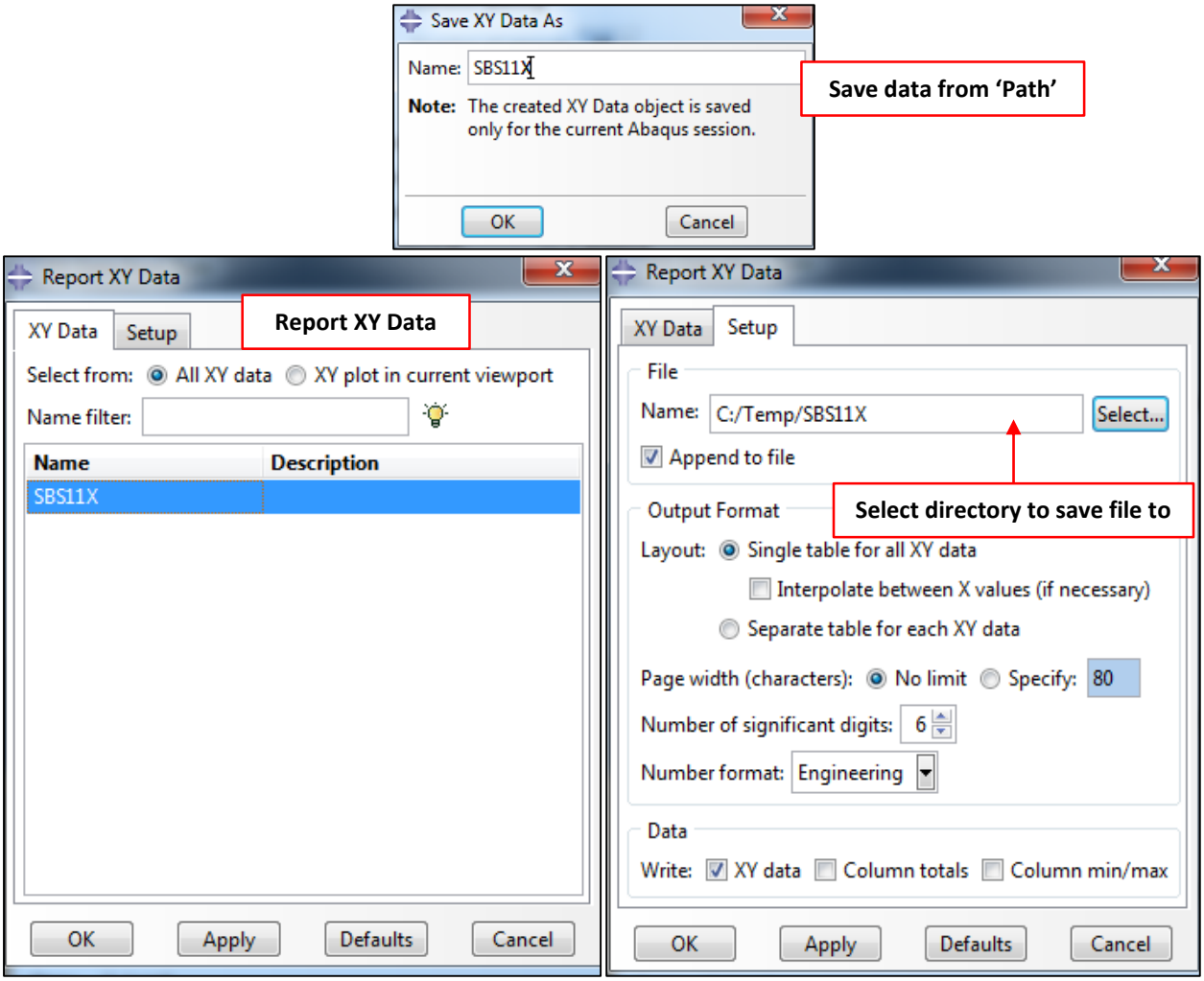

Figure C. 16 - Save extracted data.

C.2 SUMMARY

A method for successfully compiling linear-elastic finite element models were discussed in this Appendix. Various modules in Abaqus/CAE were completed to create all models as identified in the test matrix in Table 6.2 of *Chapter 2*. The results obtained by this modelling were extracted and saved to a Microsoft Excel spreadsheet for further processing.

APPENDIX D – SAMPLE INFORMATION SHEET

Sample number	MN001
Sample mass calculation	
Max Theoretical Density (Rice) kg/m^3	2500
Voids in mix (%)	4.6
Sample diameter (m)	0.15
Sample height (m)	0.075
Sample volume (m^3)	0.001325
Sample mass (g)	**3160.98**

Grading requirements				Date of weighing	07 August 2015
Sieve size (mm)	**Retained on (mm)**	**Passing percentage required (%)**	**Fraction required (g)**	**Fraction weighed (g)**	**Actual passing percentage (%)**
19	14	100	31.60	33	100
14	10	99	379.31	380	99
10	7.1	87	442.54	443	87
7.1	5	73	252.88	252.9	73.0
5	2	65	663.81	663.8	65.0
2	1	44	505.76	505.7	44.0
1	0.6	28	316.10	316.1	28.0
0.6	0.3	18	189.66	189.6	18.0
0.3	0.15	12	94.83	94.8	12.0
0.15	0.075	9	50.58	50.5	9.0
0.075	Pan	7.4	233.91	233.9	7.4
		Total mass (g)	**3160.98**	**3163.30**	

Asphalt contents		Date of mixing	17 August 2015
	Content (%)	**Mass required (g)**	**Content weighed (g)**
Aggregate mass	-	3160.98	3185.00
Binder	5.5	183.97	185.4
Lime	1	31.61	31.61
Sand (Semi gap, CCC graded mix designs)	0	0.00	N/A
A-E2	0	0.00	N/A
EVA	0	0.00	N/A
Polyamine	0	0.00	N/A
Sasobit	0	0.00	N/A
	Total briquette mass (g)	**3402.01**	

Mixing quality control	
Temperature requirement during mixing (°C) (Specified on mix design sheets)	150-160
Asphalt temperature after mixing (°C)	164
Asphalt temperature before adding to compaction mould (°C)	162
Gyratory compactor mould temperature before compaction (°C)	144
Temperature of moulds outside wall after compaction (°C)	132
Briquette temperature after removing from mould (°C)	134

Results from Gyratory compactor	
Voids (%)	-
Density (kg/m^3)	-

Bulk relative density (BRD) calculation	
Mass of briquette: Dry (g) A	3279.69
Mass of briquette: Surface dry (g) B	3288.72
Mass of briquette: In water (g) C	1899.82
Sample height (mm)	78.33
BRD result	**2.361**
Voids in mix (%)	**5.0**

MIST Conditioning				
Conditioning type	Date	Time		Total conditioning time (hours)
		In	out	
No water	N/A	N/A	N/A	N/A

MIST Conditioning quality control	
Water temperature requirement during conditioning (°C)	60
Briquette temperature after 4 hours in oven (°C)	-
Water temperature before testing (°C)	N/A
Water temperature after testing (°C)	N/A

ITS test			Date of testing	20 August 2015
Conditioning type	Maximum applied load (kN)	Sample diameter (cm)	Sample height (cm)	Indirect tensile strength (kPa)
No water	12.301	15	7.83	666.47

ITS test quality control	
Temperature requirement for testing (°C)	25
Sample temperature after 4 hours in oven (°C)	28
ITS climate chamber temperature (°C)	25
Sample inside temperature after testing (°C)	25.1

APPENDIX E – ASPHALT MIXTURE DESIGNS

SOUTH AFRICA
COLTO
Committee of Land Transport Officials

Much Asphalt

ASPHALT MIX DESIGN
ASFALT MENGSELONTWERP

CONTINUOUSLY MEDIUM GRADED ASPHALT SURI
WITH 50/70 BINDER - April'15
EX EERSTERIVIER

Aggregates / Aggregate

Sample / Monster No.	Nom. Size / Growwe	Type and Source / Tipe en Bron
1	13.2 mm	Malmesbury Hornfels ex Peak Quarry
2	9.5 mm	Malmesbury Hornfels ex Peak Quarry
3	Crusher Dust	Malmesbury Hornfels ex Peak Quarry
6	Lime	Cape Lime

NOTE: Tests Methods Refer To TMH1[ ], SABS[ ]
NOTA: Toetsmetodes Verwys Na TMH1[ ], SABS[ ]

Sieve Analysis / Sifanalise (B 4) - % Passing Sieves / % Deur Siwwe

Sample No. / Monster No.		1	2	3	4	5	6		Design / Ontwerp	
% In Mix / Mengsel		15	15	69			1		Mix / Mengsel	Spec. / Spes.
Sieve Size (mm)	37,5									
	26,5									
	19,0	100							100	100
	13,2	92	100						99	100
	9,5	19	93						87	82-100
Sifgrootte (mm)	6,7	2	15	100					73	
	4,75	1	5	92					65	54-75
	2,36		3	61					44	35-50
	1,18		3	39					28	27-42
	0,600		2	24			100		18	18-32
	0,300		1	16			100		12	11-23
	0,150			12			96		9	7-16
	0,075			9,5			81		7,4	4-10
BRD	[B14+15]	2.729	2.723	2.700			2.595		2.707	
Sand equ./eku.	[B19]			56						
Water absorp.	[B14+15]	0.3	0.4	0.8						
ACV / AWW	[B1]	13.3								
10% FACT / FAWW	[B1]	435D/500W								
Flak. Index / Plath. Indeks	[B3]	21.2	22.5							
PSV / KPW	[B4]	54								
AIV / AIW	[ ]									

Sieve analysis Sifanalise

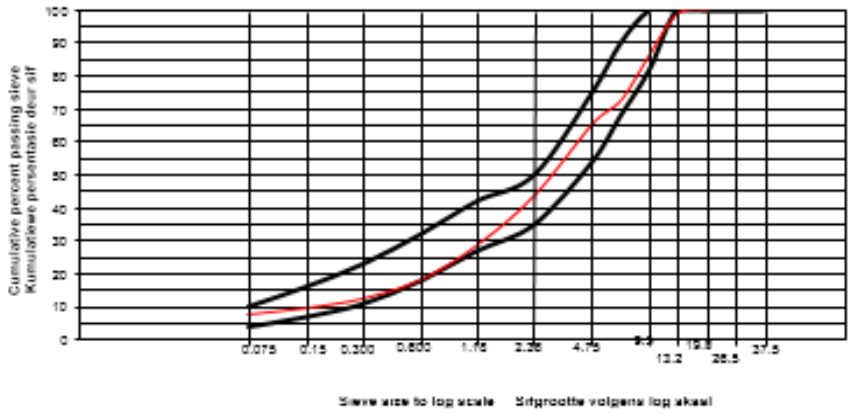

Sieve size to log scale Sifgrootte volgens log skaal

Filler / Vulstof

	Type / soort	% in mix / meng
6	Lime	1.0

Notes / Notas

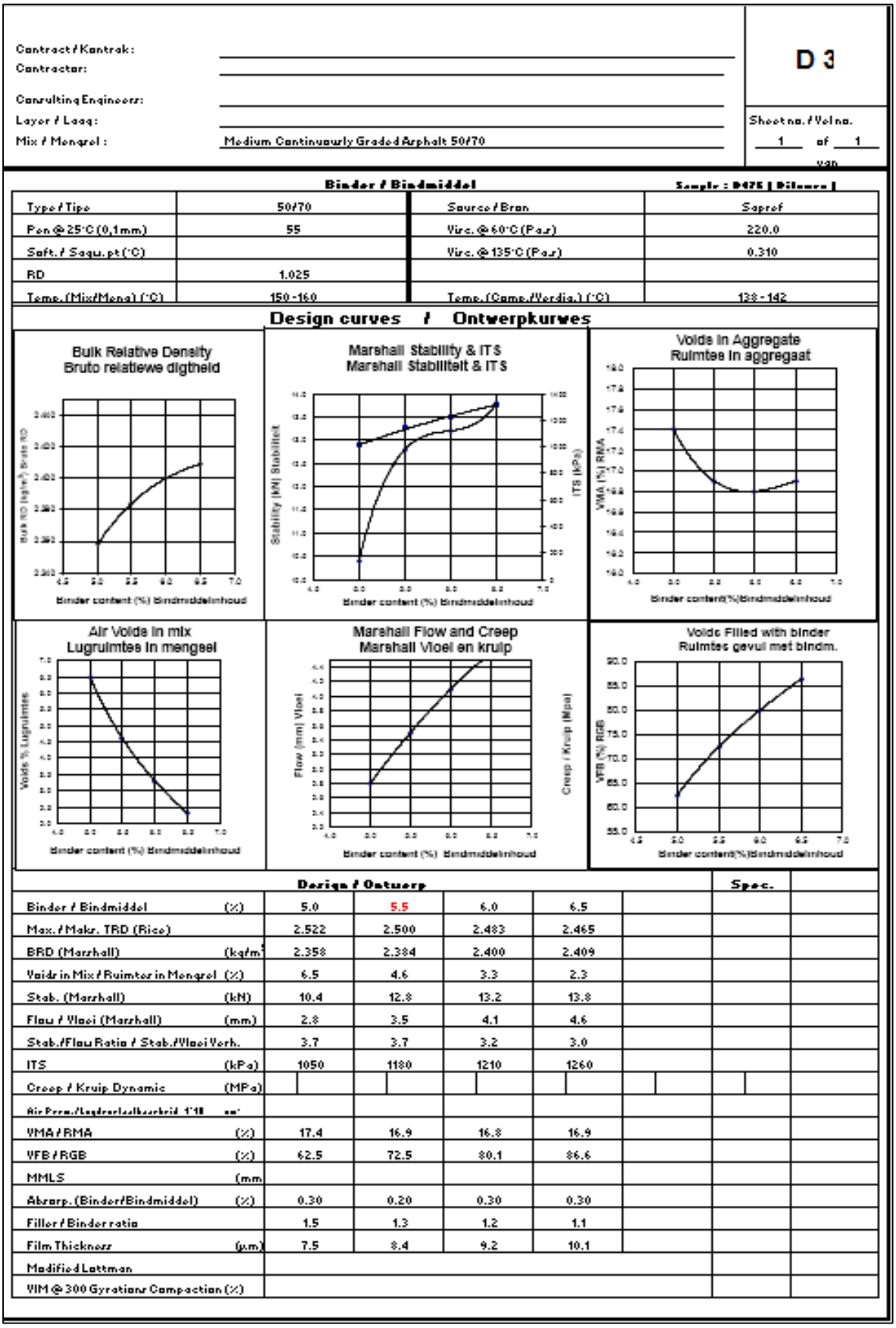

Figure E. 1 - COLTO medium continuous grade asphalt mixture.

Much Asphalt

ASPHALT MIX DESIGN
ASFALT MENGSELONTWERP

19mm Semi Gap GRADED ASPHALT
- August 2015
EX EERSTERIVIER

Aggregates / Aggregate

Sample / Monster No.	Nom. Size / Growwe	Type and Source / Tipe en Bron
1	13.2 mm	Malmesbury Hornfels ex Peak Quarry
2	6.7 mm	Malmesbury Hornfels ex Peak Quarry
3	Crusher Dust	Malmesbury Hornfels ex Peak Quarry
4	Sand	Brackenfell
5	Lime	Cape Lime

NOTE: Test Methods Refer To TMH1 [ ], SABS [ ]
NOTA: Toetsmetodes Verwys Na TMH1 [ ], SABS [ ]

Sieve Analysis / Sifanalise (B 4) - % Passing Sieves / % Deur Siwwe

Sample No. / Monster No.		1	2	3	4	5	6		Design / Ontwerp	
% In Mix / Mengsel		24	24	16	35	1	0		Mix / Mengsel	Spec. / Spes.
	37,5									
	26,5									
Sieve Size	19,0	100							100	100
(mm)	13,2	92							98	82-100
	9,5	29	100						83	73-86
Sifgrootte	6,7	4	67	100					68	59-73
(mm)	4,75	3	15	96	100				55	45-60
	2,36	3	6	69	99				48	40-52
	1,18	3	5	45	97	100			44	36-47
	0,600	3	4	32	79	97			35	32-42
	0,300	3	4	20	46	90			22	22-35
	0,150	3	4	16	7	85			8	10-20
	0,075	3	4	13,3	1	81			5,0	4-10
BRD	[B14+15]	2.725	2.731	2.701	2.578	2.595			2.670	
Sand eqv./eku.	[B19]									
Water absorp.	[B14+15]	0.2	0.2	0.6	0.9					
ACV / AWW	[B1]	10.4								
10% FACT / FAVW	[B1]	310								
Flak. Index / Plath. Indeks	[B3]	19.4	24.1							
PSV / KPW	[B4]	52								
AIV / AIW	[ ]									

Sieve analysis Sifanalise

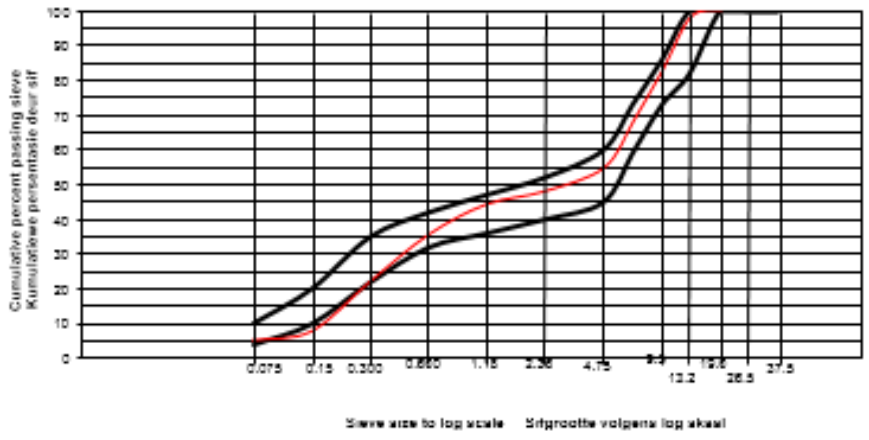

Sieve size to log scale Sifgrootte volgens log skaal

Filler / Vulstof

	Type / soort	% in mix / meng
5	Lime	

Notes / Notas

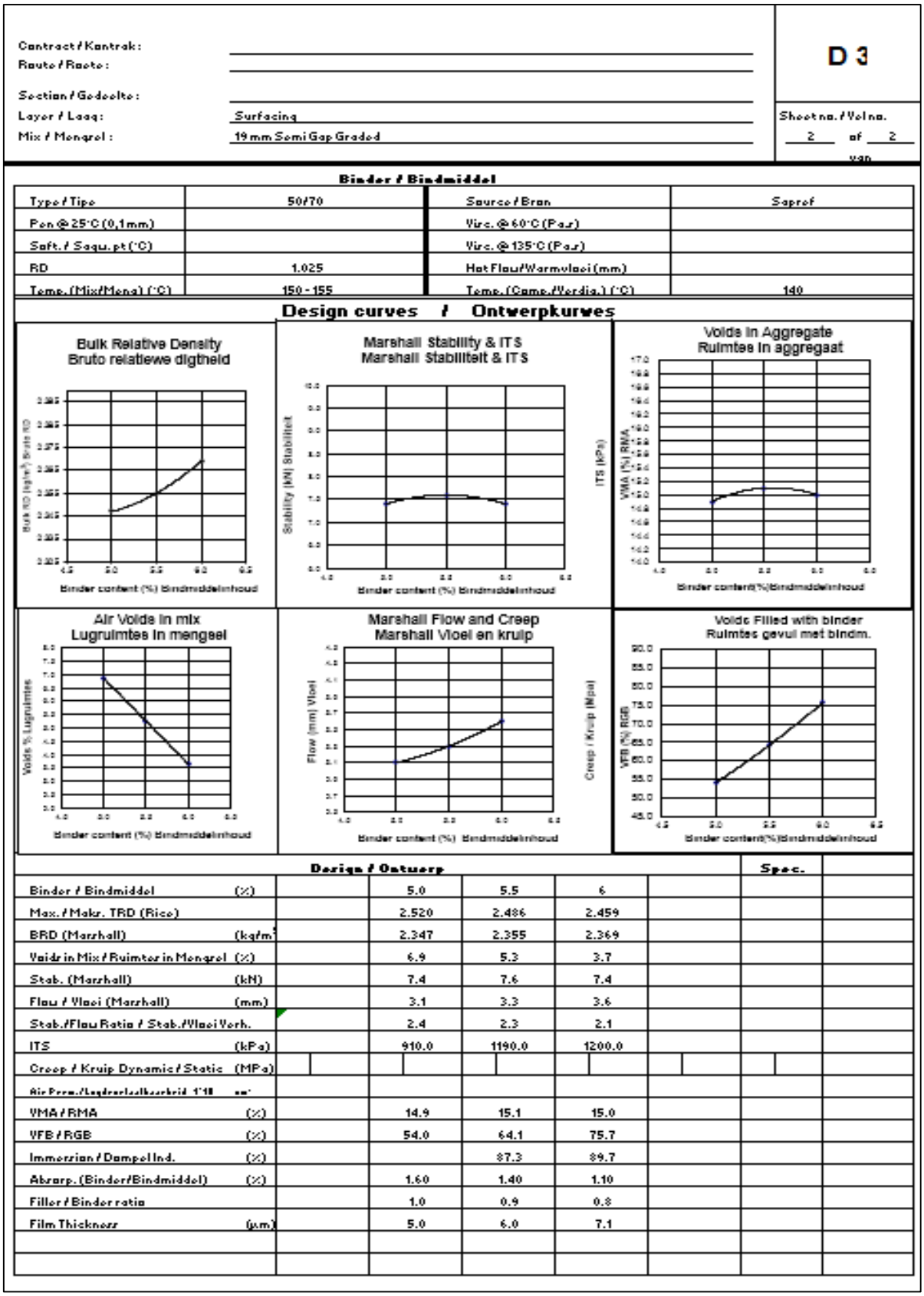

Figure E. 2 - Semi-gap grade asphalt mixture.

Much Asphalt

ASPHALT MIX DESIGN
ASFALT MENGSELONTWERP

CONTINUOUSLY GRADED ASPHALT
- February 2015
EX EERSTERIVIER

Aggregates / Aggregate

Sample / Monster No.	Nom. Size / Growwe	Type and Source / Tipe en Bron
1	13.2 mm	Malmesbury Hornfels ex Peak Quarry
2	9.5 mm	Malmesbury Hornfels ex Peak Quarry
3	Crusher Dust	Malmesbury Hornfels ex Peak Quarry
4	Sand	Brackette

NOTE: Test Methods Refer To TMH1[ ], SABS[ ]
NOTA: Toetsmetodes Verwys Na TMH1[ ], SABS[ ]

Sieve Analysis / Sifanalise (B 4) - % Passing Sieve / % Deur Sif

Sample No. / Monster No.		1	2	3	4	5	6		Design / Ontwerp	
% In Mix / Mengsel		16	15	59	10	0	0		Mix / Mengsel	Spec. / Spes.
	37,5									
	26,5									
Sieve Size	19,0	100							100	100
(mm)	13,2	90	100						98	100
	9,5	16	94						86	82-100
Sifgrootte	6,7	2	15	100					72	65-86
(mm)	4,75	2	2	93					65	54-75
	2,36	2	2	60	100				46	38-56
	1,18	2	2	37	97				32	27-42
	0,600	1	2	27	87				25	18-32
	0,300		2	17	66				17	11-23
	0,150		1	13	10				9	7-16
	0,075			10,2	1				6,1	4-10
BRD	[B14+15	2,733	2,725	2,716	2,562				2,705	
Sand equ./eku.	[B19]			53	61					
Water absorp.	[B14+15	0,2	0,2	0,6	0,7					
ACV / AWW	[B1]	10,4								
10% FACT / FAWW	[B1]	310								
Flak. Index / Plath. Indeks	[B3]	19,4	24,1							
PSV / KPW	[B48	52								
AIV / AIW	[ ]									

Sieve analysis Sifanalise

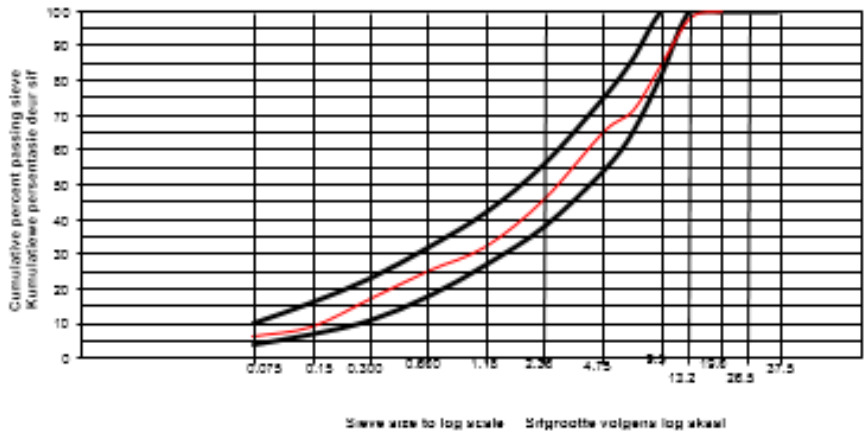

Sieve size to log scale Sifgrootte volgens log skaal

Filler / Vulstof

	Type/soort	% in mix/meng
	Lime	

Water / Water

Contract / Kontrak:

Route / Roete:

Section / Gedeelte:

Layer / Laag: Surfacing

Mix / Mengsel: SABS / CCC Wearing Course 50/70 Bitumen

D 3

Sheet no. / Vel no. 2 of 2 van

Binder / Bindmiddel

Type / Tipe	50/70 (B429)	Source / Bron	Sapref
Pen @ 25°C (0,1mm)	56	Visc. @ 60°C (Pa.s)	210.3
Soft. / Sagu. pt (°C)		Visc. @ 135°C (Pa.s)	0.400
RD	1.025	Hot Flow / Warmvloei (mm)	
Temp. (Mix/Menge) (°C)	150 - 155	Temp. (Comp./Verdig.) (°C)	140

Design curves / Ontwerpkurwes

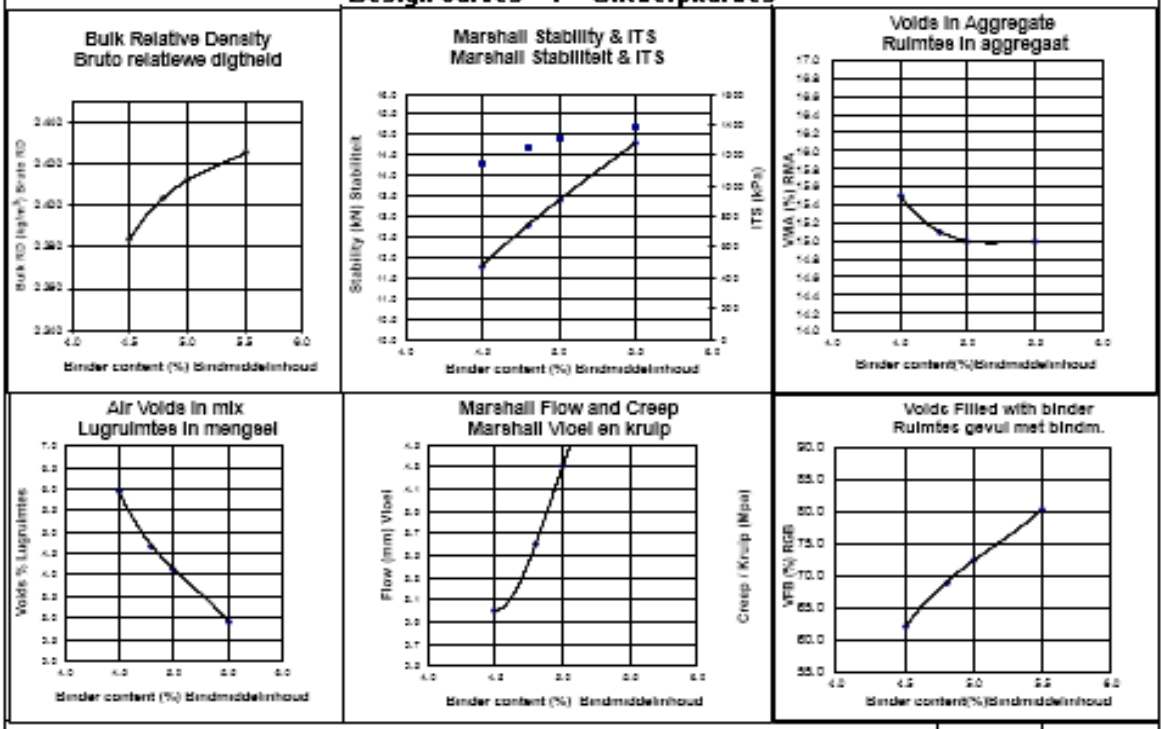

		Design / Ontwerp					Spec.	
Binder / Bindmiddel	(%)	4.5	4.8	5.0	5.5			
Max. / Maks. TRD (Rice)		2.534	2.522	2.516	2.498			
BRD (Marshall)	(kg/m³)	2.384	2.404	2.412	2.425			
Voids in Mix / Ruimtes in Mengsel	(%)	5.9	4.7	4.1	2.9			
Stab. (Marshall)	(kN)	11.8	12.8	13.4	14.8			
Flow / Vloei (Marshall)	(mm)	3.0	3.6	4.3	4.8			
Stab./Flow Ratio / Stab./Vloei Verh.		3.9	3.6	3.1	3.1			
ITS	(kPa)	1150.0	1250.0	1310.0	1390.0			
Creep / Kruip Dynamic / Static	(MPa)							
Air Perm./Lugdeurlaatbaarheid 1*10	m²							
VMA / RMA	(%)	15.5	15.1	15.0	15.0			
VFB / RGB	(%)	61.9	69.0	72.4	80.5			
Immersion / Dompel Ind.	(%)	83.5	86.2	87.3	89.7			
Abrasp. (Binder/Bindmiddel)	(%)	0.40	0.40	0.40	0.40			
Filler / Binder ratio		1.4	1.3	1.2	1.1			
Film Thickness	(µm)	6.7	7.2	7.5	8.3			
Resilient Modulus	(mPa)							

Figure E. 3 - CCC continuous grade asphalt mixture.

Much Asphalt

ASPHALT MIX DESIGN
ASFALT MENGSELONTWERP

COLTO FINE
20 January 2015
EX EERSTERIVIER

Aggregates / Aggregate

Sample / Monster No.	Nom. Size / Grootte	Type and Source / Tipe en Bron
1	6mm	Malmesbury Hornfels ex Peak Quarry
2	Crusher Dust	Malmesbury Hornfels ex Peak Quarry
3	Lime	Cape Lime

NOTE : Test Methods Refer To TMH 1 [ ], SABS [ ]
NOTA: Toetsmetodes Verwys Na TMH 1 [ ], SABS [ ]

Sieve Analysis / Sifanalise (B 4) - % Passing Sieves / % Deur Siwwe

Sample No. / Monster No.		1	2					3	Design / Ontwerp	
% In Mix / Mengsel		13	86					1	Mix / Mengsel	Spec. / Spes.
	37,5									
	26,5								100	
Sieve Size	19,0								100	
(mm)	13,2								100	
	9,5	100							100	100 - 100
Sifgrootte	6,7	85	100						98	
(mm)	4,75	25	94						85	64 - 88
	2,36	5	63						56	45 - 60
	1,18	3	41						37	35 - 54
	0,600	3	28						25	24 - 40
	0,300	2	18					100	17	16 - 28
	0,150	1	12					99	11	10 - 20
	0,075		9.5					88	9.1	4 - 12
BRD [B14+15]		2.721	2.696					2.595	2.698	
Sand eqv./ekw. [B19]			58							
Water absorp. [B14+15]		0.4	0.7							
ACV / AVW [B1]										
10% FACT / FAVW [B1]		370w/390d								
Flak. Index / Plath. Indeks [B3]		26.2								
PSV / KPW [B48]										
AIV / AIW [ ]										

Sieve analysis Sifanalise

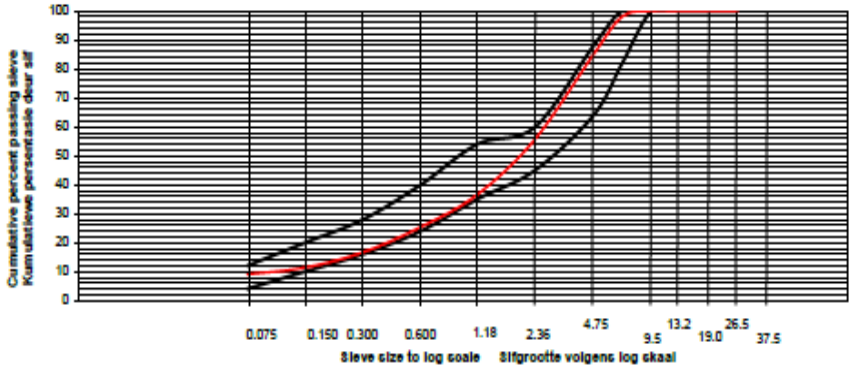

Filler / Vulstof

	Type/soort	%in mix/meng
3	Lime	1.0

Notes / Notas

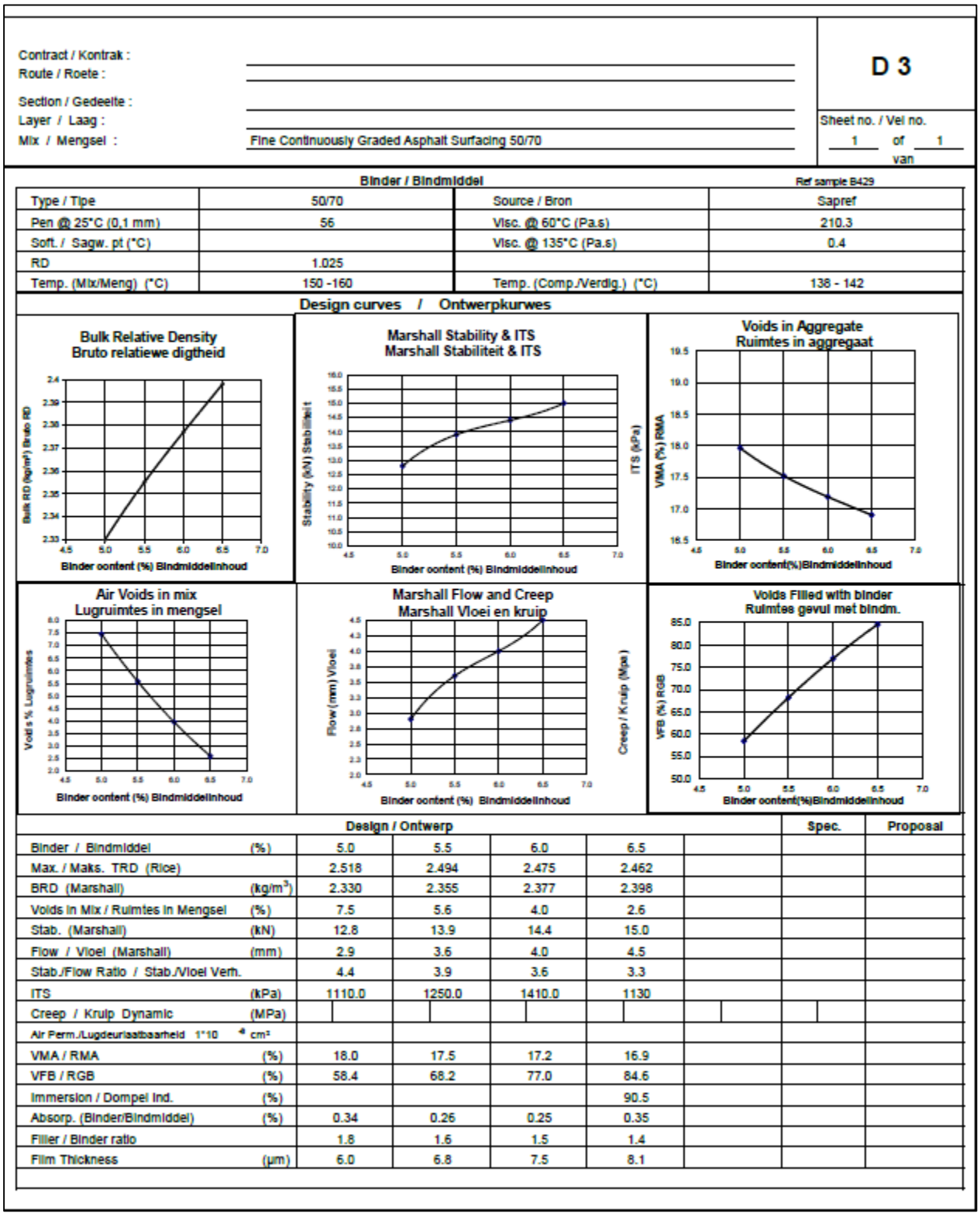

Design / Ontwerp							Spec.	Proposal
Binder / Bindmiddel	(%)	5.0	5.5	6.0	6.5			
Max. / Maks. TRD (Rice)		2.518	2.494	2.475	2.462			
BRD (Marshall)	(kg/m³)	2.330	2.355	2.377	2.398			
Voids in Mix / Ruimtes in Mengsel	(%)	7.5	5.6	4.0	2.6			
Stab. (Marshall)	(kN)	12.8	13.9	14.4	15.0			
Flow / Vloei (Marshall)	(mm)	2.9	3.6	4.0	4.5			
Stab./Flow Ratio / Stab./Vloei Verh.		4.4	3.9	3.6	3.3			
ITS	(kPa)	1110.0	1250.0	1410.0	1130			
Creep / Kruip Dynamic	(MPa)							
Air Perm./Lugdeurlaatbaarheid 1*10⁻⁴ cm²								
VMA / RMA	(%)	18.0	17.5	17.2	16.9			
VFB / RGB	(%)	58.4	68.2	77.0	84.6			
Immersion / Dompel Ind.	(%)				90.5			
Absorp. (Binder/Bindmiddel)	(%)	0.34	0.26	0.25	0.35			
Filler / Binder ratio		1.8	1.6	1.5	1.4			
Film Thickness	(µm)	6.0	6.8	7.5	8.1			

Figure E. 4 - COLTO fine continuous grade asphalt mixture.